UNIVERSITÀ DELLA CALABRIA

UNIVERSITA' DELLA CALABRIA

Dipartimento di INGEGNERIA CIVILE

Dottorato di Ricerca in

INGEGNERIA CIVILE E INDUSTRIALE

CICLO

XXX

MULTI-LEVEL ASSESSMENT OF THE ENVIRONMENTAL BENEFITS OF A PERMEABLE PAVEMENT: NUMERICAL ANALYSIS AND EXPERIMENTAL INVESTIGATIONS

Settore Scientifico Disciplinare ICAR/02

Coordinatore: Ch.mo Prof. Franco Furgiuele

Firma _____

Supervisore/Tutor: Ch.mo Prof. Patrizia Piro

Firma _____

Dottorando: Dott. Michele Turco

Firma _____

I would like to dedicate this thesis to my children Enzo and Emilio, for having changed my life in a wonderful way.

"Figlio mio, vivi in modo da non doverti vergognare di te stesso, dì la tua parola in modo che ciascuno debba dire di te che ci si può fidare; e non dimenticare che dare gioia ci dà anche gioia. Impara a tempo che la fame dà sapore ai cibi, e rifuggi la comodità perché rende insipida la vita. Un giorno dovrai fare qualcosa di grande: a tale scopo devi diventare tu stesso qualcosa di grande." (F. Nietzsche).

Declaration

I hereby declare that except where specific reference is made to the work of others, the contents of this dissertation are original and have not been submitted in whole or in part for consideration for any other degree or qualification in this, or any other University. This dissertation is the result of my own work and includes nothing which is the outcome of work done in collaboration, except where specifically indicated in the text.

Dott. Michele
Turco

2018

Acknowledgements

And I would like to acknowledge all the people that supported me during this path. First, my family, then my friends and my colleagues.

ABSTRACT

The increasing frequency of flooding events in urban catchments related to an increase in impervious surfaces highlights the inadequacy of traditional urban drainage systems whose aim is to rapidly collect and convey overland flows to the treatment plants.

Recently, scientific community has focused its attention on Low-impact developments (LIDs) techniques that have proven to be valuable alternatives for stormwater management and hydrological restoration, by reducing stormwater runoff by reproducing natural hydrological processes in urban areas. However, the lack of diffusion of adequate modelling tools represents a barrier in designing and constructing such systems.

In general, Permeable Pavement (PP) represents a good solution to solve stormwater management problems both in quantitative and qualitative way. This thesis focused on assessing the hydraulic behaviour and water quality performance of permeable pavements based on laboratory experiments and developing a modelling approach for the water flow in order to assisting engineers and researchers in the design of these systems.

In this way, an adequate hydrological description of water flow in the pavement system relies heavily on the knowledge of the unsaturated hydraulic properties of the construction materials. Although several modelling tools and many laboratory methods already exist in the literature to determine the hydraulic properties of soils, the importance of an accurate description of hydraulic properties of materials used in the permeable pavement, is increasingly recognized in the fields of urban hydrology. Thus, the aim of this study is to propose techniques/procedures on how to interpret water flow through the structural system using the HYDRUS model. The overall analysis includes experimental and mathematical procedures for model calibration and validation to assess the suitability of the HYDRUS-2D

model to interpret the hydraulic behaviour of a lab-scale permeable pavement system. The system consists of three porous materials: a wear layer of porous concrete blocks, a bedding layers of fine gravel, and a sub-base layer of coarse gravel. The water regime in this system, i.e. outflow at the bottom and water contents in the middle of the bedding layer, was monitored during ten irrigation events of various durations and intensities. The hydraulic properties of porous concrete blocks and fine gravel described by the van Genuchten functions were measured using the clay tank and the multistep outflow experiments, respectively. Coarse gravel properties were set at literature values. In addition, some of the parameters (K_s of the concrete blocks layer, and α, n and K_s of the bedding layer) were optimized with the HYDRUS-2D model from water fluxes and soil water contents measured during irrigation events. The measured and modelled hydrographs were compared using the Nash-Sutcliffe efficiency (NSE) index (varied between 0.95 and 0.99) while the coefficient of determination R^2 was used to assess the measured water content versus the modelled water content in the bedding layer (R^2= 0.81÷0.87). The parameters were validated using the remaining sets of measurements resulting in NSE values greater than 0.90 (0.91÷0.99) and R^2 between 0.63 and 0.91. Results have confirmed the applicability of HYDRUS-2D to describe correctly the hydraulic behaviour of the lab-scale system. Water quality performance aimed to improve the knowledge of the system to remove heavy metals (Copper and Zinc) from stormwater runoff. It was assessed by using batch and contaminant flow experiments. Batch experiments were conducted on each construction material of the PP and highlighted that, among the pavement materials tested, only concrete blocks had the potential to adsorb the heavy metals investigated. Results shown that the adsorption capacity of the porous concrete is higher in adsorbing Cu (70% ÷ 90%) than Zn (69% ÷ 75%). Flow contaminant experiment were performed under different inflow concentrations. Results show

that removal rates of Cu and Zn of the lab-scale pavements range from 85% to 92% and from 65% to 82%, respectively.

SOMMARIO

L’aumento della frequenza degli eventi alluvionali a scala urbana, strettamente legato all’aumento delle superfici impermeabili, evidenzia l'inadeguatezza, nella gestione delle acque meteoriche, dei sistemi di drenaggio urbano tradizionali il cui scopo è quello di collettare e trasportare rapidamente le acque di deflusso superficiale agli impianti di trattamento.

Recentemente, la comunità scientifica ha focalizzato la sua attenzione sulle tecniche di sviluppo a basso impatto (LID) le quali si sono rivelate valide alternative per la gestione delle acque piovane e il ripristino del ciclo idrologico, riducendo il deflusso superficiale nelle aree urbane mediante la riproduzione di processi idrologici naturali. Tuttavia, la mancanza di diffusione di strumenti di modellazione adeguati rappresenta una barriera nella progettazione e nella costruzione di tali sistemi.

In generale, la Pavimentazione Permeabile, rappresenta una buona soluzione per risolvere i problemi di gestione delle acque piovane sia in termini quantitativi che in termini qualitativi.

Il lavoro proposto in questa tesi è stato incentrato sulla valutazione del comportamento idraulico di una pavimentazione permeabile e sulle sue potenzialità di riduzione del carico inquinante. La valutazione degli effetti di queste opere è stata basata sull’evidenza di esperimenti condotti in laboratorio e sullo sviluppo di un approccio di tipo modellistico al fine di assistere ingegneri e ricercatori nella progettazione di tali tecniche.

Un'adeguata descrizione idrologica del flusso d'acqua nel sistema “pavimentazione” dipende in gran parte dalla conoscenza delle proprietà idrauliche insature dei materiali da costruzione. Sebbene numerosi strumenti di modellazione e molti metodi di laboratorio esistano già in letteratura per determinare le proprietà idrauliche dei terreni, l'importanza di una descrizione idraulica accurata dei materiali del pacchetto drenante rappresenta un valore aggiunto nel campo dell'idrologia urbana. Pertanto, uno degli scopi di questo lavoro è stato quello di proporre tecniche / procedure su come interpretare il flusso dell'acqua attraverso il sistema drenante utilizzando il modello HYDRUS. L'analisi generale del sistema ha riguardato l’utilizzo di procedure sperimentali e matematiche per la calibrazione e validazione del modello idraulico proposto al fine di valutare l'idoneità del modello HYDRUS-2D ad interpretare il comportamento idraulico di un modello fisico a scala ridotta di una pavimentazione permeabile. Il sistema è costituito da tre materiali porosi: uno strato di usura costituito da blocchi di calcestruzzo poroso, uno strato di allettamento in ghiaia fine e uno strato inferiore in pietrame. Il regime idrico in questo sistema, cioè il deflusso sul fondo e il contenuto idrico nello strato di allettamento, è stato monitorato durante dieci eventi di pioggia a varie durate e intensità. Le proprietà idrauliche dei blocchi di calcestruzzo poroso e della ghiaia fine descritti dalle funzioni di van Genuchten, sono state misurate utilizzando rispettivamente gli esperimenti “clay tank” e “multistep outflow”. Le proprietà idrauliche del pietrame sono state definite in base a valori di letteratura. Inoltre, alcuni dei parametri (Ks dello strato superficiale e α, n e Ks dello strato di allettamento) sono stati ottimizzati con il modello HYDRUS-2D in base al deflusso sul fondo misurato e al contenuto idrico durante la campagna sperimentale. Gli idrogrammi misurati e modellati sono stati confrontati usando l'indice di Nash-Sutcliffe (NSE) (compreso tra 0,95 e 0,99) mentre il coefficiente di determinazione R^2 è stato utilizzato per valutare il contenuto idrico misurato rispetto a quello

modellato nello strato di allettamento (R^2 = 0,81 ÷ 0,87). I parametri sono stati validati utilizzando le serie di misurazioni rimanenti con risultati dell'indice di Nash NSE superiori a 0,90 (0,91 ÷ 0,99) e R^2 compreso tra 0,63 e 0,91. I risultati hanno confermato l'applicabilità di HYDRUS-2D per descrivere correttamente il comportamento idraulico del sistema. Le prestazioni qualitative del sistema hanno aiutato a migliorare la conoscenza sulle potenzialità di questi sistemi nel rimuovere contaminanti quali metalli pesanti (rame e zinco) dalle acque di pioggia. Due diversi esperimenti hanno permesso di valutare l'efficienza di rimozione del carico inquinante, il "batch experiment" ed il "flow contaminat experiment". I "batch experiment" sono stati effettuati su ogni materiale da costruzione della PP e hanno evidenziato come solo i blocchi di calcestruzzo abbiano il potenziale di assorbire i metalli pesanti esaminati. I risultati hanno mostrato che la capacità di adsorbimento del calcestruzzo poroso è più alta nell'adsorbimento di Cu (70% ÷ 90%) rispetto allo Zn (69% ÷ 75%). I "contamint flow experiment" sono stati eseguiti con diverse concentrazioni in ingresso al sistema. I risultati hanno mostrato che i tassi di rimozione di Cu e Zn del modello a scala ridotta variano dall'85% al 92% per il Rame e dal 65% all'82% per lo Zinco.

Contents

Turco, M., Kodešová, R., Brunetti, G., Nikodem, A., Fér, M., Piro, P. (2017). Unsaturated hydraulic behaviour of a permeable pavement: Laboratory investigation and numerical analysis by using the HYDRUS-2D model. Journal of Hydrology Volume 554, November 2017, Pages 780-791, https://doi.org/10.1016/j.jhydrol.2017.10.005

Brunetti, G., Simunek, J., **Turco, M**., Piro, P. (2017). On the use of surrogate-based modeling for the numerical analysis of Low Impact Development techniques. Journal of Hydrology Volume 548, May 2017, Pages 263-277, http://dx.doi.org/10.1016/j.jhydrol.2017.03.013

Turco, M., Brunetti, G., Nikodem, A., Fér, M., Kodešová, R., Piro, P. (2017). The use of the RETC code and HYDRUS-1D to define soil hydraulic properties of permeable pavement. In Proceeding of 14th IWA/IAHR International Conference on Urban Drainage, Prague, Czech Republic.

Brunetti, G., Simunek, J., **Turco, M**., Piro, P. (2017). On the use of global sensitivity analysis for the numerical analysis of permeable pavements. In Proceeding of 14th IWA/IAHR International Conference on Urban Drainage, Prague, Czech Republic.

Brunetti, G.F., **Turco, M**., Brunetti, G., Frega, F., Fortunato, G., Piro P. (2017). Modellazione idraulica di una pavimentazione drenante: dal rilievo all'analisi numerica. In Atti del 38° Corso di Aggiornamento in Tecniche per la Difesa del Suolo dall'Inquinamento, Guardia Piemontese Terme, Italia. ISBN: 978-88-97181-57-6, ISSN 2282-5517.

Turco, M., Brunetti, G., Nikodem, A., Fér, M., Kodešová, R. and P. Piro. (2017). Water flow modeling in the highly permeable pavement using Hydrus-2D. In Proceeding of 5th International Conference on HYDRUS Software Applications to Subsurface Flow and Contaminant Transport Problems, Prague March 2017, p. 46, ISBN: 978-80-213-2749-8

Brunetti, G., Šimůnek, J., Wöhling, T., **Turco**, **M.** and Piro, P. (2017). A Computationally Efficient Pseudo-2D Model for the Numerical Analysis of Permeable Pavements. In Proceeding of 5th International Conference on HYDRUS Software Applications to Subsurface Flow and Contaminant Transport Problems, Prague March 2017, p. 17, ISBN: 978-80-213-2749-8

Turco, M., Carbone, M., Brunetti, G., Sansone, E., Piro, P. (2016). Modellazione idraulica delle pavimentazioni drenanti: risultati sperimentali. In Atti del XXXV Convegno Nazionale di Idraulica e Costruzioni Idrauliche, Bologna Settembre 2016, pagine 947-950, ISBN: 9788898010400, DOI: 10.6092/unibo/amsacta/5400

Carbone, M., **Turco, M.,** Brunetti, G., Piro, P. (2015). A Cumulative Rainfall Function (CRF) for sub-hourly design storm in Mediterranean urban areas. Advances in Meteorology, vol. 2015, Article ID 528564, 10 pages, 2015. doi:10.1155/2015/528564;

Carbone, M., **Turco, M.,** Brunetti, G., Piro, P. (2015). Minimum Inter-event Time to identify independent rainfall events in urban catchment scale. Advanced Materials Research Vols. 1073-1076 (2015) pp 1630-1633 © (2015) Trans Tech Publications, Switzerland doi:10.4028/www.scientific.net/AMR.1073-1076.1630

Carbone, M., **Turco, M.,** Nigro, G., Piro, P. (2014). Modeling of hydraulic behaviour of green roof in catchment scale. In Proceedings of International Multidisciplinary Scientific GeoConferences SGEM 2014, Albena, Bulgaria, 2014, pp. 471-478 (ISBN 978-619-7105-13-1; ISSN 1314-2704; DOI: 10.5593/sgem2014B31

LIST OF FIGURES

LIST OF TABLES

CHAPTER 1 BACKGROUND ON STORMWATER MANAGEMENT PROBLEM

This chapter examines the background of the research. It explains the structure of the document in different chapters as well as the objectives of the research.

1.1 The influence of urbanization on natural drainage

In recent decades, due to rapid expansion of urbanization, urban areas have experienced an increase of impermeable surfaces such as rooftops, sidewalks, roads and parking lots that are constructed with impermeable materials such as asphalt, concrete and stone. This urban development has diminished natural soil drainage and has increased runoff volumes (Finkenbine et al., 2000).

In Figure 1.1 the influence of the urbanization on natural drainage is described.

This figure shows that in rural areas, about 5% of the rainfall converts into surface runoff, while 95% infiltrates into soils (these percentage may change in areas rich in vegetation in relation to the magnitude of evapotranspiration). When the development of the area changes due to the increase of impermeable surfaces, there is an increase in the amount of surface runoff.

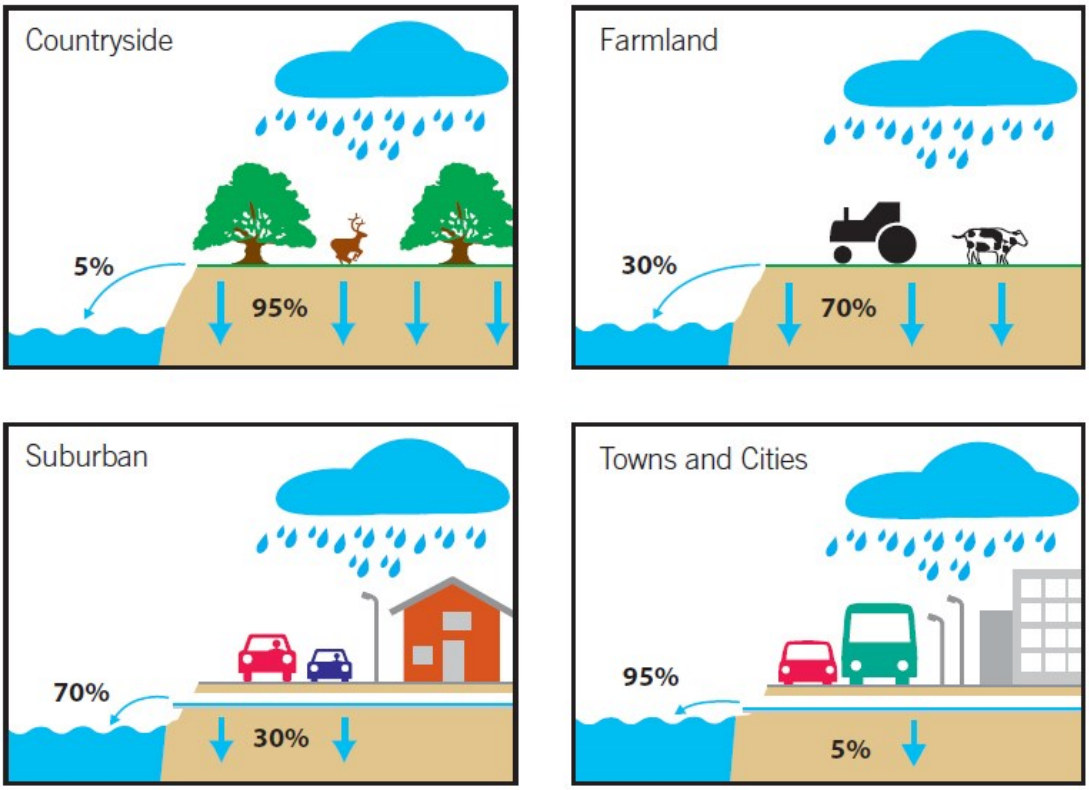

Figure 1.1 The influence of urbanization on natural drainage

This phenomenon, coupled with a progressive increase of precipitation, due to climate change, negatively affects urban water environment in terms of both water quantity and quality. Thus, urbanization consisting of replacing permeable areas with impermeable materials, prevents precipitation from infiltrating into native soils and leads to water quantity problems such as high peak flows and surface runoff volumes, and the loss of groundwater recharge. In addition, the increased surface runoff contains various pollutants and becomes a potential source of pollution of receiving water bodies (Chai et al., 2012; Davis et al., 2001; Pratt, 1995).

Types and concentrations of pollutants depend on land use. In urban areas, there are several mechanisms for deposition of pollutants, including the atmospheric deposition (wet and dry),

applications of chemicals (e.g., fertilizers and pesticides), and unintentional releases of pollutants during normal urban activities, like crankcase oil dripping from motor vehicles.

Several studies in the literature highlight that one of the main source of pollution of the residential areas is given by the traffic vehicles on the roads and one of the main pollutant site could be the car parks with different pollutants coming from the combustion processes of the motor vehicles or directly from the vehicles materials (Bedan and Clausen, 2009; Davis et al., 2001; Huber et al., 2016; Kumar et al., 2016; Sansalone et al., 2012, 2008; Zhang et al., 2011).

Several studies reported in the literature characterized urban runoff pollution; a dataset done by (Brombach et al., 2005) analyzed the main components of the urban runoff. In this study emerged that runoff pollutant are very diversified.

More negative effects of urbanization are:

- Urban Heat Island: parking lots and other paved surfaces tend to absorb solar energy more easily than natural lands and also release the solar energy very slowly. This phenomenon is called Urban Heat Island (UHI) and it could be represented as an urban area or metropolitan area that is significantly warmer than its surrounding rural areas.
- River habitat degradation: intensive artificial land use induced by urbanization is the main factor that impacted on the river habitat quality (Ding et al., 2015).

In this way, urban drainage traditional techniques, designed to collect stormwater in pipe and transport it away from urban areas in the shortest possible time, seem to be inadequate for the current expectations placed on urban drainage systems. In addition, traditional solutions used to reduce the impact of the impervious surfaces, such as storage tanks or ponds, require

a lot of space to store temporarily the captured runoff volume and often this space is not available in cities or other high urbanized areas.

1.2 Low Impact Development systems

Recently, to mitigate the negative effects of urbanization, Low Impact Development systems (LID), an innovative stormwater management approach, have gained popularity, despite the debate in the scientific community about their advantages against traditional drainage systems (Burns et al., 2012; Shuster and Rhea, 2013). LID systems consist of a series of facilities whose purpose is to reproduce the site predevelopment hydrological processes using design techniques that infiltrate, filter, store, evaporate, and detain runoff close to its source. These techniques usually do not require large capital investments, but rather a major commitment to maintenance. Because LID utilizes a variety of useful techniques for controlling runoff, designs can be customized according to local regulatory and resource protection requirements, as well as site constraints.

Among the most common LID techniques are:

- **Infiltration systems**: these systems are designed to catch a volume of the stormwater and then allow to infiltrate it into the native soils. The benefits of using this solution include both quantity (reduce peak flow and total volume) and water quality. In this category are permeable pavements (Figure 1.2), infiltration trenches (Figure 1.3).

Figure 1.2 Permeable pavement (www.marshalls.co.uk/watermanagement)

Figure 1.3 Infiltration trenches (www.marshalls.co.uk/watermanagement)

- **Stormwater wetlands:** these systems are designed for several reasons such as improving water quality, improving flood control, enhancing wildlife habitat, and providing education and recreation. Moreover, the types of pollutants targeted to be removed can influence the design. Wetlands in general, and stormwater wetlands in particular, use several mechanisms to remove pollutants. Stormwater wetlands

employ perhaps more ways to remove sediments, nutrients, metals and chemicals, and even bacteria (Li et al., 2014; Marchand et al., 2010; Qasaimeh et al., 2015; Yi et al., 2010) (Figure 1.4).

Figure 1.4 Stormwater wetland (www.archdaily.com)

- **Constructed Filters:** Constructed filters are structures or excavated areas containing a layer of sand, compost, organic material, peat, or other media that reduce pollutant levels in stormwater runoff by filtering sediments, metals, hydrocarbons, and other pollutants. Constructed filters are suitable for sites without sufficient surface area available for bioretention. The filter media may be comprised of materials such as sand, peat, compost or inorganic materials (Llorens et al., 2015; Vacca et al., 2005). Surface vegetation is another good option for pretreatment, as long as it is extensive enough to protect the filter from sediment during large storm events (Figure 1.5)

Figure 1.5 Constructed sand filter (www.storm-tex.com)

- **Vegetated systems:** Vegetated systems are designed to manage the stormwater both in quantitative and qualitative way. The most popular and fancy technique of this category is green roof (Figure 1.6). This system involves growing plants on rooftops, thus replacing the vegetated footprint that was removed when the building was constructed. Green roof covers are an "at source" measure for reducing the rate and volume of runoff released during rainfall events. The water retention and detention properties of vegetated roof covers can be enhanced through selection of the engineered media and plants. Depending on the plant material and planned usage for the roof area, modern vegetated roofs can be categorized as systems that are intensive, semi-intensive, or extensive (Vijayaraghavan, 2016).

  Vegetated swales (Figure 1.7) are structures resembling open channels or linear depressions with dense vegetation. They are typically used to convey, dissipate and treat surface runoff. Essentially, these swales are long open drainage channels, integrated within the surrounded landscape, affected by grass growth or other kind

of dense vegetation, resistant to drought during time. Widely used in residential and commercial areas, along curbsides alternatively to the classic drainage systems, they allow pollutant abatement through infiltration processes. In addition, they decrease overland flow rate, reducing peak flows and increasing time of concentration (Ainan et al., 2003; Mustaffa et al., 2016).

Figure 1.6 Green roof at University of Calabria (www.giare.eu)

Figure 1.7 Vegetated swale (www.uvm.edu)

Benefits of LIDs in terms of runoff reduction and pollutants removal have been widely discussed in the literature (Carbone et al., 2014a; Huang et al., 2016; Kamali et al., 2017). For example, Kamali et al., (2017) investigated the performance of a permeable pavement under sediment loadings during its life span by evaluating the temporal and spatial clogging trends of this facility and by finding its vulnerability to sediment loadings during rainfalls. Newcomer et al. (2014) demonstrated the benefits of LIDs, in particular of an infiltration trench, for recharge and local groundwater resources for future climate scenarios. In another study, Berardi et al. (2014) demonstrated how green roofs may contribute to the development of more sustainable buildings and cities. Furthermore, LID techniques also provide benefits by improving biodiversity and wildlife community structures, and reduce heat island effects (Bates et al., 2013; Karteris et al., 2016). Other numerous benefits in implementing LIDs are:

- Protects/restores the water quality of the water bodies.
- Protects stream channels.
- Reduces energy consumption.
- Improves air quality.
- Preserves ecological and biological systems.
- Maintains consistent dry weather flow (baselow) through groundwater recharge.
- Enhances carbon sequestration through preservation and planting of vegetation.
- Improves quality of life for residents.
- Increases energy and cost savings for heating, cooling, and irrigation.

Although each technique mentioned above exhibits very good performance in the stormwater management, in urban areas buildings represent 30-35% of impermeable surfaces, while

pavements occupy the remaining 65-70% and they are most pervasive in highly developed urban areas (Ferguson, 2005).

Therefore, to reverse the dynamics of the urbanization negative aspects, it could be helpful to propose solutions on pavement systems.

1.3 Permeable Pavement

Permeable pavement (PP) is an infiltration technique that combines stormwater infiltration, storage, and structural pavement consisting of a permeable surface underlain by a storage reservoir. Permeable pavement is well suited for parking lots, walking paths, sidewalks, playgrounds, plazas, tennis courts, and other similar uses.

This technique represents a good solution to solve stormwater management problems both in quantitative and qualitative terms. In general, PP systems are layered systems consisting of a wear layer, generally concrete, a filter layer, mainly constituted of coarse sand or fine gravel, a gravel aggregate base layer, and a crushed stones sub-base layer. The heterogeneity of the materials that compose PPs, and its strongly unsaturated hydraulic behaviour, pose significant modelling challenges. Considering the complexity of the physical processes involved, there is a need of modelling tools able to accurately interpret the hydraulic behaviour of PP. Although there are in the literature several stormwater models that can be used to analyze PP, most of them lack a comprehensive description of the hydrological processes involved, and often do not include any parameters optimization techniques, which are crucial to calibrate a model against experimental data. For these reasons, in recent years, scientific community has focused its attention to physically based models to describe hydraulic behaviour of permeable pavement and in general of LID.

In literature, most of the works related to permeable pavement are focused on the hydrological performance of PP both in qualitative and quantitative terms (Al-rubaei et al., 2013; Brown and Borst, 2015a, 2015b; Chandler and Wheater, 2002; Dreelin et al., 2006; Haselbach et al., 2014; Huang et al., 2016; Kamali et al., 2017; Kuang et al., 2011; Legret et al., 1996; Lin et al., 2016; Palla and Gnecco, 2015; Sansalone et al., 2012). Moreover, a correct characterization/identification of the parameters controlling the water regime and solute transport in construction materials is a crucial task (when using physically based models).

Despite the hydrological benefits of permeable pavements, these techniques are not yet widespread probably because modelling tools often used simplified methodologies, based on empirical and conceptual equations, which do not take into account hydrological processes in a physical way. In addition, the hydraulic properties of pavement materials have not been investigated in a comprehensive manner, limiting the investigation only to specific properties. For example, Chandrappa and Biligiri, (2016) investigated the permeability characteristics of porous concrete mixtures using falling head permeameter method. This study showed the relationship between material porosity and permeability in order to have a good design of the concrete mixture. In another work, Zhong et al., (2016) recognized the influence of pore tortuosity on hydraulic conductivity of pervious concrete. This study showed that several parameters influenced the prediction of hydraulic conductivity and this parameter was not solely affected by effective porosity. A limit of this study is that it is only focused on the concrete material and also it does not explore other hydraulic properties different than hydraulic conductivity. In another paper, Huang et al. (2016) proposed a numerical model for permeable pavements and also proved its applicability by applying it to simulate both hydraulics and water quality. The results of this study demonstrated a good

agreement between field measurements and modelled results for three types of pavement in terms of hydraulics and water quality variables including peak flow, time to peak, outflow volume and TSS removal rates.

Another problem in using these systems is the one related to maintenance. The susceptibility of a permeable pavement to clogging is a major disadvantage in permeable pavement applications (Tan et al., 2003). Clogging is defined as the processes of reducing porosity and hydraulic conductivity due to physical, biological and chemical processes (Bouwer, 2002). The main cause of this phenomenon is related to the deposition of sediments on the pavement surface. Although several studies has been conducted to evaluate clogging phenomena in permeable pavement systems (Coughlin et al., 2012; Deo et al., 2010; Kia et al., 2017; Lin et al., 2016; Lucke and Beecham, 2011; Pezzaniti et al., 2009; Sansalone et al., 2012; Winston et al., 2016; Yong et al., 2013), this phenomenon remains one of the major problems that requires attention in the use of such facilities.

1.4 Rationale, aims and objectives

To fill the identified research gap, this work will undertake an assessment of a permeable pavements with regards to the unsaturated hydraulic behaviour and water quality performance, provide the fundamental knowledge on the hydraulic properties of the pavement materials and even their absorption properties, and provide practical and robust modelling tools for assisting in the engineering design of permeable pavements.

Thus in this work, a technique/procedure was proposed for intercepting water flow through the structural system using HYDRUS programs, i.e. to suggest experimental and mathematical procedure for model calibration, which consists of: a) experimental design

(system construction, and number and character of measured transient flow data), b) methods for independent evaluation of soil hydraulic properties, c) additional optimization of soil hydraulic parameters using the transient flow data, and d) model validation.

In order to assess the quality performances of the PP, some absorption experiments, related to Zinc and Copper, were conducted to define absorption properties of the pavement materials, and the laboratory installation of the PP model was further tested for contaminant (Cu and Zn) removals for several simulated rainfall events mimicking contaminant influx.

Finally, to describe the unsaturated water flow within the system, the van Genuchten-Mualem model included in HYDRUS-2D software was used (van Genuchten, 1980). Thus, the work was organized as follows. First, following the experimental procedures proposed by (Kodešová et al., 2014), several analyses have been conducted on the wear and bedding material of the lab-scale porous system made of porous concrete blocks and fine gravel. Results of these analyses have been fundamental in order to obtain the Soil Water Retention Curve (SWRC) of the materials so as limit the next parameters optimization phase. The effect of remaining parameters has been investigated through a sensitivity analysis carried out using the Morris screening method. Therefore, a model calibration procedure using the parameter optimization procedure included in HYDRUS-2D that makes use of the Levenberg-Marquardt Optimization Algorithm, has been conducted. Finally, the calibrated model was validated on an independent set of measurements.

Therefore, the primary objectives of this dissertation include:

1. Investigating the hydraulic properties of the pavement construction materials by using some experimental investigation already used in the literature with soils.
2. Proposing procedure how to interpret water flow by using the HYDRUS model.

3. Developing robust experimental and mathematical procedures for model calibration and validation.
4. Investigating the absorption properties of the pavement materials related to Zinc and Copper heavy metals.
5. Evaluating the potential performances of the permeable pavement in removing dissolved zinc and copper from runoff.

1.5 Thesis outline

Following this chapter, Chapter 2 is dedicated to a general literature review of permeable pavements to present key findings and research gaps in the literature. Chapters 3 and 4 are the core of the research project. They present the methodology, the results and discussions of the water flow modelling and water quality performance of lab-scale porous pavements. A description of the experimental design and detailed methodologies are included in these chapters. Chapter 5 states general conclusions and summarizes the novel contributions of this research and recommendations for future studies.

Parts of the materials of these chapters have been submitted and accepted for publication in Journal of Hydrology.

1.6 References

Al-rubaei, A.M., Stenglein, A.L., Viklander, M., Blecken, G., 2013. Long-Term Hydraulic Performance of Porous Asphalt Pavements in Northern Sweden 499–505. doi:10.1061/(ASCE)IR.1943-4774.0000569.

A. Ainan, N.A. Zakaria, A. Ab. Ghani, R Abdullah, L.M. Sidek, M.F.Y., Wong, L.P., 2003. Peak Flow Attenuation Using Ecological Swale and Dry Pond. Water VI, 9

Bates, A.J., Sadler, J.P., Mackay, R., 2013. Vegetation development over four years on two green roofs in the UK. Urban For. Urban Green. 12, 98–108. doi:10.1016/j.ufug.2012.12.003

Bedan, E.S., Clausen, J.C., 2009. Stormwater Runoff Quality and Quantity From Traditional and Low Impact Development Watersheds(1). J. Am. Water Resour. Assoc. 45, 998–1008. doi:Doi 10.1111/J.1752-1688.2009.00342.X

Berardi, U., GhaffarianHoseini, A., GhaffarianHoseini, A., 2014. State-of-the-art analysis of the environmental benefits of green roofs. Appl. Energy 115, 411–428. doi:10.1016/j.apenergy.2013.10.047

Bouwer, H., 2002. Artificial recharge of groundwater: Hydrogeology and engineering. Hydrogeol. J. 10, 121–142. doi:10.1007/s10040-001-0182-4

Brombach, H., Weiss, G., Fuchs, S., 2005. A new database on urban runoff pollution: Comparison of separate and combined sewer systems. Water Sci. Technol. 51, 119–128.

Brown, R. a., Borst, M., 2015a. Nutrient infiltrate concentrations from three permeable

pavement types. J. Environ. Manage. 164, 74–85. doi:10.1016/j.jenvman.2015.08.038

Brown, R. a., Borst, M., 2015b. Quantifying evaporation in a permeable pavement system. Hydrol. Process. 29, 2100–2111. doi:10.1002/hyp.10359

Burns, M.J., Fletcher, T.D., Walsh, C.J., Ladson, A.R., Hatt, B.E., 2012. Hydrologic shortcomings of conventional urban stormwater management and opportunities for reform. Landsc. Urban Plan. 105, 230–240. doi:10.1016/j.landurbplan.2011.12.012

Carbone, M., Turco, M., Nigro, G., Piro, P., 2014. Modeling of hydraulic behaviour of green roof in catchment scale, in: 14th sgem geoconference on water resources. Forest, marine and ocean ecosystems. P. 471–478 pp. Doi:10.5593/sgem2014/b31/s12.061

Chai, L., Kayhanian, M., Givens, B., Harvey, J.T., Jones, D., 2012. Hydraulic Performance of Fully Permeable Highway Shoulder for Storm Water Runoff Management. J. Environ. Eng. 138, 711–722. doi:10.1061/(asce)ee.1943-7870.0000523

Chandler, R.E., Wheater, H.S., 2002. Analysis of rainfall variability using generalized linear models: A case study from the west of Ireland. Water Resour. Res. 38, 10-1-10–11. doi:10.1029/2001WR000906

Chandrappa, A.K., Biligiri, K.P., 2016. Comprehensive investigation of permeability characteristics of pervious concrete: A hydrodynamic approach. Constr. Build. Mater. 123, 627–637. doi:10.1016/j.conbuildmat.2016.07.035

Coughlin, J.P., Campbell, C.D., Mays, D.C., 2012. Infiltration and Clogging by Sand and Clay in a Pervious Concrete Pavement System. J. Hydrol. Eng. 17, 68–73. doi:10.1061/(ASCE)HE.1943-5584.0000424

Davis, A.P., Shokouhian, M., Ni, S., 2001. Loading estimates of lead, copper, cadmium, and zinc in urban runoff from specific sources. Chemosphere 44, 997–1009. doi:10.1016/S0045-6535(00)00561-0

Deo, O., Sumanasooriya, M., Neithalath, N., 2010. Permeability Reduction in Pervious Concretes due to Clogging: Experiments and Modeling. J. Mater. Civ. Eng. 22, 741–751. doi:10.1061/(ASCE)MT.1943-5533.0000079

Ding, Y., Shan, B., Zhao, Y., 2015. Assessment of river habitat quality in the Hai River Basin, northern China. Int. J. Environ. Res. Public Health 12, 11699–11717. doi:10.3390/ijerph120911699

Dreelin, E. a., Fowler, L., Ronald Carroll, C., 2006. A test of porous pavement effectiveness on clay soils during natural storm events. Water Res. 40, 799–805. doi:10.1016/j.watres.2005.12.002

Ferguson, B., 2005. Progress in porous pavements, in: Proceedings of the StormCon Conference.

Finkenbine, J.K., Atwater, J.W., Mavinic, D.S., 2000. Stream Health After Urbanization. J. Am. Water Resour. Assoc. 36, 1149–1160. doi:10.1111/j.1752-1688.2000.tb05717.x

Haselbach, L., Poor, C., Tilson, J., 2014. Dissolved zinc and copper retention from stormwater runoff in ordinary portland cement pervious concrete. Constr. Build. Mater. 53, 652–657. doi:10.1016/j.conbuildmat.2013.12.013

Huang, J., He, J., Valeo, C., Chu, A., 2016. Temporal evolution modeling of hydraulic and water quality performance of permeable pavements. J. Hydrol. 533, 15–27. doi:10.1016/j.jhydrol.2015.11.042

Huber, M., Welker, A., Helmreich, B., 2016. Critical review of heavy metal pollution of traffic area runoff: Occurrence, influencing factors, and partitioning. Sci. Total Environ. doi:10.1016/j.scitotenv.2015.09.033

Kamali, M., Delkash, M., Tajrishy, M., 2017. Evaluation of permeable pavement responses to urban surface runoff. J. Environ. Manage. 187, 43–53. doi:10.1016/j.jenvman.2016.11.027

Karteris, M., Theodoridou, I., Mallinis, G., Tsiros, E., Karteris, A., 2016. Towards a green sustainable strategy for Mediterranean cities: Assessing the benefits of large-scale green roofs implementation in Thessaloniki, Northern Greece, using environmental modelling, GIS and very high spatial resolution remote sensing data. Renew. Sustain. Energy Rev. 58, 510–525. doi:10.1016/j.rser.2015.11.098

Kia, A., Wong, H.S., Cheeseman, C.R., 2017. Clogging in permeable concrete: A review. J. Environ. Manage. doi:10.1016/j.jenvman.2017.02.018

Kodešová, R., Fér, M., Klement, A., Nikodem, A., Teplá, D., Neuberger, P., Bureš, P., 2014. Impact of various surface covers on water and thermal regime of Technosol. J. Hydrol. 519, 2272–2288. doi:10.1016/j.jhydrol.2014.10.035

Kuang, X., Sansalone, J., Ying, G., Ranieri, V., 2011. Pore-structure models of hydraulic conductivity for permeable pavement. J. Hydrol. 399, 148–157. doi:10.1016/j.jhydrol.2010.11.024

Kumar, K., Kozak, J., Hundal, L., Cox, A., Zhang, H., Granato, T., 2016. In-situ infiltration performance of different permeable pavements in a employee used parking lot - A four-year study. J. Environ. Manage. 167, 8–14. doi:10.1016/j.jenvman.2015.11.019

Legret, M., Colandini, V., Le Marc, C., 1996. Effects of a porous pavement with reservoir structure on the quality of runoff water and soil. Sci. Total Environ. 189–190, 335–340. doi:10.1016/0048-9697(96)05228-X

Llorens, M., Pérez-Marín, A.B., Sáez, J., Aguilar, M.I., Ortuño, J.F., Meseguer, V.F., Ruiz, J.A., 2015. Sewage treatment with a hybrid constructed soil filter, in: International Journal of Chemical Reactor Engineering. pp. 161–168. doi:10.1515/ijcre-2015-0008

Li, Y., Zhu, G., Ng, W.J., Tan, S.K., 2014. A review on removing pharmaceutical contaminants from wastewater by constructed wetlands: Design, performance and mechanism. Sci. Total Environ. doi:10.1016/j.scitotenv.2013.09.018

Lin, W., Park, D.G., Ryu, S.W., Lee, B.T., Cho, Y.H., 2016. Development of permeability test method for porous concrete block pavement materials considering clogging. Constr. Build. Mater. 118, 20–26. doi:10.1016/j.conbuildmat.2016.03.107

Lucke, T., Beecham, S., 2011. Field investigation of clogging in a permeable pavement system. Build. Res. Inf. 39, 603–615. doi:10.1080/09613218.2011.602182

Marchand, L., Mench, M., Jacob, D.L., Otte, M.L., 2010. Metal and metalloid removal in constructed wetlands, with emphasis on the importance of plants and standardized measurements: A review. Environ. Pollut. doi:10.1016/j.envpol.2010.08.018

Mustaffa, N., Ahmad, N.A., Razi, M.A.M., 2016. Hydraulic performance of grassed swale as stormwater quantity control. ARPN J. Eng. Appl. Sci. 11, 5439–5444

Newcomer, M.E., Gurdak, J.J., Sklar, L.S., Nanus, L., 2014. Urban recharge beneath low impact development and effects of climate variability and change. Water Resour. Res. 50, 1716–1734. doi:10.1002/2013WR014282

Palla, A., Gnecco, I., 2015. Hydrologic modeling of Low Impact Development systems at the urban catchment scale. J. Hydrol. 528, 361–368. doi:10.1016/j.jhydrol.2015.06.050

Pezzaniti, D., Beecham, S., Kandasamy, J., 2009. Influence of clogging on the effective life of permeable pavements. Proc. Inst. Civ. Eng. - Water Manag. 162, 211–220. doi:10.1680/wama.2009.00034

Pratt, C.J., 1995. A Review of Source Control of Urban Stormwater Runoff. J. Chart. Inst. Water Environ. Manag. 9, 132–139. doi:10.1111/j.1747-6593.1995.tb01602.x

Qasaimeh, A., Alsharie, H., Masoud, T., 2015. A Review on Constructed Wetlands Components and Heavy Metal Removal from Wastewater. J. Environ. Prot. (Irvine,. Calif). 6, 710–718. doi:10.4236/jep.2015.67064

Sansalone, J., Kuang, X., Ranieri, V., 2008. Permeable Pavement as a Hydraulic and Filtration Interface for Urban Drainage. J. Irrig. Drain. Eng. 134, 666–674. doi:10.1061/(ASCE)0733-9437(2008)134:5(666)

Sansalone, J., Kuang, X., Ying, G., Ranieri, V., 2012. Filtration and clogging of permeable pavement loaded by urban drainage. Water Res. 46, 6763–74. doi:10.1016/j.watres.2011.10.018

Shuster, W., Rhea, L., 2013. Catchment-scale hydrologic implications of parcel-level stormwater management (Ohio USA). J. Hydrol. 485, 177–187. doi:10.1016/j.jhydrol.2012.10.043

Tan, S.-A., Fwa, T.-F., Han, C.-T., 2003. Clogging Evaluation of Permeable Bases. J. Transp. Eng. 129, 309–315. doi:10.1061/(ASCE)0733-947X(2003)129:3(309)

Vacca, G., Wand, H., Nikolausz, M., Kuschk, P., Kästner, M., 2005. Effect of plants and filter materials on bacteria removal in pilot-scale constructed wetlands. Water Res. 39, 1361–1373. doi:10.1016/j.watres.2005.01.005

van Genuchten, M.T., 1980. A Closed-form Equation for Predicting the Hydraulic Conductivity of Unsaturated Soils1. Soil Sci. Soc. Am. J. 44, 892. doi:10.2136/sssaj1980.03615995004400050002x

Vijayaraghavan, K., 2016. Green roofs: A critical review on the role of components, benefits, limitations and trends. Renew. Sustain. Energy Rev. doi:10.1016/j.rser.2015.12.119

Winston, R.J., Al-Rubaei, A.M., Blecken, G.T., Viklander, M., Hunt, W.F., 2016. Maintenance measures for preservation and recovery of permeable pavement surface infiltration rate - The effects of street sweeping, vacuum cleaning, high pressure washing, and milling. J. Environ. Manage. 169. doi:10.1016/j.jenvman.2015.12.026

Yi, Q., Yu, J., Kim, Y., 2010. Removal patterns of particulate and dissolved forms of pollutants in a stormwater wetland. Water Sci. Technol. 61, 2083–2096. doi:10.2166/wst.2010.159

Yong, C.F., McCarthy, D.T., Deletic, a., 2013. Predicting physical clogging of porous and permeable pavements. J. Hydrol. 481, 48–55. doi:10.1016/j.jhydrol.2012.12.009

Zhang, W., Ye, Y., Tong, Y., Ou, L., Hu, D., Wang, X., 2011. Modeling time-dependent toxicity to aquatic organisms from pulsed exposure of PAHs in urban road runoff. Environ. Pollut. 159, 503–508. doi:10.1016/j.envpol.2010.10.008

Zhong, R., Xu, M., Vieira Netto, R., Wille, K., 2016. Influence of pore tortuosity on hydraulic

conductivity of pervious concrete: Characterization and modeling. Constr. Build. Mater. 125, 1158–1168. doi:10.1016/j.conbuildmat.2016.08.060

CHAPTER 2 REVIEW OF PERMEABLE PAVEMENT SYSTEMS

In this chapter, an overview of permeable pavement systems is given. Starting from the construction materials of these systems, a description of the hydrological and qualitative performance of the experiences present in the literature is given.

2.1 Overview of permeable pavement

Permeable pavement is one of the most popular LID, suitable for pedestrian and/or vehicular traffic, such as pathways, driveways, parking lots and access roads, used to manage stormwater with respect to both water quantity and quality (Scholz and Grabowiecki, 2007). It allows stormwater to infiltrate through the surface and into the underlying structural layers. Then stormwater is temporarily stored below the overlying surface before use, infiltration to the ground, or controlled discharge downstream.

The infiltration process through the pavement is related primarily to the surface material of the system: it can occur across the entire surface of the surface material (when the pavement is constructed with reinforced grass or gravel surfaces, porous concrete and porous asphalt) or within the void space through the surface (impermeable concrete blocks).

The main types of surfaces used as part of permeable pavement construction are:

- Permeable Interlocking Concrete Pavement (PICP): the most common surface is concrete block permeable paving, but other modular surfacing materials can also be used. The main potential uses of this type can include pedestrian areas, pathways, car parks, private driveways (Figure 2.1).

Figure 2.1 Car park constructed with PICP at Unical University

- Porous asphalt: this type can be used as an independent surface or to provide a stronger base to PICP. It also reduces traffic noise (when the pavement is trafficked by heavy vehicles). The main potential uses of this type can include pedestrian areas, car parks, private driveways, and lightly trafficked roads (Figure 2.2).

Figure 2.2 Car park constructed of Porous Asphalt (www.wolfpaving.com)

- Grass grid pavement: this solution is an eco-friendly type of pavement most suitable for lightly trafficked locations. Grass is usually reinforced with plastic or concrete grids. The main potential uses of this type can include leisure facilities car parks, private driveways, and office car parks (Figure 2.3).

Figure 2.3 Private driveways constructed of concrete grid pavement (www.icpi.org)

- Porous concrete: this type of surface can be used as an independent surface or to provide improved structural stability to the base of the PCIP permeable pavements where it is to be trafficked frequently by heavy vehicles. The main potential uses of this type can include car parks, and lightly trafficked roads (Figure 2.4).

Figure 2.4 Car park constructed of porous concrete (www.coloradohardscapes.com)

2.2 Construction materials

The first experiences in using PP date back early 1970's in the UK and in the USA.

Although there are no approved structural design methods for pervious pavements in Italy, there are a number of general principles that should be followed when permeable pavements are designed. In general, guidance given by several author in literature (Pratt at al., 2002) and specific guidance on material gradations (Burak, 2007) should be referenced for supporting detail on pervious pavement design methods and materials.

Similar to traditional pavement, PP can consist of a variety of structural components and configurations.

The main principle of a pavement design is that the constructed layers distribute the concentrated loads from wheels below the road. The wheels pressure is very high at wear layer, thus it is necessary to adopt high quality materials for this layer. Conversely, pressure decreases with depth and allows the use of weaker materials in the lower layers of the

pavement. For these reasons, the choice of constituent materials and their gradations are fundamental.

In this way, the materials used for permeable pavement construction should be graded to give the right balance in order to have a good structural performance and sufficient permeability and void space for water storage.

Generally, the main layers of a permeable pavement are a wear layer, a bedding layer, a base layer and a sub-base layer (Figure 2.5). The choice to have base and sub-base layer, as the choice of the type of wear materials, is due to the structural integrity of the pavement system and it is strictly related to its traffic load.

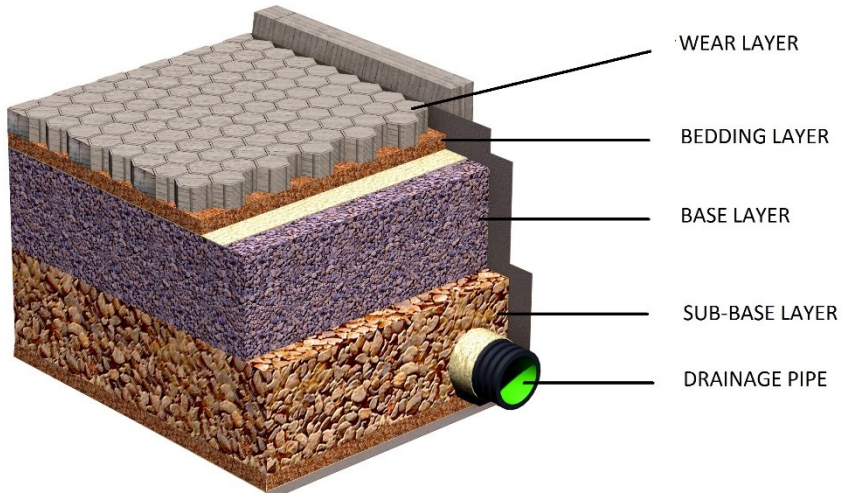

Figure 2.5 General structure of a permeable pavement (Piro et al., 2015)

As discussed earlier, the traffic category plays an important role in choosing the thickness of the various layers as well as the type of material to be used in the structure (especially for the wear layer).

In general, following Knapton et al. (2012) a permeable pavement is designed considering the traffic load as follows:

- For lightly trafficked pavements, the loads applied by wheels are the critical factor, and the guidance for those pavements is based upon wheel loads;
- For more heavily trafficked highway pavements, the pavements are designed on the basis of the cumulative number of standard 8000 kg axles.

A detailed description of the traffic categories is given in Table 2.1 (Kellagher et al., 2015).

Traffic category	Standard axles per day	Life time traffic (msa)	Number of commercial vehicles per day	Typical Application
10	≤4000	≤60	Site specific	Adopted highways and commercial/industrial developments used by a high number of commercial vehicles, Ports and airport landside, Bus stops and bus lanes
9	≤2000	≤30	Site Specific	
8	≤700	<10	420	
7	≤275	<2.5	170	
6	≤60	<0.5	35	Adopted highways and other roads used by a moderate number of commercial vehicles. Pedestrian areas subjected to regular overrun of commercial vehicles, Industrial premises, Petrol station forecourts
5	≤5	<0.05	3	Pedestrian areas subjected to occasional overrun of commercial vehicles and maintenance/cleaning machines Car parks receiving occasional commercial vehicular traffic
4	1	-	Mainly car or pedestrian traffic	Urban footways with no planned vehicular overrun

			with emergency HGV vehicles only	Pedestrian areas or car parks used by light commercial vehicles emergency vehicles and by maintenance vehicles
3	0	-	No HGV	Small car parks subject to car, light van and motorcycle access
2	0	-	No HGV	Pedestrian and cycle areas, domestic driveways
1	0	-	No HGV	Pedestrian-only areas, including domestic applications
0	0	-	No vehicular traffic	No requirement (decoration)

Table 2.1 Traffic loading categories (adapted from Kellagher et al., 2015)

One of the key factors to be taken into account in the design criteria of a permeable pavement is the bearing of the ground on which the pavement should be installed. To estimate this value, the most common index used in literature is the Californian Bearing Ratio (CBR) and its value varies inversely with moisture content (as the latter increases the CBR value decreases).

To design a permeable pavement, the equilibrium CBR value should be estimated. This value represents the long-term value that occurs once the pavement is constructed and the moisture content of the subgrade soil comes into equilibrium with the suction forces within subgrade pore air spaces. It can be determined by carrying out laboratory CBR tests at the equilibrium moisture content after saturation. The Interlocking Concrete Pavement Institute (ICPI) recommends a 96-hour saturation period.

In general, omitting the nature of the wear layer discussed in the previous section, the textures of the other constituent layers are recommended by the ICPI. ICPI recommends certain ASTM stone gradations for the subbase, base and bedding layers. The gradations for these

sizes are identified with numbers. These numbers and gradations are found in ASTM D 448, Standard Classification for Sizes of Aggregate for Road and Bridge Construction. ICPI recommends No. 2 stone for the subbase because it is very stable under construction equipment and it has a high-water storage capacity. Also recommended are stone No. 57 stone for the base layer and No. 8 stone for the bedding layer.

The No. 2 subbase thickness is typically 150– 450 mm, depending on the amount of water storage required, as well the amount of traffic and soil type. The water storage capacity of this layer is typically around 40% of the total base volume. The No. 57 thickness is typically around 200 mm; this material is used for the base and has a water storage capacity between 30% and 35%. The typical thickness of the No. 8 stone is around 50 mm. It functions as the bedding layer and jointing material. No. 8 stone has about 20% void space between its particles. All stone materials should be crushed for the highest interlock and stability during construction and load-spreading capacity during service. More details are available on the technical report of Burak (2007).

2.2.1 Grid pavement

In general, there are no design standard for the grid pavements, which consist of plastic or concrete grid filled with grass or gravel. However, the surfacing provides very little contribution to the load-bearing capacity of the pavement structure and therefore the sub-base thicknesses used for asphalt can be applied to these types of surface. A capping layer or increased thickness of coarse-graded aggregate may be required where the CBR values are less than 5%. This type of surface could be used up the traffic category No. 4. Typical

construction thickness for grid pavement with the subgrade of 5% CBR or greater are given in Table 2.2.

Traffic category	Grid	Bedding layer (mm)	Sub-base layer (mm)
4	Varies	50	300
3	Varies	50	225
2	Varies	50	150
1	Varies	50	100
0	Varies	50	Sufficient to provide suitable construction base

Table 2.2 Construction thickness for grid pavement (adapted from Kellagher et al., 2015)

2.2.2 Porous asphalt

Porous asphalt can be designed using analytical pavement design procedures with appropriate values of resilient modulus for the materials specified in the pavement. For pavements over lower CBR values that are trafficked by vehicles, the following precautions should be taken:

- 1% CBR, subgrade improvement required;
- 2% CBR, subgrade improvement layer required (may be incorporated into capping layer to provide a total layer thickness of 350 mm);
- 2.5% CBR, a 300 mm capping layer is recommended;
- 3% CBR, a 225 mm capping layer is recommended;
- 4% CBR, a 150 mm capping layer is recommended;

Typical construction thickness for Porous Asphalt (PA) pavement with the subgrade of 5% CBR or greater are given in Table 2.3.

Traffic category	Porous asphalt (mm)	Base layer (mm)	Sub-base layer (mm)
10	Asphalt requires specialist consideration and specification	Site specific	150
9	Asphalt requires specialist consideration and specification	Site specific	150
8	Site Specific	300	150
7	Site Specific	200	150
6	180 80	- 125	150 150
5	160 80	- 100	150 150
4	150	-	300
3	120	-	225
2	70	-	150
1	70	-	100
0	70	-	Sufficient to provide suitable construction base

Table 2.3 Construction thickness for PA pavement (adapted from Kellagher et al., 2015)

2.2.3 Porous concrete

Porous concrete is a near-zero-slump, open-graded material consisting of portland cement, coarse aggregate, admixtures and water. It has little or no fine aggregate. The combination of these ingredients will produce a hardened material with connected pores, 2–8 mm in size,

which should allow water to pass through easily. The porosity can be 15–35%, with typical compressive strengths of (2.8–28 MPa).

Typical construction thickness of Porous Concrete (PC) pavement with the subgrade of 5% CBR or greater are given in Table 2.4.

Traffic category	Porous concrete (mm)	Sub-base layer (mm)
10	Site specific	Site specific
9	Site specific	Site specific
8	Site specific	Site specific
7	Site specific	Site specific
6	Site specific	Site specific
5	150	300
4	135	300
3	125	225
2	125	150
1	100	100
0	100	Sufficient to provide suitable construction base

Table 2.4 Construction thickness for PC pavement (adapted from Kellagher et al., 2015)

2.2.4 Permeable interlocking concrete blocks

This type of surface material is one of the most widespread materials used in permeable pavement systems. It can be used for a wide range of traffic conditions from light to very

heavy-duty pavements. The structural design of the pavement using this layer is described in Table 2.5.

Traffic category	Concrete blocks (mm)	Bedding layer (mm)	Base layer (mm)	Sub-base layer (mm)
8	80	50	300	150
7	80	50	200	150
6	80	50	125	150
5	80	50	100	150
4	80	50	-	300
3	60	50	-	225
2	60	50	-	150
1	60	50	-	100
0	60	50	-	Sufficient to provide suitable construction base

Table 2.5 Construction thickness for PICP pavement (adapted from Kellagher et al., 2015)

It is important to highlight the difference between porous and permeable types of blocks. The first type allows water percolation through the paving block, as it is porous, while in the second type, which is not porous, the water infiltration occurs between the blocks using specially designed cuts.

2.3 Maintenance

Maintenance may represent the main restriction on using permeable pavement systems. PP need regular inspection and maintenance and these operations should be placed with an appropriate responsible organisation. Before handing over the pavement, it should be inspected for clogging, litter, weeds and water ponding, and all failures should be rectified. Several tests should be performed in order to assess the structural integrity of the pavement, the bearing capacity and the infiltration capacity. After handover, the pavement should be inspected regularly, preferably during and after heavy rainfall to check effective operation and to identify any areas of ponding.

Permeable pavements need to be regularly cleaned of solids and other sediments to preserve their infiltration capacity.

Experiences in their management suggest that sweeping PP once per year should be sufficient to maintain a good infiltration rate.

Anyway, more or less sweeping may be required and the frequency of these operations should be quantified specifically for individual sites. A management plan of permeable pavement is recommended and it should be implemented by the management authority of these systems. The type of cleaning is strictly related to the function for which the pavement is intended. In general, a brush and suction cleaner is used for regular sweeping. Care should be taken in adjusting vacuuming equipment to avoid removal of jointing material. Any lost material should be replaced. It is also possible to clean the surface using lightweight rotating brush cleaners combined with power spraying using hot water. An addition chemical cleaning should be performed if the pavement suffered by inorganic pollutant load such as heavy metals, hydrocarbons, nutrients.

2.4 Hydrology and hydraulics

The main operating principle of a PP is to collect, infiltrate (and eventually treat) the surface runoff of stormwater. This can support groundwater recharge (where infiltration into native soils is permitted) or direct treated runoff to open water streams. In comparison to traditional drainage systems, this solution is a sustainable and cost effective process, which is suitable for urban areas (Dierkes et al., 2002).

Several studies in literature have shown that evaporation, drainage and retention within the permeable structures were mainly influenced by the particle size distribution of the bedding material, and by the retention of water in the surface blocks (Alsubih et al., 2017; Andersen et al., 1999; Marchioni and Becciu, 2015). In addition, a considerable number of studies have been conducted on its water quantity performance that shown the capability of PP of reducing surface runoff, attenuating peak discharges and delaying time to peak (Al-rubaei et al., 2013; Brown and Borst, 2015a, 2015b; Chandler and Wheater, 2002; Dreelin et al., 2006; Haselbach et al., 2014; Huang et al., 2016; Kamali et al., 2017; Kuang et al., 2011; Legret et al., 1996; Lin et al., 2016; Palla and Gnecco, 2015; Sansalone et al., 2012).

2.5 Water quality performance

Urban runoff, as discussed in Davis et al., (2001), has been known as a primary pollutant source and significantly contributes to the degradation of waterbodies by washing off pollutants from impervious surfaces and transporting them to the receiving waterbodies.

The main pollutants in urban runoff pollutants include Total Suspended Solids (TSS) Nutrient such as Phosphorus and Nitrogen, heavy metals such as Zinc, Copper, Lead and

various Hydrocarbons (Benjamin O Brattebo and Booth, 2003; Davis et al., 2001; Finkenbine et al., 2000; Haselbach et al., 2014; Pratt, 1995). The sources of contaminants in Urban runoff are presented in Table 2.6.

Contaminant	Sources
Sediment and Floatables	Streets, lawns, driveways, roads, construction activities, atmospheric deposition, drainage channel erosion
Pesticides and Herbicides	Residential lawns and gardens, roadsides, utility right-of-ways, commercial and industrial landscaped areas, soil wash-off
Organic Materials	Residential lawns and gardens, commercial landscaping, animal wastes
Metals	Automobiles, bridges, atmospheric deposition, industrial areas, soil erosion, corroding metal surfaces, combustion processes
Oil and Grease/ Hydrocarbons	Roads, driveways, parking lots, vehicle maintenance areas, gas stations, illicit dumping to storm drains
Bacteria and Viruses	Lawns, roads, leaky sanitary sewer lines, sanitary sewer cross-connections, animal waste, septic systems
Nutrients	Lawn fertilizers, atmospheric deposition, automobile exhaust, soil erosion, animal waste, detergents

Table 2.6 Sources of contaminants in urban runoff

In recent years due to rapid urban expansion and deteriorated stormwater quality, scientific community has focused its attention on stormwater quality. In this way, recent studies on permeable pavements have been focusing on their ability of removing pollutants. The results indicate that the permeable pavement is capable of removing pollutants through the mechanisms of sedimentation, filtration and chemical absorption.

One of the main pollutants in urban runoff are Total Suspended Solids (TSS). Their sources vary, but in general, TSS originate from urban traffic, natural areas or decomposition of car components. This type of pollutant increases water turbidity, inhibits plant growth, affects river biota, and reduces the number of aquatic species. In addition, this pollutant acts as a vector of other contaminants due to attachment-detachment phenomenon between particles. Several studies shown the potential of PP structures to remove TSS (Brattebo and Booth, 2003; Carbone et al., 2014; Huang et al., 2016; Kamali et al., 2017; Sansalone et al., 2008). In this way, Particle Size Distribution (PDSD) in the effluent from permeable pavements generally has a finer gradation than influent due to filtration mechanisms. The gap to be filled in the TSS treatment remains clogging. The fine particles generally clog the surface layer (pore structure) and the bedding layer, thus reducing the lifespan of these structures. Frequent cleaning and maintenance with methods described in the previous sections are recommended.

Nitrogen and Phosphorus are the principal nutrients in urban stormwater runoff. The major sources of nutrients in urban runoff are urban landscape runoff (fertilizers, detergents, plant debris), atmospheric deposition, and improperly functioning septic systems. Animal waste can also be an important source. There are a number of parameters used to measure the various forms of nitrogen and phosphorus found in runoff. Ammonia (NH_3) nitrogen is the nitrogen form that is usually the most readily toxic to aquatic life. Nitrate (NO_3) and nitrite (NO_2) are the inorganic fractions of Nitrogen. These nutrients could cause eutrophication in

the receiving waters receiving urban drainage effluents and contribute to harmful algal blooms.

Several studies shown the potential of PP to remove TP and TN from urban runoff (Beecham et al., 2012; Brown and Borst, 2015a; Tota-Maharaj and Scholz, 2010). The treatment mechanisms are physical filtration and chemical sorption.

Heavy metals are often one of the primary source of pollutant in urban runoff. The primary sources of metals in urban storm water are industry and automobiles. Typical heavy metals found in storm runoff are Copper (Cu), Lead (Pb) and Zinc (Zn), which come from different sources including vehicular component wear, fluid leakage, engine exhaust, and roadway abrasion and degradation.

Atmospheric deposition (both wet and dry) can also make a substantial contribution as a source of heavy metals in urban runoff. These pollutants have the potential to impact water supply and cause acute or chronic toxic impacts on aquatic life.

Several studies have shown the potential of PP to remove heavy metals from urban runoff (Abustan et al., 2012; Dierkes et al., 2002; Drake et al., 2013; Legret et al., 1996; Sansalone et al., 2008, 1996; Scholz and Grabowiecki, 2007; Sounthararajah et al., 2017)

The removal efficiency could depend on various factors such as the pavement setups, the experimental conditions (materials) or climate conditions. The treatment mechanisms are physical filtration and chemical sorption.

Another pollutant usually found in urban runoff are hydrocarbons. They include oil and grease, the “BTEX” compounds such as benzene, toluene, ethyl benzene, and xylene and other polynuclear aromatic hydrocarbons (PAHs).

Sources of these pollutants include parking lots and roadways, leaking storage tanks, auto emissions, and improper disposal of waste oil. Petroleum hydrocarbons are known for their

acute toxicity at low concentrations. Hydrocarbons can endanger soil and groundwater, if they are not removed sufficiently during infiltration through the surface layer. Permeable pavements can operate as efficient hydrocarbon traps. Several studies shown the potential of PP to remove this type of pollutant (Coupe et al., 2003; Drake et al., 2013; Newmann et al., 2004,2002).

2.6 References

Abustan, I., Hamzah, M.O., Rashid, M.A., 2012. Review of permeable pavement systems in Malaysia conditions. OIDA Int. J. Sustain. Dev. 4, 27–36.

Al-rubaei, A.M., Stenglein, A.L., Viklander, M., Blecken, G., 2013. Long-Term Hydraulic Performance of Porous Asphalt Pavements in Northern Sweden 499–505. doi:10.1061/(ASCE)IR.1943-4774.0000569.

Alsubih, M., Arthur, S., Wright, G., Allen, D., 2017. Experimental study on the hydrological performance of a permeable pavement. Urban Water J. 14, 427–434. doi:10.1080/1573062X.2016.1176221

Andersen, C.T., Foster, I.D.L., Pratt, C.J., 1999. The role of urban surfaces (permeable pavements) in regulating drainage and evaporation : development of a laboratory simulation experiment. Hydrol. Process. 609, 597–609. doi:10.1002/(SICI)1099-1085(199903)13:4<597::AID-HYP756>3.3.CO;2-H

Beecham, S., Pezzaniti, D., Kandasamy, J., 2012. Stormwater treatment using permeable pavements. Proc. ICE - Water Manag. 165, 161–170. doi:10.1680/wama.2012.165.3.161

Brattebo, B.O., Booth, D.B., 2003. Long-term stormwater quantity and quality performance of permeable pavement systems. Water Res. 37, 4369–76. doi:10.1016/S0043-1354(03)00410-X

Brattebo, B.O., Booth, D.B., 2003. Long-term stormwater quantity and quality performance of permeable pavement systems. Water Res. 37, 4369–4376. doi:10.1016/S0043-1354(03)00410-X

Brown, R. a., Borst, M., 2015a. Nutrient infiltrate concentrations from three permeable pavement types. J. Environ. Manage. 164, 74–85. doi:10.1016/j.jenvman.2015.08.038

Brown, R. a., Borst, M., 2015b. Quantifying evaporation in a permeable pavement system. Hydrol. Process. 29, 2100–2111. doi:10.1002/hyp.10359

Burak, R., n.d. Contractor Focus Construction of Bases for Permeable Interlocking Concrete Pavements – Part I.

Carbone, M., Mancuso, A., Piro, P., 2014. Porous pavement quality modelling, in: Procedia Engineering. pp. 758–766. doi:10.1016/j.proeng.2014.11.504

Chandler, R.E., Wheater, H.S., 2002. Analysis of rainfall variability using generalized linear models: A case study from the west of Ireland. Water Resour. Res. 38, 10-1-10–11. doi:10.1029/2001WR000906

Coupe, S.J., Smith, H.G., Newman, A.P., Puehmeier, T., 2003. Biodegradation and microbial diversity within permeable pavements. Eur. J. Protistol. 39, 495–498. doi:10.1078/0932-4739-00027

Davis, A.P., Shokouhian, M., Ni, S., 2001. Loading estimates of lead, copper, cadmium, and zinc in urban runoff from specific sources. Chemosphere 44, 997–1009. doi:10.1016/S0045-6535(00)00561-0

Dierkes, C., Kuhlmann, L., Kandasamy, J., Angelis, G., 2002. Pollution retention capability and maintenance of permeable pavements, in: Global Solutions for Urban Drainage. pp. 1–13. doi:10.1061/40644(2002)40

Drake, J.A.P., Bradford, A., Marsalek, J., 2013. Review of environmental performance of permeable pavement systems: State of the knowledge. Water Qual. Res. J. Canada 48, 203–222. doi:10.2166/wqrjc.2013.055

Dreelin, E. a., Fowler, L., Ronald Carroll, C., 2006. A test of porous pavement effectiveness on clay soils during natural storm events. Water Res. 40, 799–805. doi:10.1016/j.watres.2005.12.002

Finkenbine, J.K., Atwater, J.W., Mavinic, D.S., 2000. Stream Health After Urbanization. J. Am. Water Resour. Assoc. 36, 1149–1160. doi:10.1111/j.1752-1688.2000.tb05717.x

Haselbach, L., Poor, C., Tilson, J., 2014. Dissolved zinc and copper retention from stormwater runoff in ordinary portland cement pervious concrete. Constr. Build. Mater. 53, 652–657. doi:10.1016/j.conbuildmat.2013.12.013

Huang, J., He, J., Valeo, C., Chu, A., 2016. Temporal evolution modeling of hydraulic and water quality performance of permeable pavements. J. Hydrol. 533, 15–27. doi:10.1016/j.jhydrol.2015.11.042

Kamali, M., Delkash, M., Tajrishy, M., 2017. Evaluation of permeable pavement responses to urban surface runoff. J. Environ. Manage. 187, 43–53. doi:10.1016/j.jenvman.2016.11.027

Kellagher, R., Martin, P., Jefferies, C., Bray, R., Shaffer, P., Wallingford, H.R., Woods-Ballard, B., Woods Ballard, B., Construction Industry Research and Information Association, Great Britain, Department of Trade and Industry, Environment Agency, 2015. The SUDS manual, Ciria, …. doi:London C697

Knapton, J., Morrell, D., Simeunovich, M., 2012. Structural Design Solutions for Permeable Pavements, in: 10th International Conference on Concrete Block Paving.

Kuang, X., Sansalone, J., Ying, G., Ranieri, V., 2011. Pore-structure models of hydraulic conductivity for permeable pavement. J. Hydrol. 399, 148–157. doi:10.1016/j.jhydrol.2010.11.024

Legret, M., Colandini, V., Le Marc, C., 1996. Effects of a porous pavement with reservoir structure on the quality of runoff water and soil. Sci. Total Environ. 189–190, 335–340. doi:10.1016/0048-9697(96)05228-X

Lin, W., Park, D.G., Ryu, S.W., Lee, B.T., Cho, Y.H., 2016. Development of permeability test method for porous concrete block pavement materials considering clogging. Constr. Build. Mater. 118, 20–26. doi:10.1016/j.conbuildmat.2016.03.107

Marchioni, M., Becciu, G., 2015. Experimental results on permeable pavements in urban areas: A synthetic review. Int. J. Sustain. Dev. Plan. doi:10.2495/SDP-V10-N6-806-817

Newman, A.P., Pratt, C.J., Coupe, S.J., Cresswell, N., 2002. Oil bio-degradation in permeable pavements by microbial communities, in: Water Science and Technology. pp. 51–56.

Newman, A.P., Puehmeier, T., Kwok, V., Lam, M., Coupe, S.J., Shuttleworth, A., Pratt, C.J., 2004. Protecting Groundwater with Oil-Retaining Pervious Pavements: Historical Perspectives, Limitations and Recent Developments. Q. J. Eng. Geol. Hydrogeol. 37, 283–291. doi:10.1144/1470-9236/04-011

Palla, A., Gnecco, I., 2015. Hydrologic modeling of Low Impact Development systems at the urban catchment scale. J. Hydrol. 528, 361–368. doi:10.1016/j.jhydrol.2015.06.050

Piro, P., 2015. Interventi Sostenibili nell'Idraulica Urbana. Edibios 2015; ISBN 978-88-97181-38-5.

Pratt, C., Wilson, S., Cooper, P., 2002. C582 Source control using constructed pervious surfaces - Hydraulic, structural and water quality performance issues, CIRIA C582.

Pratt, C.J., 1995. A Review of Source Control of Urban Stormwater Runoff. J. Chart. Inst. Water Environ. Manag. 9, 132–139. doi:10.1111/j.1747-6593.1995.tb01602.x

Sansalone, J., Kuang, X., Ranieri, V., 2008. Permeable Pavement as a Hydraulic and Filtration Interface for Urban Drainage. J. Irrig. Drain. Eng. 134, 666–674. doi:10.1061/(ASCE)0733-9437(2008)134:5(666)

Sansalone, J., Kuang, X., Ying, G., Ranieri, V., 2012. Filtration and clogging of permeable pavement loaded by urban drainage. Water Res. 46, 6763–74. doi:10.1016/j.watres.2011.10.018

Sansalone, J.J., Buchberger, S.G., Al-Abed, S.R., 1996. Fractionation of heavy metals in pavement runoff, in: Science of the Total Environment. pp. 371–378. doi:10.1016/0048-9697(96)05233-3

Scholz, M., Grabowiecki, P., 2007. Review of permeable pavement systems. Build. Environ. 42, 3830–3836. doi:10.1016/j.buildenv.2006.11.016

Sounthararajah, D.P., Loganathan, P., Kandasamy, J., Vigneswaran, S., 2017. Removing heavy metals using permeable pavement system with a titanate nano-fibrous adsorbent column as a post treatment. Chemosphere 168, 467–473. doi:10.1016/j.chemosphere.2016.11.045

Tota-Maharaj, K., Scholz, M., 2010. Efficiency of permeable pavement systems for the removal of urban runoff pollutants under varying environmental conditions. Environ. Prog. Sustain. Energy 29, 358–369. doi:10.1002/ep.10418

CHAPTER 3 MATERIALS AND METHODS

This chapter presents the methodology used to study the hydraulic behaviour and the water quality performance of the permeable pavement system tested, starting from the theory and governing equations of the phenomena studied.

3.1 The Lab-scale permeable pavement system

In order to study the behaviour of a permeable pavement, a lab-scale test bed was constructed. It consisted of a Plexiglas container (dimensions of the bottom 59 x 59 cm, height of 41 cm) with a circular outlet in the centre of the bottom (diameter of 10 cm) and layers of construction materials (Figure 3.1) for a total thickness of 41 cm. The main principle of a pavement design is that the constructed layers distribute the concentrated loads from wheels below the road. The wheels pressure is very high at the wear layer, thus it is necessary to adopt high quality materials for this layer. Conversely, pressure decreases with depth and allows the use of weaker materials in the lower layers of the pavement. For these reasons, the choice of constituent materials and their gradations are fundamental. Generally, the main layers of a permeable pavement are a wear layer, a bedding layer, a base layer and a sub-base layer. The layer types and their construction thickness for the lab-scale porous modular pavement were chosen according to the CIRIA report (Kellagher et al., 2015), considering a traffic category of 3 (small car parks subject to cars, light vans and motorcycle access) and a California Bearing Ratio index (CBR) of 5% or greater. The wear layer consists of porous concrete blocks characterized by high permeability. Sub-base and bedding layers were constructed following the suggestions of the Interlocking Concrete Pavement Institute (ICPI), which recommends some ASTM stone gradations. The gradations for these sizes are

identified with numbers. These numbers and gradations are found in ASTM D 448, Standard Classification for Sizes of Aggregate for Road and Bridge Construction. ICPI recommends No. 2 stone for the sub-base layer because it is very stable under construction equipment and has a high water storage capacity with a porosity of about 40%. The ASTM No. 8 is used for the bedding layer and has a porosity of about 20% of volume. The bedding layer consists of a mixture of fine gravel and glass sand to improve the pollutant removal efficiency for typical contaminants of stormwater runoff. At the interface between the bedding layer and the sub-base layer, a high permeability geotextile with a fiber area weight of 60 g m^{-2} is placed in order to prevent migrating of fine material into the bottom layer.

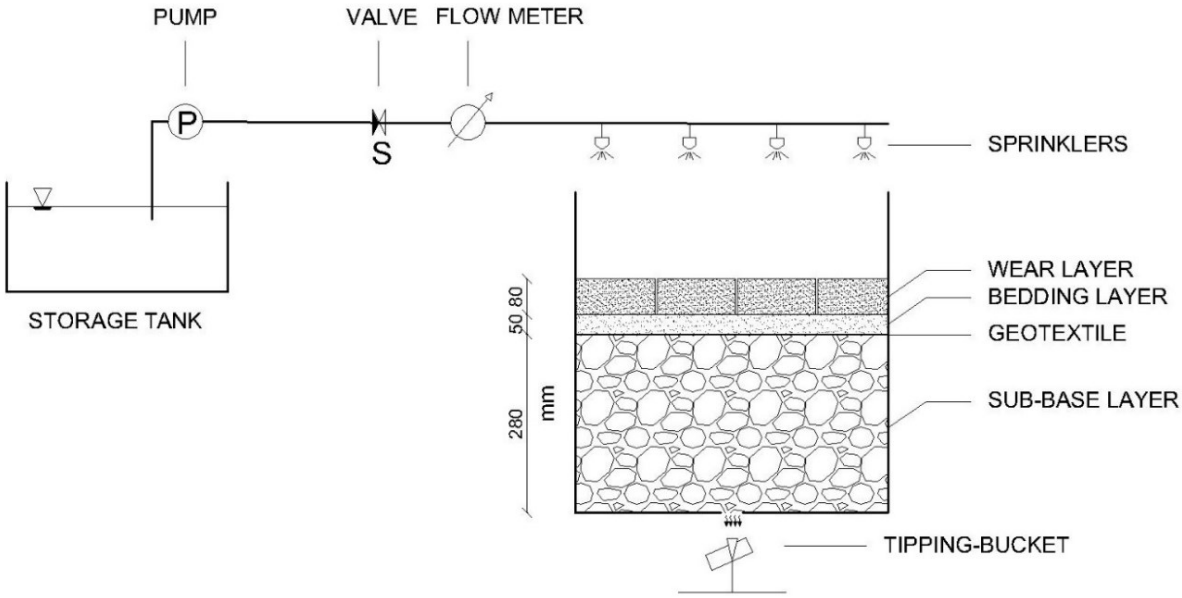

Figure 3.1 A schematic of the lab-scale permeable pavement system

Further details on the mixture and construction of the Interlocking Concrete Pavements materials can be found in the technical paper of Burak (2007). In order to study the water regime in this system several rainfall events were simulated using 12 sprinklers (Figure 3.1). Water was pumped from a storage tank by a pump into the sprinklers. Rainfall intensity was

regulated by a valve and the actual rainfall intensity was measured by a flow meter. Preferential flows along the test box side walls were prevented by sealing them. In urban areas, rains that deserve special attention are those of short duration such as subhourly. In this way, critical rainfall events occur in a very short time (Carbone et al., 2015). Given that, 10 irrigation events were simulated (Table 1). The Impervious/Pervious ratio reported in Table 3.1 represents the ratio of impervious run-on area to permeable pavement. It must be emphasized that the rainfall simulator was not able to reproduce variable precipitation patterns. Thus, a constant precipitation has been simulated in the laboratory.

Rainfall events [-]	Duration [min]	Rainfall Intensity [mm/h]	Volume [l]	Impervious/Pervious
Day 1	30	73.00	12.30	<5:1
Day 2	30	64.00	10.70	<5:1
Day 3	30	66.00	11.10	<5:1
Day 4	15	85.60	7.20	<5:1
Day 5	15	95.10	8.00	<5:1
Day 6	15	71.90	6.05	<5:1
Day 7	30	69.60	11.70	<5:1
Day 8	30	69.00	11.60	<5:1
Day 9	30	69.30	11.65	<5:1
Day 10	15	77.30	6.50	<5:1

Table 3.1 Characteristic of the rainfall events simulated during the experimental campaign

The system response was assessed by measuring water contents and fluxes from the container outlet. An FDR probe SM100 WATERSCOUT was used to measure the volumetric water

content in the middle of the bedding layer. The probe was calibrated on the sample of this material following the calibration procedure published by Kodešová et al. (2011). Experiments were performed under 20°C laboratory conditions.

A linear calibration equation was obtained by fitting the experimental data points (relating sensor readings in volts and water contents evaluated gravimetrically) with a coefficient of determination R^2= 0.904.

The outflow from the bottom outlet was measured by a pre-calibrated tipping-bucket flow meter. According to Molini et al. (2005), records from tipping-bucket were post-processed by using an analytic equation $I_a = \alpha I_r \beta$ (where I_a and I_r represent the actual and the recorded rainfall intensity while α and β are calibration parameters) in order to correct the errors caused by water losses. Measured inflow (i.e. applied rainfall), outflow and volumetric water content were logged online by a Personal Computer installed near the test-bed.

3.2 Modelling of permeable pavement systems

Modelling of permeable pavement is a relatively new topic along with the widespread application of permeable pavement. The purpose of modelling is to simulate the hydraulic and water quality performance of a permeable pavement structure in order to provide useful information to improve current design. In spite of many well-known benefits of these structures, the transition to sustainable urban drainage systems is very slow. One of the key limiting factors in the widespread adoption of such systems is the lack of adequate analytical and modelling tools (Elliott and Trowsdale, 2007).

Although several stormwater models can be applied to the PP analysis, most of them do not incorporate accurate descriptions of hydrological processes involved, which leads to

inaccurate predictions. Moreover, existing tools do not incorporate automatic parameter optimization techniques and sensitivity analysis routines, which have proven to be fundamental when the model includes multiple parameters (Brunetti et al., 2016b). In recent years, researchers have focused their attention on applying and developing physically based models for the PP analysis and in this work the same approach was developed.

3.2.1 Introduction to water flow in porous media

Water flow in the vadose zone is generally described by the combination of the continuity equation (3.1) and the Darcy-Buckingham law (3.2).

$$\frac{\partial \theta}{\partial t} = \frac{\partial q_i}{\partial z_i} \tag{3.1}$$

$$q = -K(\theta)\frac{\partial h}{\partial z} \tag{3.2}$$

where θ is the volumetric water content [L^3L^{-3}], t is the time [T], q is the volumetric flux density [$L\ T^{-1}$], h is the soil water matric head [L], K is the hydraulic conductivity [$L\ T^{-1}$] and z is the vertical axis [L].

The previous combination is generally reported in literature as the Richards equation (3.3), formulated by Lorenzo A. Richards in 1931 (Richards, 1931).

$$\frac{\partial \theta}{\partial t} = \frac{\partial}{\partial z}\left[K(\theta)\frac{\partial h}{\partial z} - 1\right] \tag{3.3}$$

It is a nonlinear partial differential equation, which is often difficult to approximate since it does not have a closed-form analytical solution. Moreover, it might be solved analytically

only for limited boundary conditions. If relationships between θ-h-K are known, numerical solutions may solve the equation for various boundary conditions.

3.2.2 Soil properties

Soil is a three-phase system and it consists of a solid, liquid and gaseous phase which are distributed spatially. The main forces which are responsible for holding water in a soil are capillary and adsorptive forces. Water flow through porous media heavily depends on the soil matrix. In this way, several porous media characteristics are listed.

Porosity of a soil [L^3 L^{-3}] might be expressed as:

$$\varepsilon = 1 - \frac{\rho_b}{\rho_s} \tag{3.4}$$

where ρ_b is a bulk density of the soil and ρ_s is soil particle density.

Soil water content [L^3 L^{-3}] may be defined as:

$$\theta = \frac{V_w}{V_t} \tag{3.5}$$

where V_w represents the volume of water [L^3], Vt is the volume of the solid fraction [L^3].

Soil water content can be also expressed by the degree of saturation S [−] as follows:

$$S = \frac{\theta}{\varepsilon} \tag{3.6}$$

The volumetric water content varies between 0 (totally dry soil) to the saturated water content θ_s, which is supposed to be equal to the porosity if the soil were completely saturated. The degree of saturation ranges between one (soil completely filled with water) to zero (completely dry soil). By replacing porosity by θs and subtracting residual water content θ_r effective saturation S_e has been obtained:

$$S_e = \frac{\theta - \theta_r}{\theta_S - \theta_r} \tag{3.7}$$

3.2.3 Soil Water Retention Curve

Modelling of water flow in unsaturated soils by means of the Richards equation requires the knowledge of the water retention function $\theta(h)$ and the hydraulic conductivity function. In general, water retention functions describe the soil ability to retain or release water (Figure 3.1) , and differ for individual soils.

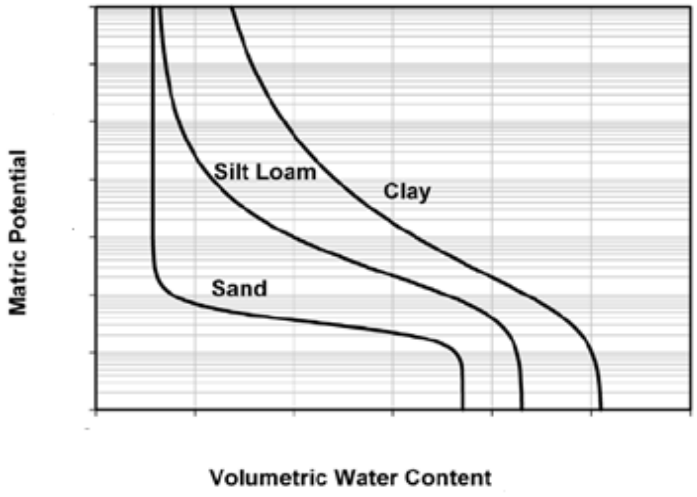

Figure 3.2 Water retention curves for soils of different texture

Soil Water Retention Curve (SWRC) is an important hydraulic property related to size and connectedness of pore spaces, hence it is strongly affected by soil texture and structure (i.e. the aggregation of solid particles in soil) and by other constituents including organic matter. Typically, a SWRC is highly nonlinear and is relatively difficult to obtain accurately. Several methods are available in the literature to obtain the measurements required for SWRC estimation. Among the primary experimental problems in determining a SWRC are:

- the limited functional range of the tensiometers, which are often used for in-situ measurements;
- inaccurate or imprecise θ field measurements;
- the difficulty in obtaining undisturbed samples for laboratory determinations;
- a slow rate of equilibrium under low matric potential values associated with dry soils.

3.2.4 In-situ methods

Among the methods to be preferred in the estimation of the SWRC are the in-situ methods. An effective method for obtaining simultaneous measurements of potential matric and volumetric water content, involves the use of Time-Domain Reflectometer probes (TDR), installed in the soil, coupled with transducer tensiometers, and recording the changing values of each measurement in time as the soil wetness varies. Although this method is very suitable to define SWRC, an accurate calibration procedure of the TDR sensor should be performed as an accurate refilling process of tensiometer is required.

The principle of this method is based on the relationship between the soil bulk dielectric constant ε_b, measured by TDR, and the volumetric water content θ_v while to define soil matric potential measurement in time, tensiometers are used. A tensiometer consists of a porous cup, usually made of ceramic material with very fine pores, placed in a direct contact to a vacuum gauge through a water-filled tube. The porous cup is placed in intimate contact with the bulk soil at the depth of measurement. When the matric potential of the soil is lower (more negative) than inside the tensiometer, water moves from the tensiometer along a potential energy gradient to the soil through the saturated porous cup, thereby creating suction sensed by the gauge. Water flow into the soil continues until equilibrium is reached and the suction

inside the tensiometer equals the soil matric potential. When the soil is wetted, flow may occur in the reverse direction, i.e., soil water enters the tensiometer until a new equilibrium is attained. The tensiometer governing equation is defined as:

$$\psi_m = \psi_g + (z_g - z_c) \tag{3.8}$$

where ψ_m is the potential matric [L], ψ_g is the reading at the vacuum gauge location and z indicate the depth of the gauge and cup.

Electronic sensors called pressure transducers often replace the mechanical vacuum gauges. The transducers convert mechanical pressure into an electric signal which can be more easily and more precisely measured. In practice, pressure transducers can provide more accurate readings than other gauges, and in combination with data logging equipment are able to supply continuous measurements of matric potential.

3.2.5 Laboratory experiments

In-situ methods were not applied for the case study. Several experimental procedures for defining the SWRC of soils already exist in the literature. However, in this study, the materials examined are construction materials, rather than soils. Consequently, the determination of hydraulic properties of construction materials has been an intricate and fundamental step for the next phase of water flow modelling. Depending on the material used in the layers of the lab-scale PP used in the analysis, several tests have been used.

Evaporation method

The evaporation method is one of the most widely and easily used methods to determine the retention curve and hydraulic conductivity of unsaturated soils. This method is based on measuring both soil moisture and pressure head during a soil drying cycle under the effect of evaporation. The method was developed by Wind (1968) who introduced an iterative graphical procedure to estimate, firstly, the water retention curve from average soil moisture and pressure head readings, and to determine hydraulic conductivities from measured pressure head profile and variations of the water content distribution. Then several authors have proposed simplifications to this method. The most recent are (Peters and Durner, 2008; Schindler et al., 2010a; Schindler et al., 2010b).

In this work the hydraulic properties of the bedding layer were measured in the laboratory using a simplified evaporation method as proposed by Schindler et al. (2010a,b) by using the HYPROP® device.

HYPROP® is a fully automated measuring and evaluation system to determine the hydraulic properties of soil samples. HYPROP measures the water tension at two levels of a sample using two tension-shafts (Figure 3.2)

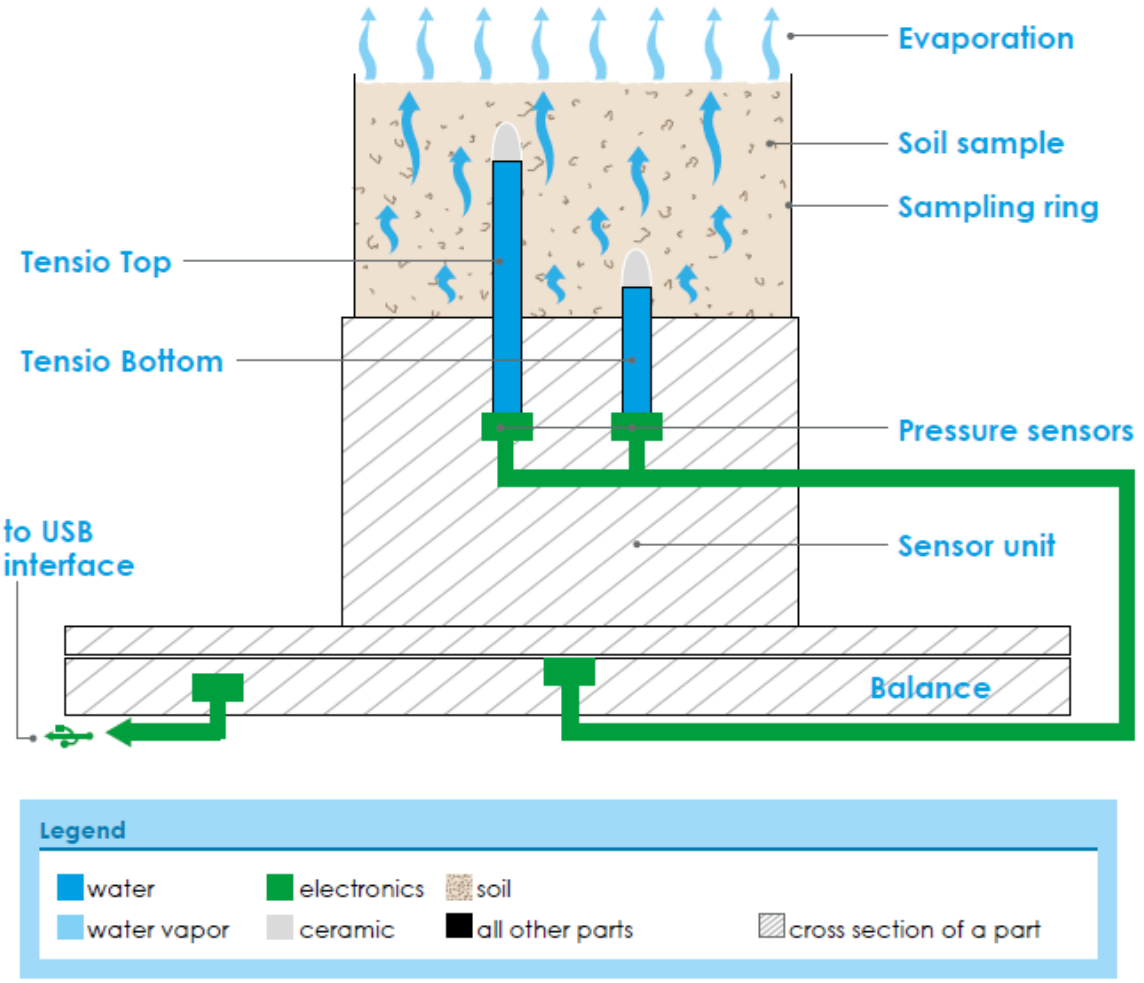

Figure 3.3 The HYPROP device (UMS HYPROP manual)

With this method two tensiometers are positioned in two depths of a soil sample sitting in a sample ring. The plane in the middle between the two tensiometers is identical with the horizontal symmetry plane of the column. The sample is saturated with water, basally closed and set on a balance. The soil surface is open to the ambient atmosphere so that the soil water can evaporate.

HYPROP measures the water tension in two horizons of the soil sample over the evaporation process by means of two vertical tension-shafts (similar to T5 tensiometers). The change of the sample mass over time is determined by weighing. The medial tension value of the sample

is calculated based on the average value of the two tensions. The medial water content is calculated based on the mass change. This results in one measuring value per point in time for the retention curve.

The bedding layer for the laboratory analysis was packed using a stainless-steel sampling ring with a volume of 250 ml. The soil sample was saturated from the bottom before starting the evaporation test. The measurement unit and tensiometers were degassed using a vacuum pump, in order to reduce the potential nucleation sites in the demineralized water. At the end of the experiment, the sample was placed in an oven at 105° C for 24 h, and then the dry weight was measured.

For a complete description of the system, please refer to UMS GmbH (2015).

The numerical optimization procedure, HYPROP-FIT (Pertassek et al., 2015), was used to simultaneously fit retention and hydraulic conductivity functions to experimental data obtained using the evaporation method. Fitting was accomplished using a non-linear optimization algorithm that minimizes the sum of weighted squared residuals between model predictions and measurements. Unfortunately, this method produced unsatisfactory results in fitting the measured data with the literature models. The problem is probably due to the coarse nature of the bedding layer material which makes this method unsuitable for the purpose. In this way, the multistep outflow experiment was proposed.

Multistep outflow experiment

Laboratory outflow experiments, are generally used to define the water retention functions and the unsaturated hydraulic conductivity function simultaneously. The Multistep Outflow experiment (MSO), evaluated by inverse modelling, is an efficient way to determine simultaneously the water retention and hydraulic conductivity functions of soils (Durner et

al., 1999; Durner and Iden, 2011; Van Dam et al., 1994). The method used flow cell known as Tempe Cell. Tempe Cell is used to determine the water-holding characteristics of a soil sample in a specified range. Tempe cell comes with top and bottom Plexiglass plates, a porous ceramic plate, a brass cylinder, and all sealing and connecting hardware. A variety of porous ceramic plates and brass cylinders are available. An external pressure source is connected to the Tempe cell using Neoprene tubing. A schematic of a Tempe Cell is presented in Figure 3.4.

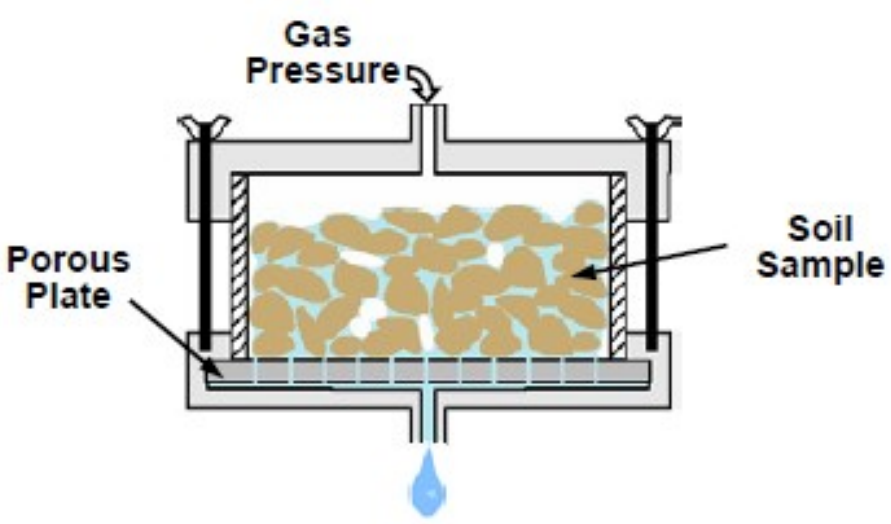

Figure 3.4 A schematic of Tempe Cell

MSO used air pressure that is increased by several smaller steps during the experiment. The first applied pressure after saturation must be larger than the soil air-entry value and is maintained until equilibrium is reached. This equilibrium state serves as the initial condition in the optimization process (Van Dam et al., 1994). The time interval between subsequent pressures steps is flexible, as the numerical analysis assumes a dynamic process. Most likely, the optimization results will be better if the soil water is closer to steady state within a pressure step.

In this work, two 100 cm^3 columns were placed in the Tempe cells, in which the fine gravel material of the bedding layer was packed. Samples were fully saturated, and then slowly drained using 5 pressure head steps (a minimum pressure head of -12.5 cm) during several days and cumulative outflow in time was measured. Points of the soil water retention curve were calculated from the final water content determined gravimetrically and the water discharge from the sample was observed. HYDRUS-1D was used to simulate the observed cumulative outflow and the measured points of the retention curve, and to optimize material hydraulic parameters. For both samples, the θ_s parameter was measured, and the θ_r value was set at 0 $cm^3\ cm^{-3}$.

Clay tank experiment

As stated in the previous sections, materials used in the pavement structures are rather construction materials than soils. In this way, a novel contribution of this work is recognized that some common procedures used with soils with soils were applied to the aggregates containing soil to define their hydraulic properties.

Thus, SWRC of the concrete pavement was measured in the laboratory using the clay tank experiment proposed by Fér and Kodešová (2012) for soil aggregates.

The experiment was conductued on two fragments of this material. Firstly, vertical sides of the fragments were covered by wax. Fragments were saturated by water, then placed in the clay tank and slowly drained using pressure heads from 0 to -220 cm. The clay tank consists in a large funnel with a sintered disc, which was covered by a 5 cm thick kaolin layer with a filter paper on the top. The clay tank (the funnel outlet) was connected to a water reservoir by a plastic tube (Figure 3.5).

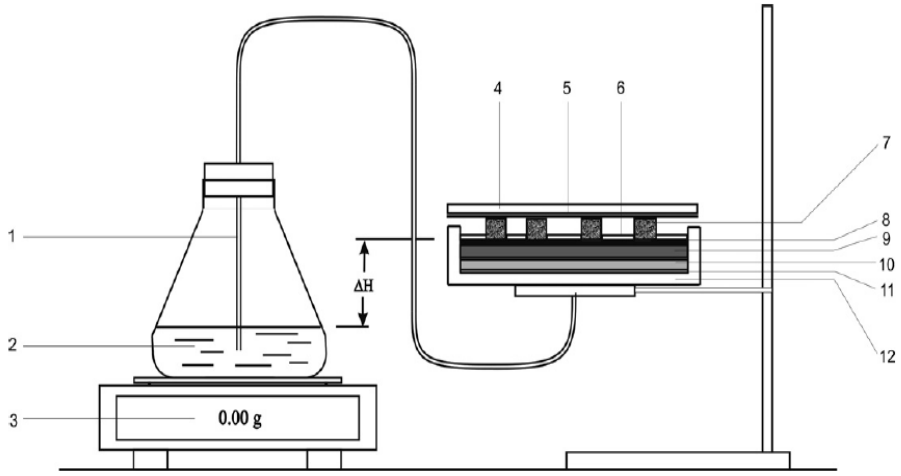

Fig. 1. Schematic cross-section of the sand–kaolin apparatus for measuring cumulative capillary rise into the aggregates: plastic tube (1), water container (2), balance (3), lid (4), plastic foil (5) (6), soil aggregates (7), filter paper (8), kaolin layer (9), fine sand layer (10), plastic drainage mesh (11), plastic container. Apparatus proposed by Gerke and Köhne (2002) was slightly modified. The filter paper (8), kaolin layer (9), fine sand layer (10) were used instead of the 30-μm pore-size membrane, sand bed and the elastic foam bed.

Figure 3.5 A schematic of the clay tank experiment (Fér and Kodešová, 2012)

This tank was designed to measure the soil water retention curve in the range of pressure heads applied during the experiment (0 to -220 cm). In order to obtain a maximal saturation of the material, considering the fact that it is very porous, saturation was encouraged by using ultrasound technique. Soil water contents related to particular pressure heads were evaluated gravimetrically. Parameters of the retention curves were obtained by fitting of the experimental data points using the RETention Curve code (RETC) (van Genuchten et al., 1991). For a more detailed explanation of the clay tank please refer to Fér and Kodešová (2012). Generally, gaps have a high influence in interlocking concrete pavements in which all the infiltration capacity is deputed to them (impervious concrete blocks). Conversely, in porous pavement, such as discussed here, the concrete blocks have a high permeability and infiltrate most of the incoming water. In the lab scale system, the gaps between porous concrete blocks were reduced to minimize preferential flows and assume a homogeneous wear layer.

Regarding the hydraulic parameters of the sub-base layer, all parameters were fixed according to Brunetti et al. (2016a) considering that the material used for the construction of the lab-scale system is similar to the one used in the cited work.

3.3 Water flow modelling using the HYDRUS model

The HYDRUS model is one of the most widespread models used to simulate the movement of water, heat, and multiple solutes in variably-saturated porous media. In particular, among the applications, the following are listed:

- predict the movement of water and solutes in the unsaturated zone;
- analyzing laboratory or field experiments involving water flow and/or solute transport;
- extract information from field experiments on different soils with different climatic conditions;
- simulate heat transport in porous media;
- assess CO_2 transport.

The HYDRUS model can numerically solves the Richards equation for variably-saturated water flow. The water flow equation incorporates a sink term to account for water uptake by plant roots if needed. The model can also implement the flow equation considering the dual-porosity type flow in which one fraction of the water content is mobile and another fraction immobile, or dual-permeability type flow involving two mobile regions, one representing the matrix and one the macropores.

Water flow can occur in the vertical, horizontal, or a generally inclined direction. The water flow part of the model can deal with prescribed head and flux boundaries, boundaries controlled by atmospheric conditions, as well as free drainage boundary conditions. The governing flow equation is solved numerically using Galerkin-type linear finite element schemes. HYDRUS also includes a Marquardt-Levenberg type parameter optimization algorithm for inverse estimation of soil hydraulic parameters from measured transient or steady-state flow.

As stated before, it is possible to implement equilibrium and non-equilibrium models, the latter could be distinguished by the introduction of the concept of dual-porosity (Gerke and van Genuchten, 1993; Gerke and Van Genuchten, 1996; Germann and Beven, 1985; Philip, 1968; Van Genuchten and Wierenga, 1976), which divides the liquid phase into the mobile regions (fluent, inter-aggregated) and immobile region (stagnant, intra-aggregated area), and the distinction between matrix and fractured region. Figure 3.6 shows diagrams for equilibrium and non-equilibrium models, where θ_{imm} and θ_m represent the water content in the immobile phase and mobile, and θ_M and θ_F represent the water content in the matrix region and in the fractured region.

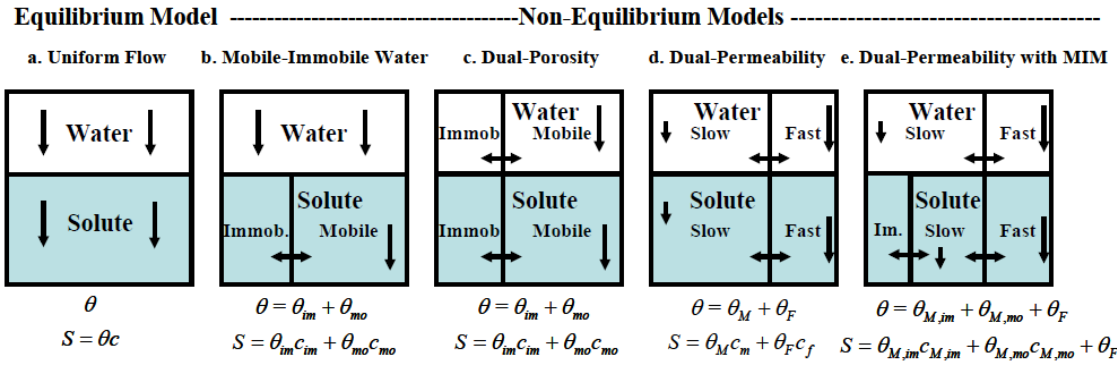

Figure 3.6 Diagrams for Equilibrium and Non-Equilibrium models in HYDRUS

The unsaturated soil hydraulic properties, *θ(h)* and *K(h)* are in general highly nonlinear functions of the pressure head. The HYDRUS software packages permit the use of five different analytical models for the hydraulic properties (Brooks and Corey, 1964; Durner, 1994; Kosugi, 1996; van Genuchten, 1980; Vogel and Cislerova, 1988).

The Van Genuchten model is the one that best simulates many types of soil, unlike the Brook and Corey model, which can be considered a particular case of the Van Genuchten formulation and which is only suitable for medium and coarse grain size. Vogel and Cislerova (1988) made changes to the Van Genuchten model to add flexibility in describing hydraulic properties near saturation.

Durner, (1994) divided the porous medium into two (or more) overlapping regions and suggested to use for each of these regions a van Genuchten-Mualem type function of the soil hydraulic properties ,whole while Kosugi (1996) suggested a lognormal distribution model for the effective water saturation S_e.

The studied permeable pavement was interpreted as a two-dimensional radially, symmetric, single-porosity, porous medium, which could be described by the Richards equation in the following form:

$$\frac{\partial \theta}{\partial t} = \frac{1}{r}\frac{\partial}{\partial r}\left[rK\frac{\partial h}{\partial r}\right] + \frac{\partial}{\partial z}\left[K\left(\frac{\partial h}{\partial z} + 1\right)\right] \tag{3.9}$$

where θ is the volumetric water content [L^3L^{-3}], t is the time [T], h is the soil water matric head [L], K is the hydraulic conductivity [L T^{-1}], r is the radial coordinate [L], and z is the vertical axis [L]. The unimodal van Genuchten–Mualem model (Mualem, 1976; van Genuchten, 1980) was used to describe the material hydraulic properties:

$$S_e = \begin{cases} \dfrac{1}{\left(1 + \left(|\alpha h|\right)^n\right)^m} & if \quad h \le 0 \\ 1 & if \quad h > 0 \end{cases} \tag{3.10}$$

$$S_e = \frac{\theta - \theta_r}{\theta_S - \theta_r} \tag{3.11}$$

$$K = \begin{cases} K_S \cdot S_e^{\,l}\left[\left(1 - \left(1 - S_e^{\frac{1}{m}}\right)^m\right)\right]^2 & if \quad h < 0 \\ K_S & if \quad h > 0 \end{cases} \tag{3.12}$$

$$m = 1 - \frac{1}{n} \tag{3.13}$$

where K_s denotes the saturated hydraulic conductivity [L T^{-1}], S_e [−] is the effective water saturation $0 \le S_e \le 1$, θ_s and θ_r [L^3 L^{-3}] are the saturated and residual water content, respectively, and α [L^{-1}], m [−], and n [−] are empirical parameters dependent on soil type and l denotes tortuosity/connectivity coefficient [−] which is found to have a value of 0.5 from the analysis of a variety of soils (Mualem, 1976). The α parameter is related to the air-

entry pressure and it is generally high for coarse soil and low for silty or clayey soils. Similarly, the *n* parameter, which determines the steepness of the SWRC.

3.3.1 Numerical domain and boundary condition

In order to reproduce the behaviour of the PP as an axisymmetrical vertical two-dimensional flow domain, the cylindrical domain was designed considering the total thickness of porous materials and planar area of the lab-scale system, i.e. the depth of the domain was 41 cm and radius was 32.70 cm (Figure 3.7). The geotextile was not included in the model considering its negligible thickness, its limited hydraulic effect due to its high permeability, and that its sole function was to separate the bedding layer from the sub-base layer.

The domain was discretized into two-dimensional rectangular elements (Figure 2) using the MESHGEN tool of HYDRUS-2D. The generated FE mesh had 1260 nodes and 2377 two dimensional elements. The quality of the FE mesh was assessed by checking the mass balance error reported by HYDRUS-2D at the end of the simulation. Mass balance errors, which in this simulation were always below 1%, are generally considered acceptable at these low levels.

At the surface of the PP, an atmospheric boundary condition (i.e. applied rainfall or potential evaporation of 6.94×10^{-5} cm min^{-1}) was assigned, while a seepage face boundary condition was specified at the bottom left corner of the flow domain (Figure 2). The outflow from a boundary exposed to atmosphere will occur only if the pressure in the porous media water exceeds atmospheric pressure. In this view, a seepage face boundary acts as a zero pressure head when the boundary node is saturated and as a no flux boundary when it is unsaturated. A zero flux boundary condition was assigned to all remaining boundaries of the domain

considering the fact that the building material of the lab-scale system is Plexiglas that is impervious. The initial condition was specified in terms of the soil water pressure head and was set to linearly increase with depth, from -30 cm at the top of the flow domain (z = 41) to -0.5 cm at the bottom (z = 0).

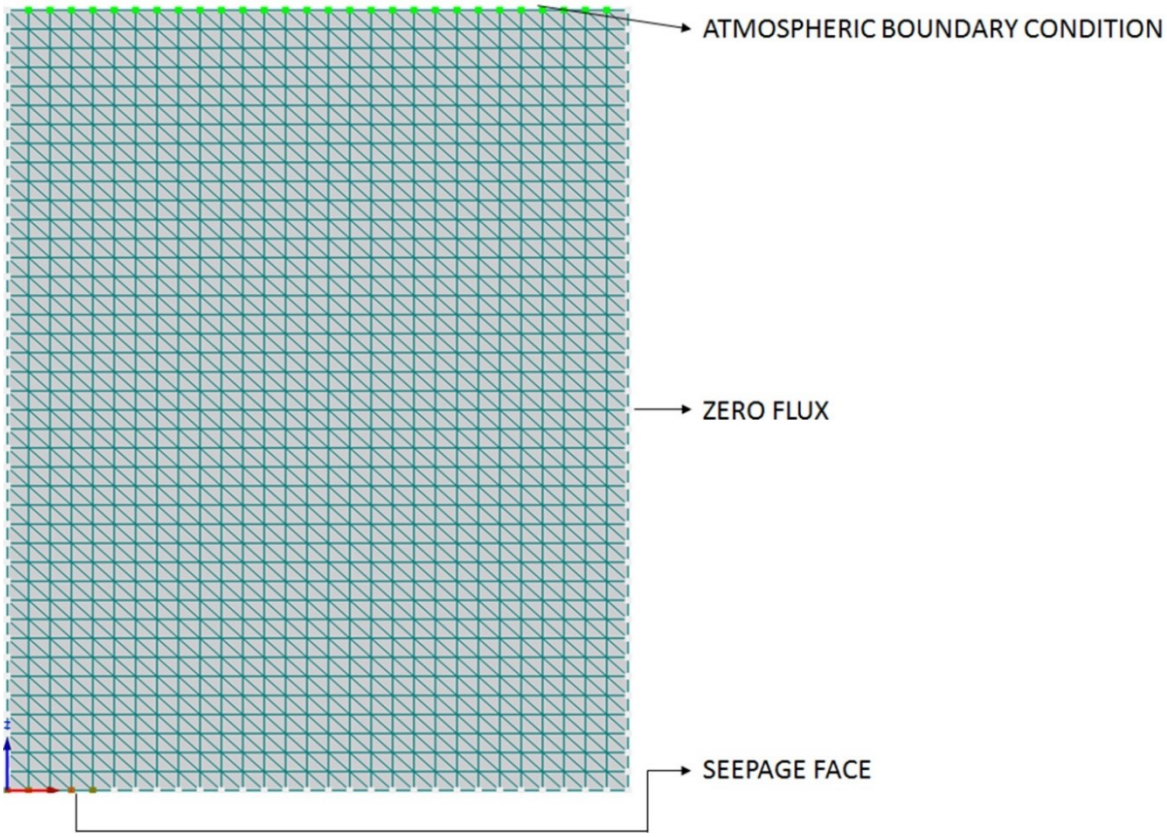

Figure 3.7 A schematic of the applied boundary conditions in the axisymmetric domain

3.3.2 Inverse parameter estimation

Inverse modelling is a procedure to estimate unknown parameters of the model from experimental data. During the past several years, its use has greatly increased joined by advances in numerical modelling and by increasing the computing power that now allows numerical inversions of saturated-unsaturated flow problems.

In general, the approach in model fitting is to select an objective function that is a measure of the agreement between measured and simulated data, and which is related to the parameters to be fitted. The best-fit parameters are obtained by minimizing this objective function.

However, to achieve the solution by inverse modelling, the inverse problem must be correctly posed. For incorrectly, or ill posed problems, inverse solutions result in non-unique, or divergent results.

On the other hand, the precision of the estimated parameters can be assessed by uncertainty analysis, which yields confidence intervals for the estimated parameters at the objective function minimum.

Numerous applications of inverse modelling for estimating soil hydraulic properties exist in the literature (Diamantopoulos et al., 2012; Hopmans et al., 2002; Le Bourgeois et al., 2016; Wohling et al., 2008).

Since the saturated hydraulic conductivity of the wear layer (concrete blocks) is not measured when using the clay tank test, numerical optimization of these parameters had to be conducted. Preliminary simulations showed that simulated transient flow data (outflow fluxes and water contents) did not closely correspond to the measured ones if only this parameter was estimated. Therefore, further 3 parameters α, n and K_s of the bedding layer were optimized. The original data set of 10 rainfall events was divided into two data sets serving calibration and validation. The calibration data set, relative to a period of three days (days 1 to 3), was characterized by having intermediate rainfall intensity in a very short time. In order to evaluate the stress conditions of the draining package, a drying time of 24 hours was secured between two events. The following 7 days were selected as the validation data.

This period was selected with the intention of having the most significant rainfall intensity and durations of between fifteen minutes and thirty minutes.

HYDRUS software packages implement a Marquardt-Levenberg type parameter estimation technique (Marquardt, 1963; Šimůnek and Hopmans, 2002) for the inverse estimation of soil hydraulic, solute transport, and/or heat transport parameters from measured transient or steady-state flow and/or transport data. This method combines the Newton and steepest descend methods, and generates confidence intervals for the optimized parameters. The method was found to be very effective and has become a standard in nonlinear least-squares fitting for hydrological models. It is a gradient-based local optimization algorithm, which has proven to be reliable when the dimensionality of the inverse problem is low. Considering that only 4 hydraulic parameters had to be estimated after the laboratory tests, this algorithm was used.

The objective function Φ to be minimized during the parameter estimation, written in a relatively general manner, may be defined as:

$$\Phi(b,q,p)=\sum_{j=1}^{m_q} v_j \sum_{i=1}^{n_{qj}} w_{i,j}\left[q_j^*(x,t_i)-q_j(x,t_i,b)\right]^2+\sum_{j=1}^{m_p}\overline{v_j}\sum_{i=1}^{n_{pj}}\overline{w_{i,j}}\left[p_j^*(x,\theta_i)-p_j(x,\theta_i,b)\right]^2 + \sum_{j=1}^{n_b}\hat{v}_j\left[b_j^*(x)-b_j(x)\right]^2 \quad (3.14)$$

where the first term on the right side represents deviations between measured and calculated space-time variables. In this term, m_q represents the number of different sets of measurements, n_{qj} is the number of measurements, q_j *(x,t_i) represents specific measurements at generic time t_i for the j_{th} measurement set at location x, $q_j(x,t_i,b)$ is the model prediction

the vector of the optimized parameters b (in this case soil hydraulic parameters), and v_j and $w_{i,j}$ are weights associated with a particular measurement set or point, respectively. In the first term water contents, at z=30.5 cm (i.e., center of the bedding layer), and actual flux across the seepage face, are included.

The second term on the right side of equation 6 represents differences between independently measured and predicted soil hydraulic properties for different soil horizons. The last term represents a penalty function for deviations between prior knowledge of the soil hydraulic parameters.

The HYDRUS code, as part of the inverse solution, produces also a correlation matrix, which specifies the degree of the correlation between the fitted coefficients. The correlation matrix measures changes in model predictions caused by small changes in the final estimate of a particular parameter, relative to similar changes as a result of changes in the other parameters. The correlation matrix reflects the nonorthogonality between two parameter values. A value of ±1 suggests a perfect linear correlation whereas 0 indicates no correlation at all. The correlation matrix may be used to select which parameters, if any, are best kept constant in the parameter estimation process because of high correlation. Interdependence of optimized parameters can cause a slow convergence rate and nonuniqueness, and increase parameter uncertainty (Šimůnek and Hopmans, 2002).

3.3.3 Sensitivity Analysis

While building and using numerical simulation models, Sensitivity Analysis (SA) methods are invaluable tools. They allow to study how the uncertainty in the output of a model can be apportioned to different sources of uncertainty in the model input. It may be used to

determine the input variables most contributing to the output behaviour or ascertain some interaction effects within the model. The objectives of SA are numerous. One can mention model verification and understanding, model simplification and factor prioritization. Finally, the SA is an aid in the validation of a computer code, guidance for research efforts, or the justification in terms of system design safety.

In this study, four material hydraulic parameters were included in the optimization framework. Preliminary to this step, a Sensitivity Analysis (SA) has been carried out to investigate the influence of different parameters on the output variance, and to identify potential important factors, which can be fixed at any value in the parameter space without significantly affecting model response. Sensitivity analyses have been widely applied in hydrological problems. However, most of the existing application used the One-factor-at-a-time (OAT) sensitivity analysis, so called as each factor is perturbed in turn while maintaining all the other parameters fixed. This type of approach is applicable only when the model is additive and parameter interaction is negligible. When the properties of the model are unknown it is necessary to use a Global Sensitivity Analysis (GSA), which is able to detect parameter interaction. Brunetti et al. (2016a) carried out a GSA, based on the Sobol method, on the material hydraulic properties of a layered permeable pavement modelled using HYDRUS-1D. The analysis revealed that the model was non-additive and characterized by significant parameter interaction, with a prominent influence of the wear layer on the hydraulic behaviour of the pavement. In another study, Brunetti et al. (2017) performed a surrogate-based sensitivity analysis on the soil hydraulic properties of a stormwater filter modelled using HYDRUS-2D. Results highlighted how the shape parameter α of the filter layer had a dominant effect on the simulated outflow.

In both cited studies, the GSA based on the Sobol method required thousands of runs to accurately determine different sensitivity measures, thus increasing substantially the computational cost of the analysis. In Brunetti et al. (2017), this problem was overcame using a surrogate model based on the kriging approximation of the response surface. An alternative, when the model is computationally expensive and the main settings of the SA are the factors fixing and prioritization, is the Morris method (Morris, 1991). The Morris method belongs to the class of *Screening* methods. Screening methods are based on a discretization of the inputs in levels, allowing a fast exploration of the code behaviour. These methods are adapted to a large number of inputs; practice has often shown that only a small number of inputs are influential. The aim of this type of method is to identify the non-influential inputs with a small number of model runs while making realistic hypotheses on the model complexity.

The Morris method is based on calculating for each input a number of *Elementary Effects* (EE), from which basic statistics are computed to derive sensitivity measures. While relying on the OAT analysis for the computation of EEs, the method can be viewed as global since it averages the EEs computed at different locations in the parameter space, thus providing a statistical base for a qualitative evaluation of different sensitivity measures.

In our analysis, each single run of the HYDRUS-2D model, for the calibration period, required approximately 30 seconds of CPU time on a laptop equipped with a CPU Intel® Core i7-4700 MQ 2.40 GHz processor and 8 GB of RAM. Since a variance-based SA would have required a significant computational cost, the modified version of the Morris method proposed by Campolongo et al. (2007) has been used. In particular, the influence of the remaining material hydraulic properties (i.e., the saturated hydraulic conductivity K_s for the both the wear and bedding layer, and the two empirical parameters α and n for the bedding layer) on the hydraulic response of the pavement has been investigated. The main outcome

of the analysis are two sensitivity measures for all investigated parameters: σ and μ^*. While the former summarizes the interaction effect, the latter reflects the overall importance of a particular parameter. For a detailed description of the method, refer to Morris (1991) and Campolongo et al. (2007). To interpret the results by simultaneously taking into account both sensitivity measures, Morris suggested their graphical representation in the (μ^*-σ) plane.

More specifically, the sensitivity analysis has investigated the influence of different material hydraulic parameters on the simulated outflow and volumetric water content in the bedding layer, respectively. The effect is quantified by comparing the simulation results with measured values of outflow and water content. In particular, the NSE index and the RMSE have been used. One of the main advantage of the Morris Method is the computational efficiency. It is able to provide a qualitative screening of the most influent factors with few model runs. There are no clear indications in the literature about the sample size. For example, Iooss and Lemaître, (2014) used a sample size of 5 to screen 8 parameters of a hydraulic model. In another study, Saltelli et al., (2004) suggested a sample size between 4 and 10. Considering that only four hydraulic parameters were investigated in the sensitivity analysis, a sample size of 8 for a total of 40 model executions has been chosen.

3.4 Statistical evaluation

In general, in order to assess the accuracy of a model it is necessary to perform a statistical evaluation to ensure the results validity. There are several statistical evaluation indices that can be used to assess the accuracy of a hydrological model. In this study, two widely used indices have been used: the coefficient of determination R^2 and the NSE index.

The coefficient of determination R^2 describes the proportion of the variance in measured data explained by the model. R^2 ranges from 0 to 1, with higher values indicating less error variance, and typically values greater than 0.5 are considered acceptable (Moriasi et al., 2007):

$$R^2 = \frac{\sum_{i=1}^{n}\left(Q_i^{\mathrm{mod}} - \overline{Q^{obs}}\right)^2}{\sum_{i=1}^{n}\left(Q_i^{obs} - \overline{Q^{obs}}\right)^2} \tag{3.15}$$

obs, mod are the observed and simulated value respectively

$\overline{obs}$ is the mean value of the observed data.

The Nash-Sutcliffe Efficiency (NSE) index (Nash and Sutcliffe, 1970), is a normalized statistic that determines the relative magnitude of the residual variance ("noise") compared to the measured data variance ("information"). NSE indicates how well the plot of observed versus simulated data fits the 1:1 line. Servat and Dezetter, (1991) also found NSE to be the best objective function in the context of rainfall-runoff modelling and for this reason was used for the proposed study:

$$NSE = 1 - \left[\frac{\sum_{i=1}^{n}\left(Q_i^{obs} - Q_i^{\mathrm{mod}}\right)^2}{\sum_{i=1}^{n}\left(Q_i^{obs} - \overline{Q_i^{obs}}\right)^2}\right] \tag{3.16}$$

where Q_i^{obs} represents the measured value, Q_i^{mod} represents the simulated value, and $\overline{Q_i^{obs}}$ is the mean value of observed data. The NSE coefficient ranges between -∞ and 1.0 .When it is equal 1 it would be perfect agreement, and, generally, values between 0.0 and 1.0 are considered acceptable (Moriasi et al., 2007).

3.5 Water quality performance

Water quality performance of the permeable pavement was assessed by spraying two dissolved heavy metals on the laboratory pavement surface during the simulated rainfall period described in the previous sections. In actual situations, besides the dissolved metal load, there would be also the particulate fraction load generally exceeding the former one (Huber et al., 2016). The pavement response to the dissolved Zinc and Copper loads was analyzed by comparing the inflow and outflow concentrations.

The concentrations of the heavy metals (Cu and Zn) applied to the PP were based on relatively high-level concentrations in stormwater runoff recommended by Reddy et al. (2014). The concentrations and the source chemicals used to prepare synthetic stormwater were: 5 ÷ 15 mg/l of dissolved Cu using $Cu(SO)_4$ and 6 ÷ 15 mg/l of Zn using $Zn(CH_3COO)_2$ $2H_2O$. The test event concentrations are listed in Table 3.2. It was recognized that the concentrations of dissolved Cu and Zn used were rather high, but deemed acceptable in these experiments considering the preliminary nature of the investigations (more or less a proof of concept), limitations of the available laboratory analytical equipment, and a higher likelihood of obtaining measurable concentrations when working at higher levels.

Rainfall events [-]	Volume [l]	Cu [mg/l]	Zn [mg/l]
Day 1	12.30	15.00	12.00
Day 2	10.70	6.85	6.00
Day 3	11.10	8.00	6.00
Day 4	7.20	5.00	8.00
Day 5	8.00	6.00	6.00
Day 6	6.05	5.00	15.00
Day 7	11.70	6.00	12.00
Day 8	11.60	5.00	6.00
Day 9	11.65	-	-
Day 10	6.50	-	-

Table 3.2 Inflow concentrations

3.6 Batch experiment

Besides the experiments with the laboratory test pavement, additional batch experiments were used to evaluate the potential dissolved metal removal efficiencies of all the pavement materials used, for individual metal concentrations provided in the laboratory rainwater. Results of these tests confirm that adsorption is one of the main mechanisms for removing heavy metals in permeable pavement systems, though metal precipitation may also occur.

3.6.1 Theory of adsorption

Adsorption is the accumulation of a molecule on the surface of an adsorbent. The materials which adsorb the molecules are called adsorbents and the materials which are being adsorbed

are called adsorbates. Adsorption is caused by the unbalanced forces associated with the surface molecules of adsorbates and adsorbents.

Adsorption is usually described through isotherms, that is, the amount of adsorbate on the adsorbent is a function of its pressure (if gas) or concentration (if liquid) at a constant temperature. So far, 15 different isotherm models have been developed (Foo and Hameed, 2010) but the two most common models reported in the literature are those of Langmuir (1916) and Freundlich (1906). A general form of the adsorption isotherm is given by equation 3.17:

$$S = \frac{K_S C^{\beta}}{1 + \eta C^{\beta}} \tag{3.17}$$

where K_S is the adsorption isotherm coefficient [$M^{-1}L^3$], S represents the adsorbed mass [M], C is the concentration of adsorbate in solution [$M\ L^{-1}$]. When β=1, the adsorption equation above becomes the Langmuir equation, when η=0, the equation becomes the Freundlich equation, and when both β=1 and η=0, it leads to a linear adsorption isotherm.

Following the methodology recommended by Fach and Geiger (2005), the concrete blocks were crushed with a jaw crusher and sieved through a mesh opening of 2 mm. The crushing increased the specific surface area of concrete fragments, compared to the monolithic concrete layer, and thereby accelerated chemical processes in the water-concrete mixture. Recently, the use of crushed concrete filters was recommended for removals of dissolved chemicals (e.g., phosphorus, heavy metals) from stormwater pond effluents (Sonderup et al. 2015). However, it is unlikely that a layer of crushed concrete could be used in the permeable pavement sub-structure, because such a material may not possess the structural strength required. The sub-base materials were tested similarly as described above. The graded material was dried in a drying oven at 105° until a constant weight was achieved.

The procedures for the adsorption tests were conducted as follows:

- Separate solutions, ranging in concentration from 40 ÷ 120 mg/l were prepared for each metal in distilled water;
- 10 g of material (concrete blocks, fine gravel, stones) as an adsorbent was added in a 250 ml conic flask of metal solution;
- the conical flasks were capped and shaken in the flask shaker at 200 rpm for four hours;
- the experiments were conducted at room temperature and the pH was adjusted to around 6.0 by adding a few drops of NaOH solution (initial pH= 5.5÷5.9).
- the sample was filtered through the 0.450 μm filter paper and the effluent concentration was measured;
- the adsorbed mass was calculated and the adsorption isotherm was assessed.

The metal concentrations of each solution were determined using the Atomic Absorption Spectrophotometer.

3.7 References

Brooks, R., Corey, A., 1964. Hydraulic properties of porous media. Hydrol. Pap. Color. State Univ. 3, 37 pp.

Brunetti, G.,Simune, J., Piro, P., 2016a. A comprehensive numerical analysis of the hydraulic behavior of a permeable pavement. J. Hydrol. 540, 1146–1161. doi:10.1016/j.jhydrol.2016.07.030

Brunetti, G., Šimůnek, J., Piro, P., 2016b. A comprehensive numerical analysis of the hydraulic behavior of a permeable pavement. J. Hydrol. 540, 1146–1161. doi:10.1016/j.jhydrol.2016.07.030

Brunetti, G., Šimůnek, J., Turco, M., Piro, P., 2017. On the use of surrogate-based modeling for the numerical analysis of Low Impact Development techniques. J. Hydrol. 548, 263–277. doi:10.1016/j.jhydrol.2017.03.013

Burak, R., n.d. Contractor Focus Construction of Bases for Permeable Interlocking Concrete Pavements – Part I.

Campolongo, F., Cariboni, J., Saltelli, A., 2007. An effective screening design for sensitivity analysis of large models. Environ. Model. Softw. 22, 1509–1518. doi:10.1016/j.envsoft.2006.10.004

Carbone, M., Turco, M., Brunetti, G., Piro, P., 2015. A Cumulative Rainfall Function for Subhourly Design Storm in Mediterranean Urban Areas. Adv. Meteorol. 2015, 1–10. doi:10.1155/2015/528564

Diamantopoulos, E., Iden, S.C., Durner, W., 2012. Inverse modeling of dynamic nonequilibrium in water flow with an effective approach. Water Resour. Res. 48. doi:10.1029/2011WR010717

Durner, W., 1994. Hydraulic Conductivity Estimation for Soils with Heterogeneus pore Structure. Water Resour. Res. doi:10.1029/93WR02676

Durner, W., Iden, S.C., 2011. Extended multistep outflow method for the accurate determination of soil hydraulic properties near water saturation. Water Resour. Res. 47. doi:10.1029/2011WR010632

Durner, W., Schultze, B., Zurmühl, T., 1999. State-of-the-art in inverse modeling of inflow/outflow experiments. Proc. Int. Work. Charact. Meas. Hydraul. Prop. Unsaturated Porous Media, Oct. 22-24, 1997, Univ. California, Riverside, CA., 1999. 661–681.

Elliott, A.H., Trowsdale, S.A., 2007. A review of models for low impact urban stormwater drainage. Environ. Model. & Softw. 22, 394–405. doi:10.1016/j.envsoft.2005.12.005

Fach, S., Geiger, W.F., 2005. Effective pollutant retention capacity of permeable pavements for infiltrated road runoffs determined by laboratory tests. Water Sci. Technol. 51, 37–45.

Fér, M., Kodešová, R., 2012. Estimating hydraulic conductivities of the soil aggregates and their clay-organic coatings using numerical inversion of capillary rise data. J. Hydrol. 468–469, 229–240. doi:10.1016/j.jhydrol.2012.08.037

Foo, K.Y., Hameed, B.H., 2010. Insights into the modeling of adsorption isotherm systems.

Chem. Eng. J. doi:10.1016/j.cej.2009.09.013

Freundlich, H.M.., 1906. Over the adsorption in solution. J. Phys. Chem 57, 385–470. doi:10.3390/ijerph9030970

Gerke, H.H., van Genuchten, M.T., 1993. A dual-porosity model for simulating the preferential movement of water and solutes in structured porous media. Water Resour. Res. 29, 305–319. doi:10.1029/92WR02339

Gerke, H.H., Van Genuchten, M.T., 1996. Macroscopic representation of structural geometry for simulating water and solute movement in dual-porosity media. Adv. Water Resour. 19, 343–357. doi:10.1016/0309-1708(96)00012-7

Germann, P.F., Beven, K., 1985. Kinematic Wave Approximation to Infiltration Into Soils With Sorbing Macropores. Water Resour. Res. 21, 990–996. doi:10.1029/WR021i007p00990

Hopmans, J.W., Šimůnek, J., Romano, N., Durner, W., 2002. 3.6.2. Inverse modeling of transient water flow. Methods Soil Anal. Part 1, Phys. Methods 963–1008. doi:10.2136/sssabookser5.4.c40

Huber, M., Welker, A., Helmreich, B., 2016. Critical review of heavy metal pollution of traffic area runoff: Occurrence, influencing factors, and partitioning. Sci. Total Environ. doi:10.1016/j.scitotenv.2015.09.033

Iooss, B., Lemaître, P., 2014. A review on global sensitivity analysis methods. Uncertain. Manag. Simulation-Optimization Complex Syst. Algorithms Appl. 23. doi:10.1007/978-1-4899-7547-8_5

Kellagher, R., Martin, P., Jefferies, C., Bray, R., Shaffer, P., Wallingford, H.R., Woods-Ballard, B., Woods Ballard, B., Construction Industry Research and Information Association, Great Britain, Department of Trade and Industry, Environment Agency, 2015. The SUDS manual, Ciria, …. doi:London C697

Kodešová, R., Kodeš, V., Mráz, A., 2011. Comparison of two sensors ECH2O EC-5 and SM200 for measuring soil water content. Soil Water Res. 6, 102–110.

Kosugi, K., 1996. Lognormal distribution model for unsaturated soil hydraulic properties. Water Resour. Res. 32, 2697–2703. doi:1029/96WR01776

Langmuir, I., 1916. The constitution and fundamental properties of solids and liquids. Part I. Solids. J. Am. Chem. Soc. 38, 2221–2295. doi:10.1021/ja02268a002

Le Bourgeois, O., Bouvier, C., Brunet, P., Ayral, P.A., 2016. Inverse modeling of soil water content to estimate the hydraulic properties of a shallow soil and the associated weathered bedrock. J. Hydrol. 541, 116–126. doi:10.1016/j.jhydrol.2016.01.067

Marquardt, D.W., 1963. An Algorithm for Least-Squares Estimation of Nonlinear Parameters. J. Soc. Ind. Appl. Math. 11, 431–441. doi:10.1137/0111030

Molini, a., Lanza, L.G., La Barbera, P., 2005. The impact of tipping-bucket raingauge measurement errors on design rainfall for urban-scale applications. Hydrol. Process. 19, 1073–1088. doi:10.1002/hyp.5646

Moriasi, D.N., Arnold, J.G., Liew, M.W. Van, Bingner, R.L., Harmel, R.D., Veith, T.L., 2007. Model Evaluation Guidelines for Systematic Quantification of Accuraccy in Watershed Simulations. Trans. Asabe 50, 885–900.

Morris, M.D., 1991. Factorial Sampling Plans for Preliminary Computational Experiments. Technometrics 33, 161. doi:10.2307/1269043

Mualem, Y., 1976. A new model for predicting the hydraulic conductivity of unsaturated porous media. Water Resour. Res. 12, 513–522. doi:10.1029/WR012i003p00513

Nash, J.E., Sutcliffe, J. V., 1970. River flow forecasting through conceptual models part I - A discussion of principles. J. Hydrol. 10, 282–290. doi:10.1016/0022-1694(70)90255-6

Pertassek, T., Peters, A., Durner, W., 2015. HYPROP-FIT Software User's Manual, V.3.0

Peters, A., Durner, W., 2008. Simplified evaporation method for determining soil hydraulic properties. J. Hydrol. 356, 147–162. doi:10.1016/j.jhydrol.2008.04.016

Philip, 1968. The theory of absorption in aggregated media. Aust. J. Soil Res. 6, 1–19. doi:10.1071/SR9680001

Reddy, K.R., Xie, T., Dastgheibi, S., 2014. Removal of heavy metals from urban stormwater runoff using different filter materials. J. Environ. Chem. Eng. 2, 282–292. doi:10.1016/j.jece.2013.12.020

Richards, L.A., 1931. Capillary conduction of liquids through porous mediums. J. Appl. Phys. 1, 318–333. doi:10.1063/1.1745010

Saltelli, A., Tarantola, S., Campolongo, F., Ratto, M., 2004. Sensitivity Analysis in Practice: A Guide to Assessing Scientific Models, in: Sensitivity Analysis in Practice. pp. 109–149. doi:10.1002/0470870958.ch5

Schindler, U., Durner, W., von Unold, G., Mueller, L., Wieland, R., 2010. The evaporation

method: Extending the measurement range of soil hydraulic properties using the air-entry pressure of the ceramic cup. J. Plant Nutr. Soil Sci. 173, 563–572. doi:10.1002/jpln.200900201

Schindler, U., Durner, W., von Unold, G., Muller, L., 2010. Evaporation Method for Measuring Unsaturated Hydraulic Properties of Soils: Extending the Measurement Range. Soil Sci Soc Am J 74, 1071–1083. doi:10.2136/sssaj2008.0358

Servat, E., Dezetter, A., 1991. Selection of calibration objective fonctions in the context of rainfall-ronoff modelling in a Sudanese savannah area. Hydrol. Sci. J. 36, 307–330. doi:10.1080/02626669109492517

Šimůnek, J., Hopmans, J.W., 2002. Parameter Optimization and Nonlinear Fitting. Methods Soil Anal. Part 1, Phys. Methods 139–158. doi:10.2136/sssabookser5.4.c7

Sonderup, M.J., Egemose, S., Bochdam, T., Flindt, M.R. (2015). Treatment efficiency of a wet detention pond combined with filters of crushed concrete and sand: a Danish full-scale study of stormwater. Environ Monit Assess 758: 1-18, DOI 10.1007/s10661-015-4975-7

UMS GmbH, 2015. UMS (2015): Manual HYPROP, Version 2015-01.

Van Dam, J.C. Van, Stricker, J.N.M., Droogers, P., 1994. Inverse Method to Determine Soil Hydraulic Functions from Multistep Outflow Experiments. Soil Sci. Soc. Am. J. 58, 647–652. doi:10.2136/sssaj1994.03615995005800030002x

van Genuchten, M.T., 1980. A Closed-form Equation for Predicting the Hydraulic Conductivity of Unsaturated Soils1. Soil Sci. Soc. Am. J. 44, 892. doi:10.2136/sssaj1980.03615995004400050002x

van Genuchten, M.T., Leij, F.J., Yates, S.R., 1991. The RETC Code for Quantifying the Hydraulic Functions of Unsaturated Soils. United States Environ. Reseach Lab. 93. doi:10.1002/9781118616871

Van Genuchten, M.T., Wierenga, P.J., 1976. Mass Transfer Studies in Sorbing Porous Media I. Analytical Solutions. Soil Sci. Soc. Am. J. 40, 473–480. doi:10.2136/sssaj1976.03615995004000040011x

Vogel, T., Cislerova, M., 1988. On the reliability of unsaturated hydraulic conductivity calculated from the moisture retention curve. Transp. Porous Media 3, 1–15. doi:10.1007/BF00222683

Wohling, T., Vrugt, J.A., Barkle, G.F., 2008. Comparison of Three Multiobjective Optimization Algorithms for Inverse Modeling of Vadose Zone Hydraulic Properties. Soil Sci. Soc. Am. J. 72, 305–319. doi:10.2136/sssaj2007.0176

CHAPTER 4 RESULTS AND DISCUSSION

This chapter presents the results of the experimental investigations and numerical analysis performed. To evaluate the accuracy of the method proposed some statistical indices have been assessed.

4.1 Hydraulic properties of the materials

The HYDRUS model is a widely used finite-element model for simulating the movement of water in variably saturated media. Although it has been mainly used to model soil infiltration, its applicability has been tested out with good results also to further types of porous media. In this view, the added value of this work is the dimensionality reduction of the material parameter space by carrying out specific experimental analyses on some materials in order to define their hydraulic properties and, therefore, to ensure a more accurate hydraulic modelling based on measured experimental data.

Hydraulic properties of the wear material were measured by using the clay tank described in the previous section. The gravimetrically determined saturated water contents for two samples, θ_{s1}, were 0.106 and 0.113 cm^3 cm^{-3}. Then, by using RETC code (van Genuchten et al., 1991), other parameters of the retention curve were obtained (Table 4.1). Results from this experiment, exhibit a satisfactory agreement between fitted and measured value of volumetric water content as indicated by the coefficient of determination for the regression of observed versus fitted values, which is equal to R^2=0.999. The value for parameter n of the SWRC value denotes that desaturation does not occur in a quick way while the high value of α denotes that the retention capacity of the material is low. A representation of the SWRC of this material is given in Figure 4.1.

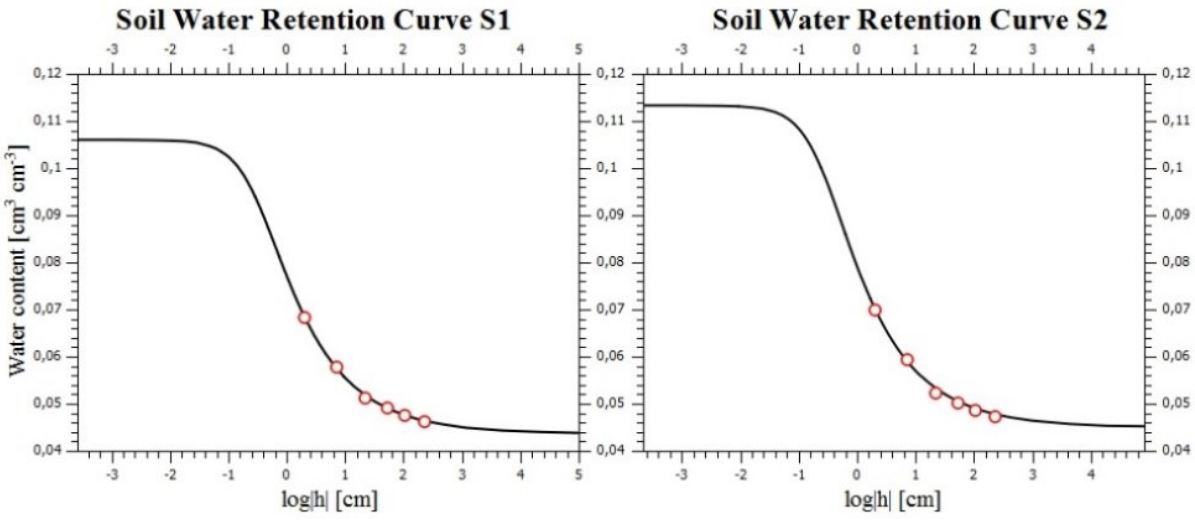

Figure 4.1 Wear layer SWRC

The structure of the porous concrete is to have voids interconnected with dimensions ranging from 2 mm to 8 mm depending on mix portion, aggregates and the degree of compaction (Deo and Neithalath, 2010; Tennis et al., 2004). The volume fraction, size distribution and topological structure of the pores are the critical parameters in controlling permeable concrete behaviour (Sansalone et al., 2008). Normally, porosity of permeable concrete is typically 7-35%, depending on a host of variables such as cement paste fraction, aggregate content, gradation and particle shape, water/cement ratio and compaction effort (Ong et al., 2016). Concretes with porosity < 7% tend to give slower water percolation while porosities > 35% result in highly permeable, but very weak concretes.

Hydraulic conductivity of porous concrete is the most investigated parameter in the literature. It varies from 0.18 cm min^{-1} to 198 cm min^{-1} (Coughlin et al., 2012; Deo et al., 2010; Haselbach, 2010; Ibrahim et al., 2014; Montes and Haselbach, 2006; Sumanasooriya and Neithalath, 2011). In the study of Kia et al. (2017), although a positive correlation between porosity and permeability is showed, the permeability is not only dependent on total porosity,

but also on other characteristics such as size distribution, shape, degree of connectivity and tortuosity of the pores. In this way, results from our experiment denotes a moderate percolation through this layer confirmed by values of θ_{s1} for both samples. By using this experimental procedure, no information can be given about hydraulic conductivity of this layer. The multistep outflow experiment has been performed on duplicate samples of the bedding layer to determine its hydraulic properties (Van Dam et al., 1994). For both samples, the saturated water content θ_{s2} was measured starting from the final water content and water balance in the sample and it was found equal to θ_{s2} = 0.41 and 0.37 cm^3 cm^{-3}, The θ_{r2} value was set at 0 cm^3 cm^{-3}. Other parameters of the hydraulic functions (van Genuchten, 1980) were optimized from the measured outflow, soil water retention data and the single porosity model in HYDRUS-1D (Table 4.1) .

Parameters obtained by using the multistep outflow experiment combined with HYDRUS-1D confirm that the bedding layer has a reduced porosity. Values of α and *n* for both samples denote that desaturation occurs very quickly. This aspect could be positive considering that one of the permeable pavements goals is to infiltrate as much water as possible in order to limit the surface runoff. Results obtained for the values of the hydraulic conductivity, are instead very variable for both samples. Confidence limits exhibit a wide range of values that suggest proceeding with further analysis. However, the estimated parameters for both materials indicated that the hydraulic behaviour of the layers was characterized by high flow rates and negligible retention capacity. A representation of the SWRC of this material is given in Figure 4.2.

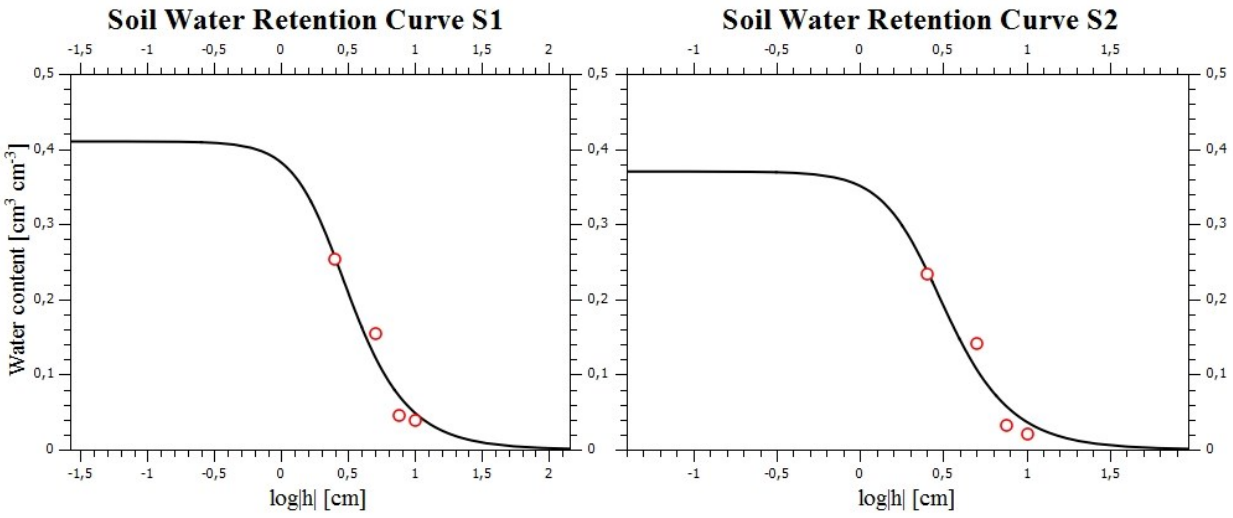

Figure 4.2 Bedding layer SWRC

4.2 Sensitivity Analysis

The clay tank and multistep outflow experiments allow to measure different material hydraulic parameters, thus reducing the dimensionality of the inverse problem to a few factors. However, before proceeding with the parameters optimization, the Morris method was used to carry out a sensitivity analysis of the unknown material hydraulic parameters. Results of the sensitivity analysis are reported in Figure 4.3. In particular, the scatter plots of the two sensitivity measures σ and μ^* for both water content (left plot in Figure 4.3) and outflow (right plot in Figure 4.3) are shown.

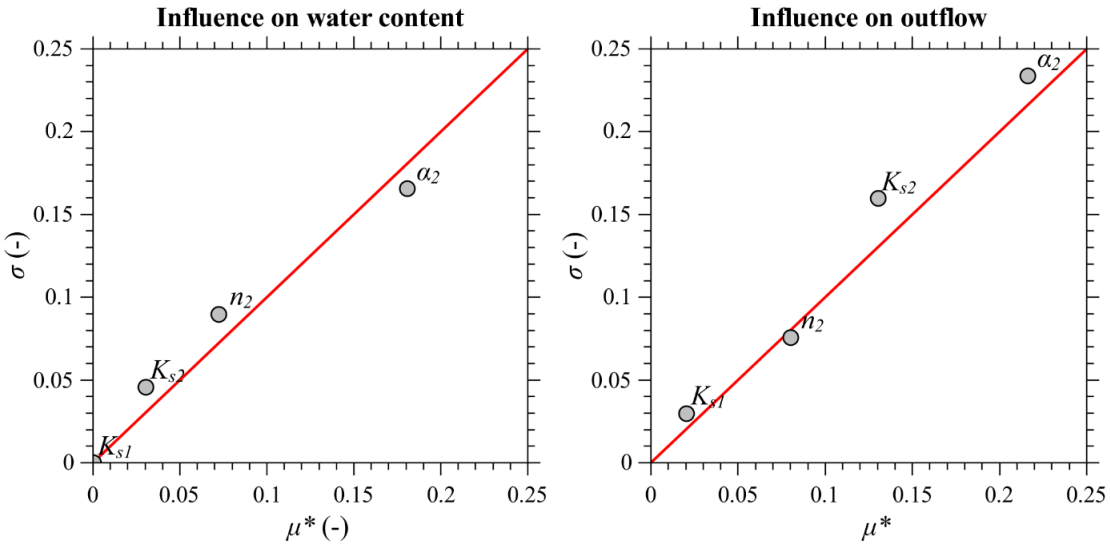

Figure 4.3 A scatter plot of sensitivity analysis measurements

At a first inspection, it is evident that for each factor σ and μ^* exhibit similar values, indicating that none of the empirical parameters has a purely linear effect. This is evident from Figure 4.3, in which all points lie around the diagonal (red line in Figure 4.3). The saturated hydraulic conductivity of the wear layer, K_{s1}, has a negligible influence on the agreement between the measured and simulated water content, as highlighted by its low values of σ and μ^*. In this case, K_{s1} can be fixed at any value in the parameter space without affecting the fitting's quality. Moreover, its effect on the simulated outflow (right plot in Figure 4.3) appears rather limited but not negligible, as for the water content in the bedding layer. In the study of Brunetti et al. (2016), who carried out a Global Sensitivity Analysis on material hydraulic parameters of a layered permeable pavement, the saturated hydraulic conductivity of the wear layer had, similarly to our findings, limited effect on the outflow, however the interaction with other parameters was significant in that study. This discrepancy could be mainly related to the differences in the adopted porous concrete, and modelling scenarios. It must be emphasized that SA results reveal that the experimental measurement

of K_{s1} would not significantly increase the accuracy of the fitting, considering its limited effect on both water content and outflow.

Conversely, the two empirical parameter α_2 and n_2 of the bedding layer have appreciable effect on both outflow and water content, with the former being the most influent parameters among those investigated in the SA. This behavior is intuitive since these two parameters both govern the shape of the van Genuchten-Mualem function, thus their influence on the retention properties of the material is significant. An accurate experimental determination of α_2 and n_2 would increase significantly the accuracy of the fitting for both the outflow and water content. The saturated hydraulic conductivity K_{s2} of the bedding layer exhibits different sensitivity for the outflow and water content. While its influence on the agreement between simulated and measured water content in the bedding layer is appreciable but limited, its impact on the simulated outflow is significant. More specifically, it is the second most influent parameter for the outflow. For both objective functions, K_{s2} exhibits a value of σ slightly higher than μ^*, indicating its nonlinear effect on the variance's output.

Summarizing, none of the analysed factors can be fixed at any feasible value in the parameter space without affecting simultaneously the quality of the fitting for the water content and outflow. Thus, the dimensionality of the inverse cannot be further reduced. The saturated hydraulic conductivity of the wear layer is relatively insensitive, while the material hydraulic properties of the bedding layer mainly drive the model's behaviour.

4.3 Inverse solution estimation

From the results obtained using clay tank experiment combined with the RETC code and multistep outflow experiments combined with HYDRUS-1D, it was possible to limit the

optimization problem to few parameters. However, in order to make the problem "well-posed" and whereas the confidence limits of the bedding layer K_{s2} exhibit a very wide range for both samples analysed, it has been decided to proceed also with the optimization of the SWRC parameters of this layer. Two sets of inverse solution data were used to yield a robust well-calibrated model. In particular, the volumetric water content in the bedding layer and the outflow at the seepage face have been used.

In this way, the list of parameters to be optimized in the inverse problem is given as follow: K_{s1} (cm min^{-1}), α_2 (cm^{-1}), n_2 (-), K_{s2} (cm min^{-1}) where the subscripts *1* and 2 are for the wear and bedding layer, respectively. In Table 4.1 results from the two previous experiments and results from the inverse solution optimization, are shown.

Layer		θ_r (cm^{3}cm^{-3})	θ_s (cm^{3}cm^{-3})	α (cm^{-1})	n (-)	K_s (cm min^{-1})
Wear layer – W1	CT	0.044	0.106	3.37	1.47	-
Wear layer - W2	CT	0.045	0.113	4.03	1.47	-
Wear layer	LSPPS	0.044	0.106	3.37	1.47	1.56±0.4
Bedding layer - B1	MSO	0	0.41	0.43	2.45	236
Bedding layer – B2	MSO	0	0.37	0.4	2.65	32
Bedding layer	LSPPS	0	0.4	0.27±0.04	2.0±0.1	69.27±14.40
Sub-base layer	Brunetti et al (2016a)	0.00	0.01	0.27	2.41	96.70

Table 4.1. Hydraulic properties of the materials; CT – clay tank, MSO – multistep outflow experiment, LSPPS – lab-scale permeable pavement system, W1, W2, and B1, B2 – sample replicates for wear and bedding layers, respectively.

Parameters obtained from the inverse solution optimization exhibit a satisfactory agreement between the fitted and measured data, as indicated by the coefficient of determination for regression of observed versus fitted values is equal to R^2=0.985, and mostly because the retention capacity of the entire system is negligible. This is also confirmed by the fact that the values confidence limits are acceptable. Saturated hydraulic conductivity of the bedding layer, K_{s2}, is in the range of measured values. Its high value indicates a high infiltration capacity, which has to be expected considering the coarse nature of the material. It is more than an order of magnitude higher than the saturated hydraulic conductivity of the wear layer, and slightly lower than the value reported for the sub-base layer, which is composed of crushed stone. The value of parameter n_2 of the SWRC value denotes that desaturation occurs in a moderate way for the bedding material while the value of α_2 denotes that the retention capacity of the material is appreciable.

The measured porosity for the bedding layer is slightly higher than the prescriptions of ICPI, which recommends a porosity of about 20%. This difference can be related to the sampling procedures of the two samples that have been difficult due to the coarse nature of the material and may have affected the determination of the saturated water content.

Figure 4.4 shows a comparison between the measured and modelled hydrographs for the calibration period. The inverse solution optimization resulted in a value of NSE > 0.90, which confirmed the high accuracy between the measured and estimated parameters. The model was able to reproduce with high accuracy the fast hydraulic response of the hydrograph during precipitation events at different intensities with negligible over- and under-estimations in the ascending and descending phases of the hydrograph.

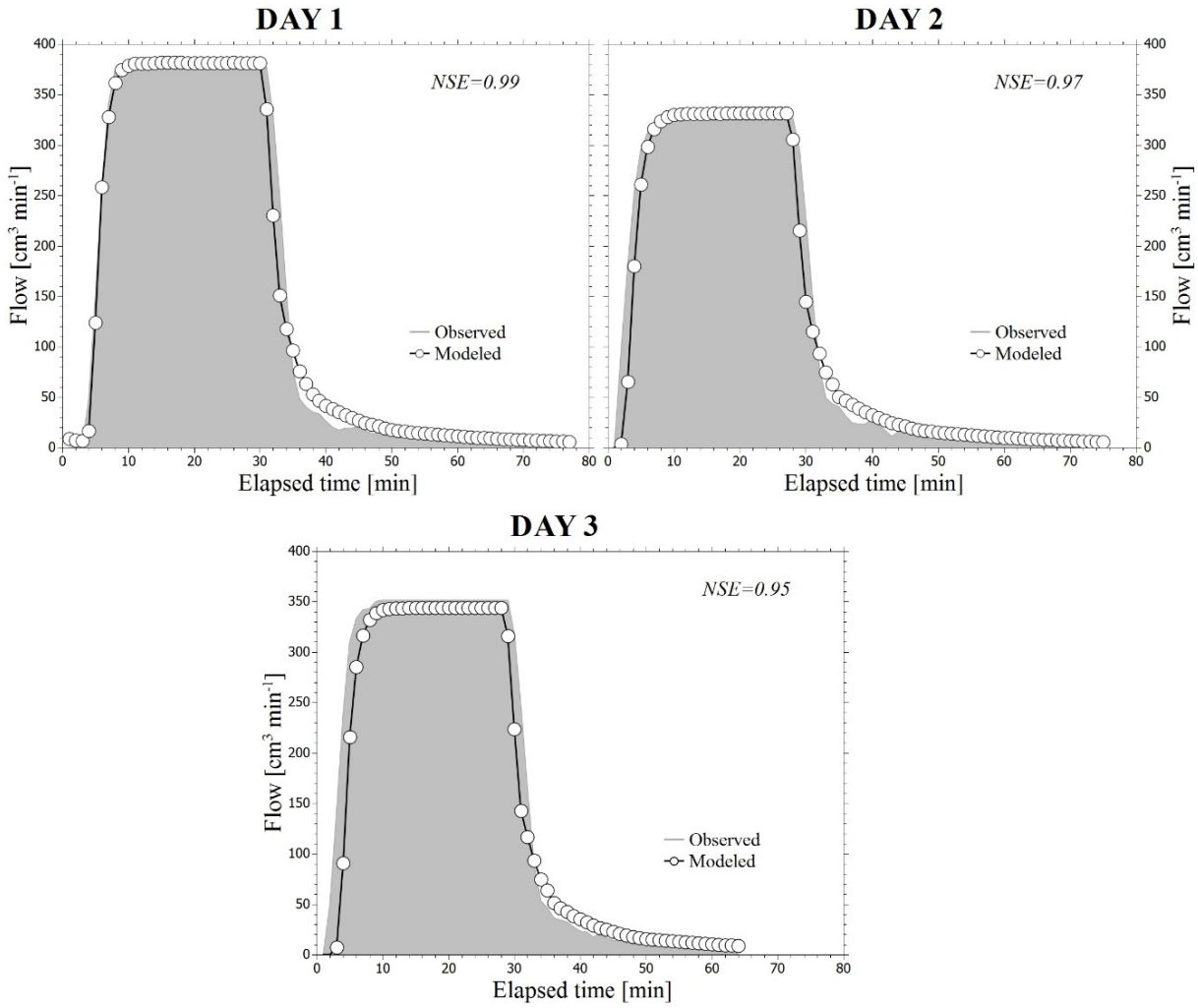

Figure 4.4 A comparison between measured and simulated outflows versus time in the calibration period

Figure 4.5 shows the simulated against measured volumetric water contents (VWC) within the bedding layer for the calibration period. This graph shows a bisector line (red full line), which indicates a good agreement between simulated and measured water content, and a linear regression line (grey dashed line). The good performance of the model is confirmed by the determination coefficient $R^2 > 0.80$. The comparison between the bisector and regression lines indicates that the model slightly underestimated the volumetric water content for the first two events and slightly overestimated the VWC for the third event. It must be

emphasized that the points in Fig. 4.5 that exhibit a relatively high bias are those related to the beginning of each precipitation event. This indicates that the model tends to underestimate the water content in the dry period. This can be related to a combined overestimation of the actual evaporation and underestimation of the retention capacity of the material.

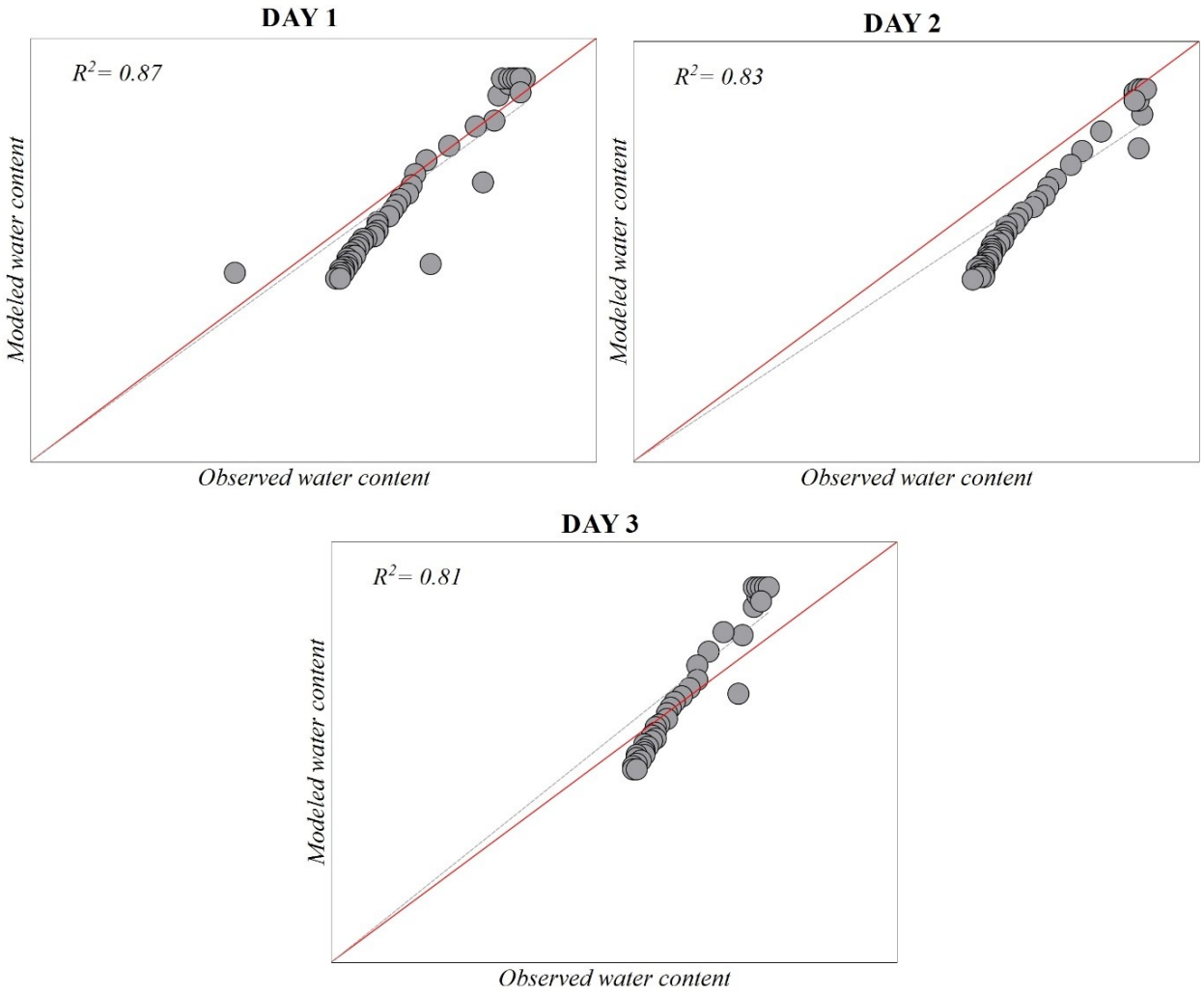

Figure 4.5 A comparison between measured and simulated water content in the calibration period

4.4 Model validation

To evaluate the reliability of the estimated parameters, the model was validated using an independent set of experimental data. Figure 5 and Figure 6 show the comparison between measured and simulated data in the validation period for hydrograph and water content respectively. Table 4.2 summarizes the material hydraulic parameters used in the validation period.

Wear layer					
θ_r (cm^3cm^{-3})	θ_s (cm^3cm^{-3})	α (cm^{-1})	n (-)	K_s (cm min^{-1})	l (-)
0.04	0.106	3.37	1.47	1.56	0.5
Bedding layer					
θ_r (cm^3cm^{-3})	θ_s (cm^3cm^{-3})	α (cm^{-1})	n (-)	K_s (cm min^{-1})	l (-)
0.00	0.40	0.27	2.00	69.27	0.5
Sub-base layer					
θ_r (cm^3cm^{-3})	θ_s (cm^3cm^{-3})	α (cm^{-1})	n (-)	K_s (cm min^{-1})	l (-)
0.00	0.01	0.27	2.41	96.70	0.5

Table 4.2 Material hydraulic parameters used in the validation period

Figure 4.6 shows a comparison between measured and modelled hydrographs during the validation period.

The NSE values remain quite similar to calibration period values and they are still close to value 1, which confirms the reliability of the calibrated model. For these reasons, the simulated hydrograph provides a very accurate description of the hydraulic behaviour of the

pavement at different rain intensities. This ability of the calibrated model is important especially regarding the analysis of traditional drainage systems and LID techniques because a correct description of the hydrograph during different precipitation events, gives information about the lag time and the intensity of peak flow, which are fundamental to establish the hydrological performance and analysis of traditional drainage systems, and for the evaluation of benefits of LID implementation. Information about volumetric water content is given in Figure 4.7. The good performance of the calibrated model is also confirmed by the determination coefficient R^2 between the simulated versus the measured volumetric water contents. The comparison between the bisector and regression lines indicates that the model slightly underestimated the VWC.

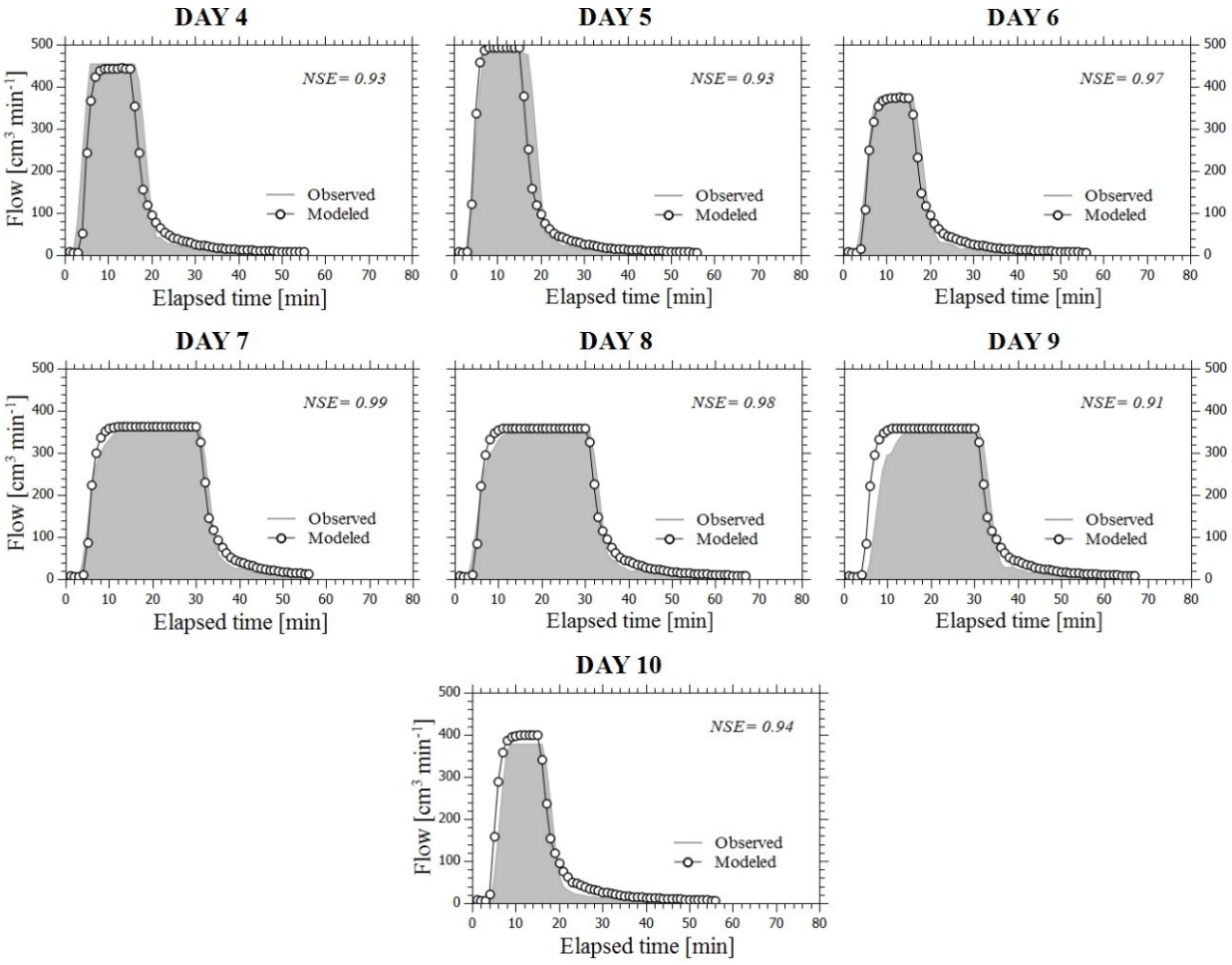

Figure 4.6 A comparison between measured and simulated outflows versus time in the validation period

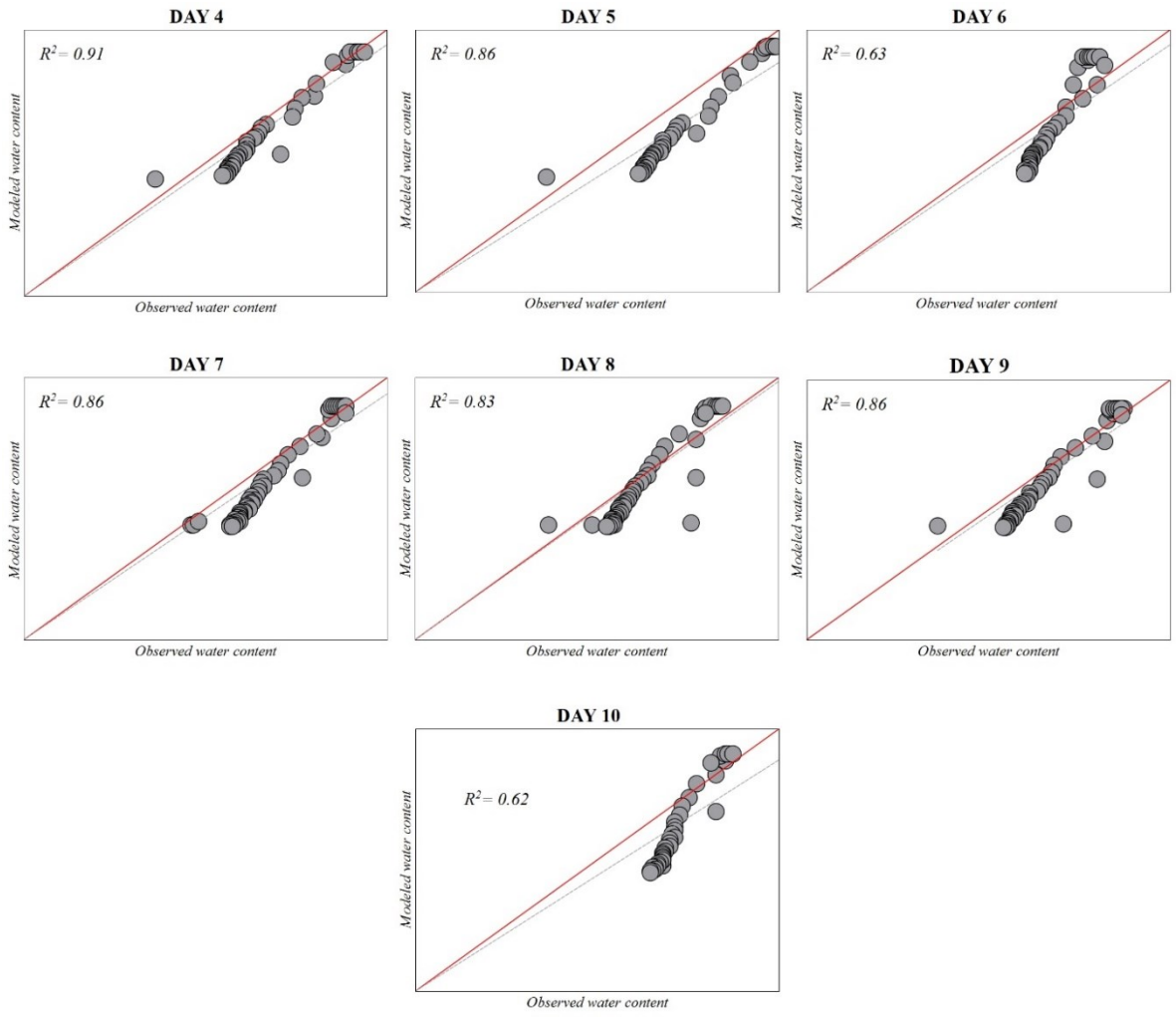

Figure 4.7 A comparison between measured and simulated VWC in the validation period

Validation of the hydraulic model aimed to identify the hydraulic behaviour of the pavement used in this study. The robustness of the model is ensured by the limited number of hydraulic parameters to be calibrated (the experiments conducted on the materials allowed to uniquely define some of the hydraulic parameters of the pavement structure) and the sensitivity analysis performed allowed to evaluate the effects of the parameters on the response of the entire system. The whole approach (experiments, SA, numerical analysis) has been a novelty in the analysis of these LID systems. Thus, previous studies in the literature on lab-scale test

bed and existing PP facilities were mainly focused on the assessment of hydrological effects, with emphasis on the peak flow and volume reduction.

Among all LID practices, permeable pavements are those that lack modelling tools able to describe their hydraulic behaviour the best. The heterogeneity of materials that compose a permeable pavement, together with the high infiltration rates (Brattebo and Booth, 2003), pose complex problems in the numerical modelling of these systems. Very few modelling tools

exist in the literature for permeable pavements. One of them is included in the Storm Water Management Model (SWMM) (Gironás et al., 2010). However, results obtained by SWMM have proven to be inaccurate, especially in the description of the effects of base and sub-base layers on the infiltration processes (Zhang and Guo, 2015). Conversely, the HYDRUS model has proven to be useful for the description of variably-saturated flow in permeable pavements. Illgen et al. (2007) used HYDRUS-2D for the numerical analysis of a permeable pavement and calibrated the model against experimental data collected at a laboratory test facility. The calibrated model was then used to simulate different scenarios not investigated during the laboratory campaign. The Illgen et al. (2007) study provided only limited details about the calibration of soil hydraulic parameters and their uncertainty and sensitivity with no experimental investigations on construction materials.

In another work of Palla et al. (2015), the hydrologic response of a lab-scale PP has been investigated under different hydrologic conditions and system settings. The laboratory test programme was designed to investigate the influence of rainfall intensity and pavement slope on the hydrologic response of permeable pavements and although laboratory test results confirm the drainage capacity of the permeable pavements, indeed no surface runoff occurs for all the investigated systems, no information was given about construction materials and

their properties. The hydrological assessment was given by using discharge index and regarding the impact of the slope condition, results indicated that the higher the slope the higher is the drainage capacity, irrespective of the stratigraphy and the rainfall intensity. This is not really true and should be confirmed by a numerical analysis and SA on physical parameters.

This thesis conversely, aimed to give a comprehensive description of the hydraulic behaviour of a permeable pavement and proposed a general methodology for the estimation of its hydraulic parameters.

4.5 Batch experiment results

To establish the adsorption isotherms and evaluate the adsorption capacity of each material, individual metal samples were tested in duplicate. The results are the average of the two sets of tests.

Table 4.3 describes the batch adsorption test results for Cu in the wear layer. Sample calculations are described below.

Observation	Influent [mg/l]	Effluent [mg/l]	Absorbed mass [mg/g]	% Absorbed
1	40	0.30	0.99	99.25
2	60	1.60	1.46	97.33
3	80	19.00	1.52	76.25
4	120	36.00	2.10	70.00

Table 4.3 Batch experiment results for Cu in the wear layer

where Influent is the concentration of the initial solution [mg/l], Effluent is the concentration of the solution after the batch experiment, Absorbed mass is the amount of Cu absorbed [mg] and % Absorbed represent the potential removal efficiency at equilibrium of the wear material. Amount of Cu adsorbed = 40-0.30 = 39.70 mg/l which is equivalent to 9.92 mg/250 ml of solution. As l0 g of material was placed in 250 ml solution, the amount of Cu adsorbed per g of concrete is 0.99 mg/g.

No absorption was detected during the performance of the batch experiment of the bedding and sub-base layer.

Table 4.4 describes the batch adsorption test results for Zn in the wear layer. Sample calculations are described below.

Observation	Influent [mg/l]	Effluent [mg/l]	Absorbed mass [mg]	% Absorbed
1	40	10	0.75	75.00
2	60	16	1.10	73.33
3	80	24	1.40	70.00
4	120	37	2.07	69.16

Table 4.4 Batch experiment results for Zn in the wear layer

No absorption was detected during the performance of the batch experiment of the bedding and sub-base layer.

In general, an adsorption isotherm is an invaluable curve describing the phenomenon governing the retention (or release) or mobility of a substance from the aqueous porous media or aquatic environments to a solid-phase at a constant temperature and pH (Allen et al., 2004; Limousin et al., 2007). Adsorption equilibrium (the ratio between the adsorbed amount with

the remaining in the solution) is established when an adsorbate containing phase has been contacted with the adsorbent for sufficient time (Foo and Hameed, 2010). Thus, adsorption isotherm can be described by a mathematical correlation usually depicted by graphically expressing the solid-phase against its residual concentration, which constitutes an important role towards the modelling analysis, operational design and applicable practice of the adsorption systems.

Results from the batch experiments on materials have shown surprisingly that only porous concrete has a remarkable adsorption potential while other materials do not play any roles in the heavy metals (Copper and Zinc) treatment. In this way, the adsorption of Cu and Zn has satisfied the linear isotherm (Figure 4.8). A linear equation was obtained by fitting the experimental data points with a coefficient of determination R^2= 0.82 for Copper and R^2 =0.99 for Zinc. Results shown that the adsorption capacity of the porous concrete is higher in Cu than Zn.

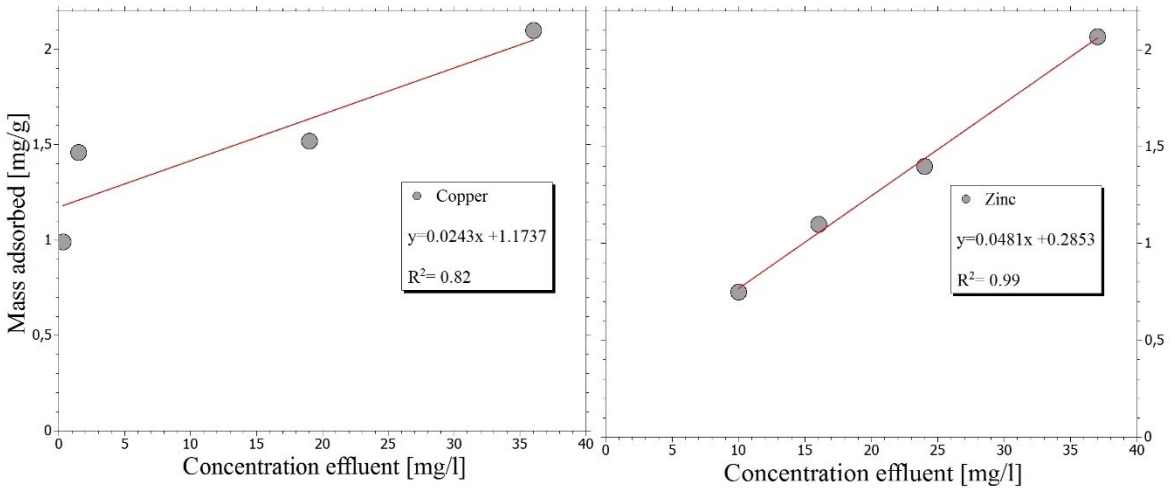

Figure 4.8 Adsorption isotherm

4.6 Water quality performance

Water quality performance of the lab-scale system has also been investigated. The inflow concentration event by event are listed in Table 3.2 of the methods section.

During the experiments, the outflows from the pavement have been collected. The samples were taken into flasks of 50 ml with a one-minute frequency and then placed in a laboratory centrifuge in order to separate any solids particles inside and filtered through the 540μm filter paper and finally the concentration of the samples was measured by using the Atomic Absorption Spectrophotometer (AAS). Before each measurement campaign, the AAS has always been calibrated by measuring some standard solutions prepared for this purpose.

Figure 4.9 represents the removal efficiency of Copper and Zinc of the permeable pavement under several inflow concentrations. As concentration outflow for each pollutant was considered the maximum value in the outflow, while inflow was constant rate.

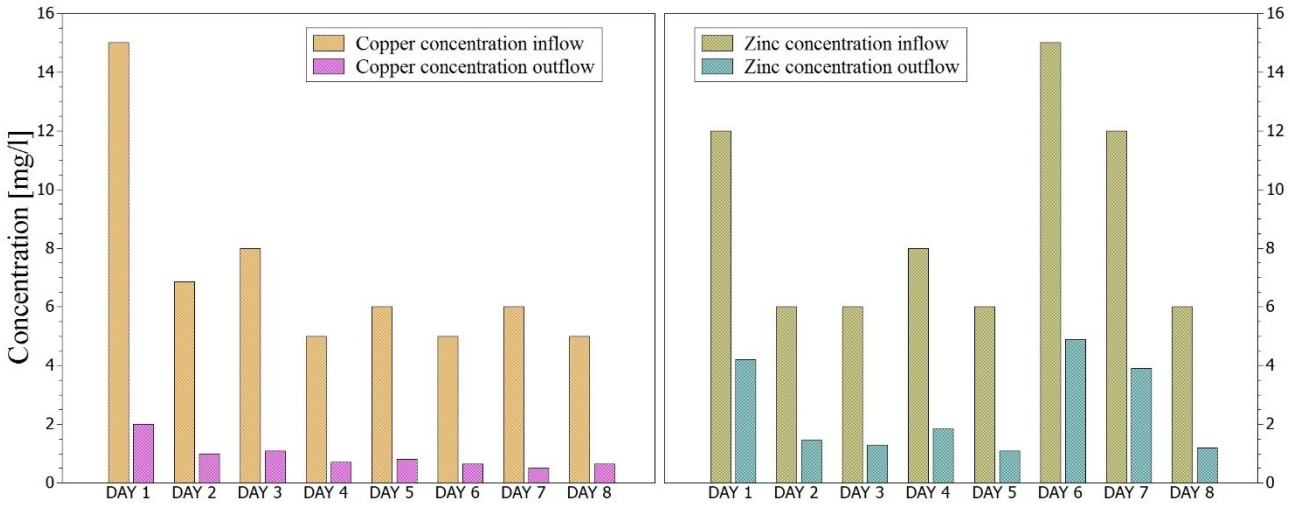

Figure 4.9 Removal efficiency of the lab-scale system

Although batch experiment gave a measure of the potential capacity of porous concrete, some flow contaminant tests have been performed. This decision was due to the fact that batch

experiment is an equilibrium test the heavy metal solution is allowed to act in contact with the material until it reach the equilibrium phase while water flow through the permeable pavement system is a fast process due to the porous nature of the structure.

So, the removal rates of Cu and Zn of the lab-scale pavements range from 85% to 92% and from 65% to 82%, respectively (Table 4.5).

Rainfall events [-]	Cu_{in} [mg/l]	Cu_{out} [mg/l]	Zn_{in} [mg/l]	Zn_{out} [mg/l]	% Cu	% Zn
Day 1	15.00	2.00	12.00	4.20	86.67	65.00
Day 2	6.85	1.00	6.00	1.45	85.40	75.83
Day 3	8.00	1.10	6.00	1.30	86.25	78.33
Day 4	5.00	0.70	8.00	1.85	86.00	76.88
Day 5	6.00	0.80	6.00	1.10	86.67	81.67
Day 6	5.00	0.65	15.00	4.90	87.00	67.33
Day 7	6.00	0.50	12.00	3.90	91.67	67.50
Day 8	5.00	0.65	6.00	1.20	87.00	80.00
Day 9	-	-	-	-	-	-
Day 10	-	-	-	-	-	-

Table 4.5 Heavy metals removal rates from lab-scale system

Similar to the results obtained from the batch experiment, the Cu removal rates of the lab-scale pavement are higher than Zn removal rates. In addition, there is no significant difference in the heavy metal removal rates between the flow contaminant experiment and the batch experiment (low concentration), it means that the equilibrium phase in the concrete

blocks is reached in the initial time of the batch experiment. Further studies and experiments are suggested in this field.

4.7 References

Allen, S.J., Mckay, G., Porter, J.F., 2004. Adsorption isotherm models for basic dye adsorption by peat in single and binary component systems. J. Colloid Interface Sci. 280, 322–333. doi:10.1016/j.jcis.2004.08.078

Brattebo, B.O., Booth, D.B., 2003. Long-term stormwater quantity and quality performance of permeable pavement systems. Water Res. 37, 4369–4376. http://dx.doi.org/10.1016/S0043-1354(03)00410-X

Coughlin, J.P., Campbell, C.D., Mays, D.C., 2012. Infiltration and Clogging by Sand and Clay in a Pervious Concrete Pavement System. J. Hydrol. Eng. 17, 68–73. doi:10.1061/(ASCE)HE.1943-5584.0000424

Deo, O., Neithalath, N., 2010. Compressive behavior of pervious concretes and a quantification of the influence of random pore structure features. Mater. Sci. Eng. A 528, 402–412. doi:10.1016/j.msea.2010.09.024

Deo, O., Sumanasooriya, M., Neithalath, N., 2010. Permeability Reduction in Pervious Concretes due to Clogging: Experiments and Modeling. J. Mater. Civ. Eng. 22, 741–751. doi:10.1061/(ASCE)MT.1943-5533.0000079

Foo, K.Y., Hameed, B.H., 2010. Insights into the modeling of adsorption isotherm systems. Chem. Eng. J. doi:10.1016/j.cej.2009.09.013

Gironás, J., Roesner, L.A., Rossman, L.A., Davis, J., 2010. A new applications manual for the Storm Water Management Model (SWMM). Environ. Model. Softw. 25, 813–814. http://dx.doi.org/10.1016/j.envsoft.2009.11.009

Haselbach, L.M., 2010. Potential for Clay Clogging of Pervious Concrete under Extreme Conditions. J. Hydrol. Eng. 15, 67–69. doi:10.1061/(ASCE)HE.1943-5584.0000154

Ibrahim, A., Mahmoud, E., Yamin, M., Patibandla, V.C., 2014. Experimental study on Portland cement pervious concrete mechanical and hydrological properties. Constr. Build. Mater. 50, 524–529. doi:10.1016/j.conbuildmat.2013.09.022

Illgen, M., Harting, K., Schmitt, T.G., Welker, A., 2007. Runoff and infiltration characteristics of pavement structures – review of an extensive monitoring program. Water Sci. Technol. 56, 133–140. http://dx.doi.org/10.2166/ wst.2007.750

Kia, A., Wong, H.S., Cheeseman, C.R., 2017. Clogging in permeable concrete: A review. J. Environ. Manage. doi:10.1016/j.jenvman.2017.02.018

Limousin, G., Gaudet, J.P., Charlet, L., Szenknect, S., Barthès, V., Krimissa, M., 2007. Sorption isotherms: A review on physical bases, modeling and measurement. Appl. Geochemistry. doi:10.1016/j.apgeochem.2006.09.010

Montes, F., Haselbach, L., 2006. Measuring Hydraulic Conductivity in Pervious Concrete. Environ. Eng. Sci. 23, 960–969. doi:10.1089/ees.2006.23.960

Ong, S.K., Wang, K., Ling, Y., Shi, G., 2016. Pervious Concrete Physical Characteristics and Effectiveness in Stormwater Pollution Reduction . InTrans Project Reports. http://www.intrans.iastate.edu

Palla, A., Gnecco, I., Carbone, M., Garofalo, G., Lanza, L. and Piro, P., 2015. Influence of stratigraphy and slope on the drainage capacity of permeable pavements: Laboratory results. Urban Water Journal, 12, 394–403.

Sansalone, J., Kuang, X., Ranieri, V., 2008. Permeable Pavement as a Hydraulic and Filtration Interface for Urban Drainage. J. Irrig. Drain. Eng. 134, 666–674. doi:10.1061/(ASCE)0733-9437(2008)134:5(666)

Sumanasooriya, M.S., Neithalath, N., 2011. Pore structure features of pervious concretes proportioned for desired porosities and their performance prediction. Cem. Concr. Compos. 33, 778–787. doi:10.1016/j.cemconcomp.2011.06.002

Tennis, P.D., Leming, M.L., Akers, D.J., 2004. Pervious Concrete Pavements. Portland Cement Association, Skokie, Illinois, and National Ready Mixed Concrete Association, Silver Spring, Maryland, USA.

Van Dam, J.C. Van, Stricker, J.N.M., Droogers, P., 1994. Inverse Method to Determine Soil Hydraulic Functions from Multistep Outflow Experiments. Soil Sci. Soc. Am. J. 58, 647–652. doi:10.2136/sssaj1994.03615995005800030002x

van Genuchten, M.T., 1980. A Closed-form Equation for Predicting the Hydraulic Conductivity of Unsaturated Soils1. Soil Sci. Soc. Am. J. 44, 892. doi:10.2136/sssaj1980.03615995004400050002x

van Genuchten, M.T., Leij, F.J., Yates, S.R., 1991. The RETC Code for Quantifying the Hydraulic Functions of Unsaturated Soils. United States Environ. Reseach Lab. 93. doi:10.1002/9781118616871

Zhang, S., Guo, Y., 2015. SWMM simulation of the storm water volume control performance of permeable pavement systems. J. Hydrol. Eng. 20, 06014010. http://dx.doi.org/10.1061/(ASCE)HE.1943-5584.0001092.

CHAPTER 5 SUMMARY, CONCLUSIONS AND FUTURE DIRECTIONS.

5.1 General conclusions

This thesis tried to improve knowledge of the hydrologic/hydraulic and water quality performance of permeable pavements in order to justify the feasibility of the use of this systems in stormwater management. The work included the application of numerical algorithms and laboratory techniques, which are rather new in urban hydrology. A lab-scale experimental facility was used as a case study to investigate the behavior of the pavement under different simulated storm events (both water flow and quality performance). More specifically, this dissertation made contributions in three aspects:

1. investigating and comparing the hydraulic and water quality performance of a permeable pavement under different simulated storm events;
2. evaluating the ability of pollutant removal by individual layers of pavement structure and assessing the pollutant removal efficiency of the entire pavement structure;
3. developing modelling tools for predicting flow through the permeable pavements by suggesting experimental and mathematical procedures for model calibration, which consists of: a) experimental design (system construction, and number and character of measured transient flow data); b) methods for independently evaluating material hydraulic properties; c) additional optimization of material hydraulic parameters using the transient flow data; and d) model validation.

Chapter 1 and Chapter 2 were dedicated to the identification of the stormwater management problem and to the solution proposed to solve it. Following regulations identified in these two chapters, a lab-scale permeable pavement system was built for the purpose.

Regarding water flow modelling, a rather new methodology was proposed to investigate the hydraulic/hydrologic behavior of the pavement systems consisting in use laboratory investigation and numerical analysis using a mechanistic model such as HYDRUS-2D in Chapter 3. In addition to give more information about the ability of each material to retain pollutants, the batch experiment method has been performed. Finally, Chapter 4 was dedicated to the evaluation of the results and discussion.

In particular, the suitability of the HYDRUS-2D software package, to correctly describe the hydraulic behaviour of a lab-scale permeable pavement system, and identifiability of the actual/effective material hydraulic parameters of the construction materials has been investigated. The single porosity model implemented by the HYDRUS software in describing the system has been considered. The coefficient of determination R^2 and the widely used Nash-Sutcliffe efficiency index have been used to assess the model. The inverse solution optimization which implements a Marquardt-Levenberg type parameter estimation technique for the inverse estimation of the material hydraulic parameters was conducted to calibrate the model. To have a very robust and well-posed model, two sets of measured data have been used.

In order to reduce the dimensionality of the inverse problem, a clay tank experiment and the multistep outflow experiment were used to determine the unsaturated material hydraulic properties of two of the three layers before the calibration of the model. Coupled with experimental procedures on some materials, a sensitivity analysis has also been performed. These two approaches allowed to obtain a model with few parameters to be calibrated which

is strictly connected with measured data from the pavement. This ensured a coherent calibration phase that reached an NSE value not lower than 0.95, which means a close agreement between the between measured and estimated parameters. The optimized parameters were then validated against an independent set of experimental data, resulting in an NSE not lower than 0.91, which indicates the reliability of the calibrated model.

The approach described above improved the identifiability of hydraulic parameters of permeable pavement and although pressure heads measurement could not be performed due the nature of our materials (concrete, fine gravel, stones), water content measurements helped to reduce uncertainty in the hydraulic parameters estimation. Finally, the results obtained with this work showed that the implementation of a model aimed at soil systems, together with accurate experimental and numerical procedures, has been able to accurately describe the hydraulic behaviour of a system of multiple layered granular materials that are not really soils.

Regarding the water quality performance, batch experiments and contaminant flow experiments have been proposed to evaluate the pollutant removal efficiency of the lab-scale systems. The batch experiment was conducted on each construction material but results shown that only concrete blocks contribute to the removal of the pollutants investigated. Both batch and flow contaminant experiment confirmed that Cu removal rates are higher than Zn removal rate. Overall, experiments confirmed the potential of this systems to treat dissolved heavy metals.

5.2 Future directions

This work was not intended as a conclusive act, but on the contrary as an intermediate step towards new and more effective applications of permeable pavements. A substantial novel approach in describing these systems concerned the merger of concepts and techniques related to other scientific fields. Laboratory investigations of construction materials by the methods commonly applied in studies of soils is an example.

Overall, based on the research results, several further investigations are recommended:

- the inclusion of different types of measurements, such as volumetric temperature and/or pressure head inside permeable pavement systems, could help in reducing the uncertainty in the estimated parameters and facilitate the calibration of mechanistic models;
- other potential applications of mechanistic models for permeable pavement can include the simulation of solute transport: the HYDRUS model could also implement solute transport through porous media but several experimental procedures are recommended in order to define reaction and transport parameter;
- further studies on removal rate of Nutrients and Hydrocarbons are suggested. It is well known that permeable pavement systems are able to retain these types of pollutants but addressing further details is recommended;
- temperature plays a key role in the solute adsorption and transport. In this way, investigations on a field-scale system (well equipped with sensors) are suggested in order to improve knowledge on the dynamics of solute transport;
- investigations on clogging phenomenon are strongly recommended. Although no clogging was detected during the experiments (conducted with clean water), further

investigations in this field are suggested because stormwater management technologies (including permeable pavements) are required to provide service to remove TSS.

Turco, M., Kodešová, R., Brunetti, G., Nikodem, A., Fér, M., Piro, P. (2017)

Unsaturated hydraulic behaviour of a permeable pavement: Laboratory investigation and numerical analysis by using the HYDRUS-2D model.

Journal of Hydrology Volume 554, November 2017

Journal of Hydrology 554 (2017) 780–791

Contents lists available at ScienceDirect

Journal of Hydrology

journal homepage: www.elsevier.com/locate/jhydrol

Research papers

Unsaturated hydraulic behaviour of a permeable pavement: Laboratory investigation and numerical analysis by using the HYDRUS-2D model

Michele Turco [a,*], Radka Kodešová [b], Giuseppe Brunetti [a], Antonín Nikodem [b], Miroslav Fér [b], Patrizia Piro [a]

[a] Department of Civil Engineering, University of Calabria, Rende, CS 87036, Italy
[b] Faculty of Agrobiology, Food and Natural Resources, Dept. of Soil Science and Soil Protection, Czech University of Life Sciences, Kamycká 129, CZ-16521 Prague 6, Czech Republic

ARTICLE INFO

Article history:
Received 4 July 2017
Received in revised form 14 September 2017
Accepted 3 October 2017
Available online 4 October 2017
This manuscript was handled by Prof. P. Kitanidis, Editor-in-Chief, with the assistance of J. Simunek, Associate Editor

Keywords:
LID
Permeable pavement
Urban drainage
Sensitivity analysis
Infiltration

ABSTRACT

An adequate hydrological description of water flow in permeable pavement systems relies heavily on the knowledge of the unsaturated hydraulic properties of the construction materials. Although several modeling tools and many laboratory methods already exist in the literature to determine the hydraulic properties of soils, the importance of an accurate materials hydraulic description of the permeable pavement system, is increasingly recognized in the fields of urban hydrology. Thus, the aim of this study is to propose techniques/procedures on how to interpret water flow through the construction system using the HYDRUS model. The overall analysis includes experimental and mathematical procedures for model calibration and validation to assess the suitability of the HYDRUS-2D model to interpret the hydraulic behaviour of a lab-scale permeable pavement system. The system consists of three porous materials: a wear layer of porous concrete blocks, a bedding layers of fine gravel, and a sub-base layer of coarse gravel. The water regime in this system, i.e. outflow at the bottom and water contents in the middle of the bedding layer, was monitored during ten irrigation events of various durations and intensities. The hydraulic properties of porous concrete blocks and fine gravel described by the van Genuchten functions were measured using the clay tank and the multistep outflow experiments, respectively. Coarse gravel properties were set at literature values. In addition, some of the parameters (K_s of the concrete blocks layer, and α, n and K_s of the bedding layer) were optimized with the HYDRUS-2D model from water fluxes and soil water contents measured during irrigation events. The measured and modeled hydrographs were compared using the Nash-Sutcliffe efficiency (NSE) index (varied between 0.95 and 0.99) while the coefficient of determination R^2 was used to assess the measured water content versus the modelled water content in the bedding layer ($R^2 = 0.81 \div 0.87$). The parameters were validated using the remaining sets of measurements resulting in NSE values greater than 0.90 ($0.91 \div 0.99$) and R^2 between 0.63 and 0.91. Results have confirmed the applicability of HYDRUS-2D to describe correctly the hydraulic behaviour of the lab-scale system.

1. Introduction

In recent decades, due to rapid expansion of urbanization, urban areas have experienced an increase of impermeable surfaces such as roofs, roads and other paved surfaces. This urban development has diminished natural soil drainage and has increased runoff volumes (Finkenbine et al., 2000). This phenomenon, coupled with a progressive increase of precipitation, due to climate change, could likely increase floods in urban areas. In this way, traditional urban drainage techniques, seem to be inadequate for the purpose.

Recently, to mitigate the effects of urbanization, Low Impact Development systems (LID), an innovative stormwater management approach, have gained popularity, despite the debate in the scientific community about their advantages compared to traditional drainage systems (Burns et al., 2012; Shuster and Rhea, 2013). LID systems consist of a series of facilities whose purpose is to reproduce the site's pre-developed hydrological processes using design techniques that infiltrate, filter, store, evaporate, and detain runoff close to its source. The most common LID techniques are green roofs, bioretention cells, infiltration trenches, wetlands, wet ponds, swales and permeable pavements. Benefits of LIDs in terms of runoff reduction and pollutants removal have been widely discussed in the literature (Carbone et al., 2014a; Huang et al., 2016; Kamali et al., 2017). For example, Kamali

* Corresponding author.
E-mail address: michele.turco@unical.it (M. Turco).

https://doi.org/10.1016/j.jhydrol.2017.10.005
0022-1694/

et al. (2017) investigated the performance of a permeable pavement under sediment loadings during its life span by evaluating the temporal and spatial clogging trends of this facility and by finding its vulnerability to sediment loadings during rainfalls.

Considering the complexity of the physical processes involved, modelling tools able to accurately interpret the behaviour of LIDs are required. Although in the literature there are several stormwater models that can be used to analyze LIDs, most of them lack a comprehensive description of the hydrological processes involved, and often do not include any parameters optimization techniques. Therefore, the scientific community has recently focused its attention on physically based models to describe the hydraulic behaviour of LIDs.

The HYDRUS software package (Šimůnek et al., 2016), is one of the most widely used software to simulate water flow and solute/heat transport in two-dimensional vertical or horizontal planes, in axisymmetrical three-dimensional domains, or in fully three-dimensional variably saturated domains. Recently, the HYDRUS models have been used in the literature for the description of the hydraulic behaviour of LIDs such as green roofs and permeable pavements with optimal results (Brunetti et al., 2016a,b; Carbone et al., 2014a,b; Carbone et al., 2015a; Hilten et al., 2008; Palla et al., 2009; Qin et al., 2016; Yang et al., 2015). However, despite the satisfactory results of the cited studies, the development and use of these numerical tools for the description of LIDs is still limited.

Permeable pavements (PP) represent a good solution to solve stormwater management problems both in quantitative and qualitative terms. In general, PP systems are layered systems consisting of a wear layer, generally concrete, a filter layer, mainly constituted of coarse sand or fine gravel, a gravel aggregate base layer, and a crushed stones sub-base layer. The heterogeneity of the materials that compose PPs, and its strongly unsaturated hydraulic behaviour, pose significant modelling challenges. In this way, most of the works related with permeable pavement are focused on the hydrological performance of PP both in qualitative and quantitative terms (Al-rubaei et al., 2013; Brown and Borst, 2015a,b; Chandler and Wheater, 2002; Dreelin et al., 2006; Haselbach et al., 2014; Huang et al., 2016; Kamali et al., 2017; Kuang et al., 2011; Legret et al., 1996; Lin et al., 2016; Palla and Gnecco, 2015; Sansalone et al., 2012).

The sustainable management of water resources requires the identification of procedures to optimize the use and the management of resources (Maiolo and Pantusa, 2016). Moreover, a correct characterization/identification of the parameters controlling the water regime in construction materials is a crucial task (when using physically based models). Despite the hydrological benefits of permeable pavements, these techniques are not yet widespread probably because modelling tools often used simplified methodologies, based on empirical and conceptual equations, which do not take into account hydrological processes in a physical way. In addition, the hydraulic properties of pavement materials have not been investigated in a comprehensive manner, limiting the investigation only to specific properties. For example, Chandrappa and Biligiri, (2016) investigated the permeability characteristics of porous concrete mixtures using falling head permeameter method. This study showed the relationship between material porosity and permeability in order to have a good design of the concrete mixture. In another work, Zhong et al. (2016) recognized the influence of pore tortuosity on hydraulic conductivity of pervious concrete. This study showed that several parameters influenced the prediction of hydraulic conductivity and this parameter was not solely affected by effective porosity. A limit of this study is that it is only focused on the concrete material and also it does not explore other hydraulic properties different than hydraulic conductivity. In another paper, Huang et al. (2016) proposed a numerical model for permeable pavements and also proved its applicability by applying it to simulate both hydraulics and water quality. The results of this study demonstrated a good agreement between field measurements and modeled results for three types of pavement in terms of hydraulics and water quality variables including peak flow, time to peak, outflow volume and TSS removal rates. Although a variety of analytical and numerical models are now available to predict water through porous media, the most popular model (maybe the best way) remains the Richards equation for variably saturated flow. A limit in using Richards equation is that its numerical solution has been criticized for being computationally expensive and unpredictable. In this way, the HYDRUS program numerically solves the Richards equation for saturated-unsaturated water flow.

Thus, the aim of this work is to propose a technique/procedure on how to interpret water flow through the construction system using the HYDRUS model. This research will suggest experimental and mathematical procedures for model calibration, which consists of: (a) experimental design (system construction, and number and character of measured transient flow data); (b) methods for independently evaluating of material hydraulic properties; (c) additional optimization of material hydraulic parameters using the transient flow data; and (d) model validation. The van Genuchten-Mualem function (van Genuchten, 1980) included in HYDRUS-2D was used to describe the unsaturated flow within the system. Following the experimental procedures proposed by Kodešová et al. (2014), several analyses have been conducted on the wear and bedding material of the lab-scale porous system made of porous concrete blocks and fine gravel. Results of these analyses have been fundamental to obtain the Soil Water Retention Curve (SWRC) of the materials so as to limit the following parameter optimization phase. The effect of the remaining parameters has been investigated through a sensitivity analysis carried out using the Morris screening method. Therefore, a model calibration procedure using the parameter optimization procedure included in HYDRUS-2D, namely the Levenberg-Marquardt optimization algorithm, has been conducted. Finally, the calibrated model was validated on an independent set of measurements.

2. Materials and methods

2.1. Lab-scale permeable pavement system

In order to study the behaviour of a permeable pavement, a lab-scale test bed was constructed. It consisted of a Plexiglas container (dimensions of the bottom 59 × 59 cm, height of 41 cm) with a circular outlet in the centre of the bottom (diameter of 10 cm) and layers of construction materials (Fig. 1) for a total thickness of 41 cm. The main principle of a pavement design is that the constructed layers distribute the concentrated loads from wheels below the road. The pressure of the wheels on the wear layer is relatively high, thus it is necessary to adopt high quality materials for this layer. Conversely, pressure decreases with depth and allows the use of weaker materials in the lower layers of the pavement. For these reasons, the choice of constituent materials and their gradations are fundamental. Generally, the main layers of a permeable pavement are a wear layer, a bedding layer, a base layer and a sub-base layer. The layer types and their construction thickness for the lab-scale porous modular pavement were chosen according to the CIRIA report (Kellagher et al., 2015), considering a traffic category of 3 (small car parks subject to cars, light vans and motorcycle access) and a California Bearing Ratio index (CBR) of 5% or greater. The wear layer consists of porous concrete blocks characterized by high permeability. Sub-base and bedding layers were constructed following the suggestions of the Interlocking Concrete Pavement

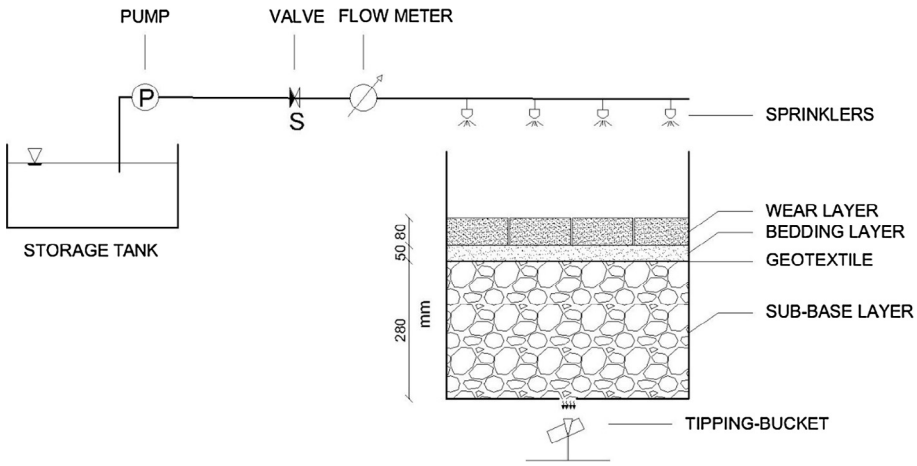

Fig. 1. A schematic of the lab-scale permeable pavement system.

Institute (ICPI), which recommends some ASTM stone gradations. The gradations for these sizes are identified with numbers. These numbers and gradations are found in ASTM D 448, Standard Classification for Sizes of Aggregate for Road and Bridge Construction. ICPI recommends No. 2 stone for the sub-base layer because it is very stable under construction equipment and has a high water storage capacity with a porosity of about 40%. The ASTM No. 8 is used for the bedding layer and has a porosity of about 20% of volume. The bedding layer consists of a mixture of fine gravel and glass sand to improve the pollutant removal efficiency for typical contaminants of stormwater runoff. At the interface between the bedding layer and the sub-base layer, a high permeability geotextile with a fiber area weight of 60 g m^{-2} is placed in order to prevent migrating of fine material into the bottom layer.

Further details on the mixture and construction of the Interlocking Concrete Pavements materials can be found in the technical paper of Burak (2007). In order to study the water regime in this system several rainfall events were simulated using 12 sprinklers (Fig. 1). Water was pumped from a storage tank by a pump into the sprinklers. Rainfall intensity was regulated by a valve and the actual rainfall intensity was measured by a flow meter. Preferential flows along the test box side walls were prevented by sealing them. In urban areas, rains that deserve special attention are those of short duration such as subhourly. In this way, critical rainfall events occur in a very short time (Carbone et al., 2015b). Given that, 10 irrigation events were simulated (Table 1). The Impervious/Pervious ratio reported in Table 1 represents the ratio of impervious run-on area to permeable pavement. It must be emphasized that the rainfall simulator was not able to reproduce variable precipitation patterns. Thus, a constant precipitation has been simulated in the laboratory.

The system response was assessed by measuring water contents and fluxes from the container outlet. An FDR probe SM100 WATERSCOUT was used to measure the volumetric water content in the middle of the bedding layer. The probe was calibrated on the sample of this material following the calibration procedure published by Kodešová et al. (2011). A linear calibration equation was obtained by fitting the experimental data points (relating sensor readings in volts and water contents evaluated gravimetrically) with a coefficient of determination $R^2 = 0.904$. The outflow from the bottom outlet was measured by a pre-calibrated tipping-bucket flow meter. According to Molini et al. (2005), records from tipping-bucket were post-processed by using an analytic equation $I_a = \alpha I_r \beta$ (where I_a and I_r represent the actual and the recorded rainfall intensity while α and β are calibration parameters) in order to correct the errors caused by water losses. Measured inflow (i.e. applied rainfall), outflow and volumetric water content were logged online by a Personal Computer installed near the test-bed.

2.2. Water flow modelling

The HYDRUS software package (Šimůnek et al., 2016) was used to model the hydraulic behaviour of the lab-scale permeable system. The studied permeable pavement was interpreted as a two-dimensional radially, symmetric, single-porosity, porous medium, which could be described by the Richards equation in the following form:

$$\frac{\partial \theta}{\partial t} = \frac{1}{r}\frac{\partial}{\partial r}\left[rK\frac{\partial h}{\partial r}\right] + \frac{\partial}{\partial z}\left[K\left(\frac{\partial h}{\partial z} + 1\right)\right] \quad (1)$$

where θ is the volumetric water content [L^3 L^{-3}], t is the time [T], h is the soil water matric head [L], K is the hydraulic conductivity [L

Table 1
Characteristic of the rainfall events simulated during the experimental campaign.

Rainfall events (–)	Duration (min)	Rainfall Intensity (mm/h)	Volume (l)	Impervious/Pervious
Day 1	30	73.00	12.30	<5:1
Day 2	30	64.00	10.70	<5:1
Day 3	30	66.00	11.10	<5:1
Day 4	15	85.60	7.20	<5:1
Day 5	15	95.10	8.00	<5:1
Day 6	15	71.90	6.05	<5:1
Day 7	30	69.60	11.70	<5:1
Day 8	30	69.00	11.60	<5:1
Day 9	30	69.30	11.65	<5:1
Day 10	15	77.30	6.50	<5:1

T^{-1}], r is the radial coordinate [L], and z is the vertical axis [L]. The unimodal van Genuchten–Mualem model (Mualem, 1976; van Genuchten, 1980) was used to describe the material hydraulic properties:

$$S_e = \begin{cases} \frac{1}{(1+(|\alpha h|)^n)^m} & if \quad h \leqslant 0 \\ 1 & if \quad h > 0 \end{cases} \tag{2}$$

$$S_e = \frac{\theta - \theta_r}{\theta_S - \theta_r} \tag{3}$$

$$K = \begin{cases} K_S \cdot S_e^l \left[\left(1 - (1 - S_e^{\frac{1}{m}})^m\right)\right]^2 & if \quad h < 0 \\ K_S & if \quad h > 0 \end{cases} \tag{4}$$

$$m = 1 - \frac{1}{n} \tag{5}$$

where K_s denotes the saturated hydraulic conductivity [L T^{-1}], S_e [–] is the effective water saturation $0 \leqslant S_e \leqslant 1$, θ_s and θ_r [L^3 L^{-3}] are the saturated and residual water content, respectively, and α [L^{-1}], m [–], and n [–] are empirical parameters dependent on soil type and l denotes tortuosity/connectivity coefficient [–] which is found to have a value of 0.5 from the analysis of a variety of soils (Mualem, 1976). The α parameter is related to the air-entry pressure and it is generally high for coarse soil and low for silty or clayey soils. Similarly, the n parameter, which determines the steepness of the SWRC.

2.3. Hydraulic properties of the materials

Brunetti et al. (2016a), who studied the hydrological behaviour of a different permeable pavement systems under natural field conditions, obtained the van Genuchten material hydraulic parameters of all layers from the inflow and outflow data via inverse numerical modelling using Particle Swarm Optimization combined with HYDRUS-1D. In our study, in order to reduce the number of parameters in the next model calibration (i.e. parameter optimization) and to better constrain the model, the material hydraulic properties of the wear material and the bedding layer were measured in the laboratory using a clay tank for the wear material and the multistep outflow experiments for the bedding material following procedures described by Kodešová et al. (2014).

SWRC of the concrete paving was measured on two fragments of this material. Firstly, vertical sides of the fragments were covered by wax. Fragments were saturated by water, then placed in the clay tank and slowly drained using pressure heads from 0 to −220 cm. The clay tank consists in a large funnel with a sintered disc, which was covered by 5 cm thick kaolin layer with a filter paper at the top. The clay tank (the funnel outlet) was connected with a water reservoir by a plastic tube. This tank was designed to measure the soil–water retention curve in the range of pressure heads applied during the experiment (0 to −220 cm). In order to obtain a maximal saturation of the material, considering the fact that it is very porous, saturation was encouraged by using ultrasound technique. Soil water contents related to particular pressure heads were evaluated gravimetrically. Parameters of the retention curves were obtained by fitting of the experimental data points using the RETention Curve code (RETC) (van Genuchten et al., 1991). For a more detailed explanation of the clay tank please refer to Fér and Kodešová (2012). Generally, gaps have a high influence in interlocking concrete pavements in which all the infiltration capacity is deputed to them (impervious concrete blocks). Conversely, in porous pavement, such in this case, the concrete blocks have a high permeability and infiltrate most of the incoming water. In the lab scale system, the gaps between porous concrete blocks were reduced to minimize preferential flows and assume a homogeneous wear layer.

The soil water retention and hydraulic conductivity curves of the bedding layer were measured using the multistep outflow experiments (Van Dam et al., 1994). Two 100 cm^3 columns were placed in the Tempe cells, in which a fine gravel material was packed. Samples were fully saturated, and then slowly drained using 5 pressure head steps (a minimum pressure head of −12.5 cm) during several days and cumulative outflow in time was measured. Points of the soil water retention curve were calculated from the final water content determined gravimetrically and the water discharge from the sample was observed. HYDRUS-1D was used to simulate the observed cumulative outflow and the measured points of the retention curve, and to optimize material hydraulic parameters. For both samples, the θ_s parameter was measured, and the θ_r value was set at 0 cm^3 cm^{-3}.

Regarding the hydraulic parameters of the sub-base layer, all parameters were fixed according to Brunetti et al., (2016a) considering that the material used for the construction of the lab-scale system is similar to the one used in the cited work.

2.4. Numerical domain and boundary condition

In order to reproduce the behaviour of the PP as an axisymmetrical vertical two-dimensional flow domain, the cylindrical domain was designed considering the total thickness of porous materials and planar area of the lab-scale system, i.e. the depth of the domain was 41 cm and radius was 32.70 cm (Fig. 2). The geotextile was not included in the model considering its negligible thickness, its limited hydraulic effect due to its high permeability, and that its sole function was to separate the bedding layer from the sub-base layer.

The domain was discretized into two-dimensional rectangular elements (Fig. 2) using the MESHGEN tool of HYDRUS-2D. The generated FE mesh had 1260 nodes and 2377 two dimensional elements. The quality of the FE mesh was assessed by checking the mass balance error reported by HYDRUS-2D at the end of the simulation. Mass balance errors, which in this simulation were always below 1%, are generally considered acceptable at these low levels.

At the surface of the PP, an atmospheric boundary condition (i.e. applied rainfall or potential evaporation of 6.94×10^{-5} cm min^{-1}) was assigned, while a seepage face boundary condition was specified at the bottom left corner of the flow domain (Fig. 2). The outflow from a boundary exposed to atmosphere will occur only if the pressure in the porous media water exceeds atmospheric pressure. In this view, a seepage face boundary acts as a zero pressure head when the boundary node is saturated and as a no flux boundary when it is unsaturated. A zero flux boundary condition was assigned to all remaining boundaries of the domain considering the fact that the building material of the lab-scale system is Plexiglas that is impervious. The initial condition was specified in terms of the soil water pressure head and was set to linearly increase with depth, from −30 cm at the top of the flow domain ($z = 41$) to −0.5 cm at the bottom ($z = 0$).

2.5. Inverse parameter estimation

Since the saturated hydraulic conductivity of the wear layer (concrete blocks) is not measured when using the clay tank test, numerical optimization of this parameter had to be conducted. Preliminary simulations showed that simulated transient flow data (outflow fluxes and water contents) did not closely correspond to measured ones if only this parameter was estimated. Therefore, further 3 parameters α, n and K_s of the bedding layer were optimized. The original data set of 10 rainfall events (Table 1) was

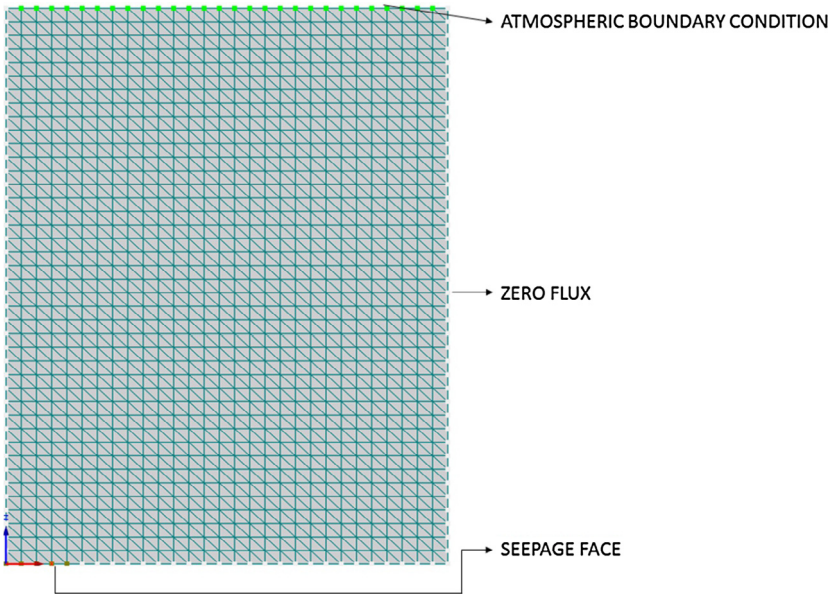

Fig. 2. A schematic of the applied boundary conditions in the axisymmetric domain.

divided into two data sets: calibration and validation. The calibration data set, relative to a period of three days (days 1–3), was characterized by having middle-high rainfall intensity in a very short time. In order to evaluate the stress conditions of the draining package, a drying time of 24 h was secured between two events. The following 7 days were selected as the validation data. This period was selected with the intention of having the most significant rainfall intensity and durations of between fifteen minutes and thirty minutes.

HYDRUS software packages implement a Marquardt-Levenberg type parameter estimation technique (Marquardt, 1963; Šimůnek and Hopmans, 2002) for the inverse estimation of soil hydraulic, solute transport, and/or heat transport parameters from measured transient or steady-state flow and/or transport data. This method combines the Newton and steepest descend methods, and generates confidence intervals for the optimized parameters. It is a gradient-based local optimization algorithm, which has proven to be reliable when the dimensionality of the inverse problem is low. Considering that only 4 hydraulic parameters had to be estimated after the laboratory tests, this algorithm was used.

The objective function Φ to be minimized during the parameter estimation, written in a relatively general manner, may be defined as:

$$\Phi(b,q,p) = \sum_{j=1}^{m_q} v_j \sum_{i=1}^{n_{qj}} w_{i,j}[q_j^*(x,t_i) - q_j(x,t_i,b)]^2 + \sum_{j=1}^{m_p} \overline{v_j} \sum_{i=1}^{n_{pj}} \overline{w_{i,j}}[p_j^*(x,\theta_i) - p_j(x,\theta_i,b)]^2 + \sum_{j=1}^{n_b} \hat{v}_j[b_j^*(x) - b_j(x)]^2 \quad (6)$$

where the first term on the right side represents deviations between measured and calculated space-time variables. In this term, m_q represents the number of different sets of measurements, n_{qj} is the number of measurements, $q_j *(x,t_i)$ represents specific measurements at generic time t_i for the jth measurement set at location x, $q_j(x,t_i,b)$ is the model prediction the vector of the optimized parameters b (in this case soil hydraulic parameters), and v_j and $w_{i,j}$ are weights associated with a particular measurement set or point, respectively. In the first term water contents, at z = 30.5 cm (i.e., center of the bedding layer), and actual flux across the seepage face, are included.

The second term on the right side of Eq. (6) represents differences between independently measured and predicted soil hydraulic properties for different soil horizons. The last term represents a penalty function for deviations between prior knowledge of the soil hydraulic parameters.

2.6. Sensitivity analysis

Four material hydraulic parameters were included in the optimization framework. Preliminary to this step, a Sensitivity Analysis (SA) has been carried out to investigate the influence of different parameter on the output variance, and to identify potential unimportant factors, which can be fixed at any value in the parameter space without significantly affecting model response. Sensitivity analyses have been widely applied in hydrological problems. However, most of the existing application used the One-factor-at-a-time (OAT) sensitivity analysis, so called as each factor is perturbed in turn while maintaining all the other parameters fixed. This type of approach is applicable only when the model is additive and parameter interaction is negligible. When the properties of the model are unknown it is necessary to use a Global Sensitivity Analysis (GSA), which is able to detect parameter interaction. Brunetti et al. (2016a) carried out a GSA, based on the Sobol method, on the material hydraulic properties of a layered permeable pavement modelled using HYDRUS-1D. The analysis revealed that the model was non-additive and characterized by significant parameter interaction, with a prominent influence of the wear layer on the hydraulic behaviour of the pavement. In another study, Brunetti et al. (2017) performed a surrogate-based sensitivity analysis on the soil hydraulic properties of a stormwater filter modeled using HYDRUS-2D. Results highlighted how the shape parameter α of the filter layer had a dominant effect on the simulated outflow.

In both cited studies, the GSA based on the Sobol method required thousands of runs to accurately determine different sensitivity measures, thus increasing substantially the computational cost of the analysis. In Brunetti et al. (2017), this problem was overcame using a surrogate model based on the kriging approximation of the response surface. An alternative, when the model

is computationally expensive and the main settings of the SA are the factors fixing and prioritization, is the Morris method (Morris, 1991). The Morris method belongs to the class of *Screening* methods. The method is based on calculating for each input a number of *Elementary Effects* (EE), from which basic statistics are computed to derive sensitivity measures. While relying on the OAT analysis for the computation of EEs, the method can be viewed as global since it averages the EEs computed at different locations in the parameter space, thus providing a statistical base for a qualitative evaluation of different sensitivity measures.

In our analysis, each single run of the HYDRUS-2D model, for the calibration period, required approximately 30 s of CPU time on a laptop equipped with a CPU Intel® Core i7-4700 MQ 2.40 GHz processor and 8 GB of RAM. Since a variance-based SA would have required a significant computational cost, the modified version of the Morris method proposed by Campolongo et al. (2007) has been used. In particular, the influence of the remaining material hydraulic properties (i.e., the saturated hydraulic conductivity K_s for the both the wear and bedding layer, and the two empirical parameters α and n for the bedding layer) on the hydraulic response of the pavement has been investigated. The main outcome of the analysis are two sensitivity measures for all investigated parameters: σ and $\mu*$. While the former summarizes the interaction effect, the latter reflects the overall importance of a particular parameter. For a detailed description of the method, refer to Morris (1991) and Campolongo et al. (2007). To interpret the results by simultaneously taking into account both sensitivity measures, Morris suggested their graphical representation in the ($\mu*$-σ) plane.

More specifically, the sensitivity analysis has investigated the influence of different material hydraulic parameters on the simulated outflow and volumetric water content in the bedding layer, respectively. The effect is quantified by comparing the simulation results with measured values of outflow and water content. In particular, the *NSE* index and the *RMSE* have been used. One of the main advantage of the Morris Method is the computational efficiency. It is able to provide a qualitative screening of the most influent factors with few model runs. There are no clear indications in the literature about the sample size. For example, Iooss and Lemaître (2014) used a sample size of 5 to screen 8 parameters of a hydraulic model. In another study, Saltelli and Tarantola (2004) suggested a sample size between 4 and 10. Considering that only four hydraulic parameters were investigated in the sensitivity analysis, a sample size of 8 for a total of 40 model executions has been chosen.

2.7. Statistical evaluation of the model

In general, in order to assess the accuracy of a model it is necessary to perform a statistical evaluation to ensure the results validity. There are several statistical evaluation indices that can be used to assess the accuracy of a hydrological model. In this study, two widely used indices (Moriasi et al., 2007) have been used: the coefficient of determination R^2 and the Nash-Sutcliffe Efficiency (NSE) index (Nash and Sutcliffe, 1970).

3. Results and discussion

3.1. Hydraulic properties of the materials

The HYDRUS model is a widely used finite-element model for simulating the movement of water in variably saturated media. Although it has been mainly used to model soil infiltration, its applicability has been poured out with good results also to further types of porous media. In this view, the added value of this work is the dimensionality reduction of the material parameter space by carrying out specific experimental analyses on some materials in order to define their hydraulic properties and, therefore, to ensure a more accurate hydraulic modelling based on measured experimental data.

Material hydraulic properties of the wear material were measured by using the clay tank described in the previous section. The gravimetrically determined saturated water contents for two samples, θ_{s1}, were 0.106 and 0.113 $cm^3\ cm^{-3}$. Then, by using RETC code (van Genuchten et al., 1991), other parameters of the retention curve were obtained (Table 2). Results from this experiment, exhibit a satisfactory agreement between fitted and measured value of volumetric water content as indicated by the coefficient of determination for the regression of observed versus fitted values, which is equal to $R^2 = 0.999$. The value for parameter n of the SWRC value denotes that desaturation does not occur in a quick way while the high value of α denotes that the retention capacity of the material is low. The structure of the porous concrete is to have voids interconnected with dimensions ranging from 2 mm to 8 mm depending on mix portion, aggregates and the degree of compaction (Deo and Neithalath, 2010; Tennis et al., 2004). The volume fraction, size distribution and topological structure of the pores are the critical parameters in controlling permeable concrete behaviour (Sansalone et al., 2008). Normally, porosity of permeable concrete is typically 7–35%, depending on a host of variables such as cement paste fraction, aggregate content, gradation and particle shape, water/cement ratio and compaction effort (Ong et al., 2016). Concretes with porosity < 7% tend to give slower water percolation while porosities > 35% result in highly permeable, but very weak concretes.

Hydraulic conductivity of porous concrete is the most investigated parameter in the literature. It varies from 0.18 cm min^{-1} to 198 cm min^{-1} (Coughlin et al., 2012; Deo et al., 2010; Haselbach, 2010; Ibrahim et al., 2014; Montes and Haselbach, 2006; Sumanasooriya and Neithalath, 2011). In the study of Kia et al. (2017), although a positive correlation between porosity and permeability is showed, the permeability is not only dependent on total porosity, but also on other characteristics such as size distribution, shape, degree of connectivity and tortuosity of the pores. In this way, results from our experiment denotes a moderate percolation through this layer confirmed by values of θ_{s1} for both samples.

Table 2
Hydraulic properties of the materials; CT – clay tank, MSO – multistep outflow experiment, LSPPS – lab-scale permeable pavement system, W1, W2, and B1, B2 – sample replicates for wear and bedding layers, respectively.

Layer		θ_r ($cm^3\ cm^{-3}$)	θ_s ($cm^3\ cm^{-3}$)	α (cm^{-1})	n (–)	K_s (cm min^{-1})
Wear layer – W1	CT	0.044	0.106	3.37	1.47	–
Wear layer – W2	CT	0.045	0.113	4.03	1.47	–
Wear layer	LSPPS	0.044	0.106	3.37	1.47	1.56 ± 0.4
Bedding layer – B1	MSO	0	0.41	0.43	2.45	236
Bedding layer – B2	MSO	0	0.37	0.4	2.65	32
Bedding layer	LSPPS	0	0.4	0.27 ± 0.04	2.0 ± 0.1	69.27 ± 14.40
Sub-base layer	Brunetti et al. (2016a)	0.00	0.01	0.27	2.41	96.70

By using this experimental procedure, no information can be given about hydraulic conductivity of this layer. The multistep outflow experiment has been performed on duplicate samples of the bedding layer to determine its hydraulic properties (Van Dam et al., 1994). For both samples, the saturated water content θ_{s2} was measured starting from the final water content and water balance in the sample and it was found equal to $\theta_{s2} = 0.41$ and $0.37\ cm^3\ cm^{-3}$, The θ_{r2} value was set at $0\ cm^3\ cm^{-3}$. Other parameters of the hydraulic functions (van Genuchten, 1980) were optimized from the measured outflow, soil water retention data and the single porosity model in HYDRUS-1D (Table 2).

Parameters obtained by using the multistep outflow experiment combined with HYDRUS-1D confirm that the bedding layer has a reduced porosity. Values of α and n for both samples denote that desaturation occurs very quickly. This aspect could be positive considering that one of the permeable pavements goals is to infiltrate as much water as possible in order to limit the surface runoff. Results obtained for the values of the hydraulic conductivity, are instead very variable for both samples. Confidence limits exhibit a wide range of values that suggest proceeding with further analysis. However, the estimated parameters for both materials indicated that the hydraulic behaviour of the layers was characterized by high flow rates and negligible retention capacity.

3.2. Sensitivity analysis

The clay tank and multistep outflow experiments allow to measure different material hydraulic parameters, thus reducing the dimensionality of the inverse problem to a few factors. However, before proceeding with the parameters optimization, the Morris method was used to carry out a sensitivity analysis of the unknown material hydraulic parameters. Results of the sensitivity analysis are reported in Fig. 3. In particular, the scatter plots of the two sensitivity measures σ and $\mu*$ for both water content (left plot in Fig. 3) and outflow (right plot in Fig. 3) are shown.

At a first inspection, it is evident that for each factor σ and $\mu*$ exhibit similar values, indicating that none of the parameters has a purely linear effect. This is evident from Fig. 3, in which all points lie around the diagonal (red line in Fig. 3). The saturated hydraulic conductivity of the wear layer, K_{s1}, has a negligible influence on the agreement between the measured and simulated water content, as highlighted by its low values of σ and $\mu*$. In this case, K_{s1} can be fixed at any value in the parameter space without affecting the fitting's quality. Moreover, its effect on the simulated outflow (right plot in Fig. 3) appears rather limited but not negligible, as for the water content in the bedding layer. In the study of Brunetti et al. (2016a,b), who carried out a Global Sensitivity Analysis on material hydraulic parameters of a layered permeable pavement, the saturated hydraulic conductivity of the wear layer had, similarly to our findings, limited effect on the outflow, however the interaction with other parameters was significant in that study. This discrepancy could be mainly related to the differences in the adopted porous concrete, and modelling scenarios. It must be emphasized that SA results reveal that the experimental measurement of K_{s1} would not significantly increase the accuracy of the fitting, considering its limited effect on both water content and outflow.

Conversely, the two empirical parameter α_2 and n_2 of the bedding layer have appreciable effect on both outflow and water content, with the former being the most influent parameters between those investigated in the SA. This behaviour is intuitive since these two parameters both govern the shape of the van Genuchten-Mualem function, thus their influence on the retention properties of the material is significant. An accurate experimental determination of α_2 and n_2 would increase significantly the accuracy of the fitting for both the outflow and water content. The saturated hydraulic conductivity K_{s2} of the bedding layer exhibits different sensitivity for the outflow and water content. While its influence on the agreement between simulated and measured water content in the bedding layer is appreciable but limited, its impact on the simulated outflow is significant. More specifically, it is the second most influent parameter for the outflow. For both objective functions, K_{s2} exhibits a value of σ slightly higher than $\mu*$, indicating its nonlinear effect on the variance's output.

Summarizing, none of the analysed factors can be fixed at any feasible value in the parameter space without affecting simultaneously the quality of the fitting for the water content and outflow. Thus the dimensionality of the inverse cannot be further reduced. The saturated hydraulic conductivity of the wear layer is relatively insensitive, while the material hydraulic properties of the bedding layer mainly drive the model's behaviour.

3.3. Inverse solution estimation

From results obtained using clay tank experiment combined with RETC code and multistep outflow experiments combined with HYDRUS-1D, it was possible to limit the optimization problem to few parameters. However, in order to make the problem "well-posed" and whereas the confidence limits of the bedding layer

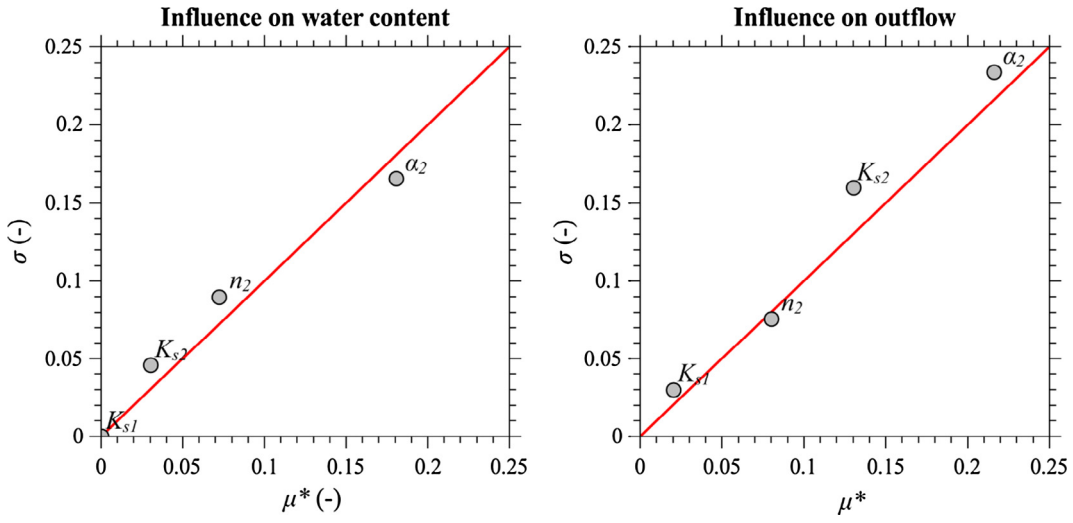

Fig. 3. A scatter plot of sensitivity analysis measurements.

K_{s2} exhibit a very wide range for both samples analysed, it has been decided to proceed also with the optimization of the SWRC parameters of this layer. Two sets of inverse solution data were used to have a robust well-calibrated model. In particular, the volumetric water content in the bedding layer and the outflow at the seepage face have been used.

In this way, the list of parameters to be optimized in the inverse problem are given as follow, K_{s1} (cm min^{-1}), α_2 (cm^{-1}), n_2 (–), K_{s2} (cm min^{-1}) where the subscript 1 and 2 are for the wear and bedding layer respectively. In Table 2 results from the two previous experiments and results from the inverse solution optimization, are shown.

Parameters obtained from the inverse solution optimization, exhibit a satisfactory agreement between fitted and measured this due to the fact that the coefficient of determination for regression of observed versus fitted values is equal to R^2 = 0.985, and mostly because the retention capacity of the entire system is negligible. This is also confirmed by the fact that the values confidence limits are acceptable. Saturated hydraulic conductivity of the bedding layer, K_{s2}, is in the range of measured values. Its high value indicates a high infiltration capacity, which has to be expected considering the coarse nature of the material. It is more than an order of magnitude higher than the saturated hydraulic conductivity of the wear layer, and slightly lower than the value reported for the subbase layer, which is composed by crushed stone. The value of parameter n_2 of the SWRC value denotes that desaturation occurs in a moderate way for the bedding material while the value of α_2 denotes that the retention capacity of the material is appreciable.

The measured porosity for the bedding layer is slightly higher than the prescriptions of ICPI, which recommends a porosity of about 20%. This difference can be related to the sampling procedures of the two samples that have been difficult due to the coarse nature of the material and may have affected the determination of the saturated water content.

Fig. 4 shows a comparison between the measured and modeled hydrographs for the calibration period. The inverse solution optimization resulted in a value of NSE > 0.90, which confirmed the high accuracy between the measured and estimated parameters. The model was able to reproduce with high accuracy the fast hydraulic response of the hydrograph during precipitation events at different intensities with negligible over- and under-estimations in the ascending and descending phase of the hydrograph.

Fig. 5 shows the simulated against measured volumetric water content (VWC) within the bedding layer for the calibration period.

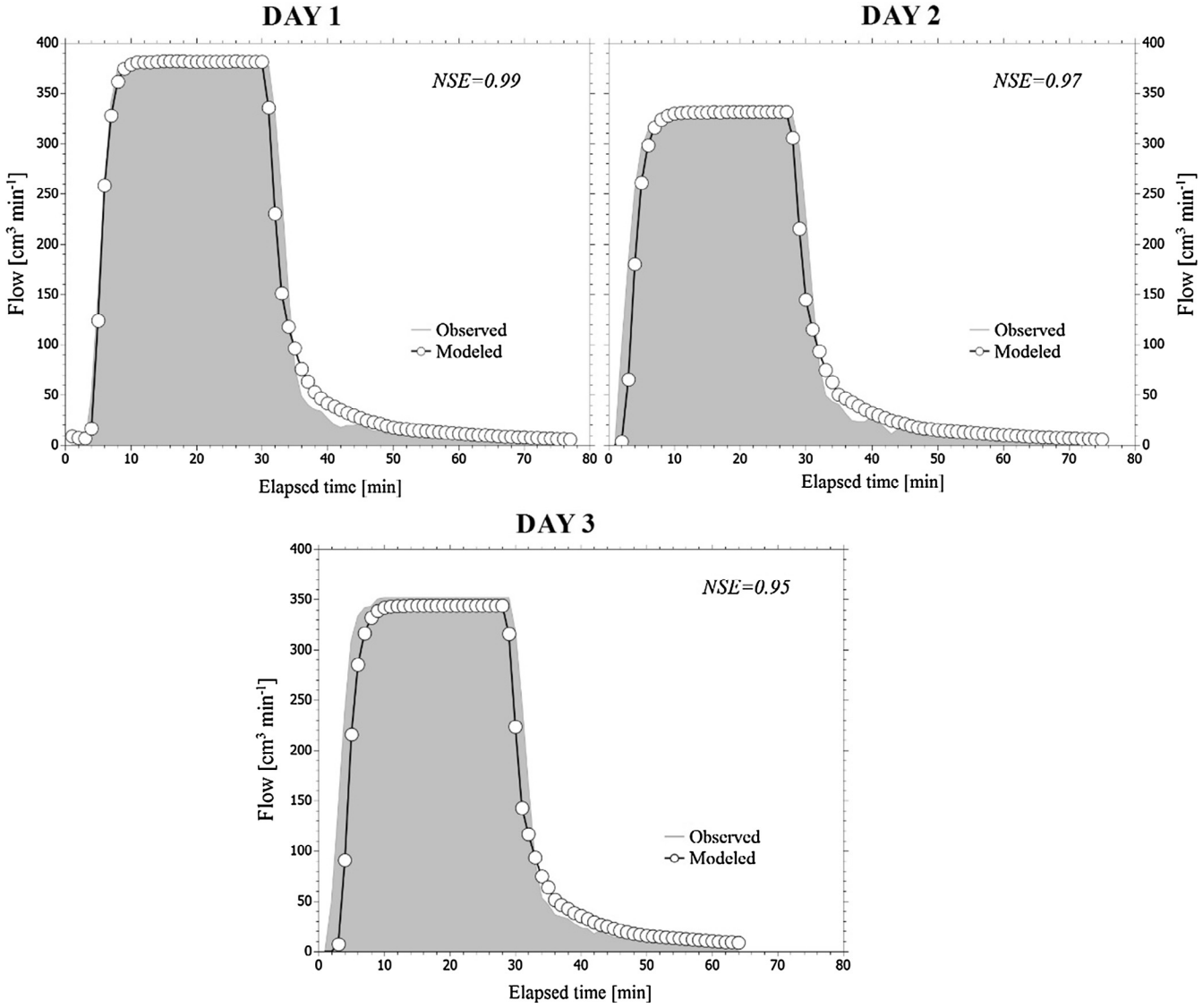

Fig. 4. A comparison between measured and simulated outflow versus time in the calibration period.

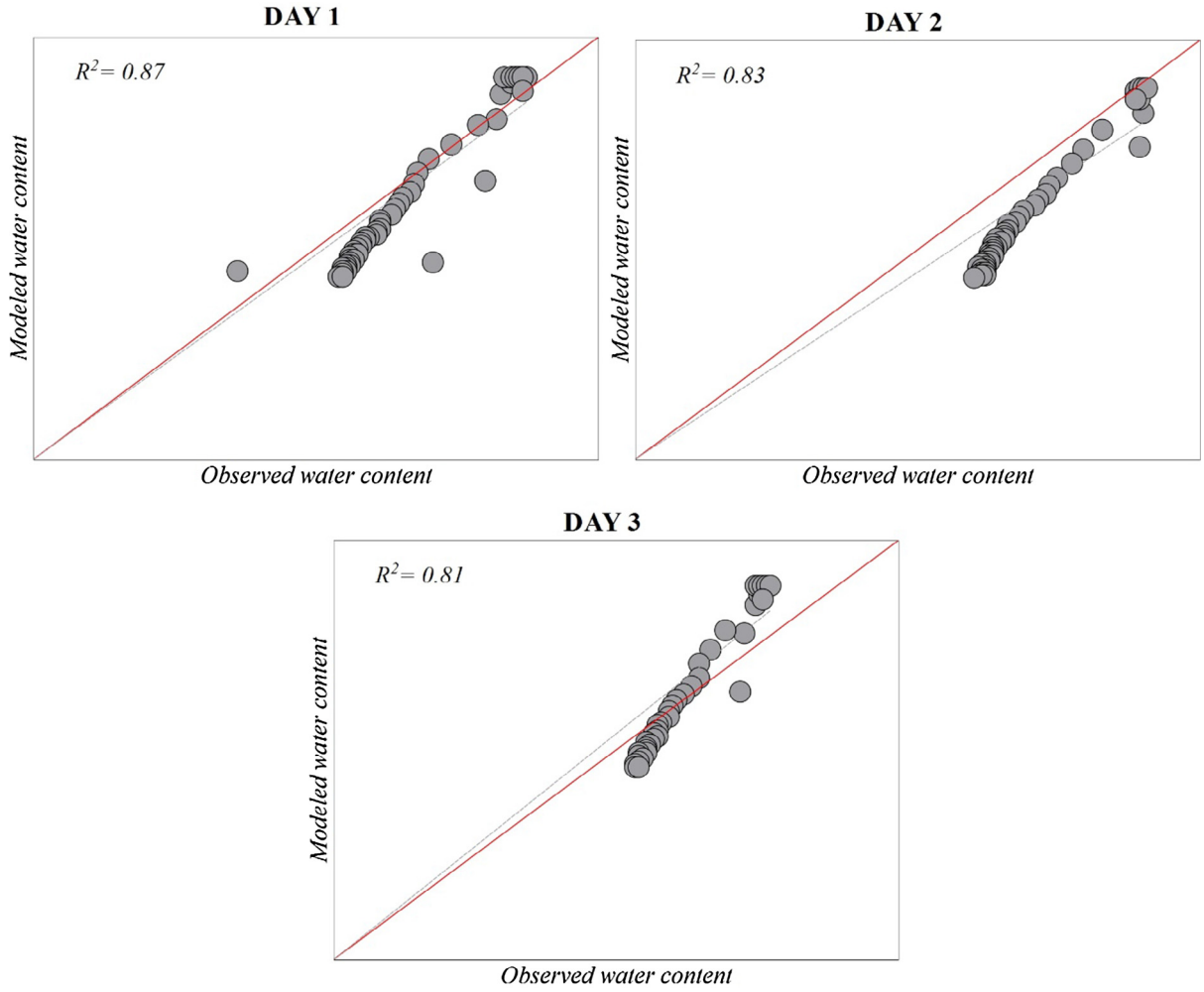

Fig. 5. A comparison between measured and simulated water content in the calibration period.

This graph shows a bisector line (red full line), which indicates a good agreement between simulated and measured water content, and a linear regression line (grey dashed line). The good performance of the model is confirmed by the determination coefficient $R^2 > 0.80$. The comparison between the bisector and regression lines indicates that the model slightly underestimated the volumetric water content for the first two events and slightly overestimated the VWC for the third event. It must be emphasized that the points in Fig. 5 that exhibit a relatively high bias are those related to the beginning of each precipitation event. This indicates that the model tends to underestimate the water content in the dry period. This can be related to a combined overestimation of the actual evaporation and underestimation of the retention capacity of the material.

3.4. Model validation

To evaluate the reliability of the estimated parameter, the model was validated using an independent set of experimental data. Figs. 5 and 6 show the comparison between measured and simulated data in the validation period for hydrograph and water content respectively. Table 3 summarize the material hydraulic parameters used in the validation period.

Fig. 6 shows a comparison between measured and modeled hydrographs during the validation period.

The NSE values remain quite similar to calibration period values and they are still close to value 1, which confirms the reliability of the calibrated model. For these reasons, the simulated hydrograph provides a very accurate description of the hydraulic behaviour of the pavement at different rain intensities. This ability of the calibrated model is important especially regarding the analysis of traditional drainage systems and LID techniques because a correct description of the hydrograph during different precipitation events, gives information about the lag time and the intensity of peak flow, which are fundamental to establish the hydrological performances and analysis of traditional drainage systems, and for the evaluation of benefits of LID implementation on them. Information about volumetric water content are given in Fig. 7. The good performance of the calibrated model is also confirmed by the determination coefficient R^2 between the simulated versus measured the volumetric water content. The comparison between the bisector and regression lines indicates that the model slightly underestimated the VWC.

4. Conclusions

In this paper, we investigated the suitability of the HYDRUS-2D software package, to correctly describe the hydraulic behaviour of a lab-scale permeable pavement system, and identifiability of the actual/effective material hydraulic parameters of the construction

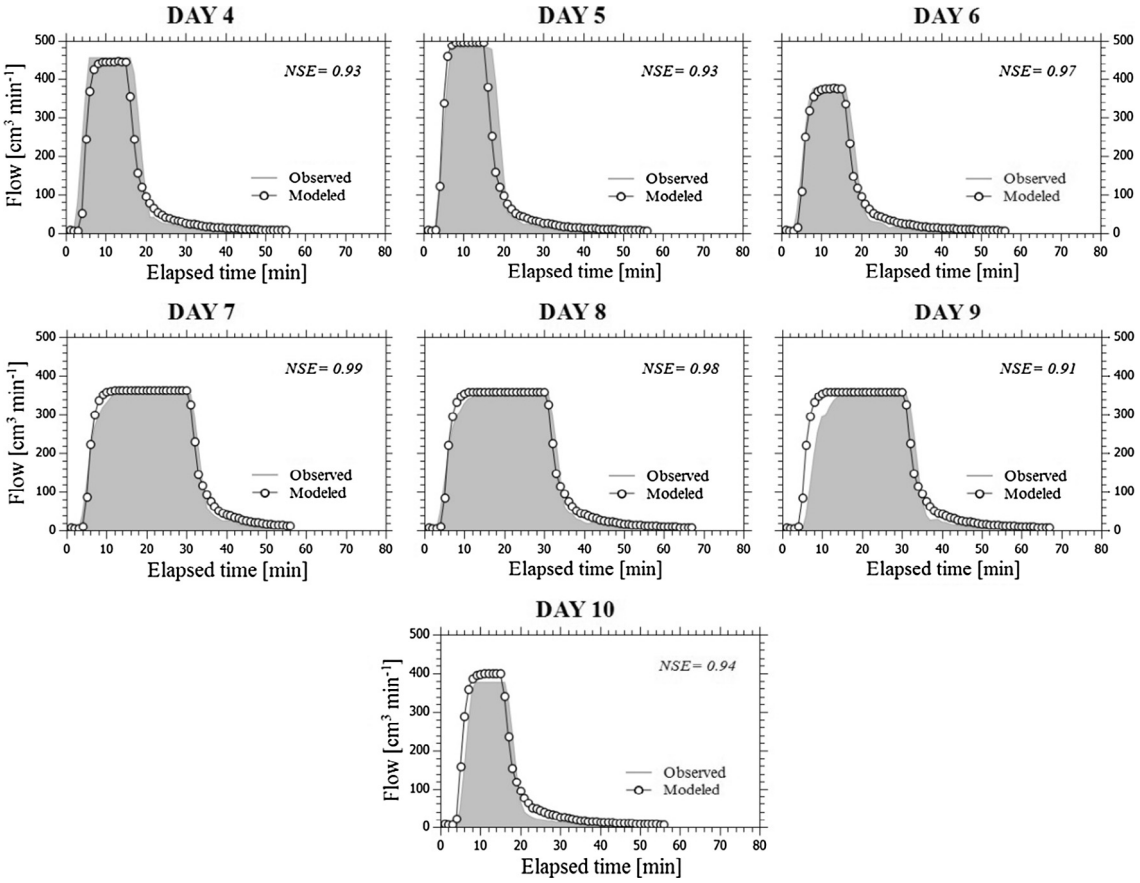

Fig. 6. A comparison between measured and simulated outflow versus time in the validation period.

Table 3
Material hydraulic parameters used in the validation period.

θ_r (cm^3 cm^{-3})	θ_s (cm^3 cm^{-3})	α (cm^{-1})	n (–)	K_s (cm min^{-1})	l (–)
Wear					
0.04	0.106	3.37	1.47	1.56	0.5
Bedding					
0.00	0.40	0.27	2.00	69.27	0.5
Sub-base					
0.00	0.01	0.27	2.41	96.70	0.5

materials. We considered the single porosity model implemented by the software in describing the system. The coefficient of determination R^2 and the widely used Nash-Sutcliffe efficiency index have been used to assess the model. The inverse solution optimization which implements a Marquardt-Levenberg type parameter estimation technique for the inverse estimation of the material hydraulic parameters was conducted to calibrate the model. To have a very robust and well-posed model, two sets of measured data have been used.

In order to reduce the dimensionality of the inverse problem, a clay tank experiment and the multistep outflow experiment were used to determine the unsaturated material hydraulic properties of two of the three layers before the calibration of the model. Coupled with experimental procedures on some materials, a sensitivity analysis has also been performed. These two approaches allowed obtainment of model with few parameters to be calibrated which is strictly connected with measured data from the pavement. This ensured a coherent calibration phase that reached an NSE value not lower than 0.95, which means a high accuracy between measured and estimated parameters. The optimized parameters were then validated against an independent set of experimental data, resulting in an NSE not lower than 0.91, which indicates the reliability of the calibrated model.

Our approach improved the identifiability of hydraulic parameters of permeable pavement and although pressure heads measurement could not be performed due the nature of our materials (concrete, fine gravel, stones), water content measurements helped to reduce uncertainty in the hydraulic parameters estimation. Finally, the results obtained with this work showed that the implementation of a model aimed at soil systems, together with accurate experimental and numerical procedures, has been able to accurately describe the hydraulic behaviour of a system of multiple layered materials that are not really soils.

Conflict of interests

The authors declare that there is no conflict of interests regarding the publication of this paper.

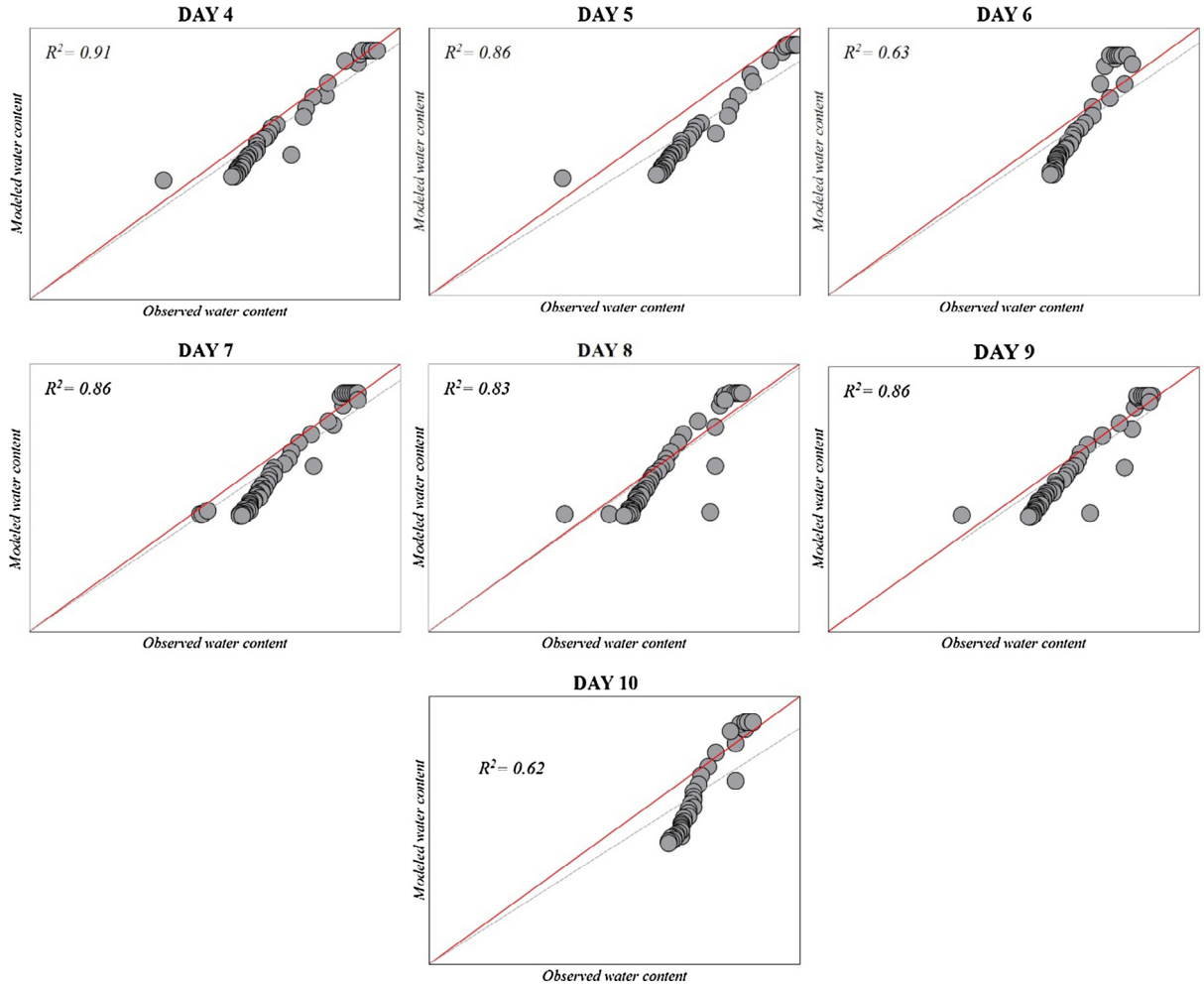

Fig. 7. A comparison between measured and simulated VWC in the validation period.

Acknowledgements

The study was co-funded by the Italian National Operative Project (PON) – Research and Competitiveness for the convergence regions 2007/2013-I Axis "Support to structural changes" operative objective 4.1.1.1. "Scientific-technological generators of transformation processes of the productive system and creation of new sectors" Action II: "Interventions to support industrial research".

References

Al-rubaei, A.M., Stenglein, A.L., Viklander, M., Blecken, G., 2013. Long-term hydraulic performance of porous asphalt pavements in Northern Sweden. J. Irrig. Drain. Eng. 499–505. https://doi.org/10.1061/(ASCE)IR.1943-4774.0000569.

Brown, R.A., Borst, M., 2015a. Nutrient infiltrate concentrations from three permeable pavement types. J. Environ. Manage. 164, 74–85. https://doi.org/10.1016/j.jenvman.2015.08.038.

Brown, R.A., Borst, M., 2015b. Quantifying evaporation in a permeable pavement system. Hydrol. Process. 29, 2100–2111. https://doi.org/10.1002/hyp.10359.

Brunetti, G., SImunek, J., Piro, P., 2016a. A comprehensive numerical analysis of the hydraulic behavior of a permeable pavement. J. Hydrol. 540, 1146–1161. https://doi.org/10.1016/j.jhydrol.2016.07.030.

Brunetti, G., Šimůnek, J., Piro, P., 2016b. A comprehensive analysis of the variably-saturated hydraulic behavior of a green roof in a mediterranean climate. Vadose Zone J. 15. https://doi.org/10.2136/vzj2016.04.0032.

Brunetti, G., Šimůnek, J., Turco, M., Piro, P., 2017. On the use of surrogate-based modeling for the numerical analysis of Low Impact Development techniques. J. Hydrol. 548, 263–277. https://doi.org/10.1016/j.jhydrol.2017.03.013.

Burak, R., 2007. Contractor focus construction of bases for permeable interlocking concrete pavements – Part I.

Burns, M.J., Fletcher, T.D., Walsh, C.J., Ladson, A.R., Hatt, B.E., 2012. Hydrologic shortcomings of conventional urban stormwater management and opportunities for reform. Landsc. Urban Plan. 105, 230–240. https://doi.org/10.1016/j.landurbplan.2011.12.012.

Campolongo, F., Cariboni, J., Saltelli, A., 2007. An effective screening design for sensitivity analysis of large models. Environ. Model. Softw. 22, 1509–1518. https://doi.org/10.1016/j.envsoft.2006.10.004.

Carbone, M., Turco, M., Nigro, G., Piro, P., 2014a. Modeling of hydraulic behaviour of green roof in catchment scale. In: 14th SGEM GeoConference on Water Resources. Forest, Marine and Ocean Ecosystems, pp. 471–478. doi:10.5593/sgem2014/b31/s12.061.

Carbone, M., Brunetti, G., Piro, P., 2014b. Hydrological performance of a permeable pavement in Mediterranean climate. In: 14th SGEM GeoConference on Water Resources. Forest, Marine and Ocean Ecosystems, pp. 381–388. doi:10.5593/SGEM2014/B31/S12.050.

Carbone, M., Brunetti, G., Piro, P., 2015a. Modelling the hydraulic behaviour of growing media with the explicit finite volume solution. Water (Switzerland) 7, 568–591. https://doi.org/10.3390/w7020568.

Carbone, M., Turco, M., Brunetti, G., Piro, P., 2015b. A Cumulative rainfall function for subhourly design storm in mediterranean urban areas. Adv. Meteorol., 1–10 https://doi.org/10.1155/2015/528564.

Chandler, R.E., Wheater, H.S., 2002. Analysis of rainfall variability using generalized linear models: a case study from the west of Ireland. Water Resour. Res. 38, 10-1–10-11. https://doi.org/10.1029/2001WR000906.

Chandrappa, A.K., Biligiri, K.P., 2016. Comprehensive investigation of permeability characteristics of pervious concrete: a hydrodynamic approach. Constr. Build. Mater. 123, 627–637. https://doi.org/10.1016/j.conbuildmat.2016.07.035.

Coughlin, J.P., Campbell, C.D., Mays, D.C., 2012. Infiltration and clogging by sand and clay in a pervious concrete pavement system. J. Hydrol. Eng. 17, 68–73. https://doi.org/10.1061/(ASCE)HE.1943-5584.0000424.

Deo, O., Neithalath, N., 2010. Compressive behavior of pervious concretes and a quantification of the influence of random pore structure features. Mater. Sci. Eng. A 528, 402–412. https://doi.org/10.1016/j.msea.2010.09.024.

Deo, O., Sumanasooriya, M., Neithalath, N., 2010. Permeability reduction in pervious concretes due to clogging: experiments and modeling. J. Mater. Civ. Eng. 22, 741–751. https://doi.org/10.1061/(ASCE)MT.1943-5533.0000079.

Dreelin, E.A., Fowler, L., Ronald Carroll, C., 2006. A test of porous pavement effectiveness on clay soils during natural storm events. Water Res. 40, 799–805. https://doi.org/10.1016/j.watres.2005.12.002.

Fér, M., Kodešová, R., 2012. Estimating hydraulic conductivities of the soil aggregates and their clay-organic coatings using numerical inversion of capillary rise data. J. Hydrol. 468–469, 229–240. https://doi.org/10.1016/j.jhydrol.2012.08.037.

Finkenbine, J.K., Atwater, J.W., Mavinic, D.S., 2000. Stream health after urbanization. J. Am. Water Resour. Assoc. 36, 1149–1160. https://doi.org/10.1111/j.1752-1688.2000.tb05717.x.

Haselbach, L., Poor, C., Tilson, J., 2014. Dissolved zinc and copper retention from stormwater runoff in ordinary Portland cement pervious concrete. Constr. Build. Mater. 53, 652–657. https://doi.org/10.1016/j.conbuildmat.2013.12.013.

Haselbach, L.M., 2010. Potential for clay clogging of pervious concrete under extreme conditions. J. Hydrol. Eng. 15, 67–69. https://doi.org/10.1061/(ASCE)HE.1943-5584.0000154.

Hilten, R.N., Lawrence, T.M., Tollner, E.W., 2008. Modeling stormwater runoff from green roofs with HYDRUS-1D. J. Hydrol. 358, 288–293. https://doi.org/10.1016/j.jhydrol.2008.06.010.

Huang, J., He, J., Valeo, C., Chu, A., 2016. Temporal evolution modeling of hydraulic and water quality performance of permeable pavements. J. Hydrol. 533, 15–27. https://doi.org/10.1016/j.jhydrol.2015.11.042.

Ibrahim, A., Mahmoud, E., Yamin, M., Patibandla, V.C., 2014. Experimental study on Portland cement pervious concrete mechanical and hydrological properties. Constr. Build. Mater. 50, 524–529. https://doi.org/10.1016/j.conbuildmat.2013.09.022.

Iooss, B., Lemaître, P., 2014. A review on global sensitivity analysis methods. Uncertain. Manage. Simul. Optim. Complex Syst. Algorithms Appl. 23. https://doi.org/10.1007/978-1-4899-7547-8_5.

Šimůnek, Jiří, Van Genuchten, Martinus Th., Šejna, Miroslav, 2016. Recent developments and applications of the HYDRUS computer software packages. Vadose Zone J. 15, 25. https://doi.org/10.2136/vzj2016.04.0033.

Kamali, M., Delkash, M., Tajrishy, M., 2017. Evaluation of permeable pavement responses to urban surface runoff. J. Environ. Manage. 187, 43–53. https://doi.org/10.1016/j.jenvman.2016.11.027.

Kellagher, R., Martin, P., Jefferies, C., Bray, R., Shaffer, P., Wallingford, H.R., Woods-Ballard, B., Woods Ballard, B., Construction Industry Research and Information Association, Great Britain, Department of Trade and Industry, Environment Agency, 2015. The SUDS manual (C697). CIRIA, London.

Kia, A., Wong, H.S., Cheeseman, C.R., 2017. Clogging in permeable concrete: a review. J. Environ. Manage. https://doi.org/10.1016/j.jenvman.2017.02.018.

Kodešová, R., Fér, M., Klement, A., Nikodem, A., Teplá, D., Neuberger, P., Bureš, P., 2014. Impact of various surface covers on water and thermal regime of Technosol. J. Hydrol. 519, 2272–2288. https://doi.org/10.1016/j.jhydrol.2014.10.035.

Kodešová, R., Kodeš, V., Mráz, A., 2011. Comparison of two sensors ECH2O EC-5 and SM200 for measuring soil water content. Soil Water Res. 6, 102–110.

Kuang, X., Sansalone, J., Ying, G., Ranieri, V., 2011. Pore-structure models of hydraulic conductivity for permeable pavement. J. Hydrol. 399, 148–157. https://doi.org/10.1016/j.jhydrol.2010.11.024.

Legret, M., Colandini, V., Le Marc, C., 1996. Effects of a porous pavement with reservoir structure on the quality of runoff water and soil. Sci. Total Environ. 189–190, 335–340. https://doi.org/10.1016/0048-9697(96)05228-X.

Lin, W., Park, D.G., Ryu, S.W., Lee, B.T., Cho, Y.H., 2016. Development of permeability test method for porous concrete block pavement materials considering clogging. Constr. Build. Mater. 118, 20–26. https://doi.org/10.1016/j.conbuildmat.2016.03.107.

Maiolo, M., Pantusa, D., 2016. An optimization procedure for the sustainable management of water resources. Water Sci. Technol. Water Supply 16 (1), 61–69. https://doi.org/10.2166/ws.2015.114.

Marquardt, D.W., 1963. An algorithm for least-squares estimation of nonlinear parameters. J. Soc. Ind. Appl. Math. 11, 431–441. https://doi.org/10.1137/0111030.

Molini, A., Lanza, L.G., La Barbera, P., 2005. The impact of tipping-bucket raingauge measurement errors on design rainfall for urban-scale applications. Hydrol. Process. 19, 1073–1088. https://doi.org/10.1002/hyp.5646.

Montes, F., Haselbach, L., 2006. measuring hydraulic conductivity in pervious concrete. Environ. Eng. Sci. 23, 960–969. https://doi.org/10.1089/ees.2006.23.960.

Moriasi, D.N., Arnold, J.G., Van Liew, M.W., Bingner, R.L., Harmel, R.D., Veith, T.L., 2007. Model evaluation guidelines for systematic quantification of accuracy in watershed simulations. Trans. ASABE 50, 885–900.

Morris, M.D., 1991. Factorial sampling plans for preliminary computational experiments. Technometrics 33, 161. https://doi.org/10.2307/1269043.

Mualem, Y., 1976. A new model for predicting the hydraulic conductivity of unsaturated porous media. Water Resour. Res. 12, 513–522. https://doi.org/10.1029/WR012i003p00513.

Nash, J.E., Sutcliffe, J.V., 1970. River flow forecasting through conceptual models: Part I. A discussion of principles. J. Hydrol. 10, 282–290. https://doi.org/10.1016/0022-1694(70)90255-6.

Ong, S.K., Wang, K., Ling, Y., Shi, G., 2016. Pervious Concrete Physical Characteristics and Effectiveness in Stormwater Pollution Reduction, p. 57.

Palla, A., Gnecco, I., 2015. Hydrologic modeling of Low Impact Development systems at the urban catchment scale. J. Hydrol. 528, 361–368. https://doi.org/10.1016/j.jhydrol.2015.06.050.

Palla, A., Gnecco, I., Lanza, L.G., 2009. Unsaturated 2D modelling of subsurface water flow in the coarse-grained porous matrix of a green roof. J. Hydrol. https://doi.org/10.1016/j.jhydrol.2009.10.008.

Qin, H.P., Peng, Y.N., Tang, Q.L., Yu, S.L., 2016. A HYDRUS model for irrigation management of green roofs with a water storage layer. Ecol. Eng. 95, 399–408. https://doi.org/10.1016/j.ecoleng.2016.06.077.

Saltelli, A., Tarantola, S., 2004. Sensitivity Analysis in Practice: A Guide to Assessing Scientific Models, p. 232.

Sansalone, J., Kuang, X., Ranieri, V., 2008. Permeable pavement as a hydraulic and filtration interface for urban drainage. J. Irrig. Drain. Eng. 134, 666–674. https://doi.org/10.1061/(ASCE)0733-9437(2008) 134:5(666).

Sansalone, J., Kuang, X., Ying, G., Ranieri, V., 2012. Filtration and clogging of permeable pavement loaded by urban drainage. Water Res. 46, 6763–6774. https://doi.org/10.1016/j.watres.2011.10.018.

Shuster, W., Rhea, L., 2013. Catchment-scale hydrologic implications of parcel-level stormwater management (Ohio, USA). J. Hydrol. 485, 177–187. https://doi.org/10.1016/j.jhydrol.2012.10.043.

Šimůnek, J., Hopmans, J.W., 2002. Parameter optimization and nonlinear fitting. Methods Soil Anal. Part 1: Phys. Methods 139–158. https://doi.org/10.2136/sssabookser5.4.c7.

Sumanasooriya, M.S., Neithalath, N., 2011. Pore structure features of pervious concretes proportioned for desired porosities and their performance prediction. Cem. Concr. Compos. 33, 778–787. https://doi.org/10.1016/j.cemconcomp.2011.06.002.

Tennis, P.D., Leming, M.L., Akers, D.J., 2004. Pervious Concrete Pavements أرصفة الخرسانة الإبتدائية. Portland Cement Association, National Ready Mixed Concrete Association, Skokie, Illinois/Silver Spring, Maryland, USA.

Van Dam, J.C., Stricker, J.N.M., Droogers, P., 1994. Inverse method to determine soil hydraulic functions from multistep outflow experiments. Soil Sci. Soc. Am. J. 58, 647–652. https://doi.org/10.2136/sssaj1994.03615995005800030002x.

van Genuchten, M.T., 1980. A closed-form equation for predicting the hydraulic conductivity of unsaturated soils. Soil Sci. Soc. Am. J. 44, 892. https://doi.org/10.2136/sssaj1980.03615995004400050002x.

van Genuchten, M.T., Leij, F.J., Yates, S.R., 1991. The RETC code for quantifying the hydraulic functions of unsaturated soils. U. S. Environ. Res. Lab. 93. https://doi.org/10.1002/9781118616871.

Yang, W.Y., Li, D., Sun, T., Ni, G.H., 2015. Saturation-excess and infiltration-excess runoff on green roofs. Ecol. Eng. 74, 327–336. https://doi.org/10.1016/j.ecoleng.2014.10.023.

Zhong, R., Xu, M., Vieira Netto, R., Wille, K., 2016. Influence of pore tortuosity on hydraulic conductivity of pervious concrete: characterization and modeling. Constr. Build. Mater. 125, 1158–1168. https://doi.org/10.1016/j.conbuildmat.2016.08.060.

Brunetti, G., Simunek, J., **Turco, M.**, Piro, P. (2017)

On the use of surrogate-based modeling for the numerical analysis of Low Impact Development techniques.

Journal of Hydrology Volume 548, May 2017

Journal of Hydrology 548 (2017) 263–277

Contents lists available at ScienceDirect

Journal of Hydrology

journal homepage: www.elsevier.com/locate/jhydrol

Research papers

On the use of surrogate-based modeling for the numerical analysis of Low Impact Development techniques

Giuseppe Brunetti [a,*], Jirka Šimůnek [b], Michele Turco [a], Patrizia Piro [a]

[a] Department of Civil Engineering, University of Calabria, Rende, CS 87036, Italy
[b] Department of Environmental Sciences, University of California, Riverside, Riverside, CA 92521, USA

ARTICLE INFO

Article history:
Received 19 October 2016
Received in revised form 28 February 2017
Accepted 6 March 2017
Available online 8 March 2017
This manuscript was handled by Corrado Corradini, Editor-in-Chief, with the assistance of Philip Brunner, Associate Editor

Keywords:
Urban hydrology
Surrogate-based modeling
Sensitivity analysis
Infiltration
LIDs

ABSTRACT

Mechanistic models have proven to be accurate tools for the numerical analysis of the hydraulic behavior of Low Impact Development (LIDs) techniques. However, their widespread adoption has been limited by their computational cost. In this view, surrogate modeling is focused on developing and using a computationally inexpensive *surrogate* of the *original* model. While having been previously applied to various water-related and environmental modeling problems, no studies have used surrogate models for the analysis of LIDs. The aim of this research thus was to investigate the benefit of surrogate-based modeling in the numerical analysis of LIDs. The kriging technique was used to approximate the deterministic response of the widely used mechanistic model HYDRUS-2D, which was employed to simulate the variably-saturated hydraulic behavior of a contained stormwater filter. The Nash-Sutcliffe efficiency (*NSE*) index was used to compare the simulated and measured outflows and as the variable of interest for the construction of the response surface. The validated kriging model was first used to carry out a Global Sensitivity Analysis of the unknown soil hydraulic parameters of the filter layer, revealing that only the shape parameter α and the saturated hydraulic conductivity K_s significantly affected the model response. Next, the Particle Swarm Optimization algorithm was used to estimate their values. The *NSE* value of 0.85 indicated a good accuracy of estimated parameters. Finally, the calibrated model was validated against an independent set of measured outflows with a *NSE* value of 0.8, which again corroborated the reliability of the surrogate-based optimized parameters.

1. Introduction

During the last few decades, stormwater management has become a major component of the prevention of floods in urban areas and for the preservation of water resources. An increase of impervious surfaces, connected with demographic growth, has altered the natural hydrological cycle by reducing the infiltration and evaporation capacity of urban catchments while also increasing surface runoff. In their report, the Organization for Economic Co-operation and Development (OECD) (2013) identified an expected increase in flash and urban floods in large parts of Europe as one of the major issues for the future.

In this context, urban drainage systems play a fundamental role in improving the resilience of cities. In recent years, an innovative approach to land development known as a Low Impact Development (LID) has gained increasing popularity. A LID is a 'green' approach to storm water management that seeks to mimic the natural hydrology of a site using decentralized micro-scale control measures (Coffman, 2002). LID practices consist of bioretention cells, infiltration wells/trenches, storm water wetlands, wet ponds, level spreaders, permeable pavements, swales, green roofs, vegetated filter/buffer strips, sand and gravel filters, smaller culverts, and water harvesting systems. Several studies have evaluated the benefits of LIDs. For example, Newcomer et al. (2014) used a numerical model to demonstrate the benefits of LIDs, and an infiltration trench in particular, on recharge and local groundwater resources for future climate scenarios. In another paper, Berardi et al. (2014) demonstrated how green roofs may contribute to the development of more sustainable buildings and cities. Green Roofs (GR) were able to significantly reduce peak rates of storm water runoff (Getter et al., 2007) and retain rainfall volumes with retention efficiencies ranging from 40% to 80% (Bengtsson et al., 2004). Permeable pavements offered great advantages in terms of runoff reduction (Carbone et al., 2014; Collins et al., 2008), water retention, and water quality (Brattebo and Booth, 2003). Even though the results of available studies are encouraging, more

* Corresponding author.
E-mail address: giusep.bru@gmail.com (G. Brunetti).

http://dx.doi.org/10.1016/j.jhydrol.2017.03.013
0022-1694/

research is needed to precisely assess the impact of LIDs on the hydrological cycle.

As pointed out by several authors (e.g., Elliot and Trowsdale, 2007; Wong et al., 2006), there is a strong demand for predictive models that can be applied across a range of locations and conditions to predict the general performance of a range of stormwater treatment measures. In recent years, researchers have focused their attention on applying and developing empirical, conceptual, and physically-based models for LIDs analysis. In their review article, Li and Babcock (2014) reported that there were >600 papers published worldwide involving green roofs, with a significant portion of them related to modeling. Several studies demonstrated that physically-based models can provide a rigorous description of various relevant processes such as variably-saturated water flow, evaporation and root water uptake, solute transport, heat transport, and carbon sequestration. Brunetti et al. (2016a, 2016b) used a mechanistic model, HYDRUS-3D (Šimůnek et al., 2016; Šimůnek et al., 2008), to analyze an extensive green roof in a Mediterranean climate. The model, previously validated against field scale measurements, was used to investigate the hydraulic response of a green roof to single precipitation events and its hydrological behavior during a two-month period. Metselaar (2012) used the SWAP model (van Dam et al., 2008) to simulate the one-dimensional water balance of a substrate layer on a flat roof with plants. Li and Babcock (2015) used HYDRUS-2D to model the hydrologic response of a pilot green roof system. The model was calibrated using water content measurements obtained with TDR (Time Domain Reflectometer) sensors. The calibrated model was then used to simulate the potentially beneficial effects of irrigation management on the reduction of runoff volumes. The VFSMOD model (Munoz-Carpena and Parsons, 2004) was extensively used for the analysis of the hydraulic behavior and solute transport of vegetated filter strips (Abu-Zreig et al., 2001; Dosskey et al., 2002).

However, physically-based modeling often involves highly nonlinear, partial, differential equations that are solved using various numerical approximation methods, requiring a high computational cost. Moreover, a comprehensive simulation framework includes model calibration, sensitivity analysis, and uncertainty quantification aimed at enhancing confidence in the model and its ability to describe real world systems. These tasks require running the simulation model hundreds or thousands of times and thus the computational cost exponentially increases.

Surrogate modeling focuses on developing and using a computationally inexpensive *surrogate* of the *original* model. The main aim is to approximate the response of an original simulation model, which is typically computationally intensive, for various quantities of interest (Razavi et al., 2012). Surrogate models have been widely applied in various water-related and environmental modeling problems. Khu and Werner (2003) used artificial neural networks (ANN) in conjunction with genetic algorithms (GA) to reduce the computational budget required in the uncertainty quantification framework of the rainfall-runoff model SWMM. The GA was first used to identify the areas of higher importance in the parameter space and ANNs were then used to approximate the response surface in these areas (Khu and Werner, 2003). Borgonovo et al. (2012) tested a surrogate model for the estimation of the sensitivity indices of an environmental model. Zhang et al. (2009) evaluated ANN and Support Vector Machine (SVM) for approximating the Soil and Water Assessment Tool (SWAT) model in two watersheds. Keating et al. (2010) used a surrogate model to carry out a comparison between the null-space Monte Carlo sampling (NSMC) and the DiffeRential Evolution Adaptive Metropolis (DREAM) algorithm for parameter estimation and uncertainty quantification. In another study, Laloy et al. (2013) used Polynomial Chaos Expansion (PCE) to emulate the output of a large-scale flow model. The surrogate model was used in a Bayesian analysis framework to derive the posterior distribution of different parameters. In their study, Younes et al. (2013) used a surrogate model to estimate three soil hydraulic parameters from a drainage experiment. In particular, PCE was used to run a Monte Carlo Markov Chain (MCMC) analysis. However, although the widespread diffusion of surrogate modeling tools could drastically reduce computational budgets, their use for physically-based modeling of LIDs is still unexploited.

The primary objective of this paper is to investigate the suitability of surrogate modeling for the numerical analysis of LIDs techniques by analyzing data from a real case study. The mechanistic model HYDRUS-2D is first used to simulate the hydraulic behavior of a Stormwater Filter (SF) at the University of Calabria, Italy. The surrogate model, based on kriging, is then used to carry out a Global Sensitivity Analysis (GSA) and a Global Optimization of soil hydraulic parameters. The use of a surrogate model for the sensitivity analysis of model outputs to soil hydraulic properties represents a new application of this technique that can provide a significant contribution in this field.

The problem is addressed in the following way. First, the evaporation method is used to measure the soil hydraulic properties of the vegetated substrate above the gravel filter, for which the hydraulic properties were unknown. The measured soil hydraulic properties of the vegetated substrate and the selected ranges of parameters of the filter layer are then used in HYDRUS-2D to set up the model. A Latin Hypercube Sampling (LHS) plan is used to build a first trial of the surrogate model. Before continuing with the other tasks, the surrogate model is validated and improved by using specific infill criteria. Once validated, the surrogate model is first used for the GSA based on Sobol's method to compute the sensitivity measures, and then for the inverse parameter estimation carried out using the Particle Swarm Optimization (PSO) algorithm. Finally, estimated parameters are used in the original mechanistic model for the validation purpose.

2. Materials and methods

2.1. Stormwater filter and site description

The University of Calabria is located in the south of Italy, in the vicinity of Cosenza (39°18′ N 16°15′ E). The climate is Mediterranean with a mean annual temperature of 15.5 °C and average annual precipitation of 881.2 mm. The stormwater filter (SF) has a surface area of 125 m^2, an average slope of 2%, and a total profile depth of 0.75 m. Fig. 1 shows a schematic of the SF.

The filter layer is covered by a vegetated soil substrate with a measured bulk density of 1.59 g/cm^3. A high permeability geotextile with a fiber area weight of 60 g/m^2 is placed at the interface between the soil substrate and the filter layer to prevent fine particles from migrating into the underlying layer. The filter layer is composed of a gravelly material characterized by a high permeability. An impervious membrane is placed at the bottom of the profile to prevent water from percolating into deeper horizons.

The SF is used to treat stormwater runoff from the adjoining impervious parking lot, which is characterized by an area of 220 m^2. Stormwater runoff from the parking lot is first conveyed into a manhole and then to an instrumented channel where the flow rate is measured by a flux meter composed of a rectangular, sharp crested weir coupled with a pressure transducer. The pressure transducer (Ge Druck PTX1830) measures the water level inside the channel and has a range of measurements of 75 cm with an accuracy of 0.1% of the full scale. The pressure transducer was calibrated in the laboratory using a hydrostatic water column, linking the electric current intensity with the water level inside the

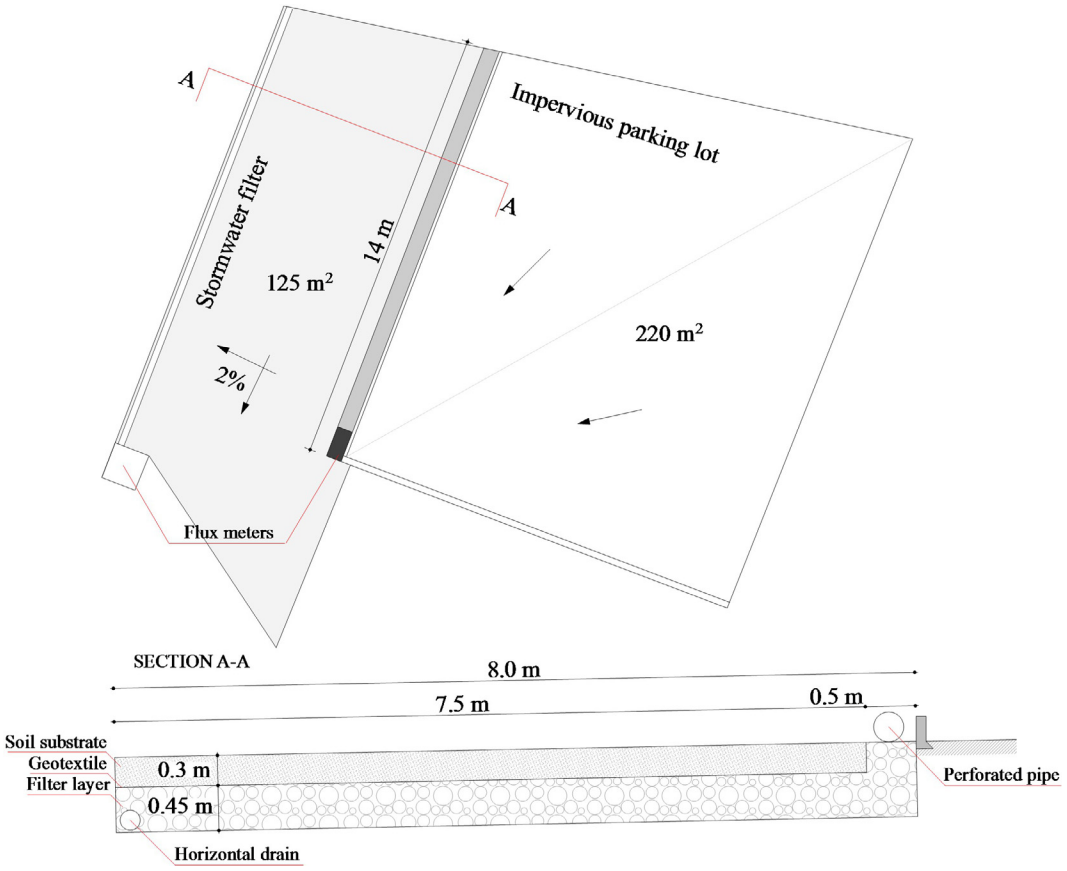

Fig. 1. A schematic of the experimental site (top) and a typical cross-section (bottom) of the stormwater filter.

column. An exponential head-discharge equation for the flux meter was obtained by fitting the experimental data.

Measured runoff is next conveyed into a 14 m long, horizontal perforated pipe where it is distributed on the top of the filter layer (Fig. 1). As shown in Fig. 1, the soil substrate is not used to treat stormwater runoff, which is directly routed into the filter, but only to increase the retention and evapotranspiration capacity of the system itself. The baseflow is collected in a horizontal drain, which consists of a perforated PVC pipe, and is conducted to a manhole for quantity and quality measurements. A second flux meter, composed of a PVC pipe with a sharp-crested weir and a pressure transducer, measures the flow rate. Runoff and baseflow data were acquired with a time resolution of one minute and stored in a SQL database. No measurements of pressure heads or volumetric water contents inside of the filter were taken.

A weather station located directly at the site measures precipitation, wind velocity and direction, air humidity, air temperature, atmospheric pressure, and global solar radiation. Rain data are measured using a tipping bucket rain gauge with a resolution of 0.254 mm and an acquisition frequency of one minute. Climatic data are acquired with a frequency of five minutes. Data are processed and stored in the SQL database.

Two month-long data sets were selected for the analysis (Fig. 2). The first data set, which started on 2014-01-15 and ended on 2014-02-15, was used for obtaining the surrogate model. The second data set, which started on 2014-03-01 and ended on 2014-03-31, was used for model validation. The precipitation totals for the first and second data sets were 274 and 174 mm, respectively. The second data set was selected because it had significantly different meteorological dynamics than during the first period. The optimization set is characterized by multiple rain events with few dry periods. The validation set has fewer rain events, which are concentrated at the beginning and end of the time period and separated by a relatively long dry period.

Hourly reference evapotranspiration was calculated using the Penman-Monteith equation (Allen et al., 1998). Considering that vegetation mainly consisted of herbaceous plants, an average value of albedo of 0.23 was assumed in calculations of net short-wave radiation (Breshears et al., 1997).

2.2. Evaporation method and parameter estimation

2.3.1. Evaporation method

Modeling of water flow in unsaturated soils by means of the Richards equation requires knowledge of the water retention function, $\theta(h)$, and the hydraulic conductivity function, $K(h)$, for each soil layer of the SF, where θ is the volumetric water content [L^3L^{-3}], h is the pressure head [L], and K is the hydraulic conductivity [LT^{-1}]. In order to reduce the dimensionality of the optimization problem, the soil hydraulic properties of the soil substrate were measured in the laboratory using a simplified evaporation method with an extended measurement range (down to −9000 cm), as proposed by Schindler et al. (2010a, 2010b). For a detailed description of the modified evaporation method, please refer to Schindler et al. (2010a, 2010b).

Peters and Durner (2008) conducted a comprehensive error analysis of the simplified evaporation method and concluded that it is a fast, accurate, and reliable method to determine soil hydraulic properties in the measured pressure head range, and that the linearization hypothesis introduced by Schindler (1980) causes only small errors. The above cited method has already been used in the LIDs analysis for the determination of the unsaturated soil

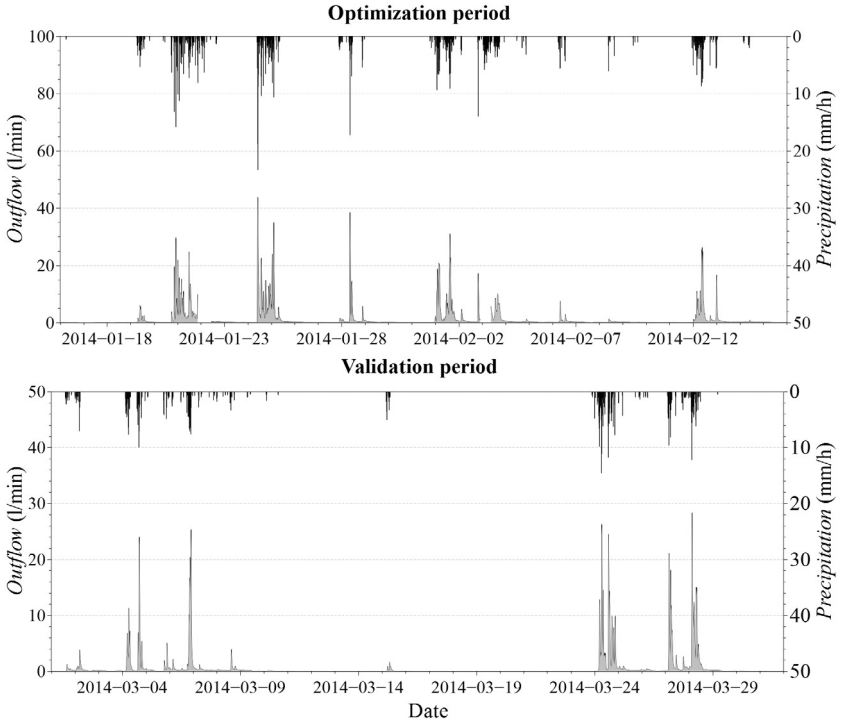

Fig. 2. Precipitation (black line) and subsurface flow (grey line) for the optimization (top) and validation (bottom) periods, respectively.

hydraulic properties of a green roof substrate (Brunetti et al., 2016a). In that study, the measured soil hydraulic properties were used in HYDRUS-3D to simulate the hydraulic behavior of a green roof and validated by providing optimal correspondence between simulated and measured outflows. The simplified evaporation method was similarly used in this study for the determination of the unsaturated hydraulic properties of the soil substrate. For a complete description of the system, please refer to UMS GmbH (2015).

The soil for the laboratory analysis was directly sampled from the SF using a stainless-steel sampling ring with a volume of 250 ml. The soil sample was saturated from the bottom before starting the evaporation test. The measurement unit and tensiometers were degassed using a vacuum pump, in order to reduce the potential nucleation sites in the demineralized water. Since Peters and Durner (2008) suggested a reading interval for structured soils of less than 0.1 day, the reading interval was set to 20 min in order to have high resolution measurements. At the end of the experiment, the sample was placed in an oven at 105 °C for 24 h, and then the dry weight was measured.

2.4. Parameter estimation

The numerical optimization procedure, HYPROP-FIT (Pertassek et al., 2015), was used to simultaneously fit retention and hydraulic conductivity functions to experimental data obtained using the evaporation method. Fitting was accomplished using a non-linear optimization algorithm that minimizes the sum of weighted squared residuals between model predictions and measurements. The software uses the Shuffled Complex Evolution (SCE) algorithm proposed by Duan et al. (1992), which is a global parameter estimation algorithm. The goodness-of-fit was evaluated in terms of the Root Mean Square Error (RMSE), while the Akaike information criterion (AIC) (Hu, 1987) was used to choose between different hydraulic conductivity functions. The software also provides 95% confidence intervals to assess the uncertainty in parameter estimation. In order to calculate the parameter uncertainties a linear approximation of the covariance matrix for each estimated parameter is calculated. The confidence interval for the i-th parameter is then computed by combining the covariance matrix and the upper $a/2$ quantile of the Students t-distribution, where a is set to 0.05 for the computation of the 95% confidence intervals.

2.5. Modeling theory

2.5.1. Water flow and root water uptake

The HYDRUS-2D software (Šimůnek et al., 2008) was used to model the hydraulic behavior of the SF. HYDRUS-2D is a two-dimensional model for simulating the movement of water, heat, and multiple solutes in variably-saturated porous media. HYDRUS-2D numerically solves the Richards equation for multi-dimensional unsaturated flow:

$$\frac{\partial \theta}{\partial t} = \nabla[k \cdot \nabla(h - z)] - S \tag{1}$$

where t is time (T), z is the vertical coordinate (L), and S is a sink term ($L^3L^{-3}T^{-1}$), defined as a volume of water removed from a unit volume of soil per unit of time due to plant water uptake. The unimodal van Genuchten–Mualem (VGM) model (van Genuchten, 1980) was used to describe the soil hydraulic properties of the two layers:

$$\Theta = \begin{cases} \frac{1}{(1+(\alpha|h|)^n)^{\overline{m}}} & \text{if } h \leqslant 0 \\ 1 & \text{if } h > 0 \end{cases} \tag{2}$$

$$\Theta = \frac{\theta - \theta_r}{\theta_s - \theta_r}$$

$$K = \begin{cases} K_s \Theta^L [(1 - (1 - \Theta^{\frac{1}{\overline{m}}}))^m]^2 & \text{if } h < 0 \\ K_s & \text{if } h > 0 \end{cases} \tag{3}$$

$$m = 1 - \frac{1}{n}$$

where Θ is the effective saturation (−), α is a shape parameter related to the inverse of the air-entry pressure head (L^{-1}), θ_s and θ_r are the saturated and residual water contents, respectively (−), n and m are pore-size distribution indices (−), K_s is the saturated hydraulic conductivity (LT^{-1}), and L is the tortuosity and pore-connectivity parameter (−).

While the soil hydraulic properties of the soil substrate were determined using the simplified evaporation method, those of the filter were optimized in the surrogate analysis framework. However, not all parameters were included in the optimization process. The residual water content θ_r was fixed to 0, considering that the filter is composed of coarse gravel, and the tortuosity L was set to 0.5, which is a common value in the literature. The initial range of the investigated parameters is reported in Table 1.

Feddes et al. (1978) defined S as:

$$S(h) = a(h) \cdot S_p \tag{4}$$

where $a(h)$ is a dimensionless water stress response function that depends on the soil pressure head h and has a range of values between 0 and 1, and S_p is the potential root water uptake rate. Feddes et al. (1978) proposed a water stress response function in which water uptake is assumed to be zero close to soil saturation (h_1) and for pressure heads larger (in absolute values) than the wilting point (h_5). Water uptake is assumed to be optimal between two specific pressure heads (h_2, h_3 or h_4), which depend on a particular plant. At high potential transpiration rates (5 mm/day in the model simulation) stomata start closing at lower pressure heads (h_3) (in absolute value) than at low potential transpiration rates (1 mm/d) (h_4). Parameters of the stress response function for a majority of agricultural crops can be found in various databases (e.g., Taylor and Ashcroft, 1972; Wesseling et al., 1991). Considering that the vegetation cover was mainly constituted of herbaceous plants, parameters reported for grass in Wesseling et al. (1991) were used in this study.

The local potential root water uptake S_p was calculated from the potential transpiration rate T_p. Beer's equation was first used to partition reference evapotranspiration, calculated using the Penman-Monteith equation (Allen et al., 1998), into potential transpiration and potential soil evaporation fluxes (e.g., Ritchie, 1972). The partitioning of evapotranspiration into potential transpiration and potential evaporation allows the computation of different actual fluxes in the soil-vegetation system. The Leaf Area Index (LAI) is needed to partition evaporation and transpiration fluxes. In this study, a LAI value of 2.29 as reported by Blanusa et al. (2013) for a *sedum* mix was used, considering its similarity with the installed vegetation. For a detailed explanation of evapotranspiration partitioning, please refer to Sutanto et al. (2012).

HYDRUS-2D allows for the consideration of a spatially variable root distribution. In this study, a homogeneous root zone within a depth of 15 cm was defined. The root density was assumed to be uniform inside the root zone and zero in the remaining part of the numerical domain. The total potential transpiration flux from a transport domain is equal in HYDRUS to potential transpiration T_p, multiplied by the surface length associated with vegetation. This total potential transpiration flux is then distributed over the entire root zone for the computation of the actual root water uptake.

Table 1
Ranges of investigated parameters for the surrogate-based analysis.

Parameter	Range
θ_s [−]	0.1–0.3
α [1/cm]	0.001–0.3
n_1 [−]	3.0–7.0
K_{s1} [cm/min]	30.0–100.0

2.6. Numerical domain and boundary conditions

The two-dimensional domain had a length of 8.0 m and a depth of 0.75 m. The geotextile was not included in the model considering its negligible thickness, its limited hydraulic effect due to its high permeability, and that its sole function was to separate the soil substrate from the filter layer. The domain was discretized into two-dimensional triangular elements using the MESHGEN tool of HYDRUS-2D. The mesh was refined in the right part of the domain, where the effect of the surface runoff from the parking lot was simulated. This refinement was necessary in order to numerically accommodate the significant pressure head gradients generated by infiltration of runoff, and thus to reduce the mass balance errors. The generated FE mesh had 736 nodes and 1350 two-dimensional elements. The quality of the FE mesh was assessed by checking the mass balance error reported by HYDRUS-2D at the end of the simulation. Mass balance errors, which in this simulation were always below 1%, are generally considered acceptable at these low levels.

The surface of the SF was exposed to precipitation, evapotranspiration, and surface runoff from the impervious parking lot. As a result, in HYDRUS, two different boundary conditions were specified at the top of the modeled domain, as well as at its bottom (Fig. 3).

The "Atmospheric" boundary condition, which was assigned on the surface of the soil substrate (green line in Fig. 3), can exist in three different states: (a) precipitation and/or potential evaporation fluxes, (b) a zero pressure head (full saturation) during ponding when both infiltration and surface runoff occurs, and (c) an equilibrium between the soil surface pressure head and the atmospheric water vapor pressure head when atmospheric evaporative demand cannot be met by the substrate. The threshold pressure head, which was set to −10,000 cm, divides the evaporation process from the soil surface into two stages: (1) a constant rate stage when actual evaporation, equal to potential evaporation, is limited only by the supply of energy to the surface, and (2) the falling rate stage, when water movement to the evaporating sites near the surface is controlled by subsurface soil moisture and the soil hydraulic properties. In such conditions, actual evaporation, calculated as a result of the numerical solution of the Richards equation, is smaller than potential evaporation.

The "Variable Flux" boundary condition, which included both precipitation and measured surface runoff, was used in the area under the perforated pipe (red line in Fig. 3). Evaporation was excluded since most of the surface was covered by the perforated pipe, which reduced the exposure of the surface to wind and solar radiation.

A seepage face boundary condition (brown line in Fig. 3) was specified at the bottom left corner of the numerical domain to simulate the effect of the horizontal drain. A seepage face boundary acts as a zero pressure head boundary when the boundary node is saturated and as a no-flux boundary when it is unsaturated. A zero flux boundary condition (black line in Fig. 3) was applied to all remaining boundaries of the domain to simulate the effect of the impervious membrane placed at the bottom and on the sides of the SF.

The initial conditions were specified in terms of the soil water pressure head and were set to linearly increase with depth, from −90 cm at the top of the flow domain (z = 0) to −0.5 cm at the bottom (z = −75). The surface layers are assumed to be drier than the bottom layers since they are directly exposed to the atmosphere.

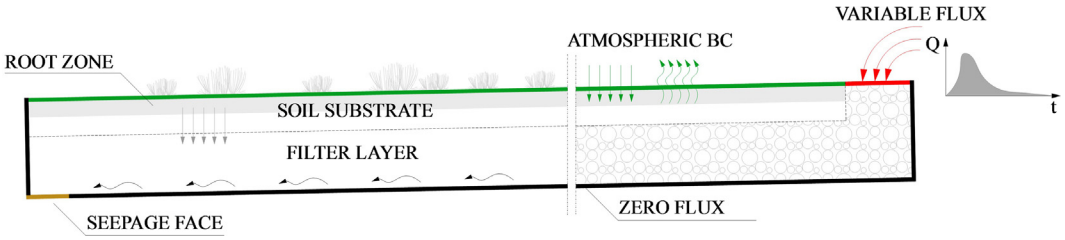

Fig. 3. The spatial distribution of applied boundary conditions.

The numerical model is expected to be sensitive to the initial conditions only during the first few simulated days.

2.7. Surrogate based model

2.7.1. Kriging

There are two broad families of surrogate modeling techniques: Response Surface Surrogates (RSS) and Lower-Fidelity Surrogates (LFS). While RSS are data-driven techniques for approximating the response surface of high-fidelity (original) models based on a limited number of original model evaluations, LFS are essentially cheaper-to-run, alternative simulation models with different levels of accuracy (Razavi et al., 2012). As pointed out by Razavi et al. (2012) in their review paper, LFS outperforms RSS when the dimensionality of the problem is high and the response surface landscape is characterized by multimodality. In such circumstances, RSS would need a higher number of original model runs to correctly approximate the response surface. O'Hagan (2006) highlighted how the same number of design sites can lead to different parameters space coverages depending on the dimensionality of the problem. However, when the problem is low-dimensional and the response surface is characterized by a low or moderate multimodality, RSS are preferred since a limited number of high-fidelity model runs is required to build a reliable surrogate model.

The present study involves a SF model with four parameters to be investigated. Considering the low dimensionality of the problem, the kriging response surface approximation technique was used. Unlike other RSS, kriging models have their origins in mining and geostatistical applications involving spatially and temporally correlated data. The kriging technique has also been referred to in the literature as a Gaussian Process (GP) prediction (Rasmussen and Williams, 2006; Sacks et al., 1989). A Gaussian Process is formally defined as being a probability distribution over a (possibly infinite) number of variables, such that the distribution over any finite subset of them is a multi-variate Gaussian. As the Gaussian distribution is fully specified by its mean and covariance matrix, the GP is specified by a mean and a covariance function (Mackay, 1998). The mean is usually assumed to be zero, and, in such circumstances, the covariance function completely describes the GP behavior. One of the most attractive features of GP is that it treats the deterministic response of a computer model as the realization of a stochastic process, in particular a Gaussian random process, thereby providing a statistical basis for fitting. This capability provides a first approximation of uncertainty associated with each value predicted by the surrogate. Another advantage of kriging against other RSS techniques such as Artificial Neural Networks (ANN) or Support Vector Machines (SVM) is that kriging is an exact emulator. An exact emulator precisely predicts all design sites used to build the surrogate, while inexact emulators can introduce bias in such sites. As described by Razavi et al. (2012), an exact emulation is recommended for approximating the deterministic response of computer simulation models. Inexact emulators have smoothing capabilities that can help when the response surface is noisy (e.g., physical experiments), however this feature can lead to poor approximation of the response surface when it is characterized by multiple local minima.

The kriging model is a combination of a polynomial model and a localized deviation model, which is based on a spatial correlation of samples (Eq. (4)):

$$y(x) = f(x) + Z(x) \tag{5}$$

where $y(x)$ is an unknown function of interest, $f(x)$ is an approximation function, and $Z(x)$ is the realization of a stochastic process with zero mean, the variance σ^2, and nonzero covariance. While $f(x)$ globally approximates the response surface through design sites, $Z(x)$ creates localized deviations. The covariance matrix of $Z(x)$ is given by Eq. (6):

$$Cov[Z(x^i), Z(x^j)] = \sigma^2 \Psi([R(x^i, x^j)]) \tag{6}$$

where Ψ is the p x p symmetric correlation matrix and $R(x^i, x^j)$ is the correlation function between two of the p sampled data points. $R(x^i, x^j)$ can assume different forms and is specified by the user. In this study, the Gaussian correlation function has been used (Eq. (7)):

$$R(x^i, x^j) = \exp\left(-\sum_{k=1}^{N} \tau_j |x_k^i - x_k^k|^2\right) \tag{7}$$

where N is the number of parameters, τ_j are the unknown correlation parameters used to fit the model, and x_k^i and x_k^j are the kth components of the sample points x^i and x^j. Correlation parameters τ_j are estimated using the maximum likelihood methodology. The "best" kriging model is found by solving a j-dimensional, unconstrained, nonlinear optimization problem. In this study, the PSO global optimization algorithm has been used to identify kriging parameters.

2.8. Design of experiments

The first step in the generation of a surrogate model is to sample the response surface at some specific design sites. This procedure is usually referred to in the literature as the Design of Experiments (DoEs). As pointed out by Razavi et al. (2012), a sufficiently large and well-distributed set of initial design sites is crucial for a successful application of a metamodeling framework. There are several DoEs methods available in the literature. Factorial design (Gutmann, 2001), Latin Hypercube Sampling (LHS) (McKay et al., 1979), and Symmetric Latin Hypercube Sampling (SLHS) (Ye et al., 2000) are the most commonly used. In this study, the LHS has been used. The size of the DoEs sample is strongly dependent on the complexity of the original response surface and computational budget available. The kriging model requires at least N+1 design sites to fit, while additional sites will improve the accuracy of the surrogate. Several relations were proposed in the literature to choose the size p of the initial sample (e.g., Gutmann, 2001; Regis and Shoemaker, 2004). In this study, the relation proposed by Jones et al. (1998) has been used (Eq. (8)):

$$p = 10N \tag{8}$$

Considering that the number of investigated parameters was 4, 40 sampling points were generated using the LHS.

2.9. Approximation uncertainty framework

The surrogate model fitted on a DoEs sample is only the first approximation of the original response function. Its accuracy can be improved using further original model runs (*infill points*) in addition to the initial sampling plan. The distribution of *infill points* strongly depends on the complexity of the original response surface and on the type of analysis conducted. When the purposes of the analysis of the surrogate model includes uncertainty and sensitivity analyses, it is necessary to have an accurate global approximation of the response surface. The adaptive-recursive framework relies on the assumption that the optimal solution of the surrogate represents well the original model. However, this is not always true, especially when the response surface is characterized by high multimodality. When the approximation of the response surface by the surrogate model is limited, this framework is not recommended for the uncertainty and/or sensitivity analysis. Jones (2001) concluded that the adaptive-framework is helpful at best for local optimization.

In this study, the approximation uncertainty framework was applied to address the shortcoming of the adaptive-recursive framework, which considers uncertainties associated with the approximation. RSS, such as kriging, explicitly provide a measure of uncertainty since they treat the deterministic response of a computer simulation as the realization of a stochastic process. The model can then be evaluated at points with the highest uncertainty, which can then be included among the design sites. Although globally convergent, such an approach requires an impractically large number of original function evaluations. An effective uncertainty based framework should balance exploitation (i.e., fine tuning of a good solution) and exploration (i.e., reducing the overall uncertainty of the surrogate). The expected-improvement approach (Schonlau, 1997) was used in this study. An expected-improvement is a measure that statistically quantifies the obtained improvement when a given point is evaluated by the original model and added to design sites. For a complete description of the expected-improvement approach please refer to Schonlau (1997).

In this study, the expected-improvement approach was used to add 15 *infill points* to the initial design sites. In order to have good accuracy, the surrogate was refitted after each new original model evaluation (Razavi et al., 2012).

2.10. Surrogate validation

Validation of the RSS model is important for evaluating the reliability of the surrogate. Although exact emulators such as kriging exactly interpolate the response surface at design sites, their accuracy in unexplored regions of the parameter space must be evaluated. The validation can be conducted by evaluating the agreement between values of the variable of interest predicted by both the surrogate and original models on an independent set of sample points. Cross validation strategies such as *k*-fold and leave-one-out cross validation have also been used in the literature (Wang and Shan, 2007). In the present study, an independent set of sample points was generated using the LHS and used to validate the model. Ten points were used to carry out the validation process. The Pearson coefficient R^2 was used to assess the agreement between predicted and modeled values. As suggested by Forrester et al. (2008), a value of the correlation coefficient higher than 0.8 indicates a surrogate model with good predictive capabilities.

2.11. Global Sensitivity Analysis (GSA)

A sensitivity analysis (SA) can identify the most influential parameters, their interactions, and how these parameters affect the output (Saltelli et al., 2005). Most SAs performed in the literature of environmental sciences are the so-called 'one-at-a-time' (OAT) sensitivity analyses, performed by changing the value of parameters one-at-a-time while keeping the other parameters constant (Cheviron and Coquet, 2009; Houska et al., 2013; Rezaei et al., 2015). However, when the model includes interactions between multiple parameters, results of the OAT analysis are inaccurate because parameter interactions can be globally identified only by simultaneously changing multiple parameters. For this reason, when the property of a model is *a priori* unknown, a Global Sensitivity Analysis (GSA) is always preferred (Saltelli and Annoni, 2010). Practitioners call this analysis a model-free setting, which means that a particular application does not depend on particular assumptions regarding the behavior of the model, such as linearity, monotonicity, etc (Saltelli and Annoni, 2010).

Variance-based methods aim to quantify the amount of variance that each parameter contributes to the unconditional variance of the model output. In Sobol's method, these measures are represented by Sobol's sensitivity indices (SIs). These indices give quantitative information about the variance associated with a single parameter or with interactions of multiple parameters. For a more complete explanation about Sobol's method, please refer to Sobol' (2001). Sobol's sensitivity indices are expressed as follows:

$$FirstOrder\ S_i = \frac{V_i}{V} \tag{9}$$

$$SecondOrder\ S_{ij} = \frac{V_{ij}}{V} \tag{10}$$

$$Total\ S_T = S_i + \sum_{j \neq i} S_{ij} + \ldots \tag{11}$$

where V_i is the variance associated with the ith parameter and V is the total variance. The first-order index, S_i, is denoted in the literature as the "main effect." When the model is additive, i.e., when it does not include interactions between input factors, the first-order index is sufficient for decomposing the model's variance. For additive models, the following relation is valid:

$$\sum_i S_i = 1 \tag{12}$$

On the other hand, the total effect index, S_T, gives information about a non-additive part of the model. $S_{Ti} = 0$ is a condition necessary and sufficient for X_i to be non-influential. For an accurate description of the calculation of Sobol's indices please refer to Saltelli et al. (2010).

When the model is nonlinear, as most environmental models are, Sobol's indices are calculated using Monte Carlo integrals. Obviously, the accuracy in the estimation of integrals becomes more accurate as the number of samples increases, which also increases the computational cost of the SA. However, this limitation is avoided when using a surrogate model since the computational cost associated with the evaluation of a large number of samples is very low (O'Hagan, 2006; Oakley and O'Hagan, 2004). For this reason, 1000 samples for a total of 30,000 surrogate model runs were used in this study. To sample the parameters' space we used Sobol's quasi-random sampling technique (Sobol', 2001).

In order to assess the accuracy of the estimations of the sensitivity indices, the bootstrap confidence intervals (BCIs) (Efron and Tibshirani, 1986) were estimated. The basic idea of the bootstrapping is that the sample contains all available information about the underlying distribution. In our particular case, we were interested in computing the uncertainty of estimated sensitivity indices. However, since their distribution is unknown it is not possible to compute the confidence intervals analytically. The rationale of the bootstrap method is to replace the unknown distribution with

its empirical distribution and to compute the sensitivity indices using a Monte Carlo simulation approach where samples are generated by resampling the original sample used for the sensitivity analysis. In our case, the samples used for the GSA were sampled 1000 times with replacement, whereby Sobol's indices were calculated for each resampling. In this way, 95% confidence intervals are constructed using the percentile method and the moment method (Archer et al., 1997).

2.12. Particle Swarm Optimization

Numerous applications of inverse modeling for the estimation of soil hydraulic properties exist in the literature (Abbaspour et al., 2004; Hopmans et al., 2002; Vrugt et al., 2008; Vrugt et al., 2004). The gradient methods (Marquardt, 1963) have been most widely used among hydrologists and soil scientists. However, these methods are sensitive to the initial values of optimized parameters and the algorithm often remains trapped in local minima, especially when the response surface exhibits a multimodal behavior. These considerations inspired researchers to develop and use global optimization techniques such as the annealing-simplex method (Pan and Wu, 1998), genetic algorithms (Ines and Droogers, 2002), shuffled complex methods (Vrugt et al., 2003), and ant-colony optimization (Abbaspour et al., 2001), among many others.

In this paper, a global search method based on Particle Swarm Optimization (PSO) (Kennedy and Eberhart, 1995) was used. This method simulates the behavior of a flock of birds collectively foraging for food (i.e., searching for the optimum of the objective function). In their recent study, Brunetti et al. (2016b) used PSO to estimate the soil hydraulic properties of a permeable pavement with satisfactory results. PSO is a relatively new algorithm for evolutionary computation methodology, but its performance has proven to be comparable to various other more established methodologies (Kennedy and Spears, 1998; Shi et al., 1999). One of the main advantages of PSO is the easiness of its implementation (Liang et al., 2006). A detailed description of the PSO algorithm is given in Shi and Eberhart (1998).

In PSO, each particle represents a possible solution of the problem. First, particles are placed in the search space, each characterized by a particular value of the objective function. Each particle then changes its position after exchanging information about its own current and best positions with other members of the swarm. The next iteration starts after all particles have changed their positions. The most important parameters in the PSO are c_1, c_2, and w. c_1 and c_2 are constant parameters known as the cognitive and social parameters, respectively, which drive the search behavior of the algorithm. Depending on the values of c_1 and c_2 the PSO can be more or less "responsive". However, their values should be selected carefully because large values of these parameters can lead to instabilities in the algorithm. w is the inertia-weight, which plays a key role in the optimization process by providing balance between exploration and exploitation. In PSO, each particle is influenced by its nearest neighbors. The arrangement of neighbors that influence a particle is called the *topology* of the swarm. Different types of neighborhoods are reported in the literature (Akat and Gazi, 2008). In this study, the *all* topology is used, in which the neighborhood encompasses the entire swarm. The PSO parameters used in this study for both scenarios are reported in Table 2 and are as suggested by Pedersen (2010).

Table 2
Parameters used in the PSO optimization.

Swarm size	c_1	c_2	w
63	−0.73	2.02	−0.36

2.13. Objective function

The Nash-Sutcliffe efficiency (NSE) index (Nash and Sutcliffe, 1970) was used to evaluate the agreement between measured and modeled hydrographs and as the variable of interest in the surrogate analysis:

$$NSE = 1 - \left[\frac{\sum_{i=1}^{T}(Q_i^{obs} - Q_i^{mod})^2}{\sum_{i=1}^{T}(Q_i^{obs} - Q_{mean}^{obs})^2}\right] \quad (13)$$

where Q_i^{obs} is the ith measured value, Q_i^{mod} is the ith simulated value, and Q_{mean}^{obs} is the mean value of observed data. The *NSE* index ranges between $-\infty$ and 1.0, is equal to 1 in case of perfect agreement, and generally, values between 0.0 and 1.0 are considered acceptable (Moriasi et al., 2007). The *NSE* index was used because it is often reported to be a valid measure for evaluating the overall fit of a hydrograph (Sevat et al., 1991).

It is important to emphasize that subsurface outflow from a LID system is among the most important outputs in the analysis of urban drainage systems. In our case, the stormwater filter was impervious at the bottom and hydraulically connected with the sewer system. An accurate numerical reconstruction of the subsurface hydrograph is thus fundamental in order to quantify its effect on the drainage system.

3. Results and discussion

3.1. Evaporation method

Soil hydraulic properties measured using the evaporation method are displayed in Fig. 4. The retention data point close to log ($|h|$) = 4 (h in cm) was obtained by using the air-entry pressure head of the ceramic cup of the tensiometers. Measured retention points were not available in the very dry range, between 2.7 and 3.8, since cavitation occurred in the tensiometers. The behavior of the retention curve appears to be sigmoidal and characterized by a clearly identifiable air-entry pressure head at log ($|h|$) = 2 (h in cm). Below this pressure head, the soil quickly desaturated, indicating a narrow pore-size distribution. Measured points of the hydraulic conductivity function were sparser and concentrated in the dry range between volumetric water contents of 0.10 and 0.20. The measured soil porosity and bulk density were 0.44 and 1.59 g/cm^3, respectively.

The unimodal van Genuchten-Mualem model (van Genuchten, 1980) was fitted to measured points using the HYPROP-FIT software. The *RMSE* values for retention and conductivity functions were 0.04 (cm^{3}cm^{-3}) and 0.6 (in log K, cm/day), respectively. The VGM function (full lines in Fig. 4) described the retention data well, especially in the dry and medium-wet regions (volumetric water contents of 0.5–0.3), while it introduced some bias near saturation where it poorly described the sharp increase in water retention at the air-entry pressure head. However, the low *RMSE* value was considered acceptable for the purposes of the present study. The *RMSE* value for the hydraulic conductivity was higher, indicating a slightly worse performance of the VGM function in describing the hydraulic conductivity of the substrate. The estimated soil hydraulic parameters (reported with their confidence intervals in Table 3) were used in HYDRUS-2D to model the hydraulic behavior of the soil substrate.

3.2. Kriging approximation of the response surface

The DoEs sample, generated with the LHS technique, was used to build the first approximation of the response surface for the investigated soil hydraulic parameters. First, the HYDRUS-2D

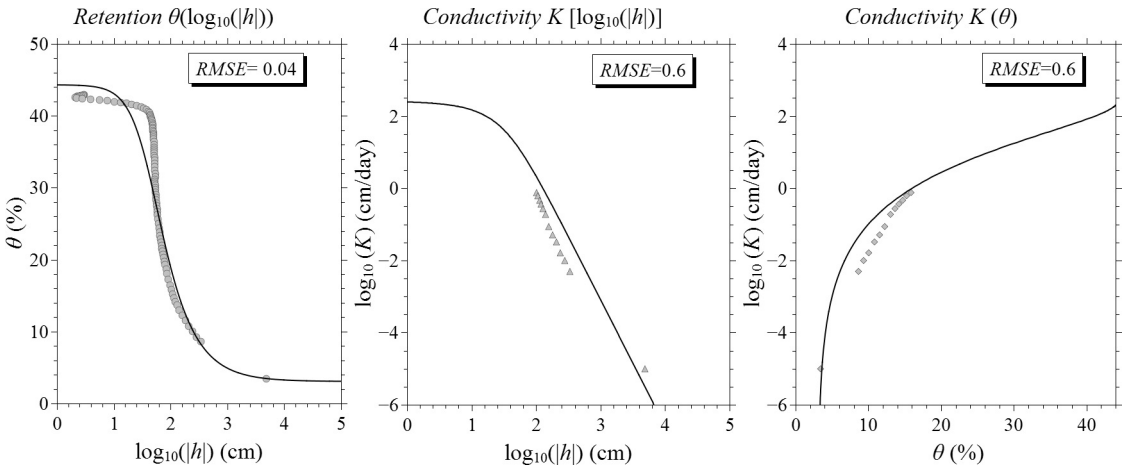

Fig. 4. Measured values and modeled functions of soil water retention, θ ($\log_{10}(|h|)$) (left) and the unsaturated hydraulic conductivity, $K(\log_{10}(|h|))$ (center) and $K(\theta)$ (right). Symbols represent the measured values, and full lines the fitted VGM functions.

Table 3
Estimated soil hydraulic parameters and their confidence intervals for the bimodal hydraulic function.

Parameter	2.5%	Estimated value	97.5%
θ_r (−)	0.02	0.03	0.04
θ_s (−)	0.43	0.44	0.45
α (1/cm)	0.021	0.025	0.029
n (−)	1.84	1.97	2.10
K_s (cm/day)	200	260	320
L (−)	−0.63	−0.44	−0.25

model was executed 40 times (Eq. (8)), and the *NSE* index was computed for each run and stored in a 1D array. A single run of the original HYDRUS-2D model required almost 1 min of CPU time on a laptop equipped with a CPU Intel® Core i7-4700 MQ 2.40 GHz processor and 8 GB of RAM. Next, the LHS sample and the *NSE* array were used in the PSO optimization framework to estimate the kriging parameters. To check its accuracy, the obtained kriging model was validated on another independent sample generated with the LHS. As shown in Fig. 5, the validation sample covered values of *NSE* ranging from 0.2 to 0.8, providing information about the response surface for both less and more accurate portions of the parameters space.

At the first inspection, the kriging model based on the initial sample exhibited a moderate accuracy. The determination coefficient R^2 for the initial kriging model was 0.91, which already indicated an overall accuracy of the surrogate model (Forrester et al., 2008). This confirmed the good coverage of the DoEs sample. However, as shown in Fig. 5, the surrogate, while being highly accurate for low values of the objective function, introduced a significant bias for high values of *NSE*, which are those of interest in an optimization framework. The regression line for the initial surrogate (a dashed grey line in Fig. 5) almost overlapped the bisector (a black line in Fig. 5), which indicates a perfect agreement between the surrogate and the original model in the range of 0.2–0.4, while it underestimated values of the response surface in the region around 0.8. The underestimation of the response surface values in the region where optimal parameter values are likely located could influence the next surrogate-based optimization of soil hydraulic properties.

To increase the accuracy of the kriging model, the approximation uncertainty framework was used next. As described in the methodology section, 15 *infilled* points were added to the initial design sites using the expected improvement approach. As shown in Fig. 5 and as expected, the infilled kriging model outperformed

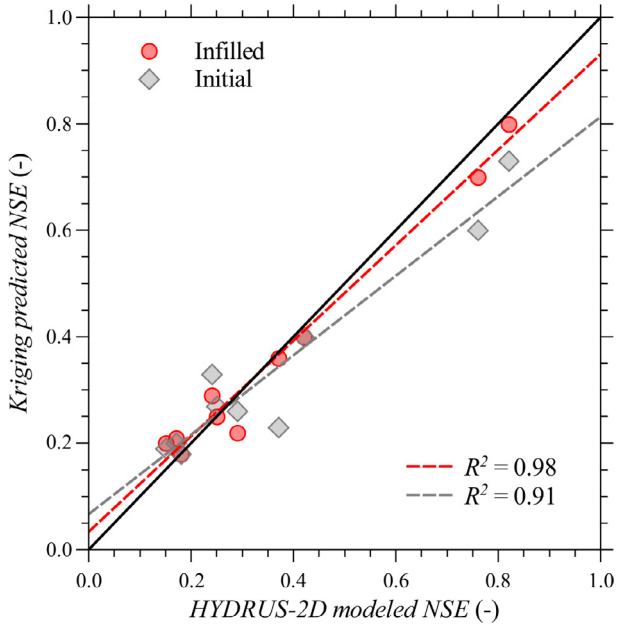

Fig. 5. Comparison between the HYDRUS-2D and kriging-predicted values of the *NSE* for the validation sample. The initial (grey diamonds) and infilled (red circles) kriging models are compared. A bisector (a black line) and regression lines for the initial (a dashed grey line) and infilled (a dashed red line) kriging models are reported.

the initial kriging model. The determination coefficient R^2 increased to 0.98, indicating that the infilled kriging improved the description of the response surface. This behavior was confirmed by the regression line (a dashed red line in Fig. 5), which almost overlapped a bisector line. Moreover, the accuracy of the kriging model improved for high values of *NSE*, which are those of interest in an optimization process, while remaining similarly high for low values of *NSE*. This global accuracy of the surrogate is fundamental for the GSA, which explores the response surface landscape. However, it should be noted that even when the surrogate accuracy improves after applying the approximation uncertainty framework, a certain degree of bias remains. A possible solution to further investigate this bias would be to increase the validation sample size. However, there are no clear indications in the literature regarding the size of the validation sample in similar problems (i.e. optimization and sensitivity analysis of soil hydraulic properties), making the choice rather subjective. Moreover,

increasing the validation sample size would significantly increase the computational cost of the analysis. In our particular case, in view of all the possible sources of uncertainty that affect the analysis, the validation of the surrogate-based optimized parameters against an independent set of data, performed towards to end of the study, was specifically intended to provide a final check on the accuracy of the estimated parameters. Considering the relatively high accuracy of the surrogate, no additional points were thus added to the design sites considering the relatively high accuracy of the surrogate, and the final surrogate was used for the GSA and optimization.

3.3. Global Sensitivity Analysis

The validated kriging model was next used in the GSA. Sobol's sensitivity indices, with their confidence intervals for each parameter, are reported in Table 4.

The sensitivity analysis revealed that the model was additive. This was confirmed by the sum of the first-order indices, which was almost 1, and by negligible differences between the first-order and total-effect indices for each parameter. An additive model $Y = f(X_1, X_2, \ldots, X_N)$ can be decomposed into a sum of N functions, where N is the number of parameters. This means that the effects of interactions between model parameters on model results were negligible.

As shown in Table 4, the most influential parameter was the shape parameter α. Its first-order (S_1) and total effect (S_T) indices were more than an order of magnitude higher than corresponding indices for the second most influential parameter K_s. The pore-size distribution index n and the saturated water content θ_s exhibited the lowest sensitivity, indicating their marginal role on the output's variance. Moreover, since their total effects were almost zero, these parameters can be fixed to any feasible value in the parameter space without affecting the value of the objective function, reducing the dimensionality of the inverse problem to only two parameters, α and K_s. Such results are very useful in an optimization framework, since they can simplify the parameter estimation procedure. Some of the total effect indices were only slightly larger than the first order indices. This is mainly due to approximation in the numerical integration of the total unconditional variance (Sobol', 2001).

It must be emphasized that additivity is quite unusual for environmental models, which are generally characterized by high nonlinearity and interactions between parameters (Brunetti et al., 2016b; Nossent et al., 2011). In our particular case, the dominant effect of the α parameter on the hydrograph makes it difficult to identify interactions between parameters. This may also indicate that water flow in the filter layer deviates from the traditional Darcian behavior and involves other physical processes, such as preferential and film flows. In such circumstances, some parameters can exhibit a negligible effect on the model's response. This may indicate that the proposed modeling approach could be affected by *model discrepancy*, a concept introduced by Kennedy and O'Hagan (2001) to assess sources of uncertainty due to underlying missing physics, numerical approximations, and other inaccuracies of the model. When the *model discrepancy* is not directly accounted for, the model parameters can be treated as simple tuning parameters, which often act as a simplified surrogate for some more complex process that is not modeled in the simulator (Brynjarsdottir and O'Hagan, 2014). In our case, it is plausible that the shape parameter α acted as a tuning parameter, condensing and representing more complex phenomena, namely preferential and film flows. It must be emphasized that the surrogate-based sensitivity analysis can be extremely useful in detecting different sources of uncertainties. Future researches should explicitly account for *model discrepancy* in the analysis (Brynjarsdottir and O'Hagan, 2014) to examine its impact on the model's behavior, or perform the same type of analysis using more complex models which account for preferential flows in the filter layer.

Table 4
The first-order (S_1) and total (S_T) effect indices (in a decreasing order) with their bootstrap confidence intervals (BCI) for the soil hydraulic parameters.

Parameter	S_1	S_1 (BCI)	S_T	S_T (BCI)
α [1/cm]	0.93	0.24	0.94	0.05
K_s [cm/min]	0.04	0.08	0.05	0.007
n [−]	0.01	0.02	0.008	0.001
θ_s [−]	0.002	0.01	0.001	0.001
Sum	≈1.0		≈1.0	

As mentioned in the methodology section, the GSA required 30,000 evaluations of the surrogate model. The computational cost of the kriging-based sensitivity analysis was limited to 1–2 s on a laptop equipped with a CPU Intel® Core i7-4700 MQ 2.40 GHz processor and 8 GB of RAM. On the other hand, since a single HYDRUS-2D model run required approximately 1 min, the same type of GSA performed using the original HYDRUS-2D model would have required approximately 21 days of continuous computation. This clearly represents one of the main advantages of surrogate-based modeling: performing the same type of analysis with negligible computation time and a similarly good level of accuracy.

3.4. Kriging-Based optimization

Using the results of the GSA, only shape parameter α and the saturated hydraulic conductivity K_s were optimized. The saturated water content θ_s and the pore-size distribution index n were assumed to be 0.15 and 3.2, respectively, considering that the filter layer consisted of coarse gravel, usually characterized by reduced porosity and narrow pore-size distribution. The soil hydraulic parameters of the filter layer, including the optimized parameters, are summarized in Table 5. The filter layer exhibited both a high value of the saturated hydraulic conductivity K_s (90 cm/min) and a very low value of the shape parameter α (0.001 1/cm).

The estimated parameters indicated that the hydraulic behavior of the filter layer was characterized by high flow rates and negligible retention capacity, which are both typical for coarse textured media. The optimized parameter values are similar to those reported in Brunetti et al. (2016b) for the base layer of a permeable pavement. In that study, the base layer consisted of crushed stones and was modeled using either the classical VGM function or the dual-porosity approach to account for preferential flow. Specifically, for the unimodal VGM function, the authors reported a value of 0.023 1/cm for the shape parameter α and a saturated hydraulic conductivity K_s of 68.7 cm/min. Moreover, the plausible occurrence of film flow in the filter layer, which can support very high flow rates, especially at near-zero matrix potential (Tokunaga, 2009), needs to be contemplated. Under such circumstances, the hydraulic behavior of the material tends to deviate from the typical Richard's type flow, and the optimized parameters attempt to approximate a combination of fingering and film flow that likely occur in this layer.

Fig. 6 shows a comparison between the measured and modeled hydrographs for the optimization period. The PSO resulted in the *NSE* value of 0.85, which confirmed the accuracy of the measured and estimated parameters. As reported by Moriasi et al. (2007), values of *NSE* between 0.75 and 1.0 indicate a very good agreement between hydrographs, and an adequate model calibration. The model was able to correctly reproduce the fast hydraulic response of the hydrograph during precipitations and to reasonably estimate peak flows. The insert of Fig. 6 shows the simulated against measured SF outflows. The same plot also shows a bisector line, which

Table 5
Unimodal VGM parameters for the filter layer. The shape parameter α and the saturated hydraulic conductivity K_s were estimated using the PSO algorithm.

Soil hydraulic parameters						
Layer	θ_r (−)	θ_s (−)	α (1/cm)	n (−)	K_s (cm/min)	L (−)
Filter	0	0.15	0.001	3.2	90	0.5

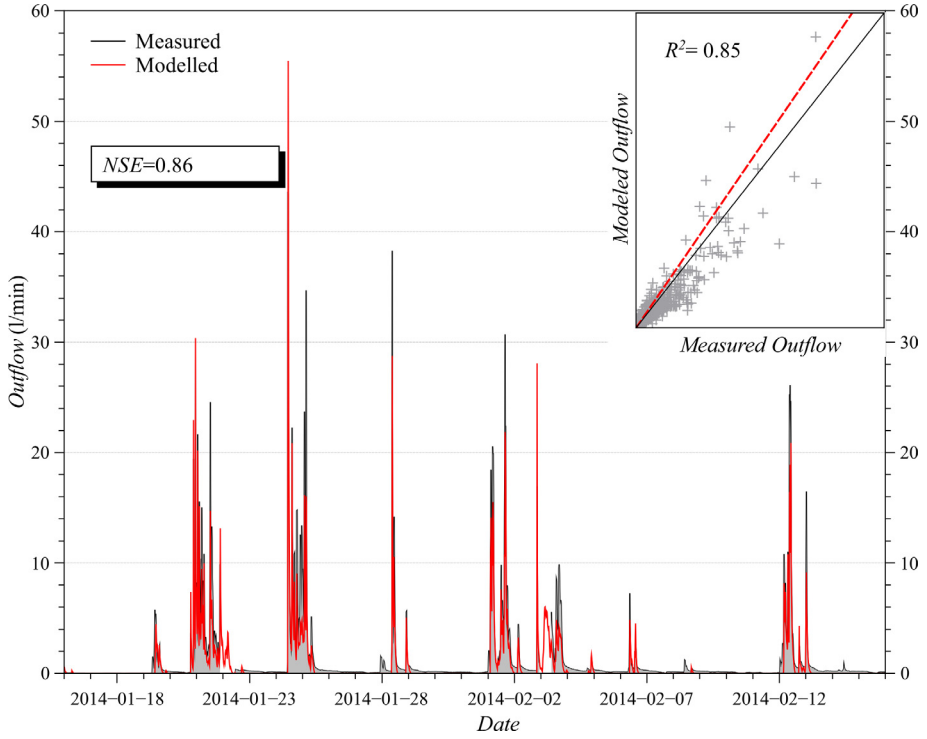

Fig. 6. A comparison between measured and simulated outflows versus time and against each other (in the insert) for the calibration period. The full and dashed lines in the insert are a bisector and linear regression line, respectively.

indicates a perfect agreement between simulated and measured outflows, and a linear regression line. The good performance of the model is confirmed by the determination coefficient R^2 = 0.85. The comparison between the bisector and regression lines indicates that, in general, the model slightly overestimated the outflow.

A careful inspection of simulated fluxes revealed that the model tends to underestimate low flows (Fig. 6). This behavior could be related to the coarse nature of the filter layer, which closely resembles "fractured aquifers". Typical breakthrough curves for fractured aquifers are characterized by early breakthrough and long tailing (Geiger et al., 2010). This is due to a delayed response in the matrix to pressure head changes that occur in the surrounding fractures. Brattebo and Booth (2003), Brunetti et al. (2016b), and Fassman et al. (2010) observed a similar behavior in permeable pavements, the base and sub-base layers of which are composed of crushed stones. In such circumstances, more complex models are needed to simultaneously describe fast preferential flow and the matrix-fracture interactions in the filter layer (Brunetti et al., 2016b).

Since the computational time associated with a single surrogate model evaluation was negligible, the approximate response surface was investigated. Fig. 7 shows the α-K_s response surface obtained using a regular grid of 40,000 points. The darkest areas represent regions of the parameter space with high values of *NSE*. At the first inspection, the response surface was characterized by a moderate multimodality. As shown in Fig. 7, optimal solutions were concentrated in the left part of the plot for values of α between 0.001 and 0.05. For α values > 0.05, the objective function dropped quickly to

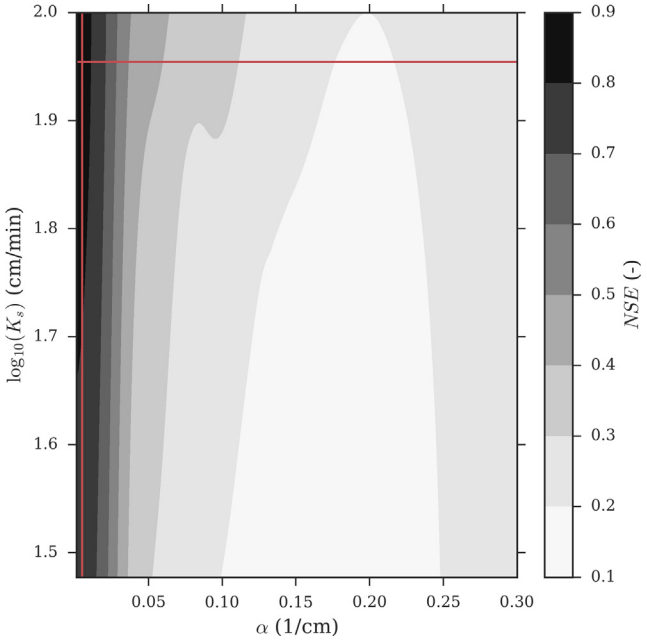

Fig. 7. The α-K_s response surface obtained using a regular grid of 40,000 points. The red lines indicate the cross sections reported in Fig. 8.

0.3–0.4. The *NSE* values slowly increased for values of $\alpha > 0.2$. This can be expected since the α parameter for gravels usually has relatively high values. However, in our case, high values of α were not able to accurately reproduce the hydraulic behavior of the SF. For large α values, the filter layer quickly desaturates and increases its retention capacity. This effect delays the hydraulic response of the system to precipitation events. On the contrary, the use of low α values delays the desaturation of the filter layer, thus reducing its retention capacity (Cey et al., 2006). This makes the filter layer more responsive to precipitation events, which was the behavior observed in the measured hydrograph. On the other hand, the response surface exhibited limited variability in the K_s direction, since high values of *NSE* were guaranteed for a broad range of saturated hydraulic conductivity values.

These results confirmed the findings of the GSA, which clearly indicated that the variance of the objective function was mainly driven by the shape parameter α, with only a limited influence of K_s. This behavior is shown in detail in Fig. 8.

Fig. 8 shows horizontal (K_s = 90 cm/min) and vertical (α = 0.001 1/cm) cross-sections (red lines in Fig. 7) through the response surface. Yellow rectangular areas are expanded in the right part of the plot. With respect to K_s, the optimum was not clearly identifiable at the first inspection. The values of the objective function ranged between 0.8 and 0.85 in the entire range of the saturated hydraulic conductivity, indicating its limited effect on the response surface. The area around the PSO-optimized value of K_s (90 cm/min) is expanded in the bottom-right corner of Fig. 8. From this plot, it is evident how the PSO algorithm well identified the optimal value K_s, even for a flat profile.

Conversely, Fig. 8 shows a completely different behavior for the α-*NSE* profile, for which an optimal region was identified in the left part of the plot for low values of the α parameter. While the gradient of the curve seemed to approach a maximum, it was not possible to clearly identify the optimum, which may have been outside of the range imposed on the α parameter. As previously discussed, this behavior could be related to a deviation from the Darcian flow in the filter layer, which requires a more complex modeling approach. The further analyzes of the response surface indicated that values of α over 0.01 1/cm corresponded to a marked decrease of *NSE*. This is evident from the expanded area in the top-right corner of Fig. 8. This finding is in agreement with the results of the GSA, which identified α as the most influential parameter.

In order to verify whether additional soil hydraulic parameters, such as the saturated water content θ_s and the pore-size distribution index n, influenced the optimum, a surrogate-based optimization, which considered four soil hydraulic parameters was carried out. The results of the optimization are listed in Table 6.

As shown in Table 6, the newly estimated parameters are very similar to those estimated when θ_s and n were fixed. The saturated water content was 0.17, which is slightly higher than the previously fixed value. Conversely, the pore-size distribution index n was slightly lower, but the difference was again very small. The two most sensitive parameters α and K_s had some small changes, however overall results are in a good agreement with those reported previously. Again, the filter layer exhibited a relatively high permeability and a low value of the α parameter, which is no longer situated at the border of the evaluated parameter space. Since α is related to the inverse of the air-entry pressure head, this suggests that its value is finite and could potentially be measured. These numerical differences could be related to the effects of interactions between parameters, which, even if small in magnitude as demonstrated by the GSA, can affect the parameters estimation. Including these parameters in the optimization process can potentially reduce the parameters uncertainty and help in better defining the problem.

3.5. Model validation

In order to evaluate the reliability of the estimated parameters, the model was validated using another independent set of experimental data. Fig. 9 shows a comparison between measured and modeled hydrographs during the validation period.

The value of the objective function was *NSE* = 0.8, which again confirmed the adequacy of the estimated parameters. The descrip-

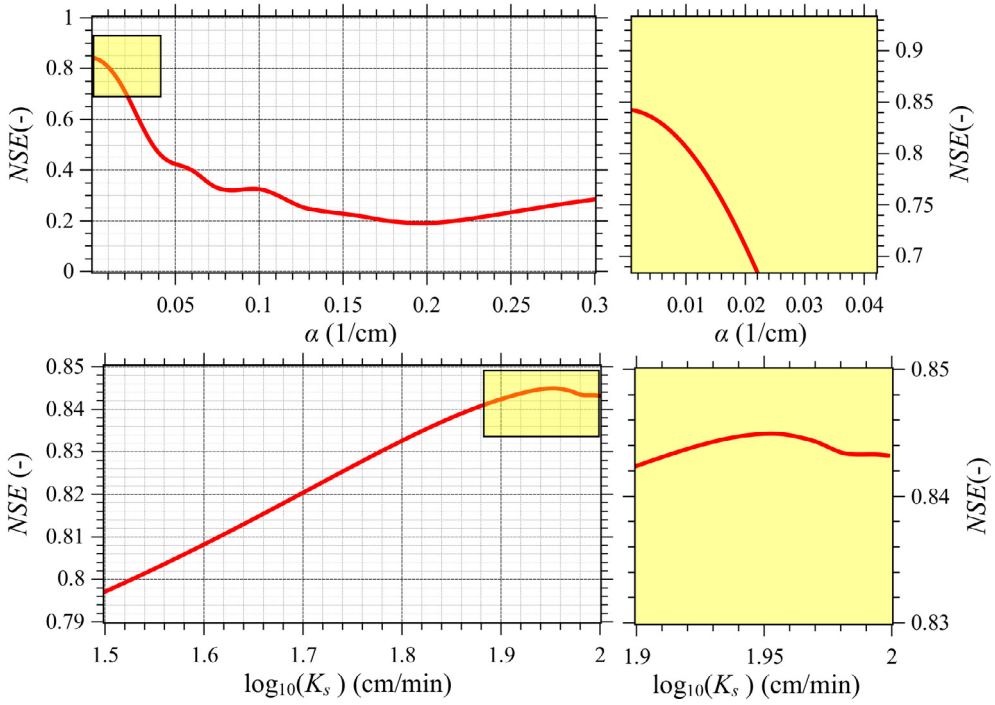

Fig. 8. Horizontal [K_s = 90 cm/min] (top), and vertical [α = 0.001 1/cm] (bottom) response surface cross-sections. The yellow rectangular areas for both plots are expanded on the right.

Table 6
Unimodal VGM parameters for the filter layer. The saturated water content θ_s, the shape parameters α and n, and the saturated hydraulic conductivity K_s were estimated using the PSO algorithm.

Soil hydraulic parameters						
Layer	θ_r (−)	θ_s (-)	α(1/cm)	n (−)	K_s (cm/min)	l (−)
Filter	0	0.17	0.003	3.1	89	0.5

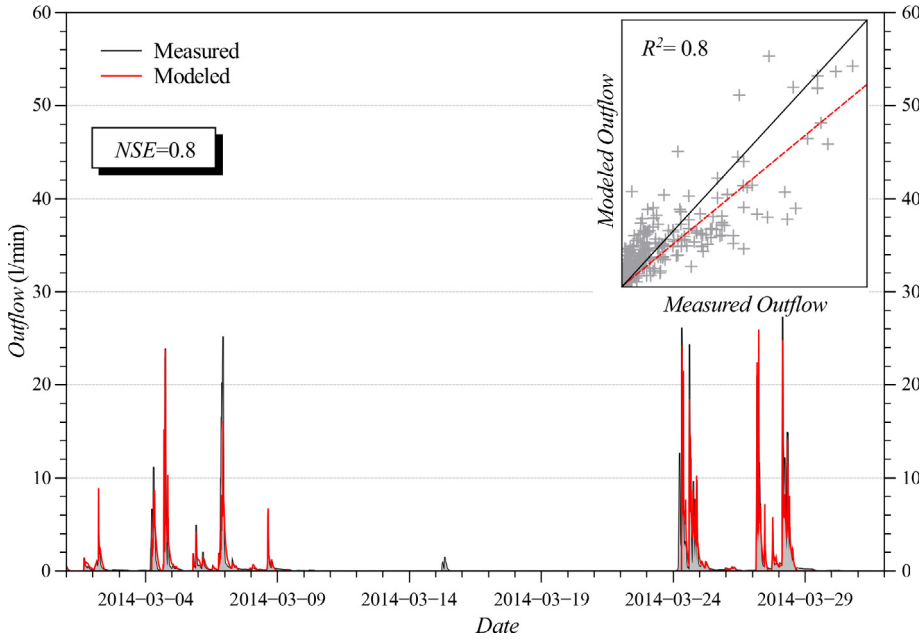

Fig. 9. A comparison between measured and simulated outflows versus time and against each other (in the insert) during the validation period. The full and dashed lines in the insert are a bisector and linear regression line, respectively.

tion of the hydraulic behavior of the stormwater filter during rainfall events was satisfactory. This capability of the calibrated model to correctly describe the hydraulic behavior of the system is important when dealing with the analysis of combined traditional drainage systems and LID techniques. A correct description of the hydrograph during precipitation events gives information about the lag time and the intensity of peak flow, which are fundamental for both a comprehensive hydraulic analysis of drainage systems, and for the evaluation of benefits of LIDs implementations. The model was not able to reproduce outflow induced by the precipitation event on March 15. This may be related to an overestimation of actual evapotranspiration calculated using values from the literature for albedo, LAI, and a hypothetical roots distribution, which could result in an overestimation of the storage capacity of the SF at the beginning of the precipitation event, which had a total volume of 6 mm. As a result, the model predicted that the SF retained all the precipitation volume. A better characterization of evapotranspiration could help in increasing the accuracy of the model, which was already high. As for the optimization data set, the model poorly described the long tailing behavior of the hydrograph after precipitations. This behavior is particularly evident for the precipitation event on March 28.

4. Conclusions and summary

The aim of this study was to demonstrate the benefit of surrogate-based modeling in the numerical analysis of Low Impact Development techniques. In particular, the unsaturated hydraulic properties of a contained stormwater filter installed at the University of Calabria were evaluated in the study. The kriging technique was used to approximate the deterministic response of the widely used mechanistic model HYDRUS-2D, which was used to simulate the variably-saturated hydraulic behavior of the filter. In order to reduce the dimensionality of the inverse problem, the simplified evaporation method was used to determine the unsaturated soil hydraulic properties of the soil substrate placed on the top of the filter layer. The Nash-Sutcliffe efficiency index was used both to compare the simulated and measured outflows, and as the variable of interest for the construction of the response surface.

The PSO heuristic algorithm was used to estimate the kriging parameters based on an initial set of design sites obtained using Latin Hypercube Sampling. The approximation uncertainty framework improved the accuracy of the surrogate model by using the expected-improvement approach to select additional points to the initial design sites. The kriging model was validated against an unexplored set of points with satisfactory results. The obtained surrogate was then used to perform a Global Sensitivity Analysis of the hydraulic parameters of the filter layer based on Sobol's method, with a negligible computational cost. The sensitivity analysis revealed that the model is additive, and that two soil hydraulic parameters, the shape parameter α and the saturated hydraulic conductivity K_s, mainly affect the hydraulic response of the filter layer. These two parameters were estimated using the PSO algorithm with a *NSE* value of 0.85, which indicated an good accuracy of the model. Moreover, the analysis of the response surface confirmed the results of the GSA, identifying α as the most influential parameter. The reliability of the surrogate-based analysis was evaluated by validating the optimized parameters on an independent dataset of measured outflows. A *NSE* value of 0.8 confirmed the reliability of the HYDRUS-2D model calibrated using the kriging technique. In both the optimization and validation, the model poorly described the long-tailed behavior of the hydrograph after precipitations. This could be related to the model inadequacy in

describing both the film and preferential flows, and the matrix-fracture interactions that occurs in the filter layer. This suggests that more complex models are needed to better describe the hydraulic processes involved.

One of the most widespread criticism against the use of mechanistic models is their computational cost, which limits their adoption. This study has demonstrated how a surrogate-based analysis can provide an effective solution in overcoming this limitation. In this paper, the kriging technique was used for highly expensive computational analyses, such as the GSA and the PSO, with good results. The sufficiently accurate reproduction of measured hydrographs, which is extremely important in the analysis of LIDs, confirmed the benefit and reliability of surrogate-based analysis.

This novel study represents the first contribution towards the use of surrogates for LIDs analysis, which does not need to be limited only to the investigation of soil hydraulic properties. For example, potential applications can be also targeted to the optimization of the morphological characteristics of the LID itself (depth, slope, plants, etc) for a particular climate, to the optimization of the adsorption properties of filter layers, or for specific design aims. Such studies could help in providing a better understanding of LID techniques while promoting the widespread adoption of such systems.

Acknowledgements

The study was co-funded by the Italian National Operative Project (PON): Research and Competitiveness for the convergence regions 2007/2013-I Axis "Support to structural changes", operative objective 4.1.1.1: "Scientific-technological generators of transformation processes of the productive system and creation of new sectors", and Action II: "Interventions to support industrial research". The surrogate-based analysis was conducted using the Python language (Python Software Foundation, 2013).

References

Abbaspour, K.C., Schulin, R., van Genuchten, M.T., 2001. Estimating unsaturated soil hydraulic parameters using ant colony optimization. Adv. Water Resour. 24, 827–841. http://dx.doi.org/10.1016/S0309-1708(01)00018-5.

Abbaspour, K.C., Johnson, C.A., van Genuchten, M.T., 2004. Estimating Uncertain Flow and Transport Parameters Using a Sequential Uncertainty Fitting Procedure. Vadose Zo. J. 3, 1340–1352. http://dx.doi.org/10.2113/3.4.1340.

Abu-Zreig, M., Rudra, R.P., Whiteley, H.R., 2001. Validation of a vegetated filter strip model (VFSMOD). Hydrol. Process. 15, 729–742. http://dx.doi.org/10.1002/hyp.101.

Akat, S.B., Gazi, V., 2008. Particle swarm optimization with dynamic neighborhood topology: Three neighborhood strategies and preliminary results. In: 2008 IEEE Swarm Intelligence Symposium. pp. 1–8. http://dx.doi.org/10.1109/SIS.2008.4668298.

Allen, R.G., Pereira, L.S., Raes, D., Smith, M., 1998. FAO Irrigation and Drainage Paper No. 56: Crop Evapotranspiration. FAO, Rome.

Archer, G.E.B., Saltelli, A., Sobol, I.M., 1997. Sensitivity measures, anova-like Techniques and the use of bootstrap. J. Stat. Comput. Simul. 58, 99–120. http://dx.doi.org/10.1080/00949659708811825.

Bengtsson, L., Grahn, L., Olsson, J., 2004. Hydrological function of a thin extensive green roof in southern Sweden. Nord. Hydrol. 36, 259–268.

Berardi, U., GhaffarianHoseini, A., GhaffarianHoseini, A., 2014. State-of-the-art analysis of the environmental benefits of green roofs. Appl. Energy 115, 411–428. http://dx.doi.org/10.1016/j.apenergy.2013.10.047.

Blanusa, T., Vaz Monteiro, M.M., Fantozzi, F., Vysini, E., Li, Y., Cameron, R.W.F., 2013. Alternatives to sedum on green roofs: can broad leaf perennial plants offer better "cooling service"? Build. Environ. 59, 99–106. http://dx.doi.org/10.1016/j.buildenv.2012.08.011.

Borgonovo, E., Castaings, W., Tarantola, S., 2012. Model emulation and moment-independent sensitivity analysis: an application to environmental modelling. Environ. Model. Softw. 34, 105–115. http://dx.doi.org/10.1016/j.envsoft.2011.06.006.

Brattebo, B.O., Booth, D.B., 2003. Long-term stormwater quantity and quality performance of permeable pavement systems. Water Res. 37, 4369–4376. http://dx.doi.org/10.1016/S0043-1354(03)00410-X.

Breshears, D.D., Rich, P.M., Barnes, F.J., Campbell, K., 1997. Overstory-imposed heterogeneity in solar radiation and soil moisture in a semiarid woodland. Ecol. Appl. 7, 1201–1215. http://dx.doi.org/10.1890/1051-0761(1997) 007[1201:OIHISR]2.0.CO;2.

Brunetti, G., Simunek, J., Piro, P., 2016a. A comprehensive analysis of the variably-saturated hydraulic behavior of a green roof in a mediterranean climate. Vadose Zo. J. 15. http://dx.doi.org/10.2136/vzj2016.04.0032. In press.

Brunetti, G., Simunek, J., Piro, P., 2016b. A comprehensive numerical analysis of the hydraulic behavior of permeable pavement. J. Hydrol. 540, 1146–1161. doi: 10.2136/vzj2016.04.0032.

Brynjarsdottir, J., O'Hagan, A., 2014. Learning about physical parameters: the importance of model discrepancy. Inverse Probl. 30, 114007. http://dx.doi.org/10.1088/0266-5611/30/11/114007.

Carbone, M., Brunetti, G., Piro, P., 2014. Hydrological Performance of a Permeable Pavement in Mediterranean Climate. In: 14th SGEM GeoConference on Water Resources. Forest, Marine and Ocean Ecosystems. pp. 381–388. http://dx.doi.org/10.5593/SGEM2014/B31/S12.050.

Cey, E., Rudolph, D., Therrien, R., 2006. Simulation of groundwater recharge dynamics in partially saturated fractured soils incorporating spatially variable fracture apertures. Water Resour. Res. 42. http://dx.doi.org/10.1029/2005WR004589.

Cheviron, B., Coquet, Y., 2009. Sensitivity analysis of transient-MIM HYDRUS-1D: case study related to pesticide fate in soils. Vadose Zo. J. 8, 1064. http://dx.doi.org/10.2136/vzj2009.0023.

Coffman, L.S., 2002. Low-impact development: an alternative stormwater management technology. In: France, R.L. (Ed.), Handbook of Water Sensitive Planning and Design. Lewis Publishers Inc., pp. 97–123.

Collins, K.A., Hunt, W.F., Hathaway, J.M., 2008. Hydrologic comparison of four types of permeable pavement and standard asphalt in eastern north Carolina. J. Hydrol. Eng. 13, 1146–1157. http://dx.doi.org/10.1061/(ASCE)1084-0699(2008)13:12(1146).

Dosskey, M.G., Helmers, M.J., Eisenhauer, D.E., Franti, T.G., Hoagland, K.D., 2002. Assessment of concentrated flow through riparian buffers. J. Soil Water Conserv. 57, 336–343. VL - 57.

Duan, Q., Sorooshian, S., Gupta, V., 1992. Effective and efficient global optimization for conceptual rainfall-runoff models. Water Resour. Res. 28, 1015–1031. http://dx.doi.org/10.1029/91WR02985.

Efron, B., Tibshirani, R., 1986. Bootstrap methods for standard errors, confidence intervals, and other measures of statistical accuracy. Stat. Sci. 1, 54–75.

Elliot, A., Trowsdale, S., 2007. A review of models for low impact urban stormwater drainage. Environ. Model. Softw. 22, 394–405. http://dx.doi.org/10.1016/j.envsoft.2005.12.005.

Fassman, E.A., Blackbourn, S., 2010. Urban runoff mitigation by a permeable pavement system over impermeable soils. J. Hydrol. Eng. 15, 475–485. http://dx.doi.org/10.1061/(ASCE)HE.1943-5584.0000238.

Feddes, R.A., Kowalik, P.J., Zaradny, H., 1978. Simulation of Field Water Use and Crop Yield. PUDOC, Wageningen.

Forrester, A.I.J., Sóbester, A., Keane, A.J., 2008. Engineering Design via Surrogate Modelling: A practical Guide. J. Wiley. http://dx.doi.org/10.1002/9780470770801.

Geiger, S., Cortis, A., Birkholzer, J.T., 2010. Upscaling solute transport in naturally fractured porous media with the continuous time random walk method. Water Resour. Res. 46. http://dx.doi.org/10.1029/2010WR009133. n/a–n/a.

Getter, K.L., Rowe, D.B., Andresen, J.A., 2007. Quantifying the effect of slope on extensive green roof stormwater retention. Ecol. Eng. 31, 225–231. http://dx.doi.org/10.1016/j.ecoleng.2007.06.004.

UMS GmbH, 2015. UMS (2015): Manual HYPROP, Version 2015-01.

Gutmann, H.M., 2001. A radial basis function method for global optimization. J. Glob. Optim. 19, 201–227. http://dx.doi.org/10.1023/A:1011255519438.

Hopmans, J.W., Šimůnek, J., Romano, N., Durner, W., 2002. Inverse modeling of transient water flow. In: Dane, J.H., Topp, G.C. (Eds.), Methods of Soil Analysis, Part 4, Physical Methods. SSSA, Madison, WI, pp. 963–1008.

Houska, T., Multsch, S., Kraft, P., Frede, H.-G., Breuer, L., 2013. Monte Carlo based calibration and uncertainty analysis of a coupled plant growth and hydrological model. Biogeosci. Discuss. 10, 19509–19540. http://dx.doi.org/10.5194/bgd-10-19509-2013.

Hu, S., 1987. Akaike information criterion statistics. Math. Comput. Simul. 29, 452. http://dx.doi.org/10.1016/0378-4754(87)90094-2.

Ines, A.V.M., Droogers, P., 2002. Inverse modelling in estimating soil hydraulic functions: a genetic algorithm approach. Hydrol. Earth Syst. Sci. Discuss. 6, 49–66.

Jones, D.R., 2001. A taxonomy of global optimization methods based on response surfaces. J. Glob. Optim. 21, 345–383. http://dx.doi.org/10.1023/A:1012771025575.

Jones, D.R., Schonlau, M., William, J., 1998. Efficient global optimization of expensive black-box functions. J. Glob. Optim. 13, 455–492. http://dx.doi.org/10.1023/a:1008306431147.

Keating, E.H., Doherty, J., Vrugt, J.A., Kang, Q., 2010. Optimization and uncertainty assessment of strongly nonlinear groundwater models with high parameter dimensionality. Water Resour. Res. 46. http://dx.doi.org/10.1029/200009WR8584. n/a-n/a.

Kennedy, J., Eberhart, R., 1995. Particle swarm optimization. Eng. Technol., 1942–1948

Kennedy, J., O'Hagan, A., 2001. Bayesian calibration of computer models. J. R. Stat. Soc. Ser. B (Statistical Methodol), 425–464. http://dx.doi.org/10.1111/1467-9868.00294.

Kennedy, J., Spears, W.M., 1998. Matching algorithms to problems: an experimental test of the particle swarm and some genetic algorithms on the multimodal problem generator. In: 1998 IEEE International Conference on Evolutionary Computation Proceedings. IEEE World Congress on Computational Intelligence (Cat. No.98TH8360). IEEE, pp. 78–83. http://dx.doi.org/10.1109/ICEC.1998.699326.

Khu, S.-T., Werner, M.G.F., 2003. Reduction of Monte-Carlo simulation runs for uncertainty estimation in hydrological modelling. Hydrol. Earth Syst. Sci. 7, 680–692. http://dx.doi.org/10.5194/hess-7-680-2003.

Laloy, E., Rogiers, B., Vrugt, J.A., Mallants, D., Jacques, D., 2013. Efficient posterior exploration of a high-dimensional groundwater model from two-stage Markov chain Monte Carlo simulation and polynomial chaos expansion. Water Resour. Res. 49, 2664–2682. http://dx.doi.org/10.1002/wrcr.20226.

Li, Y., Babcock, R.W., 2014. Green roof hydrologic performance and modeling: a review. Water Sci. Technol. 69, 727–738. http://dx.doi.org/10.2166/wst.2013.770.

Li, Y., Babcock, R.W., 2015. Modeling hydrologic performance of a green roof system with HYDRUS-2D. J. Environ. Eng. 141, 04015036. http://dx.doi.org/10.1061/(ASCE)EE.1943-7870.0000976.

Liang, J.J., Qin, A.K., Suganthan, P.N., Baskar, S., 2006. Comprehensive learning particle swarm optimizer for global optimization of multimodal functions. IEEE Trans. Evol. Comput. 10, 281–295. http://dx.doi.org/10.1109/TEVC.2005.857610.

Mackay, D.J.C., 1998. Introduction to Gaussian processes. Neural Networks Mach. Learn. 168, 133–165. http://dx.doi.org/10.1007/s10067-003-0742-1.

Marquardt, D.W., 1963. An algorithm for least-squares estimation of nonlinear parameters. J. Soc. Ind. Appl. Math. 11, 431–441. http://dx.doi.org/10.1137/0111030.

McKay, M.D., Beckman, R.J., Conover, W.J., 1979. Comparison of three methods for selecting values of input variables in the analysis of output from a computer code. Technometrics 21, 239–245. http://dx.doi.org/10.1080/00401706.1979.10489755.

Metselaar, K., 2012. Water retention and evapotranspiration of green roofs and possible natural vegetation types. Resour. Conserv. Recycl. 64, 49–55. http://dx.doi.org/10.1016/j.resconrec.2011.12.009.

Moriasi, D.N., Arnold, J.G., Van Liew, M.W., Binger, R.L., Harmel, R.D., Veith, T.L., 2007. Model evaluation guidelines for systematic quantification of accuracy in watershed simulations. Trans. ASABE 50, 885–900. http://dx.doi.org/10.13031/2013.23153.

Munoz-Carpena, R., Parsons, J.E., 2004. A design procedure for vegetative filter strips using VFSMOD-W. Trans. Asae 47, 1933–1941.

Nash, J.E., Sutcliffe, J.V., 1970. River flow forecasting through conceptual models: Part I – a discussion of principles. J. Hydrol. 10, 282–290. http://dx.doi.org/10.1016/0022-1694(70)90255-6.

Newcomer, M.E., Gurdak, J.J., Sklar, L.S., Nanus, L., 2014. Urban recharge beneath low impact development and effects of climate variability and change. Water Resour. Res. 50, 1716–1734. http://dx.doi.org/10.1002/2013WR014282.

Nossent, J., Elsen, P., Bauwens, W., 2011. Sobol' sensitivity analysis of a complex environmental model. Environ. Model. Softw. 26, 1515–1525. http://dx.doi.org/10.1016/j.envsoft.2011.08.010.

O'Hagan, A., 2006. Bayesian analysis of computer code outputs: a tutorial. Reliab. Eng. Syst. Saf. 91, 1290–1300. http://dx.doi.org/10.1016/j.ress.2005.11.025.

Oakley, J.E., O'Hagan, A., 2004. Probabilistic sensitivity analysis of complex models: a Bayesian approach. J. R. Stat. Soc. Ser. B Stat. Methodol. 66, 751–769. http://dx.doi.org/10.1111/j.1467-9868.2004.05304.x.

OECD, 2013. Water and climate change adaptation: policies to navigate uncharted waters. OECD Studies on Water. OECD Publishing, Paris. 10.1787/9789264200449-en.

Pan, L., Wu, L., 1998. A hybrid global optimization method for inverse estimation of hydraulic parameters: annealing-simplex method. Water Resour. Res. 34, 2261–2269. http://dx.doi.org/10.1029/98WR01672.

Pedersen, M.E.H., 2010. Good parameters for particle swarm optimization, Technical Report HL1001, Hvass Laboratories.

Pertassek, T., Peters, A., Durner, W., 2015. HYPROP-FIT Software User's Manual, V. 3.0.

Peters, A., Durner, W., 2008. Simplified evaporation method for determining soil hydraulic properties. J. Hydrol. 356, 147–162. http://dx.doi.org/10.1016/j.jhydrol.2008.04.016.

Python Software Foundation, 2013. Python Language Reference, version 2.7. Python Softw. Found.

Rasmussen, C.E., Williams, C.K.I., 2006. Gaussian Processes for Machine Learning. MIT Press, Cambridge, MA.

Razavi, S., Tolson, B.A., Burn, D.H., 2012. Review of surrogate modeling in water resources. Water Resour. Res. 48. http://dx.doi.org/10.1029/2011WR011527. n/a–n/a.

Regis, R.G., Shoemaker, C.A., 2004. Local function approximation in evolutionary algorithms for the optimization of costly functions. IEEE Trans. Evol. Comput. 8, 490–505. http://dx.doi.org/10.1109/TEVC.2004.835247.

Rezaei, M., Seuntjens, P., Joris, I., Boënne, W., Van Hoey, S., Campling, P., Cornelis, W. M., 2015. Sensitivity of water stress in a two-layered sandy grassland soil to variations in groundwater depth and soil hydraulic parameters. Hydrol. Earth Syst. Sci. Discuss. 12, 6881–6920. http://dx.doi.org/10.5194/hessd-12-6881-2015.

Ritchie, J.T., 1972. Model for predicting evaporation from a row crop with incomplete cover. Water Resour. Res. 8, 1204–1213. http://dx.doi.org/10.1029/WR008i005p01204.

Sacks, J., Welch, W.J., Mitchell, T.J., Wynn, H.P., 1989. Design and analysis of computer experiments. Stat. Sci. 4, 409–435. doi:10.1214/ss/1177012413.

Saltelli, A., Annoni, P., 2010. How to avoid a perfunctory sensitivity analysis. Environ. Model. Softw. 25, 1508–1517. http://dx.doi.org/10.1016/j.envsoft.2010.04.012.

Saltelli, A., Tarantola, S., Saisana, M., Nardo, M., 2005. What is sensitivity analysis? In: II Convegno Della Rete Dei Nuclei Di Valutazione E Verifica, Napoli 26, 27 Gennaio 2005, Centro Congressi Universitá Federico II, Via Partenope 36.

Saltelli, A., Annoni, P., Azzini, I., Campolongo, F., Ratto, M., Tarantola, S., 2010. Variance based sensitivity analysis of model output. Design and estimator for the total sensitivity index. Comput. Phys. Commun. 181, 259–270. http://dx.doi.org/10.1016/j.cpc.2009.09.018.

Schindler, U., 1980. Ein Schnellverfahren zur Messung der Wasserleitfähigkeit im teilgesättigten Boden an Stechzylinderproben. Arch. für Acker- und Pflanzenbau und Bodenkd. 24, 1–7.

Schindler, U., Durner, W., von Unold, G., Mueller, L., Wieland, R., 2010a. The evaporation method: extending the measurement range of soil hydraulic properties using the air-entry pressure of the ceramic cup. J. Plant Nutr. Soil Sci. 173, 563–572. http://dx.doi.org/10.1002/jpln.200900201.

Schindler, U., Durner, W., von Unold, G., Muller, L., 2010b. Evaporation method for measuring unsaturated hydraulic properties of soils: extending the measurement range. Soil Sci. Soc. Am. J. 74, 1071–1083. http://dx.doi.org/10.2136/sssaj2008.0358.

Schonlau, M., 1997. Computer experiments and global optimization (PhD thesis). University of Waterloo, Waterloo, Canada.

Sevat, E., Dezetter, A., Servat, E., 1991. Selection of calibration objective functions in the context of rainfall-runoff modelling in a sudanese savannah area. Hydrol. Sci. J. Des. Sci Hydrol. 36, 307–330. http://dx.doi.org/10.1080/02626669109492517.

Shi, Y., Eberhart, R., 1998. A modified particle swarm optimizer. In: 1998 IEEE Int. Conf. Evol. Comput. Proceedings. IEEE World Congr. Comput. Intell. (Cat. No.98TH8360), pp.69–73. http://dx.doi.org/10.1109/ICEC.1998.699146.

Shi, Y., Eberhart, R.C., 1999. Empirical study of particle swarm optimization. In: Proc. 1999 Congr. Evol. Comput. pp. 1945–1950. http://dx.doi.org/10.1109/CEC.1999.785511.

Šimůnek, J., van Genuchten, M.T., Šejna, M., 2008. Development and applications of the HYDRUS and STANMOD software packages and related codes. Vadose Zo. J. 7, 587. http://dx.doi.org/10.2136/vzj2007.0077.

Šimůnek, J., van Genuchten, M.T., Šejna, M., 2016. Recent DEVELOPMENTS and applications of the HYDRUS computer software packages. Vadose Zo. J. 15, 25. http://dx.doi.org/10.2136/vzj2016.04.0033.

Sobol', I., 2001. Global sensitivity indices for nonlinear mathematical models and their Monte Carlo estimates. Math. Comput. Simul. 55, 271–280. http://dx.doi.org/10.1016/S0378-4754(00)00270-6.

Sutanto, S.J., Wenninger, J., Coenders-Gerrits, A.M.J., Uhlenbrook, S., 2012. Partitioning of evaporation into transpiration, soil evaporation and interception: a comparison between isotope measurements and a HYDRUS-1D model. Hydrol. Earth Syst. Sci. 16, 2605–2616. http://dx.doi.org/10.5194/hess-16-2605-2012.

Taylor, S.A., Ashcroft, G.L., 1972. Physical Edaphology: The Physics of Irrigated and Nonirrigated Soils. Freeman, San Francisco, W.H.

Tokunaga, T.K., 2009. Hydraulic properties of adsorbed water films in unsaturated porous media. Water Resour. Res. 45, 1287–1295. http://dx.doi.org/10.1029/2009WR007734.

van Dam, J.C., Groenendijk, P., Hendriks, R.F.A., Kroes, J.G., 2008. Advances of Modeling Water Flow in Variably Saturated Soils with SWAP. Vadose Zo. J. 7, 640. http://dx.doi.org/10.2136/vzj2007.0060.

van Genuchten, M.T., 1980. A Closed-form Equation for Predicting the Hydraulic Conductivity of Unsaturated Soils1. Soil Sci. Soc. Am. J. 44, 892–898. http://dx.doi.org/10.2136/sssaj1980.03615995004400050002x.

Vrugt, J.A., Gupta, H.V., Bouten, W., Sorooshian, S., 2003. A Shuffled Complex Evolution Metropolis algorithm for optimization and uncertainty assessment of hydrologic model parameters. Water Resour. Res. 39. http://dx.doi.org/10.1029/2002WR001642. n/a–n/a.

Vrugt, J.A., Schoups, G., Hopmans, J.W., Young, C., Wallender, W.W., Harter, T., Bouten, W., 2004. Inverse modeling of large-scale spatially distributed vadose zone properties using global optimization. Water Resour. Res. 40. http://dx.doi.org/10.1029/2003WR002706. n/a–n/a.

Vrugt, J.A., Stauffer, P.H., Wöhling, T., Robinson, B.A., Vesselinov, V.V., 2008. Inverse modeling of subsurface flow and transport properties: a review with new developments. Vadose Zo. J. 7, 843. http://dx.doi.org/10.2136/vzj2007.0078.

Wang, G.G., Shan, S., 2007. Review of metamodeling techniques in support of engineering design optimization. J. Mech. Des. 129, 370. http://dx.doi.org/10.1115/1.2429697.

Wesseling, J., Elbers, J., Kabat, P., Broek, B. Van den, 1991. SWATRE: instructions for input. Intern. Note, Winand Star. Cent.

Wong, T.H.F., Fletcher, T.D., Duncan, H.P., Jenkins, G.A., 2006. Modelling urban stormwater treatment-A unified approach. Ecol. Eng. 27, 58–70. http://dx.doi.org/10.1016/j.ecoleng.2005.10.014.

Ye, K.Q., Li, W., Sudjianto, A., 2000. Algorithmic construction of optimal symmetric Latin hypercube designs. J. Stat. Plan. Inference 90, 145–159. http://dx.doi.org/10.1016/S0378-3758(00)00105-1.

Younes, A., Mara, T.A., Fajraoui, N., Lehmann, F., Belfort, B., Beydoun, H., 2013. Use of global sensitivity analysis to help assess unsaturated soil hydraulic parameters. Vadose Zo. J. 12. http://dx.doi.org/10.2136/vzj2011.0150.

Zhang, X., Srinivasan, R., Van Liew, M., 2009. Approximating SWAT Model using artificial neural network and support vector machine. JAWRA J. Am. Water Resour. Assoc. 45, 460–474. http://dx.doi.org/10.1111/j.1752-1688.2009.00302.x.

Turco, M., Brunetti, G., Nikodem, A., Fér, M., Kodešová, R., Piro, P. (2017).

The use of the RETC code and HYDRUS-1D to define soil hydraulic properties of permeable pavement.

14th IWA/IAHR International Conference on Urban Drainage, Prague, Czech Republic

ICUD 2017
PRAGUE

14th IWA/IAHR International Conference on Urban Drainage

September 10-15, 2017
Prague, Czech Republic

Conference Proceedings

CzWA
The Czech Water Association

CTU
CZECH TECHNICAL UNIVERSITY IN PRAGUE

IAHR AIRH
International Association for Hydro-Environment Engineering and Research
Supported by Spain Water and IWHR, China

IWA
the international water association

ICUD-0431 The use of the RETC code and HYDRUS-1D to define soil hydraulic properties of permeable pavement

M. Turco[1], G. Brunetti[1], A. Nikodem[2], M. Fér[2], R. Kodešová[2], P. Piro[1]

1 *University of Calabria, Civil Engineering, Arcavacata di Rende, Italy*
2 *Czech University of Life Sciences, Faculty of Agrobiology- Food and Natural Resources- Dept. of Soil Science and Soil Protection, Prague, Czech Republic*

Summary

LID systems, such as Permeable Pavements (PP), consist of a series of facilities with the aim to intercept stormwater runoff and solving stormwater management problems both in quantitative and qualitative terms. Knowledge about hydraulic properties of PP materials is very limited and represents a limit to the spread of these techniques. In this way, this work is focused on the determination of the soil hydraulic properties of some component materials (porous concrete and fine gravel) of PP by combining suitable experimental procedures and software modelling.

Keywords

permeable pavement, RETC, HYDRUS-1D, soil properties

Introduction

Urban development has diminished natural behaviour of soil to drain and increase runoff volume in urban areas. Recently, to avert the effects of urbanization, Low Impact Development systems (LID), an innovative stormwater management approach, have been developed and adopted. Permeable pavements (PP) represent a good solution to solve stormwater management problems both in quantitative and qualitative terms. PP systems are constructed in layers built with several materials such as concrete, coarse sand or fine gravel and crushed stones.

Despite the benefits that it would adopt by using permeable pavements, these techniques are not yet widespread probably because knowledge about their soil hydraulic properties is limited. The aim of this paper is to define the hydraulic proprieties of some of the pavement materials in order to be useful for modeling.

Methods and Materials

A permeable pavement (schematic of the PP assumed in this study is shown a Fig. 1) can be interpreted as a porous layered system and water flow in this system can be described by Richards equation:

$$\frac{\partial \theta}{\partial t} = \frac{1}{r}\frac{\partial}{\partial r}\left[rK\frac{\partial h}{\partial r}\right] + \frac{\partial}{\partial z}\left[K\left(\frac{\partial h}{\partial z} + 1\right)\right] \quad (1)$$

where θ is the volumetric content [L^3L^{-3}], *t* is the time [T], *h* is the soil water matric head [L], *z* are the spatial coordinates [L], *K* is the hydraulic conductivity [LT^{-1}], *r* is the radial coordinate [L], and *z* is the vertical axis [L]. Modeling of water flow in unsaturated soils by means of the Richards equation requires the knowledge of soil water retention function ϑ(h) and the hydraulic conductivity

function *K(h)* for each soil layer of the PP, which may be described the van Genuchten (1980) functions:

$$\theta_e = \begin{cases} \dfrac{1}{(1+(|\alpha h|)^n)^m} & if\ h < 0 \\ 1 & if\ h \geq 0 \end{cases} \quad (2)$$

$$\theta_e = \frac{\theta(h) - \theta_r}{\theta_s - \theta_r} \quad (3)$$

$$K = \begin{cases} K_s \theta_e^{l} \left[\left(1 - \left(1 - \theta_e^{\frac{1}{m}} \right)^m \right) \right]^2 & if\ h < 0 \\ K_s & if\ h \geq 0 \end{cases} \quad (4)$$

where ϑ_e is the effective soil water content (dimensionless), h is the pressure head [L], K_s is the saturated hydraulic conductivity [L T^{-1}], ϑ_r and ϑ_s are the residual and saturated soil water contents [L^3 L^{-3}], respectively, l is the pore-connectivity parameter (dimensionless), α is the reciprocal of the air-entry pressure head [L^{-1}], n (dimensionless) is related to the slope of the retention curve at the inflection point, and $m = 1 - 1/n$.

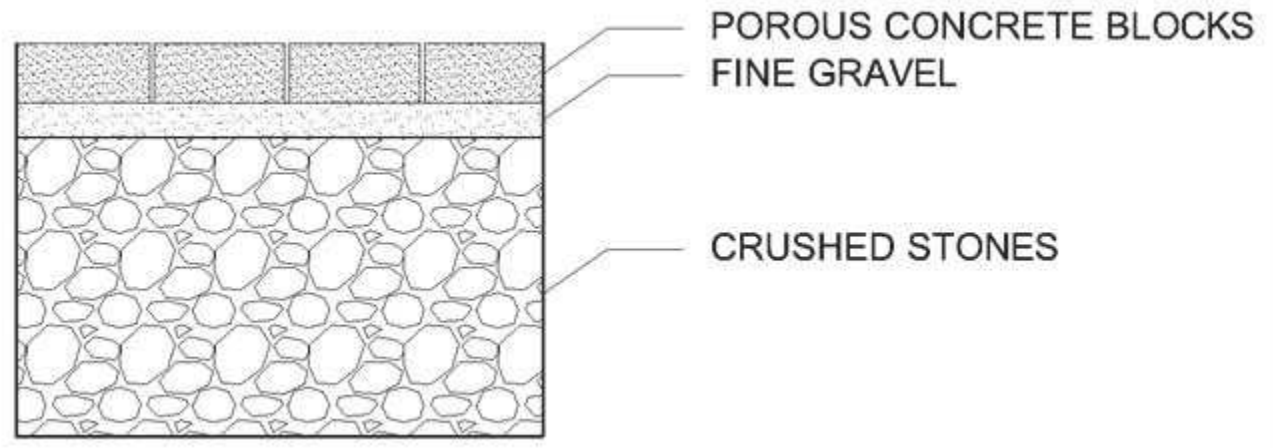

***Fig. 1**. A schematic of Permeable pavement*

By following Kodešová et al., (2014) Soil Water Retention Curve (SWRC) of the concrete paving was measured on two fragments of this material. Firstly, vertical sides of both fragments were covered by wax. Fragment were fully saturated by water using the saturation pan, next placed in the clay tank and slowly drained using pressure heads from 0 to -220 cm. Soil water contents were evaluated gravimetrically. Parameters of the retention curves were obtained by experimental data fitting using the RETC code (van Genuchten, Leij, et al., 1991). For a detailed description on the construction of the clay tank please refer to (Fér and Kodešová, 2012). The soil water retention and hydraulic conductivity curves of the bedding layer were measured using the multistep outflow experiments (Van Dam, Stricker, et al., 1994). Two 100 cm^3 columns were placed in the Tempe cells, in which a fine gravel material was packed. Samples were fully saturated, and then slowly drained using 5 pressure head steps (a minimum pressure head of -12.5 cm) during several days and cumulative outflow in time was measured. The single-porosity model in HYDRUS-1D was then applied to simulate the observed cumulative outflow in time and calculated SWRC points, and to optimize the

parameters of the soil hydraulic functions. For both samples, ϑ_s was measured, ϑr was set at 0 and the pore connectivity parameter was fix to *l* = 0.5.

Results and Discussion

Results for the wear layer are showed in Tab. 1 and Fig. 2. Parameters obtained on the highly permeable concrete used for PP constructions indicate considerably lower retention ability in comparision to that of a standard concrete paving evaluated for instance by Kodešová et al., (2014).

Tab. 1. *Hydraulic properties of the wear material*

Parameter	Sample 1	Sample 2	
θ_r [cm^3 cm^{-3}]	0.044	0.045	fitted
θ_s [cm^3 cm^{-3}]	0.106	0.113	measured
α [cm^{-1}]	3.37	4.03	fitted
n[-]	1.47	1.47	fitted

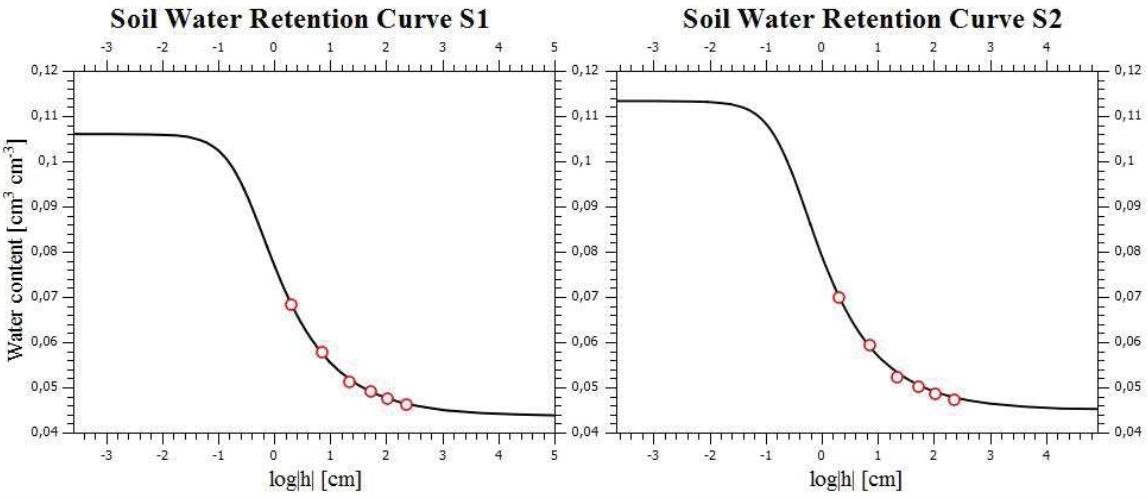

Fig. 2*. Wear layer SWRC*

Results for the bedding layer are showed in Tab. 2 and Fig. 3. Parameters again indicate negligible retention capacity and very high hydraulic conductivity of this material.

***Tab. 2**. Hydraulic proprieties of the bedding material*

Parameter	Sample 1	Sample 2	
θ_r [cm^3 cm^{-3}]	0	0	fixed
θ_s [cm^3 cm^{-3}]	0.41	0.37	measured
α [cm^{-1}]	0.43	0.40	fitted
n [-]	2.45	2.65	fitted
K_s [cm min^{-1}]	236	32	fitted

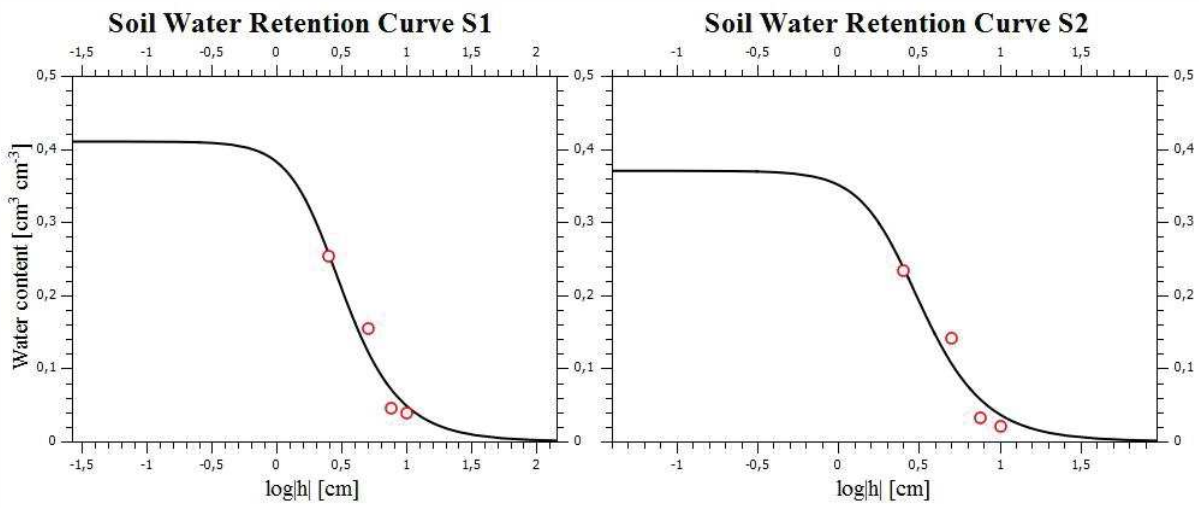

***Fig. 3**. Bedding layer proprieties*

Parameters confirm that this layer has a reduced porosity. Values of α and *n* for both samples denote that desaturation occurs in a very quick way.

Conclusions

Knowledge about hydraulic proprieties is a fundamental input to correct interpret the hydraulic behaviour of permeable pavement systems. Study therefore focused on the evaluation of the soil hydraulic properties of two construction materials of a permeable pavement by using suitable experimental procedures already present in literature coupled with RETC code and HYDRUS-1D. Both material proved very low retention ability and high permeability, thus also suitability for PP construction

Acknowledgement

The study was co-funded by the Italian National Operative Project (PON)—Research and Competitiveness for the convergence regions 2007/2013-I Axis ‘‘Support to structural changes”

operative objective 4.1.1.1. ‘‘Scientific-technological generators of transformation processes of the productive system and creation of new sectors” Action II: ‘‘Interventions to support industrial research”.

References

Van Dam, J. C. Van, Stricker, J. N. M., and Droogers, P. (1994) Inverse Method to Determine Soil Hydraulic Functions from Multistep Outflow Experiments. Soil Science Society of America Journal, 58, 647–652.

Fér, M. and Kodešová, R. (2012) Estimating hydraulic conductivities of the soil aggregates and their clay-organic coatings using numerical inversion of capillary rise data. Journal of Hydrology, 468–469, 229–240.

van Genuchten, M. T., Leij, F. J., and Yates, S. R. (1991) The RETC Code for Quantifying the Hydraulic Functions of Unsaturated Soils. United States Environmental Reseach Laboratory, (December), 93.

van Genuchten, M. T. (1980) A Closed-form Equation for Predicting the Hydraulic Conductivity of Unsaturated Soils1. Soil Science Society of America Journal, 44(5), 892. Kodešová, R., Fér, M., Klement, A., Nikodem, A., Teplá, D., Neuberger, P., and Bureš, P. (2014) Impact of various surface covers on water and thermal regime of Technosol. Journal of Hydrology, 519(PB), 2272–2288.

Brunetti, G., Simunek, J., **Turco, M**., Piro, P. (2017)

On the use of global sensitivity analysis for the numerical analysis of permeable pavements.

14th IWA/IAHR International Conference on Urban Drainage, Prague, Czech Republic

ICUD 2017
PRAGUE

14th IWA/IAHR International Conference on Urban Drainage

September 10-15, 2017
Prague, Czech Republic

Conference Proceedings

CzWA
The Czech Water Association

CTU
CZECH TECHNICAL UNIVERSITY IN PRAGUE

IAHR AIRH
International Association for Hydro-Environment Engineering and Research
Supported by Spain Water and IWHR, China

IWA
the international water association

ICUD-0434 On the use of global sensitivity analysis for the numerical analysis of permeable pavements

G. Brunetti[1], J. Simunek[2], M. Turco[3], P. Piro[3]

1 *University of Brescia, Department of Civil Engineering, Architecture, Land and Environment and Mathematic, Brescia, 25123, Italy*
2 *University of California, Riverside, Department of Environmental Sciences, CA 92521, USA*
3 *University of Calabria, Department of Civil Engineering, Rende, 87036, Italy*

Summary

The aim of this study is to investigate the use of different Global Sensitivity Analysis techniques in conjunction with a mechanistic model for the numerical analysis of a permeable pavement installed at the University of Calabria. The Morris method and the variance-based E-FAST procedure are applied to investigate the influence of soil hydraulic parameters on the pavement's behaviour. The analysis reveals that the Morris method represents a reliable computationally cheap alternative to variance-based procedures for screening important factors, and have a first inspection of the model. The study is completed by a combined GSA-GLUE uncertainty analysis used to evaluate the model accuracy.

Keywords

Urban drainage, Permeable pavement, Infiltration, Sensitivity Analysis, Modelling

Introduction

The Low Impact Development (LID) approach aims to restore the natural hydrological cycle of urban catchments by increasing their evapotranspiration and infiltration capacity. Several studies confirmed the quantitative and qualitative benefits of LIDs on the hydrological cycle. (Brattebo & Booth, 2003, Davis, 2008, Brunetti *et al.*, 2016a). Even though benefits of LID are significant, their widespread adoption at catchment scale is rather limited. One of the key limiting factor is the limited diffusion and knowledge of reliable modelling tools among practitioners. This issue is exacerbated by the complexity of the physical processes involved in LIDs (e.g., infiltration, evapotranspiration, root water uptake, solute transport, heat transport, etc), which requires a combination of high expertise and modelling accuracy. In this view, mechanistic models have proven to be a reliable and accurate tool for the numerical analysis of LIDs, as already demonstrated by several studies(Hilten *et al.*, 2008, Li & Babcock, 2015, Brunetti *et al.*, 2016a).

While mechanistic models can offer both accuracy and modelling flexibility, their calibration and computational cost represent a significant limitation in their widespread adoption. In a recent study, Brunetti *et al.* (2017) proposed the use of a Gaussian emulator to calibrate a two-dimensional mechanistic model of a stormwater filter. That study demonstrated how the surrogate model can drastically reduce the computational cost while maintaining a relatively high accuracy. A reasonable alternative would be to reduce the dimensionality of the optimization problem by fixing unimportant factors. This is usually accomplished by running a preliminary sensitivity analysis. Recently, Brunetti *et al.* (2016b) used the GSA to investigate the influence of soil hydraulic properties on the hydraulic behaviour of a permeable pavement modelled using the mechanistic model HYDRUS-1D (Šimůnek *et al.*, 2016). While results were promising, more research is needed in this direction to test alternative sensitivity analysis techniques and evaluate their use in combination with mechanistic modelling.

Thus, the aim of the present study is to investigate the use of different sensitivity analysis techniques in conjunction with a mechanistic model for the numerical analysis of a permeable pavement installed at the University of Calabria (Italy). The problem is addressed in the following way. First, the HYDRUS-1D model is selected to describe the variably saturated hydraulic behaviour of the pavement. Next, the Morris method (Morris, 1991) and the Extended Fourier Amplitude Sensitivity Test (E-FAST) (Saltelli *et al.*, 1999) are applied and compared to screen the influence of soil hydraulic properties on the likelihood function. Finally, the E-FAST is coupled with the Generalized Likelihood Uncertainty Estimation (GLUE) (Beven & Binley, 1992) to carry out an uncertainty analysis of soil hydraulic parameters, and investigate the accuracy of the model in reproducing the hydraulic behaviour of the permeable pavement.

Methods

Case study description

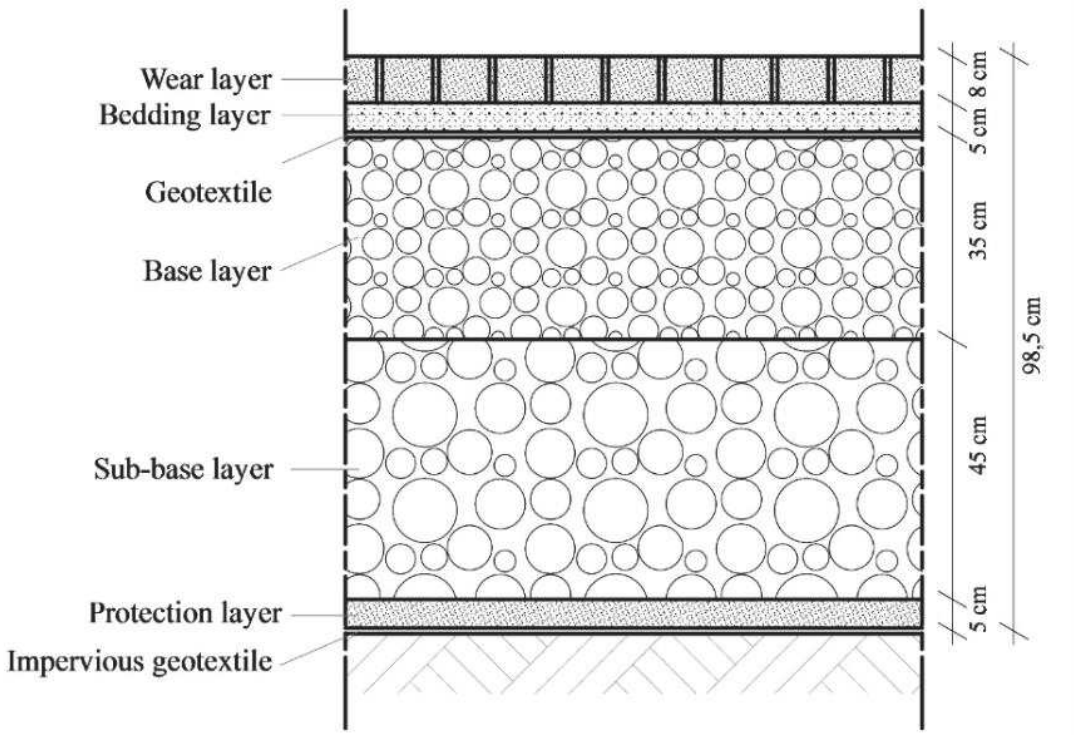

***Fig. 1**. A schematic of the permeable pavement*(Brunetti *et al.*, 2016b)

The University of Calabria is located in the south of Italy, in the vicinity of Cosenza (39°18' N 16°15' E). The climate is Mediterranean with a mean annual temperature of 15.5 °C and an average annual precipitation of 881.2 mm. The permeable pavement has an area of approximately 154 m^2, an average slope of 2%, and a total depth of the profile of 0.98 m. Figure 1 shows a schematic of the permeable pavement, consisting of 5 layers. Please refer to Brunetti *et al.* (2016b) for a thorough description of the experimental site. One month-long data set is selected for further analysis. In particular, the data set reported in one of our preceding study on the same permeable pavement (i.e.,Brunetti *et al.*, 2016b) is used. The measured subsurface outflow from the pavement is used to calculate the likelihood values, and thus to carry out both the sensitivity and uncertainty analysis. It is worth noting that no surface runoff was observed during the selected period.

Modelling theory

Water flow

The variably saturated water flow in the permeable pavement is simulated by using the HYDRUS-1D model (Šimůnek et al., 2016). The one-dimensional Richards equation describes the unsaturated water flow:

$$\frac{\partial \theta}{\partial z} = \frac{\partial}{\partial z}\left[K(h)\left(\frac{\partial h}{\partial z} + 1 \right) \right] \quad (1)$$

where θ is the volumetric water content [-], h is the soil water pressure head [L], K(h) is the unsaturated hydraulic conductivity [LT-1], t is time [T], and z is the soil depth [L]. The soil hydraulic properties are described by the van Genuchten – Mualem relation (van Genuchten, 1980):

$$\theta = \begin{cases} \dfrac{\theta_s - \theta_r}{(1 + (\alpha|h|)^n)^m} + \theta_r & \text{if } h \le 0 \\ \theta_s & \text{if } h > 0 \end{cases} \quad (2)$$

$$S_e = \frac{\theta - \theta_r}{\theta_s - \theta_r} \quad (3)$$

$$K = \begin{cases} K_s S_e^L \left[(1 - (1 - S_e^{\frac{1}{m}})^m \right]^2 & if\ h \le 0 \\ K_s & if\ h > 0 \end{cases} \quad (4)$$

$$m = 1 - \frac{1}{n} \quad (5)$$

where θr [-] is the residual water content, θs [-] is the saturated water content, Ks [LT-1] is the saturated hydraulic conductivity, n [-] and α [L-1] are two shape parameters, L indicates the tortuosity and is usually assumed to be 0.5 for many soils, and Se is the effective saturation [-]. The residual water contents are assumed to be 0.045 and 0.03 for the wear and bedding layers, respectively, and set to 0.0 for both the base and sub-base layers. The same hydraulic properties are used for the bedding and protection layers, respectively. Despite of all these considerations, the model still involves 16 unknown parameters (θs, α, n, and Ks for 4 soil layers).

Numerical domain and boundary conditions

The vertical domain is discretised into 197 finite elements, refined at the top to accommodate pressure head gradients that are likely to occur in the wear layer. An atmospheric boundary condition is set at the top of the wear layer, while a seepage face boundary condition is specified at the bottom of the protection layer. The initial conditions are specified in terms of the soil water pressure head and assumed to linearly increase with depth, from -90 cm at the top of the flow domain (z = 0) to -0.5 cm at the bottom (z = -98). The influence of the initial condition on the model's output is assumed to be limited to the first days of the simulated period, thus not affecting the likelihood.

Likelihood function

The Nash-Sutcliffe efficiency (NSE) index is used to measure the agreement between the simulated and modelled hydrograph, and as the likelihood function in the following sensitivity and uncertainty analysis:

$$NSE = 1 - \left[\frac{\sum_{i=1}^{T} (Q_i^{obs} - Q_i^{\mathrm{mod}})^2}{\sum_{i=1}^{T} (Q_i^{obs} - Q_{mean}^{obs})^2} \right] \quad (6)$$

where Q_i^{obs} is the *i*th measured value, Q_i^{mod} is the *i*th simulated value, and Q_{mean}^{obs} is the mean value of observed data.

Sensitivity analysis

Morris method

The Morris method (Morris, 1991) belongs to the class of Screening methods (SM). SMs aim to provide qualitative sensitivity measures for different factors using a relatively small number of model evaluations. In general, the Morris method is a one-factor-at-a-time (OAT) local method, since it computes the elementary effect by changing only one factor at a time. However, it can be viewed as a global method, since it averages several elementary effects computed at different points in the parameter space.

In this study, the modified version of the Morris method proposed by Campolongo et al. (2007) is used to investigate the influence of soil hydraulic properties on the pavement response. σ and μ* are the two sensitivity measures calculated in the Morris method. While the former summarizes the interaction effect, the latter reflects the overall importance of a particular parameter. For a detailed description of the method refer to Morris (1991) and Campolongo et al. (2007). To interpret the results by simultaneously taking into account both sensitivity measures, Morris suggested their graphical representation in the (μ*-σ) plane. Considering the intent of the present analysis, targeted to investigate the efficiency of the method, the sample size was set to 100, for a total of 1,700 numerical simulations.

Extended Fourier amplitude sensitivity testing (E-FAST)

The E-FAST method (Saltelli et al., 1999) belongs to the class of global variance decomposition methods. It does not require any particular assumptions on model structure, and it provides quantitative sensitivity measures for each factor. In particular, two sensitivity indices are calculated for each parameter, the main effect Si and the total effect STi. While Si measures how the ith factor contributes to the output's variance without taking into account the interactions between parameters, STi quantifies the higher order effects, thus the parameter interaction. A significant difference between STi and Si indicates an important role of an interaction for the parameter considered. STi = 0 is a condition necessary and sufficient for a factor to be non-influential, therefore, it can be fixed at any value within its range of uncertainty without affecting the output unconditional variance. For a detailed description of the E-FAST method please refer to Saltelli et al. (1999).

The E-FAST analysis requires q·N simulations, where q is the number of parameters and N is the sample size adopted. In this study, N is set to 3,000 for a total of 48,000 model executions. It is evident that the E-FAST method is more computationally demanding than the Morris method, although it provides quantitative sensitivity measures.

Uncertainty Analysis

GSA-GLUE Approach

The methodology used consists of a combination of the Generalized Likelihood Uncertainty Estimation (GLUE) (Beven & Binley, 1992) with the variance-based sensitivity analysis E-FAST. The GLUE analysis has been used extensively in the literature for the uncertainty assessment of various hydrological models (Beven & Freer, 2001, Montanari, 2005). For a detailed description of the GLUE implementation, please refer to Beven & Binley (1992). The GSA-GLUE approach was first proposed by Ratto et al. (2001). This statistical approach is rather intuitive and straightforward to implement. The sample generated for the variance-based sensitivity analysis is used also in the GLUE framework. In this way, the same sets of model runs provides the statistical base for the calculation of uncertainty bounds. In this study, the sample generated for the E-FAST analysis has been used to carry out the GLUE uncertainty estimation. The confidence interval at 5% and 95% of significance have been calculated for each soil hydraulic parameter. One of the most critical aspect of the GLUE analysis is the choice of the threshold likelihood value used to identify the so-called behavioural solutions. As pointed out by Freni et al. (2008), the threshold value strongly influences the calculated uncertainty bounds, and care should be taken in selecting the appropriate value. In this study, three values of the threshold likelihood values are investigated: 0.0, 0.1 and 0.2.

Results and Discussion

Sensitivity analysis

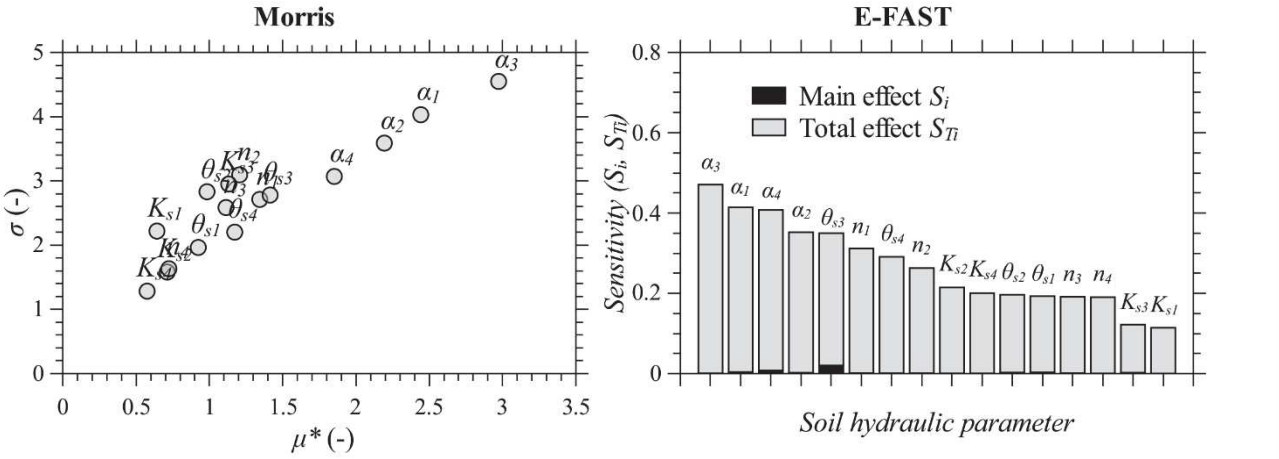

***Fig. 2**. Scatter plots of the Morris sensitivity measures (left plot) and bar chart of the E-FAST sensitivity indices (right plot) for various soil hydraulic parameters.*

Results of the sensitivity analysis carried out with the Morris method (left plot in Fig. 2) and E-FAST procedure (right plot in Fig. 2), respectively, are reported in Fig. 2. At a first inspection, it is evident how both methods identifies a modelling scenario characterized by high parameter interaction, similarly to what reported in Brunetti *et al.* (2016b). Results of the Morris analysis show that each factor with a high value of μ^*, *also has a high value of the standard deviation* σ, *indicating that none of the parameter has a purely linear effect. This is also evident from the scatter plot* μ^*-σ, *where all the points lie around the diagonal. A more careful inspection reveals the presence of two groups of factors: the first one includes the shape parameters* α, the second includes all the remaining factors. However, it must be emphasized that the groups separation is rather limited. Since all the soil hydraulic parameters exhibited significant values of μ^* *and* σ, it is not possible to fix these factors, thus reducing the dimensionality of the problem, without affecting the quality of the fitting.

Findings of the Morris method are, in general, confirmed by the results of E-FAST analysis. The main effect S_i and the total effect S_{Ti} for each factor, respectively, are reported in the right plot of Fig. 2. It is evident how all the parameters exhibit a significant S_{Ti} and a limited or negligible value of S_i.

The differences S_{Ti}-S_i indicate a strong interaction effect between factors and a high nonlinearity of the model. As for the Morris method, the shape parameters α are the most influent, although their ranking is slightly different, with α_4 being slightly more sensitive than α_2. The saturated hydraulic conductivities of the wear and base layers, respectively, are the less sensitive parameter although their total effect was still significant. The condition $S_{Ti} = 0$ *is never encountered, thus the model cannot be simplified.*

It is worth noting that the two sensitivity analysis reach similar results and conclusions. Both highlight a strong parameter interaction and nonlinearity of the model, and identify the shape parameter α *as the most influent factors. The main difference relies on the computational cost of the two methods, with the Morris method being computationally cheaper than the E-FAST.*

Uncertainty Analysis

The sample generated for the E-FAST analysis is next used to carry out the GLUE uncertainty assessment of soil hydraulic parameters. In Fig. 3, the cumulative probability distributions of the saturated hydraulic conductivity K_{s1} (left plot in Fig. 3) and the shape parameter α_1 (right plot in Fig. 3), obtained by using three different values for the NSE GLUE threshold, are reported. It is evident how the two factor exhibit a significantly different behaviour. The cumulative distribution for K_{s1} is approximately linear and insensitive to the GLUE threshold, indicating a significant parameter uncertainty and a general lack of identifiability. This confirms the findings of the sensitivity analysis that highlighted a limited influence of K_{s1} on the likelihood function. This behaviour could indicate that the informative content of the measured subsurface outflow is not sufficient to identify K_{s1}, and that other type of measurements are needed to reduce parameter uncertainty. On the other hand, the influence of the saturated hydraulic conductivity of the wear layer on a strongly unsaturated system, such as the pavement, is expected to be hydraulically limited unless surface pressure heads approach saturation (e.g., surface runoff). A situation that never occurred during the observed period.

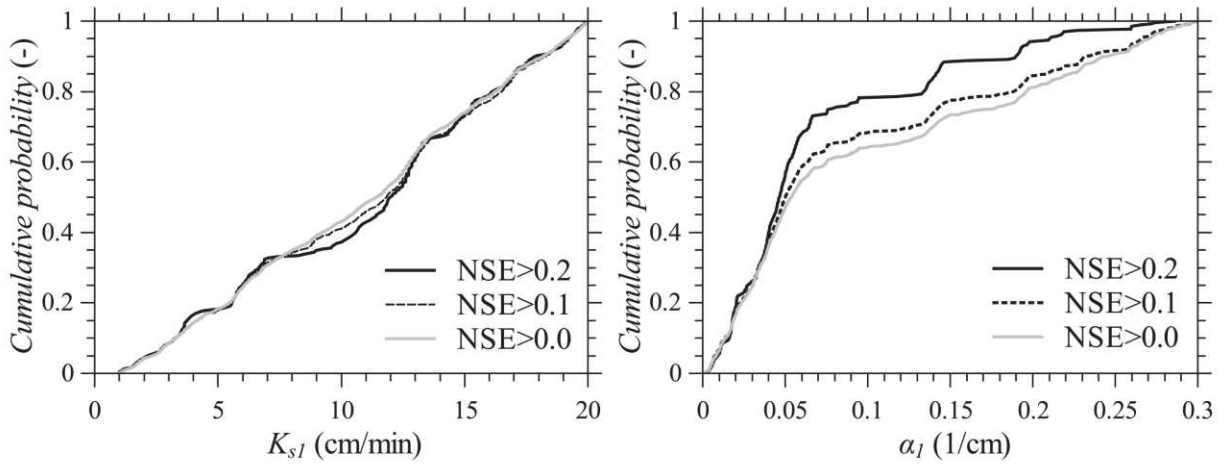

Fig. 3*. Cumulative likelihood distributions from the GSA-GLUE analysis for K_{s1} (left plot) and α_1 (right plot), for three different values of the GLUE threshold (i.e., NSE>0, NSE>0.1, NSE>0.2)*

Conversely, the cumulative distribution for α_1 indicate a leptokurtic and positively skewed posterior parameter distribution. While the 5% percentile is insensitive to the GLUE threshold, the 95% percentile changes significantly. In particular, the 95% confidence limit changes from 0.27 to 0.2, thus reducing the parameter uncertainty. This indicates that the model tends to give more accurate reproduction of the measured hydrograph for low values of α_1. Again, results agree with what found in the preceding GSA, for which α_1 is among the most sensitive parameters. In general, the analysis

reveals that selected observations allow to estimate the shape parameter of the wear layer with good confidence.

The cumulative probability distributions obtained with the GSA-GLUE approach are used to calculate the confidence interval and evaluate the accuracy of the model in reproducing the hydrograph. In particular, the *behavioural* sample obtained with the threshold value NSE>0.2 is used. Fig. 4 compares the measured hydrograph (red line in Fig. 4) with the modelled uncertainty bands (grey area in Fig. 4). The measured outflow lies only partially in the uncertainty bands, thus indicating a poor accuracy of the proposed model in reproducing the hydraulic behaviour of the pavement. Results confirm the model tendency to overestimate the hydrograph, similarly to what already reported in Brunetti *et al.* (2016b) for the same pavement modelled using the unimodal van Genuchten function for the soil hydraulic properties. The analysis suggests a general inadequacy of this formulation in describing the water flow in the pavement. However, it must be emphasized that other possible sources of uncertainty (i.e., measurement errors, input uncertainty, etc) were not accounted in the present study, thus a more comprehensive uncertainty analysis is recommended to clearly separate the effects of model input and structural errors.

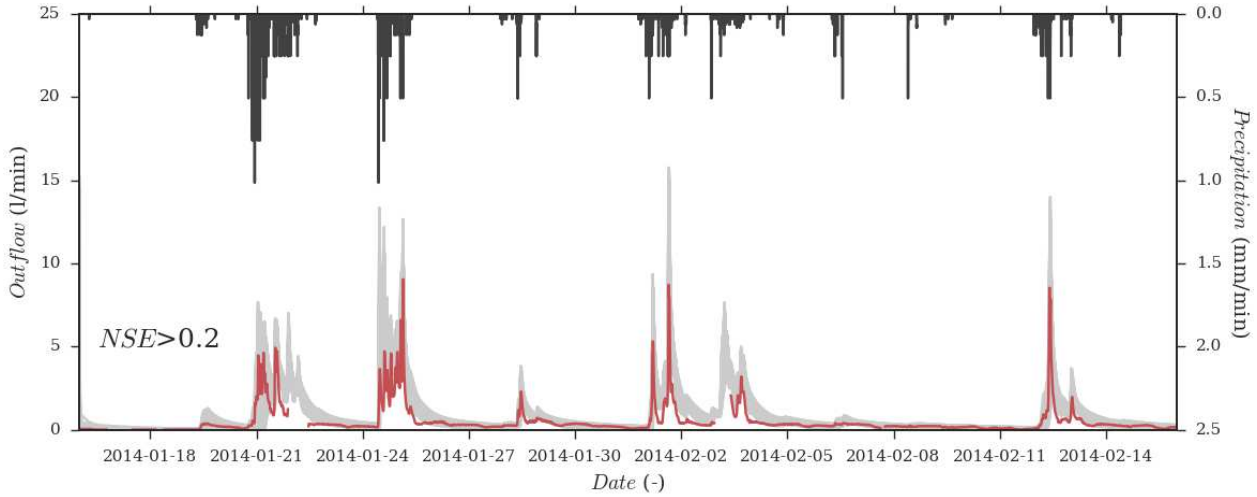

***Fig. 4**. A comparison of the measured (red line) and modelled (grey area) outflow from the pavement. The grey area represent the uncertainty band.*

Conclusions

The main aim of this study was to investigate and compare the use of Global Sensitivity Analysis techniques for the numerical analysis of the hydraulic behaviour of permeable pavements. The Morris method and the variance-based E-FAST analysis have been used, in conjunction with the mechanistic model HYDRUS-1D, to investigate the influence of soil hydraulic parameters on the ability of the model to reproduce the measured outflow from the pavement. Both methods reach similar results indicating strong parameter interaction and nonlinearity of the model. Interestingly, the analysis reveals that the Morris method represents a reliable computationally cheap alternative to variance-based GSAs, such as E-FAST. It can be used preliminarily to the model calibration to screen important and unimportant factors, and have a first inspection of the model's behaviour at a reasonable computational cost. On the other hand, the E-FAST must be chosen when the modeller's aim is to obtain quantitative sensitivity measures. Furthermore, at the same computational cost, the combined GSA-GLUE analysis allows to estimate the parameter uncertainty, and to evaluate the accuracy of the model in reproducing the behaviour of the pavement. While this and other studies report promising results, there are still other open questions, which need to be addressed in the future. In particular, how to reduce parameter uncertainty, how to maximize

the informative content of measurements, how the uncertainty in LIDs modelling propagates at catchment. However, by combining accurate modelling tools, reliable measurements and modern statistical techniques is it possible to answer to these questions and boost the adoption of LIDs.

Acknowledgement

The study was co-funded by the Italian National Operative Project (PON)—Research and Competitiveness for the convergence regions 2007/2013-I Axis "Support to structural changes" operative objective 4.1.1.1. "Scientific-technological generators of transformation processes of the productive system and creation of new sectors" Action II: "Interventions to support industrial research".

References

Beven, K. & Binley, A. (1992) The future of distributed models: Model calibration and uncertainty prediction. *Hydrol. Process.* **6**(3), 279–298. doi:10.1002/hyp.3360060305

Beven, K. & Freer, J. (2001) Equifinality, data assimilation, and uncertainty estimation in mechanistic modelling of complex environmental systems using the GLUE methodology. *J. Hydrol.* **249**(1-4), 11–29. doi:10.1016/S0022-1694(01)00421-8

Brattebo, B. O. & Booth, D. B. (2003) Long-term stormwater quantity and quality performance of permeable pavement systems. *Water Res.* **37**(18), 4369–76. doi:10.1016/S0043-1354(03)00410-X

Brunetti, G., Šimůnek, J. & Piro, P. (2016) A Comprehensive Analysis of the Variably Saturated Hydraulic Behavior of a Green Roof in a Mediterranean Climate. *Vadose Zo. J.* **15**(9), In press. doi:10.2136/vzj2016.04.0032

Brunetti, G., Šimůnek, J. & Piro, P. (2016) A comprehensive numerical analysis of the hydraulic behavior of a permeable pavement. *J. Hydrol.* **540**, 1146–1161. doi:10.1016/j.jhydrol.2016.07.030

Brunetti, G., Šimůnek, J., Turco, M. & Piro, P. (2017) On the use of surrogate-based modeling for the numerical analysis of Low Impact Development techniques. *J. Hydrol.* **548**, 263–277. doi:10.1016/j.jhydrol.2017.03.013

Campolongo, F., Cariboni, J. & Saltelli, A. (2007) An effective screening design for sensitivity analysis of large models. *Environ. Model. Softw.* **22**(10), 1509–1518. doi:10.1016/j.envsoft.2006.10.004

Davis, A. P. (2008) Field Performance of Bioretention: Hydrology Impacts. *J. Hydrol. Eng.* **13**(2), 90–95. doi:10.1061/(ASCE)1084-0699(2008)13:2(90)

Freni, G., Mannina, G. & Viviani, G. (2008) Uncertainty in urban stormwater quality modelling: The effect of acceptability threshold in the GLUE methodology. *Water Res.* **42**(8-9), 2061–2072. doi:10.1016/j.watres.2007.12.014

Genuchten, M. T. van. (1980) A Closed-form Equation for Predicting the Hydraulic Conductivity of Unsaturated Soils1. *Soil Sci. Soc. Am. J.* **44**(5), 892–898. doi:10.2136/sssaj1980.03615995004400050002x

Hilten, R. N., Lawrence, T. M. & Tollner, E. W. (2008) Modeling stormwater runoff from green roofs with HYDRUS-1D. *J. Hydrol.* **358**(3-4), 288–293. doi:10.1016/j.jhydrol.2008.06.010

Li, Y. & Babcock, R. W. (2015) Modeling Hydrologic Performance of a Green Roof System with HYDRUS-2D. *J. Environ. Eng.* **141**(11), 04015036. American Society of Civil Engineers. doi:10.1061/(ASCE)EE.1943-7870.0000976

Montanari, A. (2005) Large sample behaviors of the generalized likelihood uncertainty estimation (GLUE) in assessing the uncertainty of rainfall-runoff simulations. *Water Resour. Res.* **41**(8). doi:10.1029/2004WR003826

Morris, M. D. (1991) Factorial Sampling Plans for Preliminary Computational Experiments. *Technometrics* **33**(2), 161–174. doi:10.2307/1269043

Ratto, M., Tarantola, S. & Saltelli, A. (2001) Sensitivity analysis in model calibration: GSA-GLUE approach. *Comput. Phys. Commun.* **136**(3), 212–224. doi:10.1016/S0010-4655(01)00159-X

Saltelli, A., Tarantola, S. & Chan, K. P. S. (1999) A Quantitative Model-Independent Method for Global Sensitivity Analysis of Model Output. *Technometrics* **41**(1), 39–56. doi:10.2307/1270993

Šimůnek, J., Genuchten, M. T. van & Šejna, M. (2016) Recent Developments and Applications of the HYDRUS Computer Software Packages. *Vadose Zo. J.* **15**(7), 25. doi:10.2136/vzj2016.04.0033

Brunetti, G.F., **Turco, M**., Brunetti, G., Frega, F., Fortunato, G., Piro P. (2017)

Modellazione idraulica di una pavimentazione drenante: dal rilievo all'analisi numerica

Atti del 38° Corso di Aggiornamento in Tecniche per la Difesa del Suolo dall'Inquinamento, Guardia Piemontese Terme, Italia

2017

TECNICHE PER LA DIFESA DEL SUOLO E DALL'INQUINAMENTO

a cura di
GIUSEPPE FREGA E FRANCESCO MACCHIONE

38°

EdiBios

38°

TECNICHE PER LA DIFESA DEL SUOLO E DALL'INQUINAMENTO

UNIVERSITÀ DELLA CALABRIA
DIPARTIMENTO DI INGEGNERIA PER L'AMBIENTE
E IL TERRITORIO E INGEGNERIA CHIMICA
DIPARTIMENTO DI INGEGNERIA CIVILE
CENTRO STUDI ACQUEDOTTI E FOGNATURE
ASSOCIAZIONE IDROTECNICA ITALIANA
SEZIONE CALABRIA

Tecniche per la difesa del suolo e dall'inquinamento

ATTI DELLA XXXVIII EDIZIONE
21-24 GIUGNO 2017

a cura di
Giuseppe Frega
e Francesco Macchione

UNIVERSITÀ DELLA CALABRIA
DIPARTIMENTO DI
INGEGNERIA PER L'AMBIENTE
E IL TERRITORIO
E INGEGNERIA CHIMICA
DIATIC

EdiBios

Direttore del corso
Prof. Ing. Giuseppe Frega
Emerito di Costruzioni Idrauliche
dell'Università della Calabria

Comitato Organizzatore
Prof. Ing. Francesco Macchione (Coordinatore)
Prof. Ing. Francesco Calomino, Ing. Pierfranco Costabile,
Ing. Carmelina Costanzo, Ing. Maurizio Ponte, Ing. Alessio Siciliano

Segreteria
Ing. Carmelina Costanzo (coordinatrice), P.I. Giuseppe Cammarano,
Ing. Rosa De Santis, Ing. Francesco Rende

ISBN: 978-88-97181-57-6
ISSN 2282-5517

Via G. De Rada, 10 - 87100 Cosenza (CS)
Sito web: www.edibios.it - E-mail: info@edibios.it

In copertina: Fiume Crati (from *Wikipedia*, file licensed under the Creative Commons Attribution 2.5 Generic license)

Finito di stampare nel mese di giugno 2017

MODELLAZIONE IDRAULICA DI UNA PAVIMENTAZIONE DRENANTE: DAL RILIEVO ALL'ANALISI NUMERICA

G.F. Brunetti[1], M. Turco[1], G. Brunetti[2], F. Frega[1], G. Fortunato[1], P. Piro[1]

[1] Università della Calabria, Dipartimento di Ingegneria Civile - DINCI
[2] Università degli studi di Brescia, Dipartimento di Ingegneria Civile, Architettura, Territorio, Ambiente e Matematica - DICATAM

SOMMARIO. L'attività dell'uomo e il continuo sviluppo urbanistico degli ultimi anni hanno condotto a una drammatica e incessante diminuzione delle superfici naturali nei bacini urbani, con effetti visibilmente negativi soprattutto per il regolare deflusso superficiale delle acque meteoriche. Tetti, aree asfaltate e tutte le altre superfici impermeabili presenti nell'area urbana incrementano la portata delle acque che affluiscono negli impianti fognari, comportando non solo l'aumento dei coefficienti di afflusso ma anche dei sedimenti e delle sostanze potenzialmente inquinanti i cui effetti sulla salubrità delle acque e degli habitat acquatici dei corpi idrici ricettori risultano essere devastanti. Si rende quindi necessario rovesciare il tradizionale paradigma di progettazione dei sistemi di drenaggio urbano favorendo la transizione verso un approccio sostenibile che aiuti a ripristinare, lì dove possibile, il naturale ciclo delle acque e che allo stesso tempo proponga un modello di sviluppo sul territorio che tratti la risorsa idrica come un vero e proprio elemento di valore dal punto di vista ambientale, economico e sociale. Rientrano in questo approccio tutte le tecniche proprie dell'idraulica urbana sostenibile, riportate in letteratura scientifica con il nome di tecniche Low Impact Development (LID), le quali hanno dimostrato ampiamente i propri benefici sia in termini qualitativi che quantitativi, sebbene la transizione verso questi sistemi rimane lenta e limitata.
Uno dei fattori limitanti la diffusione di tali tecniche è la mancanza di strumenti di modellazione e analisi numerica adeguati, e precedentemente validati su installazioni sperimentali di campo. In quest'ottica, al fine di valutare le prestazioni idrologiche di una qualsiasi LID, l'interpretazione quanto più accurata possibile dei fenomeni idraulici non può prescindere da accurate tecniche rilevamento per la caratterizzazione geometrica e morfologica del manufatto indagato, aspetto preliminare e alla base della successiva analisi numerica del comportamento idraulico.
Pertanto, l'obiettivo principale del presente lavoro di tesi è di promuovere una procedura completa, replicabile e accurata, per la valutazione del comportamento idraulico di una pavimentazione drenante al fine di valutare l'apporto sulla mitigazione del fenomeno degli allagamenti urbani.

1. Introduzione

Negli ultimi decenni, a causa della rapida espansione dell'urbanizzazione, le aree urbane hanno subito un aumento delle superfici impermeabili quali tetti, strade e altre superfici di natura non permeabile a discapito delle aree naturali permeabili. Questo sviluppo urbano ha diminuito la funzione naturale del suolo di drenare e ha aumentato il volume di deflusso superficiale (Finkenbine et al., 2000). Tale problematica, accoppiata a un progressivo aumento delle precipitazioni dovute ai cambiamenti climatici, è causa del fenomeno sempre più frequente degli allagamenti in aree urbane.

Inoltre, come discusso nel lavoro di Davis et al., (2001), il deflusso superficiale urbano è una fonte primaria di inquinanti e contribuisce in modo significativo al degrado dei corpi idrici ricettori mediante il trasporto di inquinanti.

È evidente, quindi, che le tecniche tradizionali utilizzate nei sistemi di drenaggio urbano, consistenti nel trasportare l'acqua nella rete fognaria e allontanarla dalle aree urbane nel più breve tempo possibile, sembrano inadeguate allo scopo (Piro et al., 2014).

Recentemente, per mitigare gli effetti dell'urbanizzazione sopra descritti, sono stati sviluppati e

adottati dei nuovi sistemi di sviluppo a basso impatto meglio noti con l'acronimo anglosassone di LID, Low Impact Development. Questi sistemi consistono in un approccio innovativo e sostenibile per la gestione delle acque di pioggia e nonostante siano diventati molto popolari e diffusi nella pratica progettuale, ancora oggi nella comunità scientifica è aperto il dibattito su quale sia la migliore tecnica da utilizzare.

In generale, i sistemi LID sono costituiti da una serie di soluzioni che hanno lo scopo di ripristinare i processi idrologici dei suoli a un tempo antecedente al loro sviluppo urbanistico utilizzando tecniche di progettazione che infiltrano, filtrano, immagazzinano, evaporano e bloccano il deflusso superficiale vicino alla sorgente dello stesso. Tra le più comuni tecniche LID si ricordano i tetti verdi, i bacini di bioritenzione, le trincee filtranti, le zone umide e le pavimentazioni drenanti.

Sebbene esistono in letteratura diversi modelli matematici che possono essere implementati nell'analisi dei sistemi LID, la maggior parte di essi trascura la descrizione accurata dei processi idrologici alla base di tali tecniche. A ciò si aggiunge che il risultato modellistico è spesso ottenuto senza procedere all'ottimizzazione dei parametri, operazione cruciale al fine per ottenere la soluzione corretta.

Per questi motivi, negli ultimi anni, la comunità scientifica ha focalizzato l'attenzione sui modelli fisicamente basati per descrivere il comportamento idraulico delle LID.

Il software HYDRUS (Šimůnek et al., 2016) è uno dei software più diffusi al mondo per simulare il flusso d'acqua e il trasporto di soluti o di calore in piani verticali o orizzontali nei domini bidimensionali e tridimensionali variabilmente saturi. Di recente tale strumento è stato ampiamente utilizzato in letteratura per la descrizione del comportamento idraulico di alcune LID, quali il tetto verde e le pavimentazioni drenanti, con risultati ottimali tra simulazioni numeriche e misure sperimentali (Brunetti et al., 2016; Carbone, 2014; Hilten et al., 2008; Qin et al., 2016; Yang et al., 2015).

In generale, le pavimentazioni drenanti rappresentano una buona soluzione per risolvere le problematiche di gestione delle acque piovane sia in termini quantitativi che qualitativi. Sono strutture realizzate in strati e consistono di uno strato superficiale generalmente in blocchi di calcestruzzo, di uno strato filtrante, generalmente realizzato con sabbia grossolana o ghiaia fine, di uno strato base realizzato con aggregati in ghiaia e, infine, di uno strato di sub-base realizzato in materiale di grossa pezzatura.

Le pavimentazioni drenanti si distinguono poi in permeabili e porose in base al tipo di calcestruzzo utilizzato per lo strato di usura. Mentre nelle permeabili l'infiltrazione avviene esclusivamente nelle fughe tra un blocco e l'altro, in quelle porose l'infiltrazione può avvenire anche nel blocco stesso. Nel lavoro di Scholz e Grabowiecki, (2007), è presente una descrizione dettagliata delle pavimentazioni permeabili e porose.

Nonostante i vantaggi che si avrebbero nell'adottare le pavimentazioni drenanti, queste tecniche non sono ancora molto diffuse probabilmente perché gli strumenti di modellazione spesso utilizzano metodologie semplificate, basate su equazioni empiriche e concettuali, che non tengono in considerazione i processi idrologici in modo fisico. Inoltre, le proprietà idrauliche dei materiali costituenti i pacchetti drenanti spesso si riferiscono solo ad indagini sulla conducibilità idraulica. Diversi studi infatti (Chandrappa e Biligiri, 2016; Zhong et al., 2016) hanno investigato le caratteristiche di permeabilità delle miscele di calcestruzzi porosi evidenziando la relazione tra la porosità e la permeabilità del materiale al fine di ottenere un buon mix della miscela del calcestruzzo.

Al fine, quindi, di valutare le prestazioni idrologiche di una pavimentazione drenante è necessario dotarsi di strumenti di modellazione adeguati allo scopo. L'obiettivo di questo lavoro quindi, è di promuovere tecniche/procedure per l'interpretazione del comportamento idraulico di una pavimentazione drenante mediante l'utilizzo della software suite di HYDRUS, ovvero suggerire procedure matematiche e sperimentali per la definizione del modello stesso, che consistono in: a) ricostruzione in 3D della superficie della pavimentazione; b) metodologie per la caratterizzazione idraulica dei materiali componenti il pacchetto drenante; c) ottimizzazione dei parametri del modello idraulico utilizzando i dati misurati da un impianto sperimentale.

2. Metodologia

2.1 Descrizione del sito sperimentale

La pavimentazione drenante, di cui si dispongono le caratteristiche tecniche e i dati misurati di volume di acqua infiltrato per singolo evento meteorico, è stata installata nell'ambito del progetto

PON01_02543 "Servizio di gestione integrata e sostenibile del ciclo acqua – energia nei sistemi di drenaggio urbano" nei pressi del Dipartimento di Ingegneria Civile dell'Università della Calabria in un'area a parcheggio di fronte al cubo 42B. L'area di parcheggio prima dell'intervento risultava essere completamente impermeabile.

Il sito sperimentale ha una superficie di circa 154 m^2 e spessore circa pari a 98 cm (Fig. 1).

Una stazione meteo, che si trova in prossimità del sito sperimentale, misura le precipitazioni, la velocità e la direzione del vento, l'umidità dell'aria, la temperatura dell'aria, la pressione atmosferica e la radiazione solare globale. I dati di pioggia sono misurati da un pluviometro con vaschetta basculante con risoluzione di 0,254 mm e frequenza di acquisizione di 1 min. I dati climatici vengono invece acquisiti con una frequenza di 5 minuti. Tutti i dati vengono elaborati e memorizzati in un database SQL.

Un misuratore di flusso, composti da un tubo misuratore in PVC con luce a stramazzo e da un trasduttore di pressione, misurano la portata in uscita dal pacchetto drenante. Il trasduttore di pressione è stato calibrato in laboratorio utilizzando una colonna idrostatica.

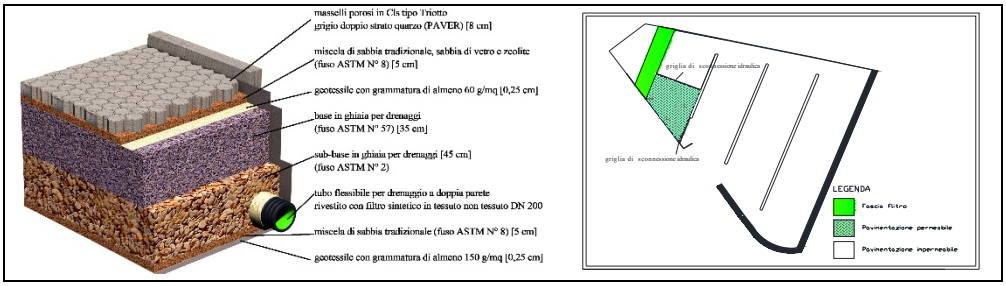

Fig. 1 - *Descrizione del sito sperimentale (Piro et al., 2015)*

2.2 Ricostruzione della superficie della pavimentazione in 3D

Al fine di costruire un modello idraulico quanto più corrispondente al vero, si è deciso di rilevare l'area oggetto di studio mediante laser scanner 3D. La fase di acquisizione della nuvola di punti, si è svolta in condizioni meteo stabili e soleggiate mediante laser scanner 3D modello Geosystems Leica HDS3000. Sono stati scelti 2 punti di presa e posizionati 4 target, in modo da avere una restituzione il più possibile densa e omogenea della nuvola di punti, per l'intera area oggetto di studio. Mentre il posizionamento dei target è stato guidato dalla necessità di garantire il corretto orientamento e l'unione delle due nubi rilevate, la scelta del secondo punto di presa è stata resa indispensabile dalla necessità di rilevare eventuali "zone d'ombra", relativa alla prima postazione, e di avere una nuvola quanto più densa e dettagliata possibile nell'area oggetto di studio. Operazioni di unione e pulizia delle nuvole di punti ottenute dalle due scansioni sono state ottenute mediante l'utilizzo di software specifici.

2.3 Caratterizzazione idraulica dei materiali componenti il pacchetto drenante

Al fine di ridurre il numero di parametri nella successiva fase di modellazione e quindi per ottenere un miglior risultato dal modello idraulico, si è proceduto a misurare in laboratorio le proprietà idrauliche dello strato di usura, in blocchi di calcestruzzo poroso, e dello strato di allettamento in sabbia e sabbia mista letto. Per lo strato in calcestruzzo si è utilizzato il "clay tank experiment" mentre per lo strato di sabbia si è utilizzato il "multistep outflow experiment" seguendo, per entrambi gli esperimenti, le procedure di Kodešová et al., (2014).

La curva di ritenzione idrica dello strato in calcestruzzo è stata misurata su due campioni (blocchetti di dimensioni ridotte). Si è proceduto per prima cosa col sigillare le facce verticali dei blocchetti con della cera, quindi i campioni sono stati saturati in acqua per poi essere posizionati in un serbatoio costituito da più strati di argilla e sabbia. I campioni sono poi stati drenati applicando diverse pressioni da 0 a -220 cm. I contenuti idrici volumetrici sono stati misurati per via gravimetrica ad ogni step di pressione applicata. I parametri della curva di ritenzione sono stati ottenuti ottimizzando i dati sperimentali mediante l'utilizzo del software RETC (van Genuchten et al., 1991).

Per quanto riguarda la misura dei parametri della curva di ritenzione idrica dello strato in sabbia, è stato utilizzato il "multistep outflow experiment" (Van Dam et al., 1994).

L'esperimento è stato condotto su due campioni di materiale precedentemente saturati e posti in due diverse "Tempe Cell". Dopo la completa saturazione, i campioni sono stati lentamente drenati utilizzando 5 step di pressione (pressione minima -12 cm). Per entrambi i modelli è stato utilizzato il modello di van Genuchten-Mualem a singola porosità (VM) implementato in HYDRUS-1D.

Per quanto riguarda i valori incogniti dei restanti parametri idraulici, si è proceduto con la procedura di ottimizzazione del modello idraulico in base ai valori misurati di portata in uscita dal pacchetto drenante.

2.4 Ottimizzazione del modello idraulico

Per interpretare il comportamento idraulico della pavimentazione è stato utilizzato il software HYDRUS 3D (Šimůnek et al., 2016). HYDRUS 3D è un modello tridimensionale molto utilizzato per simulare il flusso di acqua, calore e diversi soluti nei mezzi porosi variabili. HYDRUS-3D risolve numericamente l'equazione Richards per il flusso insaturo multidimensionale:

$$\frac{\partial \theta}{\partial t} = -\nabla \cdot \left[K \cdot \nabla (h - z) \right] \tag{1}$$

dove θ è il contenuto volumetrico dell'acqua [$cm^3\ cm^{-3}$], t è il tempo [T], h è è il carico matriciale [L], z è la coordinata spaziale [L], K è la conducibilità idraulica insatura [$L\ T^{-1}$]

Mentre nello strato di usura e in quello di allettamento è stato utilizzato il modello a singola porosità di VM (van Genuchten, 1980), per gli strati base e sub-base, composti da materiali grossolani e non omogenei, è stato utilizzato il modello a doppia porosità (van Genuchten and Wierenga, 1976). In questi modelli, si presuppone che il flusso d'acqua sia limitato alle fratture (ovvero ai pori tra gli aggregati e ai macropori), e che l'acqua nella matrice (ovvero nei pori interni agli aggregati o nella matrice rocciosa) non si muova affatto. In tal modo i pori tra gli aggregati rappresentano delle tasche immobili che possono scambiare, trattenere e immagazzinare l'acqua, ma non consentono il flusso convettivo. Questa concettualizzazione porta all'utilizzo di modelli, a due regioni e a doppia porosità, che descrivono i tipi di flusso e di trasporto partizionando la fase liquida nella regione mobile (che scorre tra gli aggregati)-θ_m e in quella immobile (stagnante, interna agli aggregati)- θ_{im}. Si ha infatti:

$$\theta = \theta_m + \theta_{im} \tag{2}$$

dove il pedice m in riferimento alle fratture, ovvero ai pori tra gli aggregati o macro-pori, mentre im fa riferimento alla matrice del terreno, ovvero ai pori interni all'aggregato e alla matrice rocciosa.

La formulazione della doppia porosità per il flusso d'acqua può essere basata su una formulazione mista dell'equazione di Richards, per descrivere il flusso d'acqua nelle fratture, e di un'equazione di equilibrio di massa, per descrivere le dinamiche di umidità nella matrice:

$$\begin{aligned} \frac{\partial \theta_m}{\partial t} &= -\nabla \cdot \left[K \cdot \nabla (h - z) \right] - S_m - \Gamma_w \\ \frac{\partial \theta_{im}}{\partial t} &= -S_{im} + \Gamma_w \\ \Gamma_w &= \omega \left(S_e^m - S_e^{im} \right) \end{aligned} \tag{3}$$

dove S_m e S_{im} sono i termini di assorbimento per entrambe le regioni, e Γ_w è la velocità di trasferimento dell'acqua presente nei pori tra l'aggregato, verso i pori all'interno dell'aggregato, ω rappresenta invece un coefficiente del primo ordine.

Il domino numerico che rappresenta la stratigrafia della pavimentazione è stato diviso in 5 strati.

Per il bordo superiore è stata adottata la *Atmospheric Boundary Condition*, una condizione che specifica i valori di flusso entrante ed uscente, in particolare i valori di precipitazione ed evapotraspirazione. Per il bordo inferiore è stata specificata una condizione di tipo *Seepage*, che essenzialmente permette che ci sia flusso in uscita solo quando il mezzo sia saturo sul bordo. La condizione iniziale è stata specificata in termini di pressione, e in particolare ipotizzando una distribuzione lineare delle stesse nella stratigrafia con valore superiore pari a -90 cm e -0.5 cm inferiore

La procedura cosiddetta di "inverse modeling", consente la stima dei parametri incogniti di un modello a partire da dati sperimentali misurati. Negli ultimi anni, il suo utilizzo è notevolmente aumentato grazie ai progressi della modellazione numerica e all'incremento della potenza di calcolo dei personal computer che consentono ora la risoluzione di problemi inversi. In generale, l'approccio nella modellazione inversa, è quello di selezionare una funzione obiettivo che è una misura dell'accuratezza tra i dati misurati e quelli simulati dal modello e che è strettamente correlata ai parametri da ottimizzare. La soluzione di ottimo dei parametri sarà ottenuta minimizzando tale funzione obiettivo.

Tuttavia, per ottenere la soluzione mediante la modellazione inversa, il problema inverso deve essere posto correttamente.

In letteratura numerose sono le applicazioni di modellazione inversa per la stima dei parametri idraulici di un modello e tra i metodi più utilizzati si ricorda il metodo di Marquardt, (1963) che forse il più utilizzato tra gli idrologi e i fisici del suolo. Tuttavia, questi metodi sono sensibili ai valori iniziali di parametri ottimizzati e l'algoritmo spesso rimane intrappolato in minimi locali, specialmente quando la superficie di risposta mostra un comportamento multimodale.

La procedura di ottimizzazione dei parametri è stata quindi effettuata utilizzando l'algoritmo "*Particle Swarm Optimization*" (PSO) (Kennedy and Eberhart, 1995), un metodo di ricerca globale molto utilizzato per l'ottimizzazione dei parametri in modelli ambientali complessi. Per l'implementazione dell'algoritmo è stato utilizzato il tool *pyswarm* in ambiente python.

Per valutare l'accuratezza della risposta del modello, stato utilizzato l'indice di Nash-Sutcliffe (Nash and Sutcliffe, 1970). Tale indice indica l'accuratezza tra i dati osservati rispetto ai dati simulati ed inoltre, in letteratura, è identificato quale migliore funzione obiettivo per i modelli rainfall-runoff. Il coefficiente di Nash varia da -∞ ad 1.0 dove il valore 1 rappresenta il valore di ottimo tra misurato e simulato. Valori superiori a 0.45 sono da considerarsi accettabili.

$$NSE = 1 - \left[\frac{\sum_{i=1}^{n} \left(Q_i^{obs} - Q_i^{\mathrm{mod}} \right)^2}{\sum_{i=1}^{n} \left(Q_i^{obs} - \overline{Q_i^{obs}} \right)^2} \right] \tag{4}$$

3. Risultati

3.1 Ricostruzione della superficie della pavimentazione in 3D

A seguito delle operazioni di pulitura e unione delle nuvole di punti dai diversi punti di presa, ha portato alla sintesi di una nuvola di punti più densa e omogenea e quindi rappresentativa dell'area di studio. Mediante l'utilizzo del software Geomagic Studio 2014 è stato avviato il processo di triangolazione tra i punti rilevati, al fine di ricostruire la mesh dell'area dopo aver eseguito operazioni di "fill holes" (chiusura dei buchi), operazione necessaria a seguito dell'unione di due scansioni (Fig. 2).

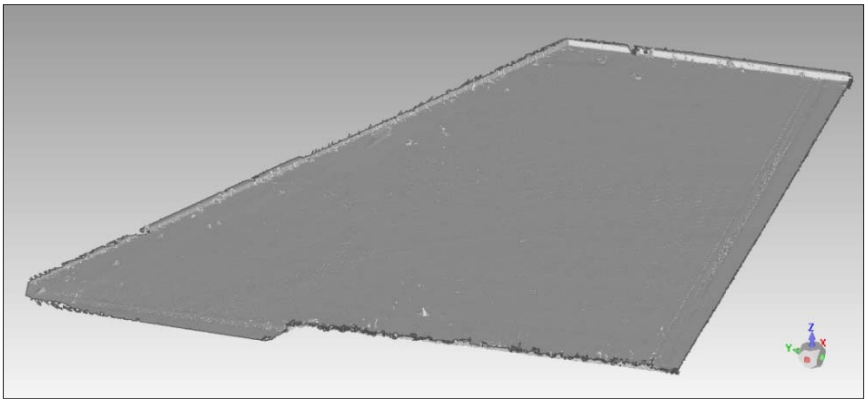

Fig. 2 - *Mesh della pavimentazione ottenuta alla fine del processo*

Ottenuto il modello della pavimentazione, sono state condotte alcune indagini necessarie ai fini della modellazione idraulica mediante Hydrus. L'analisi con gradiente di colore relativa deviazione standard della mesh e l'operazione di slicing orizzontale della pavimentazione, che ha permesso di individuare le curve di livello della stessa e identificare una doppia pendenza della pavimentazione.

A seguito di queste analisi è stata estrapolata la lunghezza media della pavimentazione che risulta essere di 9.646 m, i valori delle 2 pendenze percentuali individuate che sono all'incirca del 2%, e le coordinate dei vertici della mesh riportati nella tabella 1.

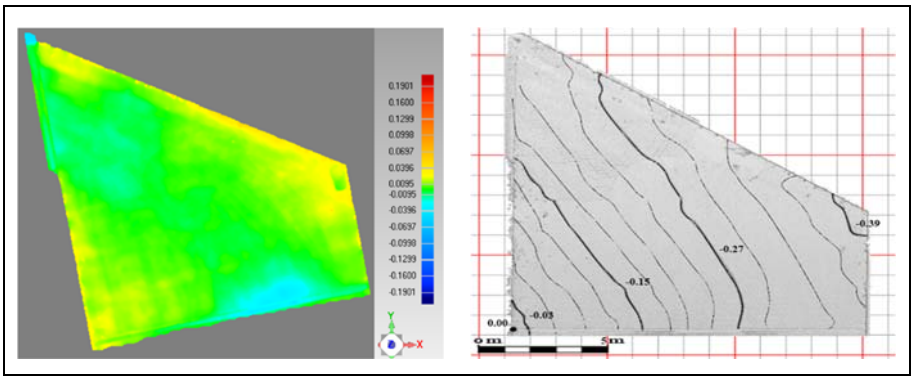

Fig. 3 - *Analisi di deviazione standard delle pavimentazione e studio della pendenza attraverso curve di livello*

	X	Y	Z
PUNTO 1	4.553	8.702	-2.301
PUNTO 2	5.691	3.068	-2.261
PUNTO 3	-7.776	0.398	-1.924
PUNTO 4	-10.53	14.79	-2.134

Tab. 1 - *Coordinate geometriche dei vertici della mesh*

3.2 Caratterizzazione idraulica dei materiali componenti il pacchetto drenante

I risultati degli esperimenti condotti sui materiali presentano un buon grado di accuratezza tra i valori osservati di contenuto idrico ed i valori simulati con gli strumenti software citati nella metodologia. Ciò è confermato da valori del coefficiente di determinazione pari a $R^2 = 0.90$. Nella tabella 2, si riportano i valori dei parametri idraulici dei materiali.

Layer 1 – strato di usura in cls	Campione 1	Campione 2
θ_r [cm^3 cm^{-3}]	0.044	0.045
θ_s [cm^3 cm^{-3}]	0.106	0.113
α [cm^{-1}]	3.37	4.03
n [-]	1.47	1.47
K_s [cm min^{-1}]	-	-
Layer 2 – strato di allettamento in sabbia	**Campione 1**	**Campione 2**
θ_r [cm^3 cm^{-3}]	0	0
θ_s [cm^3 cm^{-3}]	0.41	0.37
α [cm^{-1}]	0.43	0.40
n [-]	2.45	2.65
K_s [cm min^{-1}]	30	32

Tab. 2 – *Proprietà idrauliche dei blocchi in cls poroso e del misto sabbia*

Nella tabella, θ_r e θ_s [$L^3\ L^{-3}$] rappresentano rispettivamente il contenuto idrico residuo e a saturazione del materiale, α [L^{-1}], m [−], e n [−], sono parametri empirici che dipendono dal tipo di suolo, K_s [$L\ T^{-1}$] rappresenta la conducibilità idraulica del mezzo a saturazione.

I parametri stimati per entrambi i materiali indicano che il comportamento idraulico degli strati è caratterizzato dall'avere un drenaggio moderato e capacità di ritenzione trascurabile. Questo aspetto è senza dubbio positivo considerando che l'obiettivo di una pavimentazione drenante è infiltrare quanta più acqua possibile al fine di limitare il deflusso superficiale.

3.3 Ottimizzazione del modello idraulico

Una volta completata la definizione del modello e la caratterizzazione idraulica dei primi due materiali, si è passati all'analisi numerica del modello stesso mediante la modellazione inversa dei rimanenti parametri idraulici, degli strati base e sub-base, su un periodo di simulazione mensile utilizzando l'algoritmo di ottimizzazione globale *"Particle Swarm Optimization"*. Nella tabella 3 sono riportate le caratteristiche idrauliche dei materiali componenti il pacchetto drenante dopo le analisi sui materiali e la fase di ottimizzazione.

Layer	θ_r	θ_s	α	n	K_s	L	$\theta_{r,\,imm}$	$\theta_{s,\,imm}$	ω
Blocchi cls - 1	0.044	0.106	3.37	1.47	-	0.5			
Blocchi cls - 2	0.045	0.113	4.03	1.47	-	0.5			
Blocchi cls – simulazione	0.044	0.106	3.37	1.47	1.56	0.5			
Misto sabbia - 1	0	0.41	0.43	2.45	30	0.5			
Misto sabbia - 2	0	0.37	0.4	2.65	32	0.5			
Base in ghiaia per drenaggi - simulazione	0	0.044	0.021	4.33	93.20	0.5	0	0.35	0.00017
Sub-base in ghiaia per drenaggi	0.00	0.01	0.27	2.41	96.70	0.5	0	0.29	0.0013

Tab. 3 – *Proprietà idrauliche dei materiali dell'intero pacchetto drenante*

Al fine di investigare l'adeguatezza del modello nel riprodurre il reale comportamento della pavimentazione, l'idrogramma numerico in uscita e quello misurato sono stati comparati. Il valore dell'indice di Nash-Sutcliffe è stato inoltre computato.

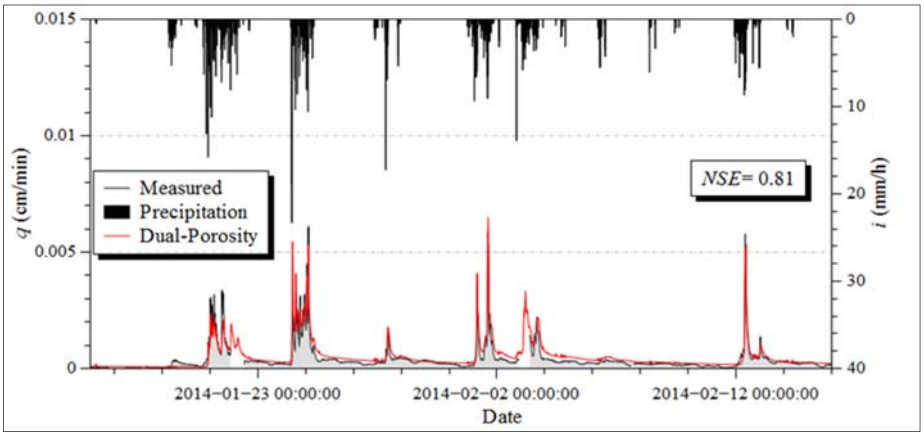

Fig. 4 - *Confronto tra idrogramma in uscita modellato e idrogramma misurato*

L'analisi numerica è risultata essere convergente e con errori di integrazione numerica sotto al 2% durante tutta la simulazione. Ciò indica l'adeguatezza nella definizione del modello numerico.

I risultati ottenuti dalla simulazione tridimensionale della pavimentazione valore dell'indice di Nash–Sutcliffe è risultato essere pari a 0.81 per il periodo considerato. Ciò indica che il modello riesce a riprodurre accuratamente il comportamento insaturo della pavimentazione, come confermato dalla buona sovrapponibilità dei due idrogrammi.

4. Conclusioni

In questo lavoro si è voluto proporre una metodologia replicabile e accurata per l'analisi del comportamento idraulico di una pavimentazione drenante.

Nella fase preliminare si è provveduto a effettuare il rilievo con il laser scanner, da due diversi punti di presa, della pavimentazione. Sono state quindi ottenute due nuvole di punti e successivamente con l'utilizzo di software specifici è stato possibile unirle, ridurre il rumore, decimare i punti in eccesso. La nuvola di punti ottenuta è stata poi importata nel software Geomagic Studio 2014 con il quale, attraverso un processo di triangolazione tra i punti, è stata ricostruita la mesh della pavimentazione.

Le analisi sperimentali condotte su alcuni materiali hanno aiutato a ridurre la dimensionalità del problema inverso di ottimizzazione e la scelta di un algoritmo globale per la modellazione inversa ha assicurato la validità della fase di ottimizzazione dei rimanenti parametri.

Le informazioni ottenute hanno reso possibile la definizione di un modello idraulico accurato.

Lo studio, quindi, ha evidenziato come la costruzione di un modello numerico fisicamente basato, unitamente all'utilizzo delle più moderne tecniche di rilievo, in particolare quella del laser scanning, alle procedure sperimentali per la caratterizzazione idraulica dei materiali e infine all'analisi numerica computazione avanzata, consenta di ottenere un elevato grado di precisione nello studio dei fenomeni di infiltrazione e deflusso delle acque in area urbana.

Infine si è dimostrato che la modellazione degli strati in ghiaia con la formulazione a doppia porosità, ha fornito risultati soddisfacenti in termini comparazione tra dati misurati e modellati, e ha confermato la validità dell'ipotesi sul comportamento idraulico di tali strati, comportamento simile al comportamento nelle matrici rocciose.

Bibliografia

1. Finkenbine, J.K., Atwater, J.W., Mavinic, D.S., (2000) - *Stream Health After Urbanization.* J. Am. Water Resour. Assoc. 36, 1149–1160. doi:10.1111/j.1752-1688.2000.tb05717.x
2. Davis, A.P., Shokouhian, M., Ni, S., (2001) - *Loading estimates of lead, copper, cadmium, and zinc in urban runoff from specific sources*. Chemosphere 44, 997–1009. doi:10.1016/S0045-6535(00)00561-0
3. Piro P., Carbone M., (2014) - *A modelling approach to assessing variations of total suspended solids (TSS) mass fluxes during storm events.* Hydrological Processes, 28(4), 2014, pp. 2419-2426.
4. Šimůnek, J, Van Genuchten, M.T., Šejna, M., (2016) - *Recent Developments and Applications of the HYDRUS Computer Software Pac*. Vadose Zo. J. 15, 25. doi:10.2136/vzj2016.04.0033
5. Brunetti, G., Simunek, J., Piro, P., (2016) - *A comprehensive analysis of the variably-saturated hydraulic behavior of a green roof in a mediterranean climate*. Vadose Zo. J. 15, doi: 10.2136/vzj2016.04.0032
6. Carbone, M., Brunetti, G., Piro, P (2014) - *Hydrological performance of a permeable pavement in mediterranean climate*. In: 14th SGEM GeoConference on Water Resources. Forest, Marine and Ocean Ecosystems, pp. 381–388. doi:10.5593/SGEM2014/B31/S12.050
7. Hilten, R.N., Lawrence, T.M., Tollner, E.W., (2008) - *Modeling stormwater runoff from green roofs with HYDRUS-1D*. J. Hydrol. 358, 288–293. doi:10.1016/j.jhydrol.2008.06.01010. Qin, H.P., Peng, Y.N., Tang, Q.L., Yu, S.L., (2016) - *A HYDRUS model for irrigation management of green roofs with a water storage layer*. Ecol. Eng. 95, 399–408. doi:10.1016/j.ecoleng.2016.06.077
8. Yang, W.Y., Li, D., Sun, T., Ni, G.H., (2015) - *Saturation-excess and infiltration-excess runoff on green roofs*. Ecol. Eng. 74, 327–336. doi:10.1016/j.ecoleng.2014.10.023
9. Scholz, M., Grabowiecki, P., (2007) - *Review of permeable pavement systems*. Build. Environ. 42, 3830–3836. doi:10.1016/j.buildenv.2006.11.016
10. Chandrappa, A.K., Biligiri, K.P., (2016) - *Comprehensive investigation of permeability characteristics of pervious concrete: A hydrodynamic approach*. Constr. Build. Mater. 123, 627–637. doi:10.1016/j.conbuildmat.2016.07.035

11. Zhong, R., Xu, M., Vieira Netto, R., Wille, K., (2016) - *Influence of pore tortuosity on hydraulic conductivity of pervious concrete: Characterization and modeling*. Constr. Build. Mater. 125, 1158–1168. doi:10.1016/j.conbuildmat.2016.08.060
12. Kodešová, R., Fér, M., Klement, A., Nikodem, A., Teplá, D., Neuberger, P., Bureš, P., (2014) - I*mpact of various surface covers on water and thermal regime of Technosol*. J. Hydrol. 519, 2272–2288. doi:10.1016/j.jhydrol.2014.10.035
13. van Genuchten, M.T., Leij, F.J., Yates, S.R., (1991) - *The RETC Code for Quantifying the Hydraulic Functions of Unsaturated Soils*. United States Environ. Reseach Lab. 93. doi:10.1002/9781118616871
14. Van Dam, J.C. Van, Stricker, J.N.M., Droogers, P., (1994) - *Inverse Method to Determine Soil Hydraulic Functions from Multistep Outflow Experiments*. Soil Sci. Soc. Am. J. 58, 647–652. doi:10.2136/sssaj1994.03615995005800030002x
15. van Genuchten, M.T., (1980) - *A Closed-form Equation for Predicting the Hydraulic Conductivity of Unsaturated Soils*. Soil Sci. Soc. Am. J. 44, 892. doi:10.2136/sssaj1980.03615995004400050002x
16. van Genuchten, M.T., Wierenga, P.J., (1976) - *Mass transfer studies in sorbing porous media* I. Analytical solutions. Soil Sci. Soc. Am. J. 40, 473–480
17. Marquardt, D.W., (1963) - *An Algorithm for Least-Squares Estimation of Nonlinear Parameters*. J. Soc. Ind. Appl. Math. 11, 431–441. doi:10.1137/0111030
18. Kennedy, J., Eberhart, R., (1995) - *Particle swarm optimization*. Eng. Technol., 1942-1948
19. Nash, J.E., Sutcliffe, J. V., (1970) - *River flow forecasting through conceptual models part I - A discussion of principles*. J. Hydrol. 10, 282–290. doi:10.1016/0022-1694(70)90255-6

ISSN 2282-5517

ISBN 978-88-97181-57-6

9 788897 181576

€ 39,00

Turco, M., Brunetti, G., Nikodem, A., Fér, M., Kodešová, R. and P. Piro. (2017).

Water flow modeling in the highly permeable pavement using Hydrus-2D

5th International Conference on HYDRUS Software Applications to Subsurface Flow and Contaminant Transport Problems, Prague, Czech Republic

Water Flow Modeling in the Highly Permeable Pavement Using Hydrus-2D

Michele Turco[1], Giuseppe Brunetti[1], Antonín Nikodem[2], Miroslav Fér[2], Radka Kodešová[2], and Patrizia Piro[1]

[1]*Department of Civil Engineering, University of Calabria, Rende, CS 87036, Italy*
[2]*Faculty of Agrobiology, Food and Natural Resources, Dept. of Soil Science and Soil Protection, Czech University of Life Sciences, Kamycká 129, CZ-16521 Prague 6, Czech Republic*

The increase of urbanization in the last decades has caused, among others, the increase of impervious surfaces in spite of those permeable. This is one of the major aspects of the increasing frequency of flooding events in urban catchments that highlighted all the critical issues of the traditional urban drainage systems and oriented science and technical towards new stormwater management approaches such as Low Impact Development techniques (LID). LID systems consist of a series of facilities whose purpose is to intercept stormwater runoff. Among the most common LID, permeable pavement (PP) is a facility constructed in layers that represent a good solution to solve stormwater management problems.

Despite the benefits that it would adopt by using PP, these techniques are not yet widespread probably because modeling tools often used simplified methodologies, based on empirical and conceptual equations, that do not take into account hydrological processes in a physical way.

The aim of this work is to assess the suitability of the HYDRUS-2D model correctly describe the hydraulic behavior of a lab-scale permeable pavement system. The hydraulic properties of two (porous concrete blocks and fine gravel used for bedding layers) of the three layers that composed the system were measured using two experimental procedures (clay tank and the multistep outflow experiment, respectively). Soil water retention and hydraulic conductivity curves were described by the van Genuchten functions. In addition some of the parameters were optimized with the HYDRUS-2D model from observed water fluxes in the lab-scale porous pavement system and soil water contents measured in bedding layer. The inverse solution optimization, which implements a Marquardt-Levenberg type parameter estimation technique for the estimation of the soil hydraulic parameters, was carried out to calibrate the model. Measured and modeled hydrographs were compared using the Nash-Sutcliffe efficiency (NSE) index, while the coefficient of determination R^2 was used to assess the measured water content versus modeled ones in the bedding layer. Obtained results have confirmed the suitability of HYDRUS-2D to correctly interpret the hydraulic behavior of the lab-scale permeable pavement system.

Brunetti, G., Šimůnek, J., Wöhling, T., **Turco, M.** and Piro, P. (2017)

A Computationally Efficient Pseudo-2D Model for the Numerical Analysis of Permeable Pavements

5th International Conference on HYDRUS Software Applications to Subsurface Flow and Contaminant Transport Problems, Prague, Czech Republic

A Computationally Efficient Pseudo-2D Model for the Numerical Analysis of Permeable Pavements

Giuseppe Brunetti[1], Jirka Šimůnek[2], Thomas Wöhling[3], Michele Turco[1], and Patrizia Piro[1]

[1]*Department of Civil Engineering, University of Calabria, Rende, CS 87036, Italy*
[2]*Department of Environmental Sciences, University of California, Riverside, CA 92521, USA*
[3]*Department of Hydrology, Technische Universität Dresden, Dresden, Germany*

Mechanistic models have proven to be accurate and reliable tools for simulating the hydraulic behavior of permeable pavements. However, their widespread adoption is limited by their complexity and computational cost. Recent studies have tried to address this issue by investigating the application of new techniques, such as surrogate-based modeling. One of such approaches includes the development of Lower-Fidelity Physically-Based Surrogates (LFS). LFSs focus on reducing the computational complexity of a numerical problem by computing an approximation of the original model. While this technique has been extensively used in water-related problems, no studies have evaluated its use in LIDs modeling. Thus, the main aim of this study is the development of the LFS model for the numerical analysis of the hydraulic behavior of permeable pavements. The proposed model decouples the subsurface water dynamics of a permeable pavement into a) a one-dimensional (1D) vertical infiltration process and b) one-dimensional saturated lateral flow along the impervious base. The pavement is horizontally discretized in *N* elements. HYDRUS-1D is used to simulate the infiltration process. Simulated outflow from the vertical domain is used as a recharge term for saturated lateral flow, which is described using the kinematic wave approximation of the Boussinesq equation. The proposed model has been compared with HYDRUS-2D, which numerically solves the Richards equation for the entire two-dimensional domain. Results confirmed the accuracy of the LFS model, which was able to reproduce both subsurface outflow and the moisture distribution in the permeable pavement, while significantly reducing the computational cost.

Turco, M., Carbone, M., Brunetti, G., Sansone, E., Piro, P. (2016)

Modellazione idraulica delle pavimentazioni drenanti: risultati sperimentali

Atti del XXXV Convegno Nazionale di Idraulica e Costruzioni Idrauliche, Bologna, Italia

MODELLAZIONE IDRAULICA DELLE PAVIMENTAZIONI DRENANTI: RISULTATI SPERIMENTALI

Michele Turco [1], Marco Carbone[1], Giuseppe Brunetti [1], Eugenio Sansone [1] & Patrizia Piro [1]

(1) Dipartimento di Ingegneria Civile Università della Calabria via P. Bucci, 87036 Arcavacata di Rende (CS)

ASPETTI CHIAVE

- *Analisi dei processi di infiltrazione nei mezzi porosi mediante l'utilizzo del modello S.W.M.M*
- *Schematizzazione del processo di infiltrazione mediante un modello a serbatoi con efflusso controllato*
- *Validazione del modello sulla base di un controllo volumetrico a partire da dati misurati in situ*

1 PREMESSA

Negli ultimi decenni i cambiamenti climatici e la crescente impermeabilizzazione del territorio hanno favorito nelle aree urbane il verificarsi di situazioni critiche che hanno causato un vero e proprio sconvolgimento del ciclo idrologico naturale con conseguenti fenomeni allagamenti superficiali a causa dell'inefficienza dei sistemi di drenaggio urbano utilizzati. I sistemi fognari tradizionali non sono quindi più in grado di gestire questo aumento del deflusso superficiale e le inondazioni stanno diventando frequenti, anche per eventi di pioggia di bassa magnitudo. Per tale motivo, la comunità scientifica ha rivolto da anni il suo interesse verso soluzioni tecnologiche innovative sostenibili volte a ripristinare il ciclo idrologico "Pre-development" mediante la riproduzione dei processi naturali. Tra le tecniche più diffuse, l'approccio Low Impact Development (LID) mira a preservare e ripristinare il ciclo idrologico naturale, ridurre al minimo l'impermeabilità dei bacini urbani migliorandone le loro capacità di infiltrazione ed evapotraspirazione. Tra le tecniche LID si ricordano bacini di bio-ritenzione, le trincee filtranti, le coperture a verde, le pavimentazioni drenanti e molte altre *(Dietz, 2007)*.

Le pavimentazioni drenanti rappresentano una delle tecniche LID più diffuse. Rispetto alle tradizionali pavimentazioni in asfalto impermeabile, esse sono in grado di ridurre il deflusso superficiale, ridurre le portate di picco e laminare i volumi di deflusso tuttavia le prestazioni complessive dipendono da diversi fattori quali ad esempio le caratteristiche dei materiali di costruzione o le caratteristiche delle precipitazioni (*Pratt et al., 1995*). Un limite alla diffusione di tali infrastrutture è senza dubbio rappresentato da una scarsa conoscenza di strumenti di modellazione adeguati.

Obiettivo principale di questo lavoro è analizzare il processo di infiltrazione all'interno di una pavimentazione drenante, installata nel Parco di Idraulica Urbana dell'Università della Calabria, mediante l'utilizzo di un modello a serbatoi implementato all'interno dello Storm Water Management Model (SWMM) sviluppato dall'Environment Protection Agency degli Stati Uniti.

2 METODOLOGIA

2.1 Modello di calcolo

Caratteristica principale delle pavimentazioni drenanti è quella di avere una struttura fortemente insatura. Il flusso all'interno di un mezzo poroso può essere descritto attraverso l'equazione di Richards *(Richards, 1931)*:

$$\frac{\partial\theta(\psi)}{\partial t} - \nabla \cdot K(\theta(\psi))\nabla(\psi - z) = 0 \tag{1}$$

dove θ rappresenta il contenuto idrico (L^3/L^3), ψ rappresenta il carico di suzione (L), K la conducibilità idraulica del mezzo insaturo (L/T), t il tempo (T) e z la profondità (L). Non esistono soluzioni analitiche per risolvere tale equazione e quindi molto spesso si utilizzano per la sua risoluzione metodi numerici alle differenze finite o ai volumi finiti *(Carbone et al., 2015)*.

A partire dall'equazione di Richards è stato elaborato un modello di calcolo a serbatoi per determinare il processo di infiltrazione all'interno del quale ogni strato della pavimentazione è schematizzato da un serbatoio caratterizzato da una certa legge di efflusso definita dalla relazione

$$q(h) = a \cdot h^b \tag{2}$$

dove q rappresenta l'aliquota di volume uscente dal singolo serbatoio (L^3/T), h il tirante idrico all'interno del serbatoio (L), a e b sono invece i parametri caratteristici del mezzo poroso ricavabili, a partire da alcune semplificazione dell'equazione di Richards, o direttamente, se note la curva di ritenzione idrica e la conducibilità satura del mezzo in questione, o mediante calibrazioni su dati sperimentali osservati.

Il modello di calcolo implementato si basa perciò sull'utilizzo di moduli e oggetti fisici presenti nello SWMM quali nodi serbatoio, nodi outlet, nodi dividers e sottobacini. Semplificando si può dire che lo SWMM è stato utilizzato come piattaforma per una progettazione ad oggetti: ad esempio il nodo serbatoio è stato utilizzato come blocco in grado di gestire l'equazione di bilancio idraulico, il nodo divider come nodo selettivo del percorso etc.

Il modello descrive perciò il processo di infiltrazione attraverso i vari strati della pavimentazione drenante concettualizzandolo come un processo di deflusso attraverso una cascata di serbatoi; I vari strati della pavimentazione sono visti come serbatoi con efflusso controllato posti in serie.

2.2 Descrizione del sito sperimentale

La pavimentazione drenante, di cui si dispongono le caratteristiche tecniche e i dati di volume di acqua infiltrato per singolo evento meteorico è stata installata nell'ambito del progetto PON01_02543 "Servizio di gestione integrata e sostenibile del ciclo acqua – energia nei sistemi di drenaggio urbano" nei pressi del Dipartimento di Ingegneria Civile dell'Università della Calabria in un'area a parcheggio di fronte al cubo 42B. L'area di parcheggio prima dell'intervento risultava essere completamente impermeabile.

Il sito sperimentale ha una superficie di circa 154 m^2 e spessore circa pari a 98 cm (Figura 1)

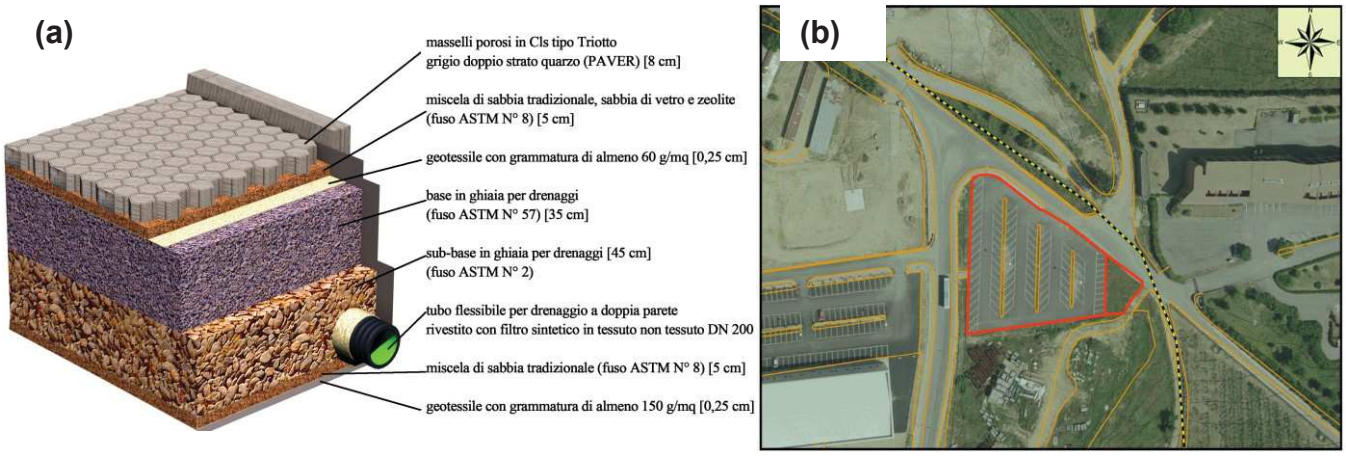

Figura 1. Descrizione del sito sperimentale: nel pannello (a) è riportata la stratigrafia della pavimentazione drenante, il pannello (b) illustra invece la posizione planimetrica della stessa installazione sperimentale (Piro ed. 2015).

In sintesi le caratteristiche dei vari strati sono le seguenti:

- Masselli porosi in CLS tipo Triotto filtrante grigio doppio strato quarzo (PAVER) per uno spessore di 8 cm
- miscela fuso ASTM 8 di Sabbia tradizionale (50%), Sabbia di vetro (50%) e Zeolite (5%) per uno spessore di 5 cm
- geotessile ad elevata permeabilità con grammatura non superiore a 60 g/m^2

- ghiaia per drenaggi (fuso ASTM No 57) per uno spessore di 35 cm
- ghiaia per drenaggi (fuso ASTM No 2) per uno spessore di 45 cm
- sabbia con fuso ASTM 8 (tradizionale), spessore di 5 cm, con funzione anti-punzonamento del sottostante geotessile
- geotessile accoppiato a una pellicola impermeabile con grammatura non superiore a 150 g/m^2

Per quanto riguarda le pendenze attribuite all'opera, è stato scelto come criterio progettuale quello della doppia pendenza longitudinale (2.00 %) e trasversale (2.00 %), in modo da far confluire le acque sia superficiali che sotterranee verso un univoco punto di raccolta.

2.3 Dati sperimentali

L'analisi effettuata in questo lavoro è un'analisi sui parametri quantitativi della pavimentazione drenante (volume totale di acqua infiltrato per ogni evento meteorico considerato) che ha l'obiettivo di valutare in maniera critico-sperimentale il modello implementato all'interno del motore di calcolo SWMM confrontando i dati modellati con quelli misurati in situ. Per quanto riguarda l'input del modello esso è costituito dai dati di pioggia misurati attraverso una stazione meteorologica installata in prossimità del sito sperimentale; la portata in uscita dalla pavimentazione invece è misurata in modo indiretto mediante un tubo misuratore con luce a stramazzo munito di un trasmettitore di pressione immergibile in grado di misurare il livello idrico da 0 a 750 mm con precisione standard dello 0.1%.

3 RISULTATI E DISCUSSIONE

Il modello di calcolo parte dal considerare il sottobacino ricevente l'evento di pioggia, che nel nostro caso di studio corrisponde all'intera superficie della pavimentazione drenante, come un semplice mezzo che trasforma totalmente l'afflusso di pioggia in deflusso. La trasformazione delle precipitazioni in deflusso, dipende da diversi parametri caratteristici del sottobacino tra cui il D-Store, la width o larghezza equivalente, il coefficiente di Manning e la pendenza media. Si è confrontato il volume totale di pioggia caduto sul sottobacino, quindi dato idrologico acquisito in sito, con il volume di deflusso modellato al variare della width del D-store e del coefficiente di Manning e si è visto che il valore di deflusso varia di poco al variare della larghezza equivalente o width in quanto tale parametro ha molta più influenza sul tempo di rilascio (più è basso tale valore più tempo impiega il sottobacino a trasformare l'afflusso in deflusso) che non sul volume totale di deflusso. Lo stesso è invece molto influenzato dal parametro "D-store" e dal coefficiente di Manning che fisicamente rappresentano rispettivamente l'altezza delle depressioni superficiali della pavimentazione e la scabrezza; le depressioni superficiali possono essere riempite dall'acqua meteorica di afflusso del bacino ricevente e quindi sottraggono parte delle precipitazioni al processo di deflusso, rappresentando perciò una perdita secca; cosi come minore è la scabrezza minore è la resistenza al moto offerta dal sottobacino al volume di afflusso.

La validazione del modello di calcolo è stata effettuata ad un criterio di tipo volumetrico, cioè i parametri dell'analisi sono stati calibrati nel rispetto del bilancio dei volumi. Ciò che la prima parte dello studio sperimentale ha messo in evidenza è che il parametro regolatore del bilancio volumetrico, partendo dalle misurazioni in sito, è il D-store. Tale parametro nel motore di calcolo dello SWMM caratterizza l'altezza delle depressioni superficiali del sottobacino rappresentando di fatto una perdita nel processo di deflusso superficiale in quanto parte dell'acqua di pioggia non partecipa al deflusso riempiendo tali depressioni; nel modello di calcolo implementato in realtà il processo simulato è di infiltrazione dell'acqua di pioggia attraverso la pavimentazione drenante e quindi tale parametro D-store rappresenta sempre una perdita per il processo di infiltrazione ma intesa come "volume ritenuto" dal pacchetto drenante. Per meglio specificare tale parametro si può dire che è la capacità del mezzo drenante di immagazzinare acqua prima che si inneschi il moto di percolazione a gravità tra gli strati della pavimentazione stessa. Tale capacità del mezzo dipende ovviamente oltre che dalle caratteristiche di tessitura e granulometria degli strati anche e soprattutto dalle condizioni idrologiche specifiche iniziali dell'evento meteorico. I risultati delle simulazioni dimostrano una correlazione tra il tempo secco che precede l'evento meteorico e il D-store. I risultati sono sintetizzati nella seguente tabella e nel grafico sottostante:

Evento	Volume modellato(m^3)	Volume misurato(m^3)	D-store (mm)	Dry-Time (giorni)
19-23/01/2014	6.05	5.92	20	19
31/01-01/02/2014	2.7	2.59	9	3
12/02/2014	1.77	1.77	9	3
04-06/03/2014	3.9	3.54	7	1.5
24-25/03/2014	3.49	3.58	17	8
04-06/04/2014	1.1	1.16	15	6
28-30/04/2014	1.32	1.33	18.5	10

Tabella 1. Risultati della modellazione effettuata

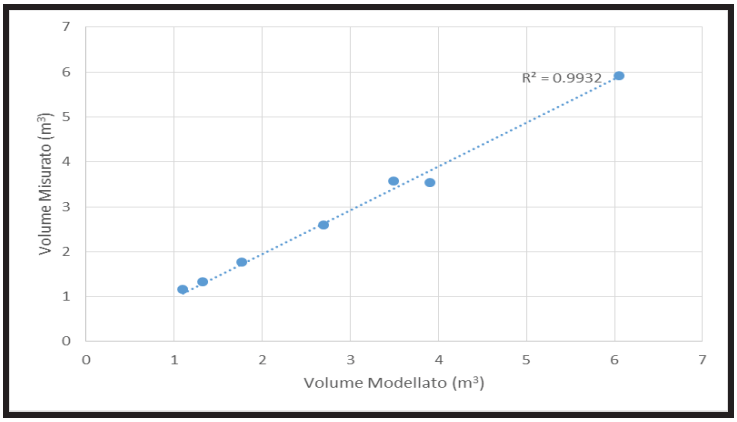

Figura 2. Confronto tra Volume misurato in situ e Volume modellato

4 CONCLUSIONI

Scopo del presente lavoro è stato quello di mostrare peculiarità e limiti del modello di calcolo proposto ancora oggi oggetto di studio. Tale modello propone l'analisi del processo di infiltrazione dell'acqua descrivendolo, a partire da oggetti fisici e blocchi già presenti in SWMM, come un processo di deflusso attraverso i vari strati della pavimentazione drenante. Tali strati sono visti come una cascata di serbatoi con efflusso controllato. La validazione del modello è stata effettuata a scala di evento a partire dai dati misurati in situ. L'analisi sperimentale ha mostrato l'accuratezza del modello da un punto di vista del bilancio volumetrico sebbene presenta ancora delle accuratezze in termini di idrogrammi simulati.

RINGRAZIAMENTI

Il presente lavoro è cofinanziato dal Programma Operativo Nazionale italiana - Ricerca e Competitività per le regioni la convergenza 2007/2013 - Asse I "Sostegno ai mutamenti strutturali" obiettivo operativo 4.1.1.1. "Aree scientifico-tecnologiche generatrici di processi di trasformazione del sistema produttivo e la creazione di nuovi settori" Azione II: "Interventi a sostegno della ricerca industriale".

RIFERIMENTI BIBLIOGRAFICI

Dietz, M.E. Low Impact Development Practices: A Review of Current Research and Recommendations for Future Directions, Water, Air, and Soil Pollution, 2007, Volume 186, Issue 1, pp 351-363.

Pratt, C., Mantle, J. & Schofield, P. UK Research into the performance of permeable pavement, reservoir structures in controlling stormwater discharge quantity and quality, Water Sci Technol, 1995, 32, 63–9.

Richards, L.A. Capillary conductions of liquids through porous mediums, J. Appl. Phys. 1931, 1, 318–333

Carbone, M., Brunetti, G. & Piro, P. Modelling the Hydraulic Behaviour of Growing Media with the Explicit Finite Volume Solution, Water, 2015, 7, 568–91.

Mancuso, A., Carbone, M., Piro, P. Progettazione e installazione pavimentazione drenante: parco di Idraulica Urbana - Unical In: Piro P. (ed.), "Interventi sostenibili nell'idraulica urbana. Ciclo Acqua-Energia: Ricerca - Progettazione - Innovazione", Cosenza, Edibios, 2015, pp.147-161, ISBN 978-88-97181-38-5.

Carbone, M., **Turco, M**., Brunetti, G., Piro, P. (2015)

A Cumulative Rainfall Function (CRF) for sub-hourly design storm in Mediterranean urban areas

Advances in Meteorology

Hindawi Publishing Corporation
Advances in Meteorology
Volume 2015, Article ID 528564, 10 pages
http://dx.doi.org/10.1155/2015/528564

Research Article

A Cumulative Rainfall Function for Subhourly Design Storm in Mediterranean Urban Areas

Marco Carbone, Michele Turco, Giuseppe Brunetti, and Patrizia Piro

Department of Civil Engineering, University of Calabria, Via P. Bucci, Cubo 42/b, 87036 Rende, Italy

Correspondence should be addressed to Michele Turco; michele.turco@unical.it

Received 24 March 2015; Revised 17 June 2015; Accepted 21 June 2015

Academic Editor: Guillermo Baigorria

Design storms are very useful in many hydrological and hydraulic practices and are obtained from statistical analysis of precipitation records. However considering design storms, which are often quite unlike the natural rainstorms, may result in designing oversized or undersized drainage facilities. For these reasons, in this study, a two-parameter double exponential function is proposed to parameterize historical storm events. The proposed function has been assessed against the storms selected from 5-year rainfall time series with a 1-minute resolution, measured by three meteorological stations located in Calabria, Italy. In particular, a nonlinear least square optimization has been used to identify parameters. In previous studies, several evaluation methods to measure the goodness of fit have been used with excellent performances. One parameter is related to the centroid of the rain distribution; the second one is related to high values of the standard deviation of the kurtosis for the selected events. Finally, considering the similarity between the proposed function and the Gumbel function, the two parameters have been computed with the method of moments; in this case, the correlation values were lower than those computed with nonlinear least squares optimization but sufficiently accurate for designing purposes.

1. Introduction

In recent years, climate change and the growing waterproofing land have favoured the occurrence, in urban areas, of critical situations causing surface flooding. Floods are the most dangerous meteorological hazard in the Mediterranean areas due to both the number of people involved and the relatively high frequency by which human activities and goods suffer damage and losses [1]. Flooding in urban areas can occur due to several factors that vary according to the kind of drainage system used (separate or combined sewers) and its design characteristics. In addition to these variables, rainfall plays the main role for flooding characterization although this one is characterized by a substantial uncertainty as much from the spatial point of view as from the temporal point of view [2]. Also its triggering factors are very complex, so it represents one of the most difficult variables to predict [3, 4]. Several studies concluded that the factors of heavy rainfall generation are various; in particular they are summarized as (a) high moisture content of the air mass present over the zone, (b) vertical movement on one or more scales, and (c) static instability.

Heavy rainfall can be the result of persistent moderate precipitation or very intense precipitation of short duration. In this way critical rainfall events are represented by heavy precipitation that occur in a very short time [5].

The use of design storms is very popular among hydraulic engineers. Several techniques to develop design storms have been studied, including intensity-duration-frequency (IDF) curve, stochastic models, and profiles obtained directly from rainfall records. A critical characteristic of IDF curves is that intensities are averaged over the specified duration and do not represent the real distribution of rainfall. Usually, design storms are developed by statistical analysis of rainfall records, but, unfortunately, sometimes they are not tested against long-term rainfall records. In addition, much of the digitised rainfall data from numerous stations is viewed as being unreliable, with important events missing and errors in the digitised data. In an attempt to overcome these problems and to improve reliability, a double exponential approach

has been applied to estimate design storm for short duration (<1 h) rainfalls.

The aim of this research is to propose a cumulative rainfall function (CRF) to assess subhourly rainfall distribution to observed data taken from three sites from the Calabria region in South Italy. Calabria region has a mean rainfall rate of about 1170 mm/years; several studies have classified Calabria Storm into four main groups: (a) storms that originate on the lee of the Alps (including those over the Gulf of Genoa); (b) storms that develop in the Western Mediterranean (Gulf of Lyon, Rhone valley, and Iberia); (c) storms that develop in Northern Africa or enter the Mediterranean from the Strait of Gibraltar; (d) storms that move over the central Mediterranean from Balkans and Eastern Europe [10]. Storms of class (a) are the most frequent ones. This research work intends to propose a multiparameter function of double exponential type applied to observed data from meteorological stations located in urban watersheds with the aim of obtaining significant input that helps in design problems of urban drainage systems; however, for urban basins, subhourly events were chosen. Several studies have been performed using stochastic models to simulate observed data [2, 11–16]. To separate a storm event from the other an appropriate minimum interevent time (MIT) was chosen. Almost all of the mathematical models used in the literature to describe or simulate hydrological processes, also stochastic, require techniques that allow the performance evaluation. In general, to evaluate the performance of a model, it needs to compare the calculated values and the corresponding measured or reference methods. The description of the various indices and the discussion on their suitability have been widely discussed in the literature [17–24]. In addition, several studies identify some common points to evaluate a mathematical model. In particular (1) a standard procedure for mathematical evaluation of a model is needed; (2) performance evaluation of a model should include at least one absolute value error indicator (in the variable units), one dimensionless index (or indicator of the relative error) for quantifying the goodness of fit, and a graphical representation of the relationship between model estimates and observations [21].

2. Materials and Methods

2.1. Data Collection and Analysis. Precipitation data, consisting of rainfall depth recorded with minute frequency, were collected from the Functional Meteorological Hydrographic and Mareographic Center database of Calabria region, South Italy. This institution has the principle role of measuring and collecting the information associated with the Earth's climate of the whole region. Three stations equipped with tipping-bucket rain gauges were selected for the data collection. The data, which covered a period of 5 years, was examined and missing records were resampled. In Figure 1 are summarized the geographical characteristics of the three stations chosen for this work.

To separate a storm event from the other, Minimum Interevent Time criterion was chosen. Minimum Interevent Time is defined as the time between the end of a storm event and the beginning of the next. Often the choice of a particular

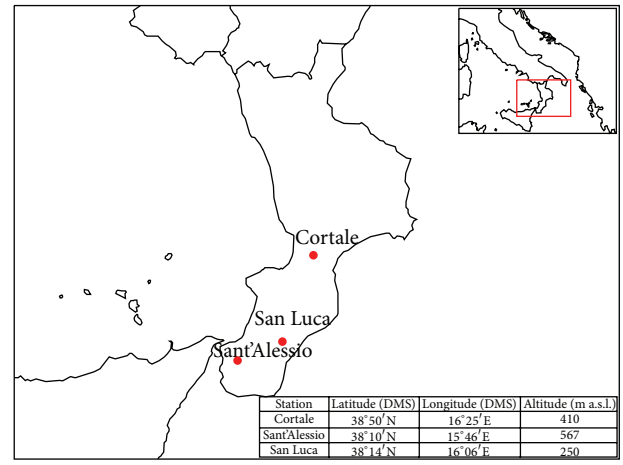

Station	Latitude (DMS)	Longitude (DMS)	Altitude (m a.s.l.)
Cortale	38°50′N	16°25′E	410
Sant'Alessio	38°10′N	15°46′E	567
San Luca	38°14′N	16°06′E	250

Figure 1: Geographical individuation of rain stations.

value of MIT was related to physical parameters changes that competed in the definition of independent rainfall events. This value therefore has never been unique but closely related to the type of analysis or observation of a particular natural phenomenon. For example, Bracken et al. [9] used MIT = 12 h in order that the ground could dry between runoff events, reducing the impact of antecedent soil moisture on runoff event. In Table 1 is summarized the typical range of rain MIT in the literature.

In urban areas, rains that deserve special attention are those of short duration such as subhourly. In this way critical rainfall events are represented by heavy precipitation that occur in a very short time [5]. As discussed by Carbone et al. [25] an appropriate value of MIT to identify independent rainfall events in urban catchment scale for subhourly rainfall events is 15 minutes. Using this value of MIT and considering a volume threshold of 8 mm, a number of rainfall events were selected from each location. Rainfall events separated by less than 15 min were merged and considered as single event. Obviously, the choice of the volume threshold can condition both the number of events resulting from the chosen MIT and the events' characteristics.

The statistical analysis is crucial for the mathematical characterization of rainfall events. In particular, skewness, kurtosis, and variation are among the most important shape parameters of a statistical distribution. Skewness, kurtosis, and variation are computed as follows:

$$\text{Skew} = \frac{\sum_{i=1}^{n}\left(X_i - \overline{X}\right)^3}{(n-1)\,\sigma^3},$$

$$\text{Kurt} = \frac{\sum_{i=1}^{n}\left(X_i - \overline{X}\right)^4}{(n-1)\,\sigma^4}, \tag{1}$$

$$\text{variation} = \frac{\sigma}{\overline{X}},$$

where X_i represents the ith data points, $\overline{X}$ is the mean, n is the number of data points, and σ is the standard deviation of data.

Table 1: Review of typical MIT value present in the literature.

MIT	Scope of the work	Reference
3 h	Forest interception processes	Lloyd [6]
0.25 days (6 h)	Dependence and internal structure of storm events	Gyasi-Agyei and Melching [7]
8 h	Depression storage recovered fully	Aryal et al. [8]
12 h	Dry ground between runoff events	Bracken et al. [9]

The skewness is a measure of the asymmetry of the probability distribution of a real-valued random variable. The skewness for a normal distribution is zero and any symmetric data should have a skewness near zero. On the other hand, the kurtosis is a measure of degree of the "peakedness" of the probability distribution of a real-valued random variable.

For these reasons, in this research, a statistical analysis of selected rainfall events has been performed in order to characterize the statistical behaviour of samples. In Table 2, the values of skewness, kurtosis, and variation are listed.

All selected events have positive skewness and are not normally distributed. Kurtosis is almost always positive; only four events exhibit negative kurtosis which indicates a uniform rain distribution. The station of Cortale exhibits always positive values of kurtosis. The mean coefficient of variation is 1.31 which indicates a high variance in the distribution of rain data.

2.2. Cumulative Rainfall Function. In general, to reproduce rainfall behaviour, stochastic processes are used in the literature [11–16]. Usually, when a statistical procedure is applied on annual maximum values the probability of exceedance might be converted into a "return period T (years)." However the critical values of the rain event refer not only to the rain intensity (or rain depth) but to the "time distribution" of the rain quantity as well. It is difficult to assign a return period to a sequence of discrete values of rainfall intensities throughout certain design storm duration. In this study, to overcome this problem, a parameterization of the cumulative historical rainfall event curve is proposed.

Rainfall depths are often described by means of the exponential distribution, sometimes by the generalized Pareto distribution hereafter referred to as GPD, and more rarely by the gamma distribution or the generalized extreme value (GEV) distribution. Results showed that although all the analysed distributions were able to satisfactorily reproduce ordinary statistics, generalized Pareto distribution was able to better reproduce the observed behaviour [26]. The selection of a particular distribution is mainly influenced by the value of the skewness of the samples considered.

In solving hydrologic problems, such as the design of urban storm sewer systems, it is much important to know the time distribution rainfall. In hydrological theory, theoretical distribution functions are usually used to set rainfall characteristics, and their parameters are calibrated using historical rainfall events.

As shown by the analysis of selected rainfall events, samples exhibit positive skewness and kurtosis, which, in general, indicate that samples are not normally distributed. In this case, considering the values of skewness and kurtosis, the sample could be represented by double exponential functions, such as Gumbel type.

If we refer to the cumulative rain depth, this function often exhibits a sigmoidal behaviour. For this reason and for what is stated above about skewness and kurtosis, the idea to propose a Gumbel-type function that parameterizes the cumulative rainfall time series has arisen.

In particular, a double exponential function is proposed:

$$F(x) = e^{-e^{-\alpha(x-\beta)}}, \tag{2}$$

where $F(x)$ represents the parametric function proposed and α and β are the parameters of the function, which depend on the characteristics of the sample considered.

In order to identify these parameters a nonlinear least squares optimization has been performed. Nonlinear optimization problems arise in numerous applications such as economy, statistic, and engineering. An optimization problem begins with a set of independent variables and often includes conditions or restrictions that define acceptable values of the variables. Such restrictions are called restraints. The essential component is the objective function, which depends in some way on the variables. The solution of an optimization problem is a set of allowed values of the variables for which the objective function assumes an optimal value. In general, a parameter of function F appears nonlinearly if the derivative is a function of the parameter. For this reason, a function $F(x, t)$ is nonlinear if at least one of the parameters appears nonlinearly.

The least squares (LS) method is a standard approach in finding an approximation to an overdetermined system of equations. It is also the most important application in data fitting. A standard example of using LS is the case of fitting a line to a given set of points, called linear regression. In general, one can distinguish between linear least squares (LLS) and nonlinear least squares (NLS).

LLS implies that the residuals are all linear. There is a closed form for the solution and it occurs mostly in regression analysis, meaning that one has a set of data points and fits function (usually a polynomial of degrees 1, 2, or 3) to best approximate the given data set.

NLS implies that the residuals are not all linear. In general, one does not have a closed form for the solution and needs to apply an iterative procedure in order to obtain a solution. Furthermore, there might exist several minimums and finding the global minimum might require high computational costs.

For these reasons the nonlinear least squares optimization has been used.

Table 2: Statistical analysis of rainfall events.

ID	Event	Skewness	Kurtosis	Variation
	Cortale			
1	2008-10-02 22:20:00	1.85	2.73	1.57
2	2008-10-04 10:43:00	1.94	3.75	1.27
3	2009-03-20 19:05:00	1.17	0.83	0.92
4	2009-06-22 01:43:00	2.13	3.70	1.71
5	2009-09-24 12:31:00	1.17	0.30	1.01
6	2009-12-04 18:55:00	1.51	1.29	1.34
7	2010-05-20 16:09:00	2.12	3.60	1.73
8	2010-07-25 09:12:00	1.56	2.21	1.12
9	2010-09-03 10:51:00	3.02	8.82	2.14
10	2010-09-25 13:44:00	1.66	2.45	1.15
11	2010-10-14 22:37:00	2.20	4.34	1.22
12	2010-11-17 17:17:00	1.98	2.89	1.40
13	2010-11-24 17:34:00	1.60	2.75	1.03
14	2011-09-20 05:30:00	1.05	0.40	1.05
15	2012-05-27 06:17:00	1.32	1.06	1.22
16	2012-09-01 14:31:00	1.59	2.93	1.14
17	2012-09-01 15:47:00	2.74	7.57	1.88
18	2012-09-04 09:43:00	2.41	5.10	1.57
19	2012-10-13 17:07:00	2.06	2.86	1.91
20	2012-10-28 13:49:00	1.30	0.49	1.22
21	2012-12-10 19:45:00	1.24	0.93	0.88
22	2013-01-21 12:41:00	1.82	2.54	1.10
23	2013-06-01 23:35:00	1.55	1.70	1.11
24	2013-08-10 13:25:00	1.90	2.85	1.30
25	2013-09-01 13:12:00	2.46	5.45	1.75
26	2013-10-01 05:41:00	1.97	3.17	1.35
27	2013-12-01 12:43:00	2.92	11.04	1.27
28	2013-12-02 13:21:00	1.35	1.69	0.89
	Mean	1.84	3.19	1.33
	Standard deviation	0.53	2.53	0.33
	Sant'Alessio			
1	2008-10-04 12:59:00	3.24	11.71	1.16
2	2009-09-16 07:39:00	2.12	4.30	1.38
3	2009-10-02 15:42:00	1.36	0.85	0.93
4	2009-12-05 20:03:00	1.41	1.97	1.10
5	2010-09-03 23:10:00	1.90	3.30	1.03
6	2010-09-09 07:16:00	0.73	−1.01	1.30
7	2010-10-13 13:12:00	1.76	2.67	1.34
8	2010-10-13 16:15:00	2.72	8.52	1.55
9	2011-06-12 07:54:00	1.99	3.10	1.60
10	2011-09-19 10:28:00	1.80	2.11	1.10
11	2011-09-21 05:24:00	1.72	3.01	1.04
12	2011-12-07 07:21:00	1.06	0.07	1.75
13	2013-07-08 11:18:00	2.31	4.43	1.07
14	2013-08-10 19:12:00	1.57	1.78	0.99
15	2013-08-21 11:31:00	0.62	−1.05	1.53
16	2013-08-30 11:00:00	1.81	2.44	1.41
17	2013-11-06 03:07:00	1.91	2.77	2.04
	Mean	1.76	2.99	1.29
	Standard deviation	0.65	3.15	0.27
	San Luca			
1	2008-01-23 01:54:00	2.37	4.82	1.00
2	2008-05-21 11:04:00	1.30	1.15	1.58
3	2008-10-25 13:38:00	1.18	0.73	1.07
4	2008-11-15 09:57:00	1.58	0.86	1.32
5	2009-01-13 17:53:00	2.15	5.29	1.70
6	2009-04-12 17:03:00	1.58	1.61	1.38
7	2009-09-17 00:18:00	2.27	4.56	1.05
8	2009-09-23 09:49:00	2.14	4.69	1.85
9	2009-09-25 12:01:00	0.68	−1.04	0.95
10	2010-09-04 00:08:00	2.05	2.74	1.23
11	2010-09-09 13:56:00	0.70	−0.80	1.70
12	2010-09-14 14:00:00	1.94	2.72	0.97
13	2010-09-14 21:30:00	2.49	6.25	1.46
14	2010-10-03 12:10:00	1.53	2.34	0.88
15	2010-11-02 12:57:00	1.56	1.11	1.12
16	2012-11-17 03:36:00	1.46	2.31	1.03
17	2013-11-12 15:44:00	1.46	1.85	1.57
18	2013-12-03 14:37:00	2.16	7.50	1.27
	Mean	1.69	2.70	1.34
	Standard deviation	0.53	2.36	0.34
	Mean	1.76	2.96	1.31
	Standard deviation	0.57	2.68	0.31

Numerical methods for nonlinear optimization problems are iterative. At the kth iteration, a current approximate solution xk is available. A new point x_{k+1} is computed by certain techniques, and this process is repeated until a point can be accepted as a solution. The classical methods for optimization are line search algorithms. Such an algorithm obtains a search direction in each iteration and searches along this direction to obtain a better point. The search direction is a descent direction, normally computed by solving a subproblem that approximates the original optimization problem near the current iterate. Therefore, unless a stationary point is reached, there always exist better points along the search direction. To set function parameter and solve nonlinear curve fitting (data fitting) problems in least squares sense, "trust-region-reflective" algorithm was used.

Nonlinear least squares problem usually makes use of one the following two algorithms:

(1) trust-region-reflective (TRR);

(2) Levenberg-Marquardt method (LM).

Levenberg-Marquardt algorithms and trust region algorithms are both Newton step-based methods (they are called "restricted Newton step methods"). Thus, they both exhibit quadratic speed of convergence near optimal value. When we are far from the solution, we can encounter a negative curvature. If this happens, Levenberg-Marquardt algorithms will slow down dramatically. In opposition, trust region algorithm will thus exhibit better performances each time a negative curvature is encountered and have thus better

performances than all the Levenberg-Marquardt algorithms. The trust region reflective algorithm has been chosen because (i) analytical first and second order derivative information can be included, (ii) upper and lower bounds on parameters can be considered easily, and (iii) it is computationally faster than LM [27].

2.3. Statistical Evaluation. In general, in order to verify the accuracy of a model, it is necessary to perform a statistical evaluation to ensure the results validity. The statistical evaluation indices of a hydrological model are varied. The use of an index instead of another depends on the type of hydrological model to validate. The description of the various indices and discussions on their suitability have been widely discussed in the literature [17–24]. The quantitative statistics are generally divided into three categories: standard regression, goodness of fit (GOF), and error index. Standard regression statistics determine the strength of the linear relationship between simulated and measured data; goodness of fit of a statistical model describes how well it fits into a set of observations. GOF indices summarize the discrepancy between the observed values and the values expected under a statistical model; error indices quantify the deviation in the units of the data of interest.

For these reasons, in order to have a global assessment of the proposed function, most widely used indices were used for each of the categories described above.

2.3.1. Statistical Evaluation (Standard Regression: Coefficient of Determination R^2). The coefficient of determination (R^2) describes the proportion of the variance in measured data explained by the model. R^2 ranges from 0 to 1, with higher values indicating less error variance, and typically values greater than 0.5 are considered acceptable [21]. Given two cumulative functions F_{exp} and F_{obs}, R^2 is given by

$$R^2 = 1 - \frac{\text{SS}_{\text{res}}}{\text{SS}_{\text{tot}}}, \tag{3}$$

where

$$\begin{aligned} \text{SS}_{\text{tot}} &= \sum \left(\text{obs} - \overline{\text{obs}}\right)^2 \quad \text{residual sum of squares,} \\ \text{SS}_{\text{res}} &= \sum \left(\text{obs} - \text{exp}\right)^2 \quad \text{total sum of squares,} \\ \overline{\text{obs}} &= \frac{1}{n}\sum_{i=1}^{n} \left(\text{obs}_i\right) \quad \text{mean of observed data.} \end{aligned} \tag{4}$$

2.3.2. Statistical Evaluation (Goodness of Fit: Kolmogorov-Smirnov Test). The Kolmogorov-Smirnov (KS) statistics provides a means of testing whether a set of observations comes from a specific continuous distribution. The usual alternative would be the chi-square test. The KS test has at least two major advantages over the chi-square test:

(1) It can be used with small sample sizes, where the validity of the chi-square test would be questionable.

(2) Often it appears to be a more powerful test than the chi-square test for any sample size.

Considering the sizes of the samples selected in this study, which are small, the KS test has been preferred.

The "one-sample" Kolmogorov-Smirnov (KS) test is the most used GOF test to decide if a sample comes from a hypothesized continuous function. It is based on the largest vertical difference between the theoretical and empirical functions. Given two cumulative functions F_{exp} and F_{obs}, the Kolmogorov-Smirnov test statistics (D_{max}) is given by

$$D_{\text{max}} = \max \left| F_{\text{exp}} - F_{\text{obs}} \right|; \tag{5}$$

values less than critical value D_{crt} are considered acceptable. D_{crt} is reported in tables function of sample size n.

2.3.3. Statistical Evaluation (Error Index: Root Mean Square Error, Percent Bias). Several error indices are commonly used in model evaluation. These include mean absolute error (MAE), mean square error (MSE), and root mean square error (RMSE). These indices are valuable because they indicate error in the units (or squared units) of the constituent of interest, which aids in analysis of the results. Root mean square error (RMSE) is one of the commonly used error index statistics; it measures the differences between value predicted by a model or an estimator and the values actually observed. RMSE values of 0 indicate a perfect fit.

Given two cumulative functions F_{exp} and F_{obs}, RMSE [L] is given by

$$\text{RMSE} = \sqrt{\frac{\sum_{i=1}^{n} \left(F_{\text{obs}} - F_{\text{exp}}\right)^2}{n}}. \tag{6}$$

Percent bias (Pbias) measures the average tendency of the expected data to be larger or smaller than their observed data. The optimal value of Pbias is 0. Low values indicate a very good performance. Positive value of Pbias indicates an underestimation bias while positive values indicate an overestimation.

Given two cumulative functions F_{exp} and F_{obs}, Pbias is given by

$$\text{Pbias} = \frac{\sum_{i=1}^{n} \left(F_{\text{obs}} - F_{\text{exp}}\right)}{\sum_{i=1}^{n} \left(F_{\text{obs}}\right)} \times 100. \tag{7}$$

Study step Methodology is described in Figure 2.

3. Results and Discussion

In this research, three rain gauge stations were selected for the analysis. The stations considered are installed in South Italy. Rain gauge has a resolution of 0.2 mm and rain data are registered with a temporal resolution of 1 min. The analysis has been carried on a period of five consecutive years, from 2008 to 2013. Pluviometric data come from the Functional Meteorological Hydrographic and Mareographic Center database of Calabria region. This database contains all rainfall records of all meteorological stations installed throughout the region. Unfortunately, stations with measurement per minute were relatively few and many of them have

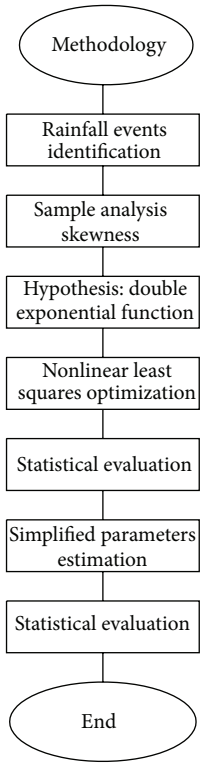

Figure 2: Study steps.

interruptions in measurements resulting in missing data. In addition, the weather stations chosen for this work measure per minute only since 2008 and it has not been possible to obtain more data in previous years. Most recent records were not available because they are still under processing.

However, five years of pluviometric data are considered to be sufficient to identify a significative sample of short duration rainfall events, which are of interest in this paper.

The rainfall series have been processed using a Python code. In specific, subhourly rainfall events were identified by setting a Minimum Interevent Time (MIT) of 15 minutes and discarding events with a volume lower than 8 mm. Under these conditions, a total of 63 subhourly rain events for the three stations were identified and then used in the analysis. The characteristics of selected events are listed in Table 3.

The two parameters of the proposed function, α and β, for each event were determined by using a nonlinear optimization procedure. The proposed parametric function has been fitted on the cumulative rainfall distribution of each event. In order to assess the quality of the fitting error indices and standard regression index were computed. Results of the curve fitting are listed in Table 4.

Results confirm the optimal fitting of the proposed function. Low values of RMSE and high values of R^2 indicate very good performance. In particular, R^2 is always above 0.5 and RMSE exhibits always values near zero. In addition, the Pbias values are considerably low indicating a good agreement between the fitted function and the observations. A graphical

Table 3: Characteristics of selected rainfall events.

ID	Event	Duration (min)	Volume (mm)	I_{max} (mm/h)
		Cortale		
1	2008-10-02 22:20:00	20	9.2	156
2	2008-10-04 10:43:00	53	12.4	84
3	2009-03-20 19:05:00	50	14	60
4	2009-06-22 01:43:00	50	9	72
5	2009-09-24 12:31:00	43	17.4	84
6	2009-12-04 18:55:00	55	10.6	60
7	2010-05-20 16:09:00	60	10.6	72
8	2010-07-25 09:12:00	60	18.4	84
9	2010-09-03 10:51:00	50	13.6	168
10	2010-09-25 13:44:00	58	9.8	48
11	2010-10-14 22:37:00	47	10.8	72
12	2010-11-17 17:17:00	54	9.6	60
13	2010-11-24 17:34:00	39	8.6	60
14	2011-09-20 05:30:00	33	15	108
15	2012-05-27 06:17:00	53	16.8	96
16	2012-09-01 14:31:00	51	13.4	84
17	2012-09-01 15:47:00	51	11.4	120
18	2012-09-04 09:43:00	48	9.2	72
19	2012-10-13 17:07:00	59	19.8	132
20	2012-10-28 13:49:00	42	12.8	84
21	2012-12-10 19:45:00	61	15.2	48
22	2013-01-21 12:41:00	47	8.6	48
23	2013-06-01 23:35:00	43	8.2	48
24	2013-08-10 13:25:00	56	13.2	72
25	2013-09-01 13:12:00	49	14.4	132
26	2013-10-01 05:41:00	46	8.8	60
27	2013-12-01 12:43:00	36	15	168
28	2013-12-02 13:21:00	43	9.6	48
	Mean	48.46	12.33	85.71
	Standard deviation	9.13	3.27	36.47
		Sant'Alessio		
1	2008-10-04 12:59:00	51	10.2	108
2	2009-09-16 07:39:00	59	8.6	48
3	2009-10-02 15:42:00	40	17	120
4	2009-12-05 20:03:00	59	8.2	36
5	2010-09-03 23:10:00	41	16	108
6	2010-09-09 07:16:00	58	20.8	72
7	2010-10-13 13:12:00	38	11.2	96
8	2010-10-13 16:15:00	54	18.4	144
9	2011-06-12 07:54:00	54	8.4	60
10	2011-09-19 10:28:00	22	13.4	204
11	2011-09-21 05:24:00	43	10.6	72
12	2011-12-07 07:21:00	52	14.4	60
13	2013-07-08 11:18:00	39	9.2	96
14	2013-08-10 19:12:00	30	8.6	72
15	2013-08-21 11:31:00	50	28	108
16	2013-08-30 11:00:00	47	19.2	144
17	2013-11-06 03:07:00	42	9.6	72
	Mean	45.82	13.63	95.29
	Standard deviation	10.36	5.58	41.88

Table 3: Continued.

ID	Event	Duration (min)	Volume (mm)	I_{max} (mm/h)
		San Luca		
1	2008-01-23 01:54:00	50	10.2	108
2	2008-05-21 11:04:00	46	15.8	96
3	2008-10-25 13:38:00	47	9.2	48
4	2008-11-15 09:57:00	38	8	60
5	2009-01-13 17:53:00	37	9.6	72
6	2009-04-12 17:03:00	54	20	108
7	2009-09-17 00:18:00	36	9.2	108
8	2009-09-23 09:49:00	49	12.4	96
9	2009-09-25 12:01:00	25	14.4	108
10	2010-09-04 00:08:00	53	8.4	60
11	2010-09-09 13:56:00	26	10	72
12	2010-09-14 14:00:00	51	8	48
13	2010-09-14 21:30:00	57	8.2	72
14	2010-10-03 12:10:00	54	24.2	120
15	2010-11-02 12:57:00	42	13	96
16	2012-11-17 03:36:00	58	16.8	72
17	2013-11-12 15:44:00	50	16.6	84
18	2013-12-03 14:37:00	53	11	72
	Mean	45.88	12.5	83.33
	Standard deviation	9.88	4.62	22.34
	Mean	46.72	12.73	87.61
	Standard deviation	9.79	4.34	34.52

Table 4: Statistical evaluation.

Station	RMSE (mm)	R^2	Pbias (%)
Cortale	0.045 ± 0.019	0.983 ± 0.023	2.601 ± 5.161
Sant'Alessio	0.046 ± 0.021	0.980 ± 0.021	2.154 ± 2.566
San Luca	0.048 ± 0.022	0.980 ± 0.027	3.656 ± 4.673

representation to describe statistics of the computed parameters α and β by indices of dispersion and position is described in Figure 3.

Considering that α is directly related to first derivative of the cumulative rainfall distribution, which indicates peakedness of the sample, the large value of the standard deviation of α could be related to high value of the standard deviation of the kurtosis for the selected events. Also β, which is a location parameter, exhibits large values of standard deviation. The meaning of β has been further investigated. In particular, the analysis has revealed that β is directly related to x-coordinate of the centroid X_g of the rain distribution.

As shown in Figure 4, the relationship between β and X_g can be explained by two types of regression: a linear regression and a bisector regression. The linear regression achieves slightly better results than the bisector, which also gives a sufficiently accurate description of the relation.

In order to assess the suitability of the proposed exponential function, the Kolmogorov-Smirnov one-sample test (KS test) has been used. The KS test is used to test whether a sample comes from a specific distribution. The test has been performed on all 63 selected events by comparing the value of the Kolmogorov-Smirnov test statistic D_{max} with the critical value D_{crit} obtained by tables already present in the literature by assuming a 5% of level of significance. The KS test has been carried out by using the parameters α and β already calculated with the NLS optimization described in the previous sections. Results of the KS test are reported in Figure 5.

As it can be seen from Figure 5, results of the KS test confirm that selected rainfall events come from the exponential distribution function proposed in this study. Only for two rain events $D_{max} > D_{crit}$.

In general, the definition of parameters by using the NLS optimization guarantees good results in terms of fitting. This is confirmed by the statistical criterion described above. Although, especially for practical applications, the NLS optimization could be complex and time consuming, in such practical cases parameters could be computed by using other statistical procedures, which are easy to implement.

It is possible to observe that function (2) closely resembles the Gumbel distribution function, where $F(x)$ represents the exceedance probability. In statistics parameters α and β may be computed by using several methods; the most common are maximum likelihood estimation (MLE) and method of moments. The MLE could be more accurate in the estimation of parameters, although the mathematical computation is very complex. On the other hand, the method of moments is fairly simple and allows calculating easily the parameters. For these reasons, in this study, the method of moments has been used.

α and β could be calculated by using the method of moments as follows:

$$\alpha = \frac{1.28255}{\sigma},$$
$$\beta = \overline{X} - 0.450 \cdot \sigma, \tag{8}$$

where $\overline{X}$ and σ are, respectively, the mean value and the standard deviation of x distribution.

Consider the assumptions:

$$F = \frac{r(t)}{r_{tot}},$$
$$x = t, \tag{9}$$

where $r(t)$ is the rainfall depth at time t, r_{tot} is the total rainfall depth of the event, and t is the casual variable x; for every event in each station the parameters α and β have been calculated by using (8). A graphical representation to describe the statistics of the computed parameters α and β by indices of dispersion and position is described in Figure 6 while results of the curve fitting are listed in Table 5.

Values of RMSE and R^2 indicate a deterioration in terms of quality of fitting when using α and β computed by using (8). In particular, R^2 exhibits a mean value of 0.771 which is still acceptable. The RMSE values are three times the values computed with NLS. However, results are still acceptable for practical applications where the degree of precision may be less accurate.

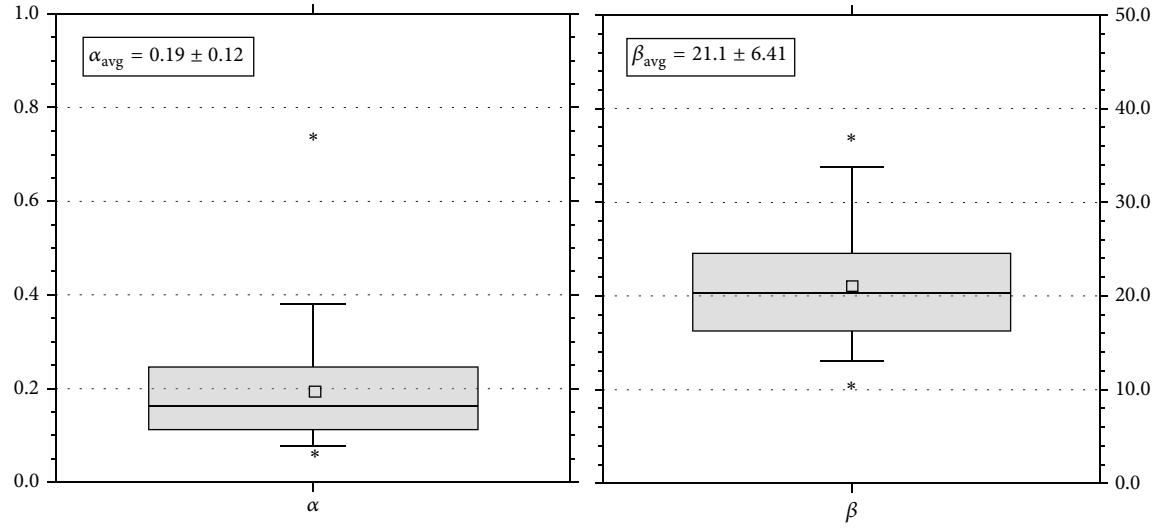

Figure 3: Statistics of the computed parameters α and β.

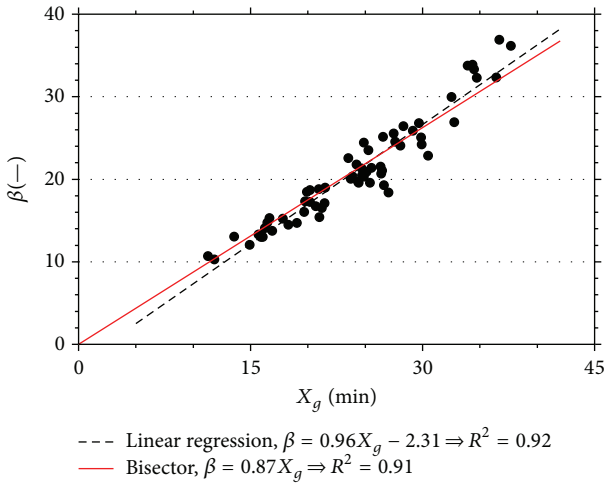

Figure 4: Relation between β and X_g.

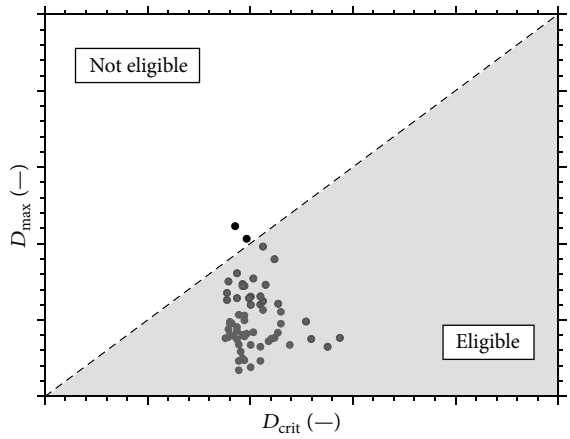

Figure 5: KS test for fitted exponential function.

Table 5: Statistical evaluation.

Station	RMSE (mm)	R^2	Pbias (%)
Cortale	0.151 ± 0.082	0.778 ± 0.269	−9.911 ± 29.412
Sant'Alessio	0.144 ± 0.070	0.811 ± 0.241	−6.941 ± 25.683
San Luca	0.180 ± 0.075	0.724 ± 0.214	−17.282 ± 30.184

In addition, the KS test has been performed. Results of the KS test are shown in Figure 7.

Results of the KS test confirm the nonoptimal performance of the proposed function when using parameters α and β computed by using (8).

4. Conclusion

This paper intends to provide a contribution on defining a "design storm" for urban drainage system. The main idea is based on the definition of a parametric cumulative function validated with an exhaustive evaluation of both model scientific basis and performance. The proposed CRF has been fitted on the cumulative rainfall distribution of each event. In order to assess the quality of the fitting RMSE, R^2 and Pbias were computed. The results highlight very good performances with low values of RMSE ranging from 0.045 ÷ 0.048 and high values of R^2 ranging from 0.980 ÷ 0.983. Finally, considering the similarity of the proposed CRF with the Gumbel function, a practical and expeditious method to assess the parameters of the CRF has been proposed. In this case, the values of RMSE and R^2 indicate a deterioration in terms of quality of fitting; however, results are still acceptable for the practical application. Further studies will go in the direction of a better definition of the parameters to allow a direct practical application of the CRF. In particular, the approach will be strengthened with the analysis of more pluviometric stations, in different countries and under different climate conditions. In addition to this, a more detailed study on the physical meaning of parameters α and β will be conducted.

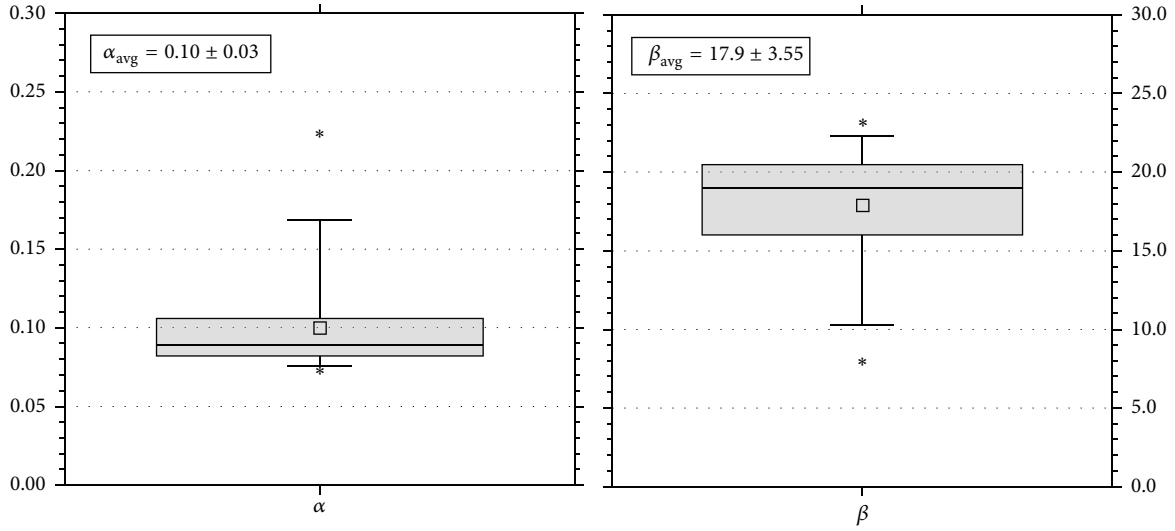

Figure 6: Statistics of the computed parameters α and β.

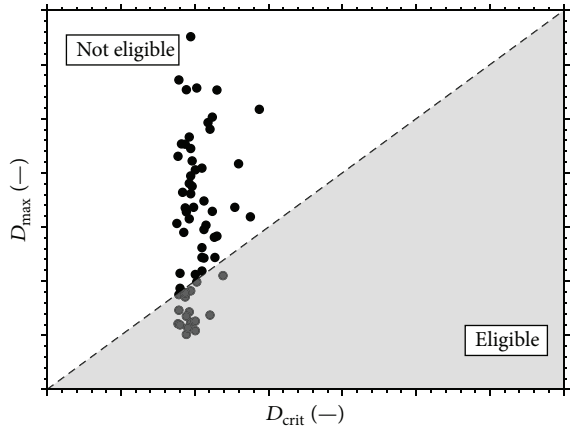

Figure 7: KS test for direct formulation.

Conflict of Interests

The authors declare that there is no conflict of interests regarding the publication of this paper.

Acknowledgments

This research study was cofunded by the Italian National Operative Project (PON)-Research and Competitiveness for the Convergence Regions 2007/2013-I Axis "Support to structural changes" operative objective 4.1.1.1 "Scientific-technological generators of transformation processes of the productive system and creation of new sectors" Action II: "Interventions to support industrial research."

References

[1] M. Llasat-Botija, M. C. Llasat, and L. Lopez, "Natural hazards and the press in the Western Mediterranean region," *Advances in Geosciences*, vol. 12, pp. 81–85, 2007.

[2] A. Tarpanelli, M. Franchini, L. Brocca, S. Camici, F. Melone, and T. Moramarco, "A simple approach for stochastic generation of spatial rainfall patterns," *Journal of Hydrology*, vol. 472-473, pp. 63–76, 2012.

[3] B. Casati, L. J. Wilson, D. B. Stephenson et al., "Forecast verification: current status and future directions," *Meteorological Applications*, vol. 15, no. 1, pp. 3–18, 2008.

[4] M. W. Rotach, P. Ambrosetti, C. Appenzeller et al., "MAP D-PHASE: real-time demonstration of weather forecast quality in the Alpine region," *Bulletin of the American Meteorological Society*, vol. 90, pp. 1321–1336, 2009.

[5] J. Riesco Martín, M. Mora García, F. de Pablo Dávila, and L. Rivas Soriano, "Severe rainfall events over the western Mediterranean Sea: a case study," *Atmospheric Research*, vol. 127, pp. 47–63, 2013.

[6] C. R. Lloyd, "The temporal distribution of Amazonian rainfall and its implications for forest interception," *Quarterly Journal of the Royal Meteorological Society*, vol. 116, no. 496, pp. 1487–1494, 1990.

[7] Y. Gyasi-Agyei and C. S. Melching, "Modelling the dependence and internal structure of storm events for continuous rainfall simulation," *Journal of Hydrology*, vol. 464-465, pp. 249–261, 2012.

[8] N. N. R. K. Aryal, H. Furumai, F. Nakajima, and H. K. P. K. Jinadasa, "The role of inter-event time definition and recovery of initial/depression loss for the accuracy in quantitative simulations of highway runoff," *Urban Water Journal*, vol. 4, no. 1, pp. 53–58, 2007.

[9] L. J. Bracken, N. J. Cox, and J. Shannon, "The relationship between rainfall inputs and flood generation in south-east Spain," *Hydrological Processes*, vol. 22, no. 5, pp. 683–696, 2008.

[10] S. Federico, E. Avolio, L. Pasqualoni, and C. Bellecci, "Atmospheric patterns for heavy rain events in Calabria," *Natural Hazards and Earth System Science*, vol. 8, no. 5, pp. 1173–1186, 2008.

[11] A. Burton, C. G. Kilsby, H. J. Fowler, P. S. P. Cowpertwait, and P. E. O'Connell, "RainSim: a spatial—temporal stochastic rainfall modelling system," *Environmental Modelling and Software*, vol. 23, no. 12, pp. 1356–1369, 2008.

[12] P. S. P. Cowpertwait, "A continuous stochastic disaggregation model of rainfall for peak flow simulation in urban hydrologic systems," *Research Letters in the Information and Mathematical Sciences*, vol. 2, pp. 81–88, 2001.

[13] R. E. Chandler and H. S. Wheater, "Analysis of rainfall variability using generalized linear models: a case study from the west of Ireland," *Water Resources Research*, vol. 38, no. 10, pp. 101–1011, 2002.

[14] P. S. P. Cowpertwait, P. E. O'Connell, A. V. Metcalfe, and J. A. Mawdsley, "Stochastic point process modelling of rainfall. I. Single-site fitting and validation," *Journal of Hydrology*, vol. 175, no. 1–4, pp. 17–46, 1996.

[15] Y. Lu and X. S. Qin, "Multisite rainfall downscaling and disaggregation in a tropical urban area," *Journal of Hydrology*, vol. 509, pp. 55–65, 2014.

[16] P. S. P. Cowpertwait, "A spatial–temporal point process model of rainfall for the Thames catchment, UK," *Journal of Hydrology*, vol. 330, no. 3-4, pp. 586–595, 2006.

[17] A. Ritter and R. Muñoz-Carpena, "Performance evaluation of hydrological models: statistical significance for reducing subjectivity in goodness-of-fit assessments," *Journal of Hydrology*, vol. 480, pp. 33–45, 2013.

[18] D. R. Legates and G. J. McCabe Jr., "Evaluating the use of 'goodness-of-fit' measures in hydrologic and hydroclimatic model validation," *Water Resources Research*, vol. 35, no. 1, pp. 233–241, 1999.

[19] B. Schaefli and H. V. Gupta, "Do Nash values have value?" *Hydrological Processes*, vol. 21, no. 15, pp. 2075–2080, 2007.

[20] A. H. Nury, M. Koch, and J. B. Alam, "Analysis and prediction of time series variations of rainfall in north-eastern Bangladesh," *British Journal of Applied Science & Technology*, vol. 4, no. 11, pp. 1644–1656, 2014.

[21] D. N. Moriasi, J. G. Arnold, M. W. van Liew, R. L. Bingner, R. D. Harmel, and T. L. Veith, "Model evaluation guidelines for systematic quantification of accuracy in watershed simulations," *Transactions of the ASABE*, vol. 50, no. 3, pp. 885–900, 2007.

[22] P. Krause, D. P. Boyle, and F. Bäse, "Comparison of different efficiency criteria for hydrological model assessment," *Advances in Geosciences*, vol. 5, pp. 89–97, 2005.

[23] S. Grimaldi, "Linear parametric models applied to daily hydrological series," *Journal of Hydrologic Engineering*, vol. 9, no. 5, pp. 383–391, 2004.

[24] C. W. Dawson, R. J. Abrahart, and L. M. See, "HydroTest: a web-based toolbox of evaluation metrics for the standardised assessment of hydrological forecasts," *Environmental Modelling and Software*, vol. 22, no. 7, pp. 1034–1052, 2007.

[25] M. Carbone, M. Turco, G. Brunetti, and P. Piro, "Minimum inter-event time to identify independent rainfall events in Urban catchment scale," *Advanced Materials Research*, vol. 1073-1076, pp. 1630–1633, 2014.

[26] S. Dan'azumi, S. Shamsudin, and A. Aris, "Modeling the distribution of rainfall intensity using hourly data," *American Journal of Environmental Sciences*, vol. 6, no. 3, pp. 238–243, 2010.

[27] R. Mínguez, F. J. Méndez, C. Izaguirre, M. Menéndez, and I. J. Losada, "Pseudo-optimal parameter selection of non-stationary generalized extreme value models for environmental variables," *Environmental Modelling and Software*, vol. 25, no. 12, pp. 1592–1607, 2010.

Carbone, M., **Turco, M.**, Brunetti, G., Piro, P. (2015)

Minimum Inter-event Time to identify independent rainfall events in urban catchment scale

Advanced Materials Research

Advanced Materials Research Vols. 1073-1076 (2015) pp 1630-1633

doi:10.4028/www.scientific.net/AMR.1073-1076.1630

Minimum Inter-event Time to identify independent rainfall events in urban catchment scale

Marco Carbone[1,a], Michele Turco[1,b], Giuseppe Brunetti[1,c], Patrizia Piro[1,d]

[1]Department of Civil Engineering, University of Calabria, Italy

[a]marco.carbone@unical.it, [b]michele_turco@yahoo.it, [c]giusep.bru@gmail.com
[d]patrizia.piro@unical.it

Keywords: Rainfall, Inter-event time, Design, Independent events.

Abstract. For many hydrologic analyses, planning or design problems, reliable rainfall estimates are necessary. For this reason, an accurate estimation of storm event properties is central to continuous simulation of rainfall. Rainfall is generally noted as single events or storms where the beginning and the end are defined by rainless of particular size duration called Minimum Inter-event Time (MIT). Starting from a critical study of the state of the art, this paper intends to investigate the definition of MIT for rainfall events shorter than an hour that, on an urban scale, are the most critical for designers, planners and operators of urban drainage system. All event characteristics such as depth and mean rain rate, are influenced by the choice of the value of MIT. This paper reviews the range of approaches used in literature and after this, based on a year of pluviograph records on an urban catchment, proposes a value of MIT according to catchment network entry time.

Introduction

In urban drainage system, short-duration rainfall events represent the main elements to be investigated in order to start critical studies on urban drainage systems.

Climatic changes of the last decades have radically changed the rainfall regime in terms of temporal and spatial scale. In this perspective, research was mainly driven towards the study of statistical properties of daily long series of rainfall depth from which emerged an increase of extreme rainfall events frequency [1]. To plan or design various hydraulic structures, extreme rainfall for a given return period is required. In particular, hourly rainfall events or shorter are necessary for the design of drainage systems in urban catchments usually characterized by fast response [2]. For these reasons it is necessary to characterize rainfall events, in particular regarding their duration. Planners and designers of urban drainage systems often select rainfall events for the design of drainage infrastructures. These choices significantly affect the sizing of the infrastructures and for these reasons are fundamental.

Most of the literature papers, summarized in Table 1, that present rain event data and that report how the events were selected, identify a fixed rainless period, MIT, required to be reached or exceeded before and after each event. In 1990 Lloyd assumed a 3 h inter-event gap in a study of forest interception processes; Aryal et al. [3] showed that depression storage recovered fully in about 8 h without rain, and so they adopted MIT = 8 h for rain event identification; also they hypothesized that the MIT changes between winter and summer. Bracken et al. [4] used MIT = 12 h in order that the ground could dry between runoff events, reducing the impact of antecedent soil wetness on event runoff; Gyasi-Agyei and Melching [5] assumed a 0.25 days (6 h) of MIT to separate rainfall event in a study for modelling the dependence and internal structure of storm events.

The focus of this paper is to give an appropriate methodology to correctly identify the MIT for solving problems in urban catchment scale.

The paper is structured into three sections: Methodology shows the experimental site and the working assumptions made; Results describes the results; finally in the Conclusion section the working assumptions made before are discussed according with results.

Methodology

Experimental site. This study proposes a methodology to set a correct MIT for rainfall events in urban catchment scale. Pluviograph records from Liguori Catchment (LC) was chosen. LC is situated in Cosenza, a city of south Italy; it has an area of 414 ha and a population of about 50,000 inhabitants. 48% of the catchment area is strongly urbanized with high imperviousness, but the rest (almost 52%) is a pervious area, covered mainly by vegetation. Combined sewer overflows are discharged into the river Crati during intensive rain events [6]. Based on more than 100 records, registered between 1996 and 2014 on LC, the mean annual rainfall is 780 mm and the mean annual flow volume, estimated on the impervious area, is approximately 1040 mm (volume per unit area). The average of the annual base flow volume (sanitary water) and the mean annual runoff were also measured, which are respectively 480 mm and 560 mm. Several studies have been conducted on this area in the past, focusing the attention on the quality and quantity of the water drained in the catchment [7, 8, 9, 10, 11].

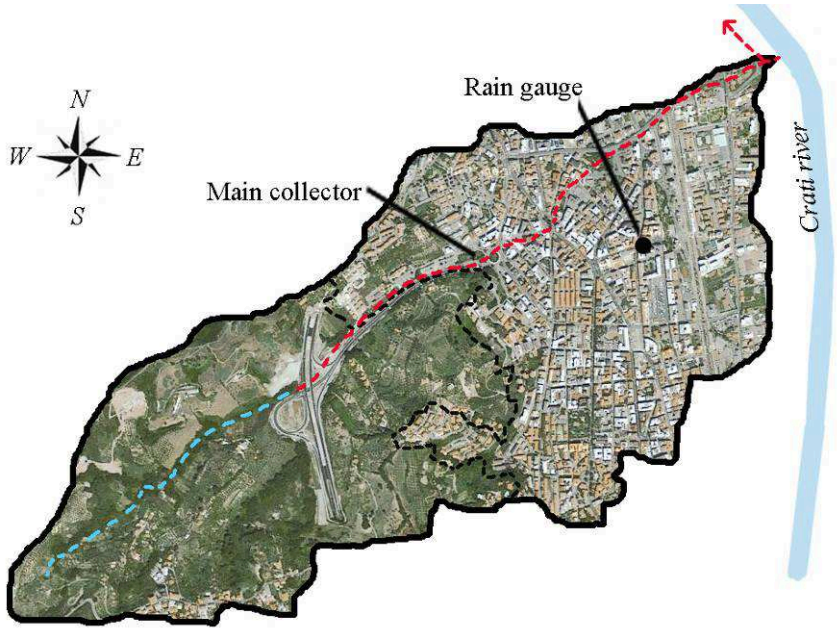

Fig. 1. Liguori Catchment

Work hypothesis. Inter-event time is defined as the time between the end of a storm event and the beginning of the next.

The selection of a MIT precise value depends on the study characteristics to be performed and on the features of the event to be considered. In table 1 are summarized the typical range of rain MIT in literature.

Table 1. Range of rain MIT in literature

MIT	Scope of the work	Reference
3 h	Forest interception processes	Lloyd 1990
0.25 days (6 h)	Dependence and internal structure of storm events	Yeboah et al. (2012)
8 h	Depression storage recovered fully	Aryal et al. (2007)
12 h	Dry ground between runoff events	Bracken et al. (2008)

In urban areas, rains that deserve special attention are those of short duration. Ulanski and Garstang [12] showed that higher rain depths were delivered in Florida by once-daily convective events than from multi-shower days having the same total rain duration. They reordered multiple events occurring on the same day if they were separated by 15 min without rain.

If we therefore relates to short duration events (shorter than 1 h) as critical events, according with above consideration, and considering the expression given by Gyasi-Agyei and Melching (2012) (MIT = 0.25 period), a correct value of MIT in urban areas could be 15 min, as time separation gap between a rainfall event and next. In order to identify independent rainfall events, it was necessary established a volume threshold to below which rainfall events were not taken into account. Then, through a numerical code implementation, MIT value was varied according with the critical event duration (one hour). MIT variation identified a number of significant events showed in the next section in Table 2.

The working hypothesis are based on finding the minimum mean event volume, computed for a specific MIT, assuming this as the ideal condition to identify independent events.

Results

As said before, on urban scale heavy rains are those with duration shorter than one hour, for this reason it was decided, in the selection of independent events, to range the value of MIT from 2 min to 30 min by setting a threshold of 3 mm in volume.

The analysis has been performed with one year rainfall data (September 2013-September 2014) measured by a tipping-bucket rain gauge located in the LC. The observed data indicate that the number of events decreases when the MIT increases (Table 2). Obviously, the choice of the volume threshold can condition both the number of events result from MIT both the events characteristics.

Table 2. Results

Value of MIT *(min)*	N. of events > 3 mm	Mean event volume *(mm)*
2	45	5.04
5	48	4.65
10	33	4.61
12	34	4.58
15	33	4.61
20	29	4.82
30	20	5.18

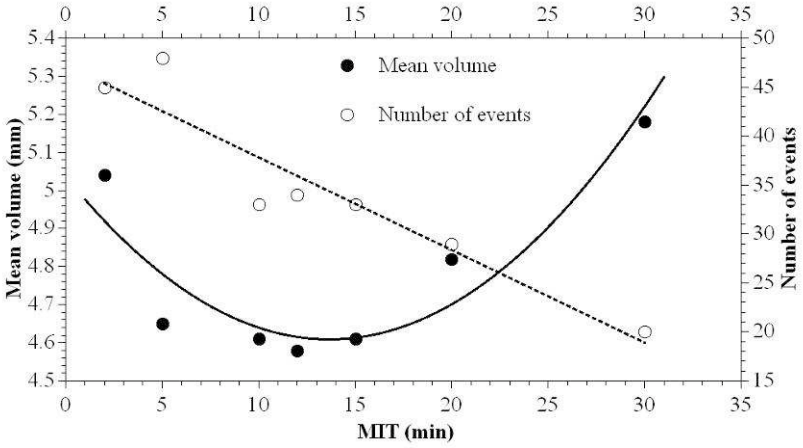

Another important factor is the individuation of the minimum in the mean event volume trend, in particular, smaller values are observed in correspondence with MIT values ranging from 10 to 15 min.

Conclusion

Results show that the MIT values substantially changes both the number and the characteristics of rain events identified in a pluviograph record. According to the literature, the trend of independent events selected decreases while MIT increases. Considering short duration events, an acceptable value of MIT can be 15 min. This is supported by table 2 where optimal point could be between 10 min and 15 min.

According to the literature, urban catchment entry time is generally small, with values ranging between 5 and 15 min [13]; then it is correct to consider MIT optimal point between the proposed ranges.

Further studies will be performed using the information from other rain gauges, checking the sensitivity of the MIT compared to other characteristic parameters of the event (intensity, duration, etc.).

Acknowledgements

The study was co-funding from the Italian National Operative Project (PON) - Research and Competitiveness for the convergence regions 2007/2013 - I Axis "*Support to structural changes*" operative objective 4.1.1.1. "*Scientific-technological generators of transformation processes of the productive system and creation of new sectors*" Action II: "*Interventions to support industrial research*".

References

[1] M. Haylock, N. Nicholls, Trends in extreme rainfall indices for an updated high quality data set for Australia, 1910–1998, International Journal of Climatology 20, pp 1533–1541 (2000).

[2] G.T. Aronica, G. Freni, Estimation of sub-hourly DDF curves using scaling properties of hourly and sub-hourly data at partially gauged site, Atmospheric Research 77, pp. 114-123 (2005).

[3] R.K. Aryal, H. Furumai, F. Nakajima, H.K.P.K Jinadasa, The role of inter-event time definition and recovery of initial/depression loss for the accuracy in quantitative simulations of highway runoff, Urban Water Journal 4, pp. 53–58 (2007).

[4] L.J. Bracken, N.J. Cox, J. Shannon, The relationship between rainfall inputs and flood generation in south-east Spain, Hydrological Processes 22, pp. 683–696. (2008).

[5] Y. Gyasi-Agyei, C. S. Melching, Modelling the dependence and internal structure of storm events for continuous rainfall simulation, Journal of Hydrology, pp. 249-261. (2012).

[6] P. Piro, M. Carbone and J.J. Sansalone, Delivery and Frequency Distributions of Combined Wastewater Collection System Wet and Dry Weather Loads, Water Environment Research 84 pp 65-75 (2012).

[7] P. Piro, M. Carbone, G. Garofalo and J.J. Sansalone, Size Distribution of Wet Weather and Dry Weather Particulate Matter Entrained in Combined Flows from an Urbanizing Sewershed, Water Air and Soil Pollution 206 pp 83-94 (2010)

[8] P. Piro, M. Carbone , G. Garofalo and J.J. Sansalone, Management of CSOs based on observations from the urbanized Liguori catchment of Cosenza, Italy, Water Science & Technology, 61(1), pp. 135-143 (2010).

[9] P. Piro, M. Carbone, G. Garofalo, Innovative monitoring of combined sewer overflow (CSO) quality in the Liguori catchnment (Cosenza, Italy), Water Quality Research Journal of Canada, 47(2), pp. 178-185 (2012).

[10] M. Carbone, G. Garofalo, G. Nigro, P. Piro, A conceptual model for predicting hydraulic behaviour of a green roof, Procedia Engineering, pp. 266-274 (2014).

[11] M. Carbone, M. Turco, G. Nigro, P. Piro, Modeling of hydraulic behaviour of green roof in catchment scale, International Multidisciplinary Scientific GeoConferences SGEM 2014, Albena, Bulgaria, pp. 471-478 (2014).

[12] S.L. Ulanski, M. Garstang, The role of surface divergence and vorticity in the life cycle of convective rainfall Part 1. Observation and analysis, Journal of the Atmospheric Sciences 35, pp. 1047–1062, (1978).

[13] S. Artina, G. Calenda, F. Calomino, G. La Loggia, C. Modica, A. Paoletti, S. Papiri, G. Rasulo, P. Veltri, Sistemi di Fognatura. Manuale di Progettazione, HOEPLI, Milano, (1997).

Carbone, M., **Turco, M.**, Nigro, G., Piro, P. (2014)

Modeling of hydraulic behaviour of green roof in catchment scale

International Multidisciplinary Scientific GeoConferences SGEM Albena, Bulgaria

MODELING OF HYDRAULIC BEHAVIOUR OF GREEN ROOF IN CATCHMENT SCALE

Dr. Marco Carbone[1]

Dr. Michele Turco[1]

Dr. Gennaro Nigro[1]

Prof. Dr. Patrizia Piro[1]

[1]University of Calabria – Dep. of Civil Engineering, **Italy**

ABSTRACT

In the last decades the increase of urbanization has drastically modified the hydrological cycle; in particular, while the extension of impervious surface has increased the runoff and hence, the potential for flooding, the reduction of green areas has caused the formation of urban heat island and consequently, the increase of the energy demand. Another negative effect of urbanization has been a severe decline of biodiversity. In this context a comprehensive land planning and engineering design approach with a goal of maintaining are needed to restore pre-development hydrologic regime of urban and developing watersheds. At the University of Calabria GIs were designed and built to develop a sustainable approach example of university campus; the project is called "Urban Water Park". The park consists of a green roof, a permeable pavement and a biofiltration system. From the hydraulic point of view the parameters retrieved are rainfall, influent and effluent flow rates, humidity and water content in the soil substrate. For each facility the main pollutant (eg. TSS, heavy metal, PAH, COD) are monitored. From a thermo-physical point of view temperature and solar parameters are measured. Green roof techniques are increasingly becoming popular among the Low Impact Developments (LIDs) techniques for urban runoff management. Of particular interest is the rooftop runoff management on large time scales (eg. annual). Several studies have shown that green roofs allow to effectively control the generation of surface runoff, significantly reducing the overall discharged volumes (40% to 80%) as well as slowing the contribution to the urban drainage network.

This study proposes a conceptual model based on the SWMM model to predict the hydrological benefit of a green roof in a large watershed for daily simulation. The model idealizes the green roof as a system consisting of three individual components in series, each characterized by a specific process hydrological and hydraulic. A mass balance equation is applied to each block, taking into account the specific physical phenomena occurring in each module, and the flow is governed by Richards equations. The model is validated with the data observed from the monitoring campaign (climatic, thermal-hydraulic parameters) of a full-scale green roof characterized by different drainage layers and vegetation species.

This study aims to provide quantitative information about the hydraulic performance of green roofs in large watershed for daily series of rainfall, and to identify the most sensitive parameters, such as retained volume, runoff delay for modeling the hydraulic behaviour. The results show that the ability of water regulation is a function of weather-climatic conditions, plant species and green roof design characteristics.

Keywords: SUDs, stormwater, green roofs, runoff, conceptual model, monitoring, water storage.

1. INTRODUCTION

Climate change and urbanization increase have promote, in recent years, critical situation in urban areas such as flood phenomena. This kind of phenomena depend specially from the urban drainage system inefficiency. Flood in urban areas can occur due to different aspects: sewer system type (separated or mixed sewers), urban drainage system design. Additionally studies also indicate that in certain areas global warming may caused increased frequency of intense precipitation events which will also lead to increased urban flooding.

Scope of this work is permeable surface increasing in urban areas using green-roof to control runoff. Green roof is a new technology that mitigates urban runoff, decreases temperature and provides an eco-friendly space [1], [2], [3], [4], [5]. Several Research have been conducted on run-off mitigation by green roof [6], [7], [8]. In the literature several study have assessed the hydrological performances of green roof in terms of volume reduction with values range between 45% to 55% of annual rainfall volume [9]. To assess the performance of a green roof in mitigating flooding, quantitative analysis of these parameters is essential [10].

The focus of this paper is to demonstrate the benefit of a green roof in terms of volume reduction on an urban catchment (situated in Cosenza, Calabria region south of Italy) using a conceptual model basing on Storm Water Management Model (SWMM). The model idealizes the green roof as a system consisting of three individual components in series, each characterized by a specific process hydrological and hydraulic. The paper is structured into sections: in section 2, Methodology, is presented the experimental site and the model used in the work; in section 3, Results and discussion, the results of model simulations, are described; in section 4, Conclusion, the benefit of green roof to the flood problem and the future development are described.

2. METHODOLOGY

Study Area

The Liguori Catchment (LC) is situated in Cosenza, a city of south Italy; it has an area of 414 ha and a population of 50,000 inhabitants. Forty-eight per cent of the catchment area is strongly urbanized with high imperviousness, but the rest (almost 52%) is occupied by a pervious area, covered mainly by vegetation. Combined sewer overflows are discharged into the river Crati during intensive rain events [11]. Based on more than 100 runoff events, recorded between 1996 and 2013 on LC, the mean annual rainfall is 780 mm and the mean annual flow volume, estimated on the impervious area, is approximately 1040 mm (volume per unit area). The average of the annual base flow volume (sanitary water) and the mean annual runoff were also measured, which are respectively 480 mm and 560 mm. Several studies have been conducted on this area in the past, focusing the attention on the quality and quantity of the water drained in the catchment [12], [13], [14]. Study area has been chosen in the city of Cosenza: in particular the area including mainly street as Corso Italia street, Via Nicola Serra and Via Riccardo Misasi has been chosen.

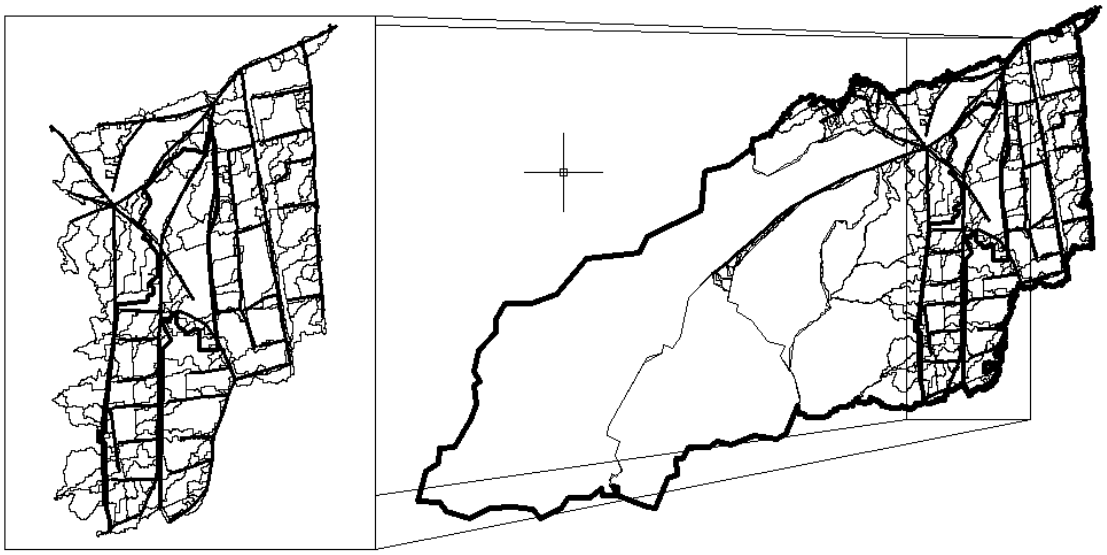

Figure 1 Liguori Catchment

Experimental model

Methods used in the literature to assess environmental benefits and hydrological performance (in terms of total volume reduction) of a green roof system are different and range from simple empirical relationships to schemas of conceptual modeling and physically based models. In this work it has been used a conceptual model that idealizes the green roof as a system consisting of three individual components in series, each characterized by a specific hydrological and hydraulic process [15]. For each block mass balance equation is applied; that takes into account physical phenomena of the specific component [15]. The goal is the modeling hydrological flows in relation to climatic conditions, basic technological components and geometric characteristics of green roof systems (substrate thickness, material, type and density of vegetation) with the aim to adapt the model to a specific soil stratigraphy designed for green roof systems. Almost all numerical simulations of infiltration processes in unsaturated porous medium are based on the classical Richards equation. The θ-based form of this equation is written as:

$$\frac{\partial \theta}{\partial t} - \nabla \cdot D(\theta) \nabla \theta - \frac{\partial K}{\partial z} = 0 \qquad \theta\text{-based} \qquad (1)$$

where θ is the volumetric soil water content, $D(\theta)$ is the unsaturated soil diffusivity [L^2/T], K is the unsaturated hydraulic conductivity [L/T], z represents the vertical dimension assumed positive upward, and porous medium is assumed isotropic. Equation (1) is non-linear, so it's not possible to obtain an analytical solution, except for special cases. This implies that numerical solutions for unsaturated flow are obtained through mathematical approximations.

SWMM Implementation

To estimate the good behavior of green roof, conceptual model has been implemented through use of Storm Water Management Model (SWMM) software using their computation models that SWMM has got. With this approach green roof in SWMM can

be modeled as a "subcatchment" linked to two different blocks in sequence, "storage units" then to the final "outlet"; the subcatchment element represents the surface schematization of the green roof while the storage units represents respectively soil layer and storage layer. The links between subcatchment, storage units and final outlet have been reproduced by outlet elements.

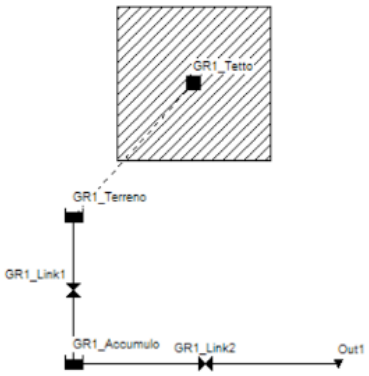

Figure 2 SWMM schematization of a green roof

Soil and storage layer of the green roof used in this work are characterized as follows:

Thickness (m)	0.15
Porosity	0.452
Field capacity	0.3
Conductivity (cm/h)	232.41
Soil retention curve slope	0.15
Wilting point	0.043
Van Genuchten parameter 'm'	0.627

Table 1 Soil layer characterization

Percentage of accumulation area compared to the total (%)	60
Weir height (cm)	2
Effluent coefficient	0.4

Table 2 Storage layer characterization

3. RESULTS AND DISCUSSION

To evaluate the benefit of green roof on the runoff control, three different scenarios have been tested on a portion of the LC. Scenario 1 consider green roof implementation equal to 15% of the total study area; scenario 2 consider green roof implementation equal to 20% of the total study area; scenario 3 consider green roof implementation

equal to 25% of the total study area. The results obtained by simulating different scenarios are shown in the following figures.

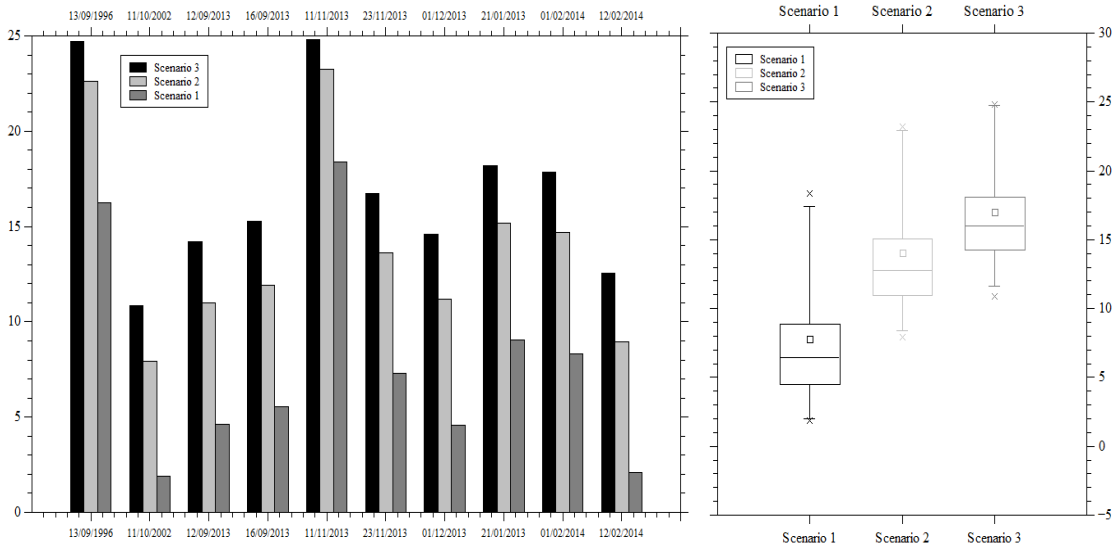

Figure 3 Flow volume reduction for each simulated event

In addition to bar plot, to describe variability of results a box plot has been used. This kink of plot is based on “quantile” definition. While providing less information than cumulative distribution function, this plot allows to describe the variable in a concise and it is very useful to compare subsets of data. The idea is to identify with a "box" the central observations and with the 'whiskers' or tails coming out from the box the most extreme observations. The "box" is bounded by the first and third quartile, $q_{1/4}$ and $q_{3/4}$, and internally divided by the median $q_{1/2}$. The segments, the "whiskers", are delimited by the minimum and maximum values. The middle square represents the average value. The “star value” (x) represents the outliers. Moreover, it shows the effects of each scenario on the runoff, in terms of volume reduction in percent. For all events, the analysis of figure above clearly shows that the increase of permeable surfaces, obtained using green roofs, causes the reduction of outflow volumes and this reduction tends to increase as green roof implementation increase.

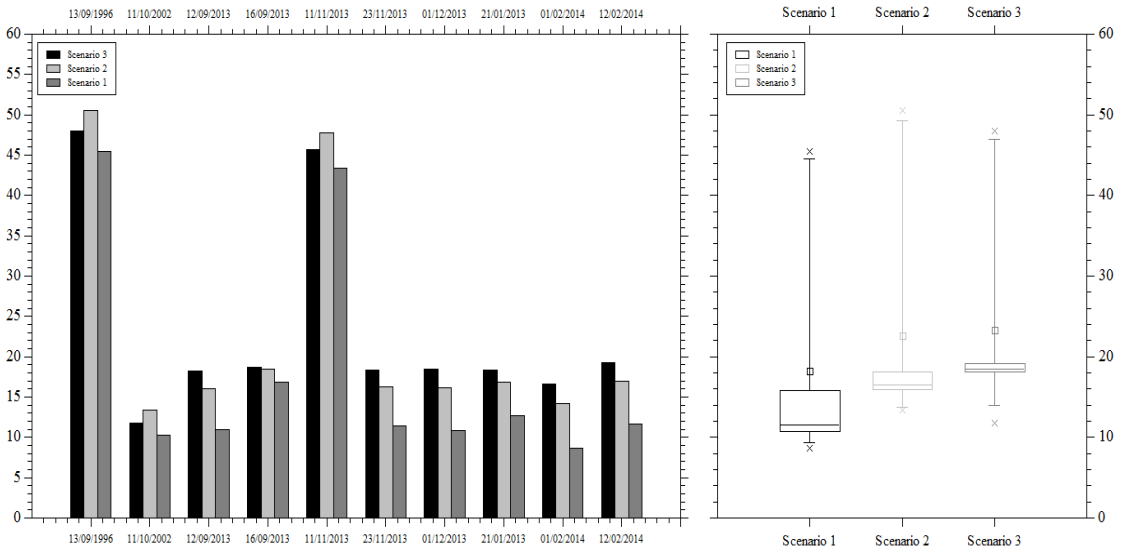

Figure 4 Peak Flow reduction for each simulated event

Figure 4 shows that on average, peak reduction tends to increase as green roof implementation increase, but results are very distributed; this is ascertained by the fact that the "whiskers" are very elongated. For these reasons distribution values it is more asymmetrical and unbalanced. Moreover, it shows the effects of each scenario on the runoff, in terms of peak reduction in percent. For all events, the analysis of figure above clearly shows that the increase of permeable surfaces, obtained using green roofs, causes the reduction of peak flow.

It should be noted that all simulations were carried out considering the green roof made up essentially of a soil whose characteristics are sandy type. This kind of soil is characterized by having low retention capacity; for this reason, results are to be understood rounded down compared to most advanced technological solutions as in the case of Unical installation.

Results shown above confirm that green roof implementation in highly urbanized catchment can be a good solution to reduce flow volume reduction and peak flow for medium-intense rainfall. That can helps sewer system when critical condition arise (flood, overflow). In particular results confirms that benefits in terms of flow volume reduction are appreciable compare to result in terms of peak flow reduction; an increment of green roof in terms of percentile on the catchment is directly connected to flow reduction in the three scenarios.

4. CONCLUSION

The aim of this work was to provide guidance to different approaches for flood management in urban area, highlighting the role and the specific utility of individual interventions. In particular, it has been demonstrated that distributed approach, consisting of green roof implementation on a strongly urbanized catchment, can give answers to the efficient management of flow volumes, due to extreme events. Green roof implementation is an effective storm water best-management practice for reducing runoff from roof surfaces in urban areas by harvesting rainfall and reducing urban flooding. This approach is preferable to the classic storm water solutions for runoff control (storm water tanks) primarily because the classic solutions needs more space in

urban areas then because the results in terms of peak and volume reduction are satisfactory and finally biodiversity can be improved.

REFERENCES

[1] Stovin, V., Dunett, N., Hallam, A., Green roofs-getting sustainable drainage off the ground, In: 6th International Conference of Sustainable Technologies and Strategies in Urban Water Management (Novatech 2007), Lyon, France, pp 11-18. 2007

[2] Yang, J., Yu, Q., Gong, P., Quantifying air pollution removal by green roofs in Chicago, Atmospheric Environment 42 (31), pp 7266-7273. 2008

[3] Berndtsson, J.C., Bengtsson, L., Jinno, K., Runoff water quality from intensive and extensive vegetated roofs, Ecological Engineering 35 (3), 369-380. 2009

[4] Teemusk, A., Mander, U., Green roof potential to reduce temperature fluctuations of a roof membrane: a case study from Estonia, Building and Environment 44 (3), 643-650. 2009

[5] Castleton, H.F., Stovin, V., Beck, S.B.M., Davison, J.B., Green roofs; building energy savings and the potential for retrofit, Energy and Buildings 42, 1582-1591. 2010

[6] Beattie, D., Berghage, R., Green roof media characteristics, The Basic, 2-4. 2004

[7] Carter, T., Rasmussen, T., Evaluation of the hydrologic behavior of green roof, Journal of the American Water Resources Association 42, pp 84-94, 2006

[8] Carter, T., Jackson, C.R., Vegetated roofs for stormwater management at multiple spatial scales, Landscape and Urban Planning 80, pp84-94. 2007

[9] Jarrett, A., Hunt, W., Berghage, R., Annual and individual storm green roof stormwater response models, In: 2006 ASABE Annual International Meeting. Sponsored by ASABE, Oregon Convention Center, Portland, Oregon, pp 9-12. 2006

[10] Lee, J.Y., Moon, H.J., Kim, T.I., Kim, H.W., Han, M.Y., Quantitative analysis on the urban flood mitigation effect by the extensive green roof system, Environmental Pollution 18, pp 257-261. 2013

[11] Piro, P., Carbone, M. and J.J. Sansalone. Delivery and Frequency Distributions of Combined Wastewater Collection System Wet and Dry Weather Loads, Water Environment Research 84 pp 65-75. 2012

[12] Piro, P., Carbone, M., Garofalo, G. and J.J. Sansalone. Size Distribution of Wet Weather and Dry Weather Particulate Matter Entrained in Combined Flows from an Urbanizing Sewershed, Water Air and Soil Pollution 206 pp 83-94. 2010

[13] Piro P., M. Carbone, G. Garofalo and J.J. Sansalone, Management of CSOs based on observations from the urbanized Liguori catchment of Cosenza, Italy. Water Science & Technology, 61(1), pp. 135-143. 2010

[14] Piro P., Carbone M., Garofalo G. Innovative monitoring of combined sewer overflow (CSO) quality in the Liguori catchnment (Cosenza, Italy), Water Quality Research Journal of Canada, 47(2), pp. 178-185. 2012

[15] Carbone M., Garofalo G., Nigro G., Piro P. A conceptual model for predicting hydraulic behaviour of a green roof, Procedia Engineering, pp. 266-274. 2014